NOVEL ANTAGONISTIC MECHANISMS BETWEEN HUMAN SEC3 EXOCYST AND FLAVIVIRUS CAPSID PROTEIN

RAGHAVAN BHUVANAKANTHAM
M.Sc. University of Madras, India

A THESIS SUBMITTED

FOR THE DEGREE OF DOCTOR OF PHILOSOPHY

DEPARTMENT OF MICROBIOLOGY
YONG LOO LIN SCHOOL OF MEDICINE
NATIONAL UNIVERSITY OF SINGAPORE
2010

PUBLICATIONS AND CONFERENCE PRESENTATIONS GENERATED DURING THE COURSE OF STUDY

Publications

Bhuvanakantham R, Cheong YK, Ng ML (2010). West Nile virus capsid protein interaction with importin and HDM2 protein is regulated by protein kinase C-mediated phosphorylation. Microbes Infect. *12*, 615-625.

Bhuvanakantham R, Li J, Tan TT, Ng ML (2010). Human Sec3 protein is a novel transcriptional and translational repressor of flavivirus. Cell Microbiol. *12*, 453-472.

Bhuvanakantham R, Chong MK, Ng ML (2009). Specific interaction of capsid protein and importin-alpha/beta influences West Nile virus production. Biochem Biophys Res Commun. *389*, 63-69.

Tan TT, **Bhuvanakantham R**, Li J, Howe J, Ng ML (2009). Tyrosine 78 of premembrane protein is essential for assembly of West Nile virus. J Gen Virol. *90*, 1081-1092.

Manuscript in preparation

Bhuvanakantham R, Ng ML. Degradation of human Sec3 protein by flavivirus capsid protein through the activation of proteasome degradation pathway.

Chapter published in a book

Bhuvanakantham R, Ng ML (2009). West Nile virus-host interaction: An immunological prospective. In RNA Viruses: Host Gene Responses to Infection. World Scientific Publishing group. Pg: 415-444.

Conference Presentations

Bhuvanakantham R, Yeo KL, Ng ML (2010). A novel antagonistic relationship between human Sec3 exocyst and flavivirus capsid protein. 14th International Congress on Infectious Diseases (ICID), Miami, Florida, USA.

Bhuvanakantham R, Ng ML (2010). Hostile affiliation of flavivirus capsid protein with host proteins. 10th Nagasaki-NUS Medical Symposium on Infectious Diseases, Singapore.

Cheong YK, **Bhuvanakantham R**, Ng ML (2010). Phosphorylation of West Nile virus capsid protein is essential for efficient viral replication. 10th Nagasaki-NUS Medical Symposium on Infectious Diseases, Singapore.

Bhuvanakantham R, Wee ML, Ng ML (2009). Identification of human Sec3 protein as a novel anti-flaviviral factor. The 18th Scientific Conference of Electron Microscopy Society of Malaysia, Kuala Lumpur, Malaysia.

Cheong YK, **Bhuvanakantham R**, ML Ng (2009). Phosphorylation is a key modulator of flaviviral capsid protein functions. Emerging Infectious Diseases 2009, Singapore.

Bhuvanakantham R, Yeo KL, Ng ML (2009). Exploitation of host cell's regulatory mechanism during West Nile virus infection. 7th ASEAN Microscopy Conference, Jakarta, Indonesia.

Bhuvanakantham R, Chong MK, Ng ML (2009). Flavivirus capsid protein and importin beta interaction influences virus replication. 8th Asia Pacific Congress of Medical Virology, Hong Kong. (Oral)

Bhuvanakantham R, Ng ML (2008). Calcium-modulating cyclophilin ligand influences flavivirus replication. The Second International Conference on Dengue and Dengue Haemorrhagic fever, Phuket, Thailand.

Tan TT, **Bhuvanakantham R**, Li J, Howe J, Ng ML (2008). Defining new elements of West Nile virus prM protein: filling gaps in the understanding of flavivirus assembly process. 14th International Congress of Virology, Turkey, Istanbul.

Bhuvanakantham R, Ng ML (2008). West Nile virus exploits host proteins to hinder apoptosis. 14th International Congress of Virology, Turkey, Istanbul.

Bhuvanakantham R, Ng ML (2008). A novel antagonistic relationship between human Sec3 exocyst and West Nile virus capsid protein. 13th International Congress on Infectious Diseases, Malaysia, Kuala Lumpur.

Tan TT, **Bhuvanakantham R**, Li J, Howe J, Ng ML (2008). Identification of critical molecular determinants of West Nile virus prM protein: A potential site for antiviral targeting. 13th International Conference of Infectious Diseases, Malaysia, Kuala Lumpur.

Chong MK, **Bhuvanakantham R**, Ng ML (2008). The role of capsid protein in cell cycle arrest during flaviviral replication. Singapore Dengue Consortium First Annual Meeting, Singapore.

Chong, MK, Shu SL, **Bhuvanakantham R**, Ng ML (2007). Characterization of nuclear localization signals in dengue virus and West Nile virus capsid protein. Proceedings for the Third Asian Regional Dengue Research Network Meeting. Taipei, Taiwan).

ACKNOWLEDGEMENT

I would like to express my sincere gratitude to my supervisor, Professor Ng Mah Lee for the immense amount of support and guidance she has provided throughout this study. Professor Ng's insights into this project and patience towards me have been a true blessing. This dissertation would not have been possible without her continued support and commitment. I am greatly indebted to her.

Special thanks to Mdm Loy Boon Pheng for sharing her skills and knowledge on tissue culture techniques. I also thank her for her speedy efforts in handling and purchasing all the materials used in this study.

I would also like to thank Terence Tan for his advice and helpful discussion during this project. I thank all the members of the Flavivirus Laboratory: Krupakar, Sameul, Fiona, Patricia, Mei Ling, Yap Han, Melvin, Mun Keat, Xiao Ling, Li Shan, Shu Min, Vincent, Edwin, Kim Long, Anthony and Audrey for their friendship and technical advice on different techniques.

Confocal microscopy would have been challenging if not for the assistance of Clement Khaw at the Nikon-Singapore Bio-imaging Consortium.

Last but not least I would like to extend my deepest gratitude to my family who never ceased loving and supporting me. I am very grateful to my husband and my daughter for their understanding, patience and support during the entire period of my study. I am greatly indebted to my parents and my sister who constantly encouraged me although they are miles away. I must thank my mother-in-law for her support and patience especially when I need to stay late in the laboratory.

Thank you.

TABLE OF CONTENTS

PAGE NUMBER

APPENDICES

SUMMARY

The *Flaviviridae* family consists of several medically important pathogens such as West Nile virus (WNV) and Dengue virus (DENV). Flavivirus capsid (C) protein is a key structural component of virus particles. However, the role of C protein in the pathogenesis of arthropod-borne flaviviruses is poorly understood. To examine whether flavivirus C protein can associate with cellular proteins, and contribute to viral pathogenesis, WNV/DENV C protein was screened against a human brain/liver cDNA yeast two-hybrid library. This study identified several interesting proteins associated with a wide variety of cellular functions. One of the exocyst components, human Sec3 protein (hSec3p) was discovered to be a novel interacting partner of WNV and DENV C protein. Mutagenesis studies showed that the SH2 domain-binding motif of hSec3p binds to the first 15 amino acids of C protein. Based on the functional roles of Sec3p in the secretory pathways and exocytosis process, it was hypothesized that flavivirus C protein might exploit hSec3p for virus trafficking and release. The knock-down of hSec3p should therefore prevent C protein-exocyst association and disrupt virus production. However, hSec3p knock-down potentiated virus replication/production in flavivirus-infected hSec3p knock-down cells while the reverse phenomenon was observed in hSec3p over-expressing cells. This contradicted the initial hypothesis and proposed hSec3p as a negative regulator of flavivirus infection. This is the first study that highlighted hSec3p as an anti-flaviviral host protein. This study reported for the first time that hSec3p modulated virus production by affecting viral RNA transcription and translation through the sequestration of elongation factor 1α (EF1α). The hSec3p sequestered EF1α and as a result, EF1α was no

longer capable of binding to flaviviral RNA efficiently. This resulted in reduced binding of EF1α with flaviviral RNA genome or RNA-associated replicative complex and led to the decrement in viral RNA synthesis. By sequestering the translational enhancer, EF1α, hSec3p also inhibited viral protein translation. This molecular discovery shed light on the protective role of hSec3p during flavivirus infection. This study also highlighted the antagonistic mechanism adopted by flavivirus C protein that activated the chymotrypsin-like proteolytic function of 20S proteasome to degrade hSec3p. This resulted in reduced hSec3p level that subsequently led to the decreased formation of EF1α-hSec3p complex. This rendered free EF1α readily available to interact with 3'UTR of viral RNA to aid viral RNA transcription and translation. In this way, C protein nullified the anti-viral effects of hSec3p to support flavivirus life-cycle. Overall, this study illustrated the antagonistic relationship between flavivirus C protein and hSec3p and highlighted the new interface for pharmaceutical intervention.

LIST OF TABLES

PAGE NUMBER

LIST OF FIGURES

PAGE NUMBER

ABBREVIATIONS

%	-	percentage
(-)	-	minus strand viral RNA
(+)	-	plus strand viral RNA
:	-	ratio
˚C	-	degrees Celsius
<	-	less than
>	-	more than
µg	-	microgram
µl	-	microlitre
µm	-	micrometer
293FT	-	Human Embryonic Kidney cells FT
3'UTR	-	3' untranslated region
5'UTR	-	5' untranslated region
α1	-	helix I
α2	-	helix II
α3	-	helix III
α4	-	helix IV
AD	-	GAL4 DNA-activation domain
α-gal	-	α-galactosidase
AQP2	-	aquaporin-2
ATF6	-	activating transcription factor 6
BC	-	background control
BC_{Lac}	-	background LacZ control
BD	-	GAL4 DNA-binding domain
BHK	-	Baby Hamster Kidney Cells 21, clone 13
BSA	-	bovine serum albumin
BSL	-	biosafety level
BVDV	-	Bovine viral diarrhea virus
C protein	-	capsid protein

C6/36	-	mosquito cells derived from *Aedes albopictus*
CAML	-	calcium-modulating cyclophilin binding ligand
CDC	-	Centers for Disease Control and Prevention
cDNA	-	complementary deoxyribonucleic acid
cm	-	centimetre
CM	-	convoluted membranes
CMC	-	carboxy-methyl-cellulose
CNS	-	central nervous system
Co-IP	-	co-immunoprecipitation
CSFV	-	Classical swine fever virus
Daxx	-	human death domain-associated protein
DENV	-	dengue virus
DENVCIP	-	DENV C protein interacting partner
DHF	-	dengue hemorrhagic fever
DMSO	-	dimethyl sulfoxide
DNA	-	deoxyribonucleic acid
Dorfin	-	E3 ubiquitin ligase
ds	-	double-stranded oligonucleotides
DSS	-	dengue shock syndrome
E	-	envelope
EF1α	-	elongation factor 1α
ER	-	endoplasmic reticulum
EtBr	-	ethidium bromide
FBS	-	foetal bovine serum
g	-	gram(s)
HCV	-	Hepatitis C virus
HEK293	-	Human Embryonic Kidney cells
hSec3p	-	human Sec3p
hSec3pKD	-	hSec3p knock-down cells
hSec3pOE	-	hSec3p over-expressing cells
HSP 27	-	heat shock protein 27
HSP 70	-	heat shock protein 70
HSP 90	-	heat shock protein 90

I2PP2A	-	phosphatase inhibitor
IP	-	immunoprecipitated sample
JEV	-	Japanese encephalitis virus
KUN	-	Kunjin virus
LB agar	-	Luria-Bertani agar
LB broth	-	Luria-Bertani broth
LiAc	-	lithium acetate
Log	-	logarithmic scale
M	-	molar
M2H	-	mammalian two-hybrid assay
min	-	minute(s)
ml	-	millilitre(s)
mm	-	millimetre(s)
MOI	-	multiplicity of infection
NC	-	negative control
nm	-	nanometre(s)
NMR	-	nuclear magnetic resonance spectroscopy
NS	-	non-structural
ORF	-	open reading frame
p	-	probability
p.i.	-	post-infection
PAGE	-	polyacrylamide gel electrophoresis
PBS	-	phosphate-buffered saline
PBST	-	phosphate-buffered saline with Tween-20
PC	-	paracrystalline arrays
PC (M2H)	-	positive control
PCR	-	polymerase chain reaction
PEG	-	polyethylene glycol
PFU	-	plaque forming unit
PIC	-	positive interaction control
PIMT	-	protein L-isoaspartyl methyltransferase
prM	-	premembrane
PTB	-	polypyrimidine-tract binding protein

PVDF	-	polyvinylidene fluoride membrane
RE	-	restriction endonuclease
RF	-	replicative form
RNA	-	ribonucleic acid
rpm	-	revolutions per minute
RT	-	room temperature
RT-PCR	-	real-time polymerase chain reaction
SD	-	synthetic drop-out medium
SDS-PAGE	-	Sodium-dodecyl sulphate PAGE
Sec3p	-	Sec3 protein
Sec6p	-	Sec6 protein
shRNA	-	short hairpin-RNA
TAE	-	tris-acetate-EDTA buffer
TBEV	-	Tick-borne encephalitis virus
TBST	-	Tris-buffered solution containing Tween-20
TGN	-	trans Golgi network
TSPY	-	testis-specific protein Y
UV	-	ultraviolet
V-ATPase	-	vacuolar ATPase
VP	-	vesicle pockets
vRNA	-	viral RNA
WB	-	Western blot
WCL	-	whole cell lysate
WNV	-	West Nile virus
WNV(NY)	-	West Nile virus, New York strain
WNV(S)	-	West Nile virus, Sarafend strain
WNVCIP	-	WNV C protein interacting partner
x	-	times magnitude
x *g*	-	centrifugal force
Y2H	-	yeast two-hybrid assay
YFV	-	Yellow fever virus
YPDA	-	yeast peptone dextrose adenine medium

CHAPTER 1

LITERATURE REVIEW

1.0. LITERATURE REVIEW

1.1. *FLAVIVIRIDAE*

The family *Flaviviridae* comprises more than 70 closely related RNA viruses under three genera, namely flavivirus, pestivirus and hepacivirus. Members of the different genera are distantly related but share a similar gene order and conserved non-structural protein motifs. The genus flavivirus consists of most medically important groups of emerging arthropod-borne viruses that includes West Nile (WNV), dengue (DENV), yellow fever (YFV), Japanese encephalitis (JEV) and tick-borne encephalitis (TBEV) viruses (Gaunt *et al.*, 2001; Heinz & Allison, 2000; Kuno *et al.*, 1998). The genus pestivirus includes classical swine fever virus (CSFV) and bovine viral diarrhea virus (BVDV). Hepatitis C virus (HCV) is the member of the genus, Hepacivirus (Taxonomy, 2000).

1.2. FLAVIVIRUS

The name, flavivirus was derived from YFV, a representative virus of the *Flaviviridae* family (In Latin, *flavus* means yellow). Flaviviruses are a group of small enveloped RNA viruses that cause serious diseases in humans and animals. Most of them are arthropod-borne viruses and are transmitted to vertebrate hosts by either mosquitoes or ticks (Gubler *et al.*, 2007). These flaviviruses cause a range of distinct clinical diseases in humans. Based on the associated clinical manifestations, flaviviruses can be clustered into two main groups. The first group includes viruses that have the capacity to cause vascular leak and haemorrhage (DENV and YFV) while the second group includes those that can cause

encephalitis (WNV, JEV and TBEV). However, relatively few infected individuals develop these severe clinical manifestations and many are asymptomatic or have an undifferentiated febrile illness. In this literature review, the focus is on WNV and DENV since these two representative viruses were chosen for studies in the following chapters although studies involving TBEV, YFV, JEV, HCV and other RNA viruses were also compared.

1.3. TRANSMISSION

West Nile virus is transmitted by *Culex* mosquitoes primarily between birds, the amplifying hosts of the virus. They also function as bridge vectors for transmission to humans, equines and other mammals (Turell *et al.*, 2005). Humans are considered dead-end hosts because they usually develop viremia at an insignificant level to facilitate further transmission of the virus. West Nile virus transmission was also reported during organ transplantation (DeSalvo *et al.*, 2004; Jain *et al.*, 2007; Murtagh *et al.*, 2005; Wadei *et al.*, 2004), blood transfusion (Dokland *et al.*, 2004; Macedo de Oliveira *et al.*, 2004; Montgomery *et al.*, 2006) pregnancy (Dokland *et al.*, 2004; Jamieson *et al.*, 2006; O'Leary *et al.*, 2006; Skupski *et al.*, 2006) and lactation (Brinton, 2002). Occupational WNV infections in laboratory workers have also been documented (Brinton, 2002; Hamilton & Taylor, 1954).

Dengue virus is transmitted by *Aedes* mosquitoes. Although the virus is transmitted by *Aedes albopictus* and *Aedes polynesiensis* as well, *Aedes aegypti* is

the principal vector. Dengue viruses are maintained in an *Aedes aegypti* - human - *Aedes aegypti* cycle with periodic epidemics. Infected humans are the main carriers and amplification host of DENV. Female mosquitoes acquire DENV by biting infected humans in the viraemic phase and become infective after an extrinsic incubation period of 7-14 days. Since female mosquitoes are nervous feeders, the slightest movement will disrupt the feeding process. Few moments later, they will continue to feed on the same person or different person. This behavioral pattern allows the infected mosquito to feed on several people during a single blood meal, which in turn transmit DENV to many people in a short duration (Gubler, 1998). Dengue virus transmission was also reported during organ transplantation (Machado *et al.*, 2009; Teo *et al.*, 2009), blood transfusion (Teo *et al.*, 2009) and pregnancy (Basurko *et al.*, 2009).

1.4. CLINICAL MANIFESTATIONS

While the majority of WNV infections are asymptomatic, it can cause debilitating disease in humans and animals, with symptoms ranging from febrile illness to fatal encephalitis. About 20% of infected patients display a range of symptoms including fever, headache, malaise, back pain, myalgias, eye pain, pharyngitis, nausea, vomiting, diarrhea and abdominal pain. Out of that 20%, maculopapular rash appears in approximately half, a subset of which would acquire a form of neuroinvasive disease (Petersen & Roehrig, 2001; Watson *et al.*, 2004). More serious manifestations of WNV are categorized as encephalitis, meningitis and flaccid paralysis with the former two being more common (Nash *et al.*, 2001).

Muscle weakness and flaccid paralysis is particularly suggestive of WNV infection (Petersen & Marfin, 2002). Asymmetric acute flaccid paralysis syndrome may also occur independent of encephalitis and has been noted to be a sign of impending respiratory failure (Sejvar *et al.*, 2005).

West Nile encephalitis is commonly reported in patients above the age of 55 and is higher among organ transplant recipients (Kumar *et al.*, 2004; O'Leary *et al.*, 2002). West Nile poliomyelitis, West Nile choreoretinitis, hepatitis, pancreatitis, cardiac dysrhythmia and myocarditis have also been documented [reviewed in (Hayes & Gubler, 2006)]. Around 381 cases of WNV infection in United States with 12 fatalities were reported to CDC between January to November 2010 (http://www.cdc.gov/ncidod/dvbid/westnile/surv&controlCaseCount10_detailed.htm). There was no reported human case of WNV infection in Singapore.

Dengue virus causes a wide range of diseases in humans, ranging from acute febrile illness dengue fever to life-threatening dengue hemorrhagic fever/dengue shock syndrome (DHF/DSS). Febrile dengue fever is self-limited though debilitating illness characterized by fever, frontal headache, retro-orbital pain, myalgia, arthralgia, nausea, vomiting, weakness and rash. Constipation, diarrhea and respiratory symptoms are occasionally reported. Lymphadenopathy is common. Rash is variable but occurs in up to 50% of patients as either early or late eruptions. In some cases, an intense erythematous pattern with islands of normal skin is observed.

Dengue hemorrhagic fever is marked by increased vascular permeability, thrombocytopenia and hemorrhagic manifestations. Common hemorrhagic manifestations include skin hemorrhages such as petechiae, purpuric lesions and ecchymoses. Epistaxis, bleeding gums, gastro-intestinal hemorrhage and hematuria occur less frequently. Dengue shock syndrome occurs when fluid leakage into the interstitial spaces results in shock, which without appropriate treatment may lead to death [reviewed from (Gubler, 1998; Halstead, 2007; Leong *et al.*, 2007)]. It has been estimated that more than 2.5 billion people in over 100 countries are at risk of DENV infection. As many as 100 million people are infected yearly with 500,000 cases of DHF and 22,000 deaths mainly among children (http://www.cdc.gov/dengue/epidemiology/index.html and http://www.who.int/csr/disease/dengue/impact/en/). Dengue virus infection poses a major health problem in Singapore. Despite the active vector sutveillence programme in Singapore, about 1200 dengue cases have been reported in 2011 (Jan to 1st week of May). The number of dengue cases would significantly increase in the period of June to October which is the actual peak period of dengue infection.

1.5. STRUCTURE OF FLAVIVIRUS

The mature flavivirus is smooth and spherical with a diameter of approximately 50 nm. The mature virus is symmetrically icosahedral with no spiky surface extensions (Mukhopadhyay *et al.*, 2003). Each virion is composed of a single positive-strand genomic RNA. The RNA genome is housed within a poorly-ordered cage-like nucleocapsid core composed of multiple copies of capsid (C) protein. The spherical nucleocapsids are about 25 nm in diameter and surrounded

by a 4 nm thick lipid bilayer derived from the endoplasmic reticulum (ER) membrane of the host cell, within which 180 copies of two viral glycoproteins, membrane (M) and envelope (E) are anchored (Kuhn *et al.*, 2002; Mukhopadhyay *et al.*, 2003; Mukhopadhyay *et al.*, 2005; Perera & Kuhn, 2008).

The M and E proteins have different conformations in immature and mature virions, thereby conferring unique structural features to both forms of particles. In immature virion, E protein exists as a heterodimer with prM protein. These heterodimers form 60 trimeric spikes that extend away from virus surface and gives the virus a 'spiky' morphology (Fig. 1.1). In mature virion, E proteins are found as 90 homodimers that lie flat against viral surface forming a 'smooth' protein shell (Fig. 1.2). The structural transitions from immature (spiky) to mature (smooth) morphology occur in Trans-Golgi Network (TGN) and are driven predominantly by pH-driven conformational changes in E protein (Modis *et al.*, 2003; 2004; 2005; Zhang *et al.*, 2004). In both mature and immature particles (Fig. 1.3), there is a gap of about 3 nm between the lipid bilayer and nucleocapsid core. Unlike alphaviruses, there are little or no connections between the viral outer coat and inner core (Kuhn *et al.*, 2002; Mukhopadhyay *et al.*, 2003; Zhang *et al.*, 2003a; Zhang *et al.*, 2003b).

1.6. FLAVIVIRUS RNA GENOME ORGANIZATION AND VIRAL PROTEINS

The flavivirus genome consists of a single-stranded RNA molecule of positive polarity. Since the genomic RNA is positive-stranded, it is infectious (Ada & Anderson, 1959). Its genome is approximately 11 kb in length and contains a

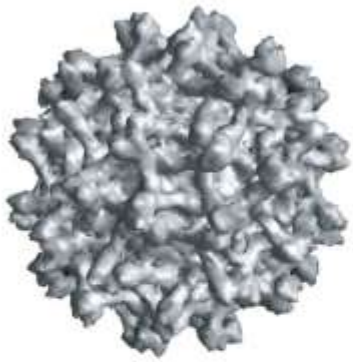

Fig. 1.1: Cryo-EM reconstruction of immature virion (Zhang *et al.*, 2004).

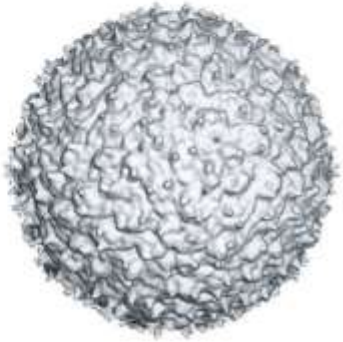

Fig. 1.2: Cryo-EM reconstruction of mature virion (Zhang *et al.*, 2003a).

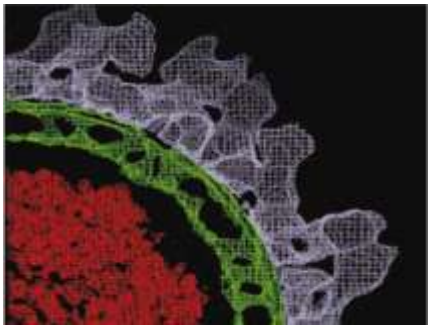

Fig. 1.3: Cross section of virus particle showing the ectodomain of prM protein in bluish white, lipid bilayer in green and nucleocapsid in orange (Zhang *et al.*, 2003b).

single open reading frame (ORF) flanked by 5'- and 3'-untranslated regions (UTRs) (Fig. 1.4). The UTRs possess secondary structures that are essential for initiation of positive strand RNA synthesis, negative strand RNA synthesis and initiation of translation (Davis *et al.*, 2007b; Paranjape & Harris, 2010; Tilgner *et al.*, 2005; Tilgner & Shi, 2004; Villordo & Gamarnik, 2009; Wei *et al.*, 2009; Yu *et al.*, 2008b; Zhang *et al.*, 2008a). In mosquito-borne flaviviruses, the 5'UTR has a type I cap, but 3' UTR lacks the 3' terminal polyadenine tract (poly-A-tail), instead terminates with conserved dinucleotide CU^{OH} (Brinton *et al.*, 1986; Westaway, 1987).

The ORF encodes a polyprotein precursor of approximately 3400 amino acids, which are co-translationally and post-translationally processed by host cell signalases and viral proteases to form three structural and seven non-structural (NS) proteins (Fig. 1.4). The structural proteins capsid (C), pre-membrane/membrane (prM/M) and envelope (E) constitute the virus particle while the NS proteins are involved in viral RNA replication, virus assembly and modulation of host cell responses (Beasley, 2005; Brinton, 2002; Chambers & Rice, 1987; Lindenbach & Rice, 2003; Rice, 1990). Table 1.1 summarizes the properties of flavivirus proteins and their functions.

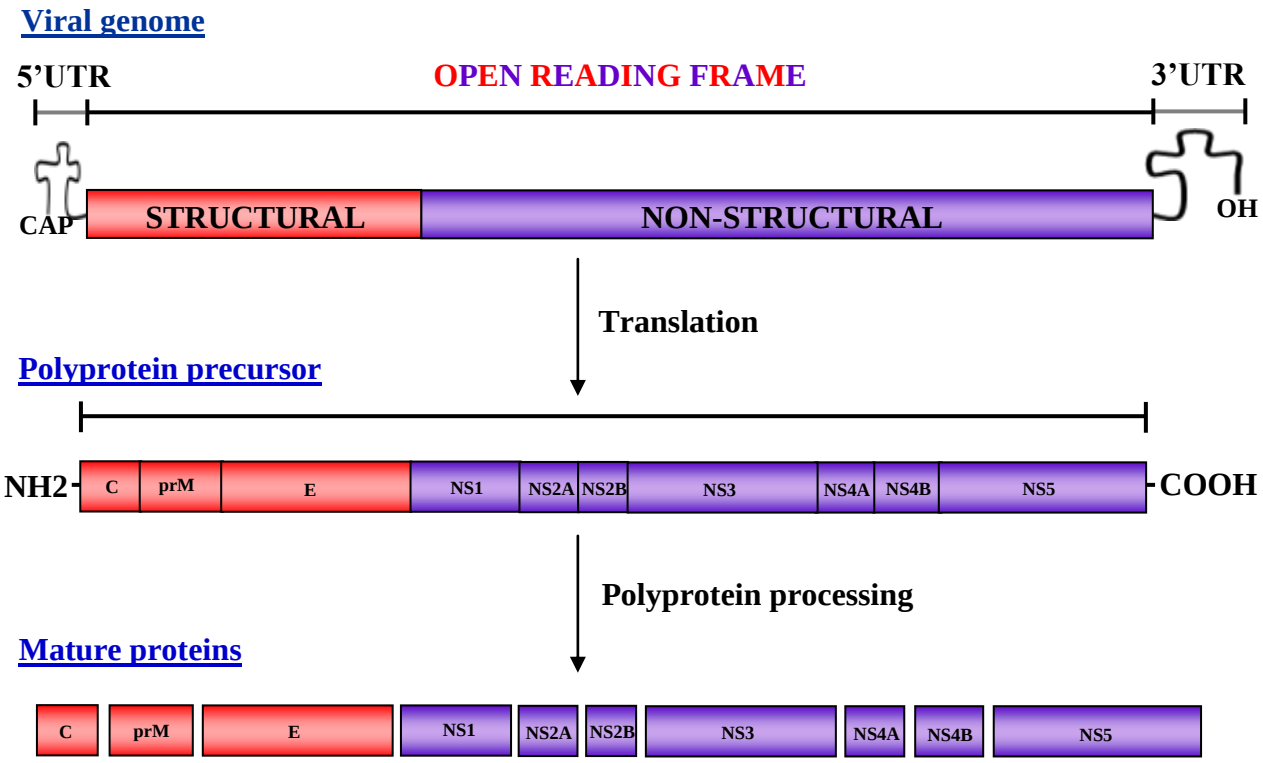

Fig. 1.4: Schematic representation of flavivirus genome organization and polyprotein processing. The 11kb positive-sense, single-stranded RNA genome contains a 5' CAP, but no 3' poly-A tail. It is translated as one long polyprotein that is cleaved by viral and host proteases to form three structural proteins and seven non-structural proteins.

Table 1.1: Summary of the properties of flavivirus proteins and their functions

Protein	MW (~kDa)	Nuclear phase	Relication complex	Functions
C	14	Yes	No	- Basic building blocks of nucleocapsid protein (Kiermayr *et al.*, 2004; Kunkel *et al.*, 2001; Patkar *et al.*, 2007) - Conserved internal hydrophobic domain aids the oligomerization of C protein and assists the anchoring of C protein to cellular ER membrane (Bhuvanakantham & Ng, 2005; Markoff *et al.*, 1997; Wang *et al.*, 2004)
prM	26	No	No	- Important for maturation of the virus with cleavage of prM to M (Chambers *et al.*, 1990a; Stadler *et al.*, 1997) - Co-expression of prM is essential for proper folding of E protein (Holbrook *et al.*, 2001; Konishi & Mason, 1993; Lorenz *et al.*, 2002) - prM protects E protein from premature acid-induced fusion in the acidic compartments of secretory pathway (Allison *et al.*, 1995; Guirakhoo *et al.*, 1992; Heinz & Allison, 2000; 2003; Heinz *et al.*, 1994; Li *et al.*, 2008; Yu *et al.*, 2008a) - prM interacts with host proteins such as V-ATPase and claudin-1 to facilitate efficient virus entry and egression (Duan *et al.*, 2008; Gao *et al.*, 2010)
E	50-60	No	No	- Mediates virus binding to host cell receptors (Chambers *et al.*, 1990a; Modis *et al.*, 2004; Rey *et al.*, 1995) - Mediates membrane fusion (Allison *et al.*, 2001; Allison *et al.*, 1995; Bressanelli *et al.*, 2004; Heinz & Allison, 2000; 2003; Rey *et al.*, 1995) - antigenic properties (Chambers *et al.*, 1990a; Modis *et al.*, 2004; Rey *et al.*, 1995)
NS1	45	Yes	Yes	- Part of viral replication complex (Lindenbach & Rice, 1999; Mackenzie *et al.*, 1996) - Attenuates complement activation (Chung *et al.*, 2006) - Elicits auto-antibodies against platelet and extracellular matrix proteins (Chang *et al.*, 2002; Falconar, 1997) - Causes endothelial cell damage through antibody-dependent complement-mediated cytolysis (Falconar, 1997; Lin *et al.*, 2005a; Lin *et al.*, 2003; Lin *et al.*, 2002)

NS2A	22	No	Yes	- Part of viral replication complex (Mackenzie *et al.*, 1998) - Modulates host interferon response (Liu *et al.*, 2004b; Liu *et al.*, 2006b) - Affects the assembly of virus particles (Liu *et al.*, 2003)
NS2B	14	No	No	- Functions as a co-factor for the serine protease activity of NS3 (Chambers *et al.*, 1993; Chang *et al.*, 1999) - Mediates membrane permeability during flavivirus infection (Chang *et al.*, 1999)
NS3	70	Yes	Yes	- possesses serine protease, RNA helicase, RNA triphosphatase (RTPase) and RNA-stimulated nucleoside triphosphatase (NTPase) activities - The protease domain cleaves viral polyprotein at several sites (Amberg & Rice, 1999; Falgout *et al.*, 1991; Preugschat *et al.*, 1990) - The helicase domain unwinds the RNA secondary structure in the 3'UTR of viral RNA genome as well as the double-stranded replicative form of viral RNA (Benarroch *et al.*, 2004; Chen *et al.*, 1997a; Matusan *et al.*, 2001) - The RTPase helps to synthesize and modify the cap structure at the 5' end of nascent viral genome (Wengler, 1993) - The NTPase activity of NS3 is essential to power RNA unwinding for helicase activity (Li *et al.*, 1999)
NS4A	16	No	Yes	- Induces membrane rearrangements, a unique feature observed with most RNA viruses (Miller *et al.*, 2007; Roosendaal *et al.*, 2006) - Modulates the host interferon response (Munoz-Jordan *et al.*, 2003)
NS4B	27	Yes	Yes	- Inhibits host-induced interferon signaling (Munoz-Jordan *et al.*, 2005) - Modulates viral replication by interacting with NS3 (Umareddy *et al.*, 2006)
NS5	105	Yes	Yes	- The RNA-dependent RNA polymerase activity is essential for virus replication (Khromykh *et al.*, 1998; Khromykh *et al.*, 1999) - Its S-adenosyl methyl transferase activity helps to methylate the type I cap at the 5' end of viral genome (Ray *et al.*, 2006; Zhou *et al.*, 2007)

1.7. FLAVIVIRUS LIFE CYCLE

Flavivirions attach to target cells through binding of E protein to the receptor(s) on host cell surfaces. Several receptors and co-receptors have been identified for flaviviruses such as integrin αVβ3, Fcγ, Rab5, heat shock cognate protein 70, C-type lectin DC-SIGN, glycosaminoglycan and heparin sulphate (Chen *et al.*, 1997b; Chu & Ng, 2004c; Krishnan *et al.*, 2007; Lee & Lobigs, 2000; Liu *et al.*, 2004a; Martina *et al.*, 2008; Miller *et al.*, 2008; Navarro-Sanchez *et al.*, 2003; Ren *et al.*, 2007). After binding to the cell receptors, virions enter the cells by receptor-mediated endocytosis (Acosta *et al.*, 2008; 2009; Ang *et al.*, 2010; Chu & Ng, 2004b; Peng *et al.*, 2009). The acidic environment of endosomes triggers major conformational changes on E protein, which results in re-organisation of E homodimers into E homotrimers. This structural re-arrangement exposes the fusion peptide which helps in the insertion of the virus into the host endosomal membrane (Allison *et al.*, 2001; Allison *et al.*, 1995; Bressanelli *et al.*, 2004; Heinz & Allison, 2000; 2003; Rey *et al.*, 1995). After fusion has occurred, the nucleocapsid is released into the cytoplasm. The nucleocapsid further dissociates into RNA and C protein and this process is believed to be spontaneous (Heinz & Allison, 2000; Koschinski *et al.*, 2003).

Flaviviral RNA genome is translated by host cell machinery into a single polyprotein that is co-translationally and post-translationally processed by viral and host proteases to generate structural and non-structural proteins (Fig. 1.5). Within ER lumen, host-encoded signalase cleaves the polyprotein at C/prM,

prM/E, E/NS1 and NS4A/NS4B junctions. As a result, C, prM, E and NS1 proteins are released from the polyprotein. The prM and E proteins remain anchored on the luminal side of the membrane, while C protein remain anchored on the cytoplasmic side of ER membrane by a conserved hydrophobic signal sequence at its carboxy-termini. Within TGN, furin cleaves prM into M protein, releasing the "pr" region, which is subsequently secreted into the extracellular medium. The NS2B/NS3 protease cleaves the polyprotein at all protein-protein junctions on the cytosolic side of ER membrane, releasing all non-structural proteins. On the cytoplasmic side of ER membrane, the NS2B/NS3 protease also cleaves the anchored C protein before the carboxy-termini hydrophobic sequence. As a result, the signal sequence for translocation of prM into ER lumen is released and mature C is produced (Chambers *et al.*, 1990a; Chambers *et al.*, 1990b; Chambers & Rice, 1987; Markoff, 1989; Perera & Kuhn, 2008; Stocks & Lobigs, 1995; 1998).

After translation of input genomic RNA, NS5 through its RNA-dependent RNA polymerase activity together with other viral non-structural proteins and some host proteins, copies complementary minus strand RNA from genomic RNA. Flaviviral RNA synthesis occurs in an asymmetric and semi-conservative manner. A single, nascent minus RNA strand is synthesised from plus strand RNA genome and forms double-stranded RNA replicative form (RF). The RF is then used as a template for the synthesis of new RNA strands through a replicative intermediate (RI), in which several plus strands can simultaneously be synthesized from a

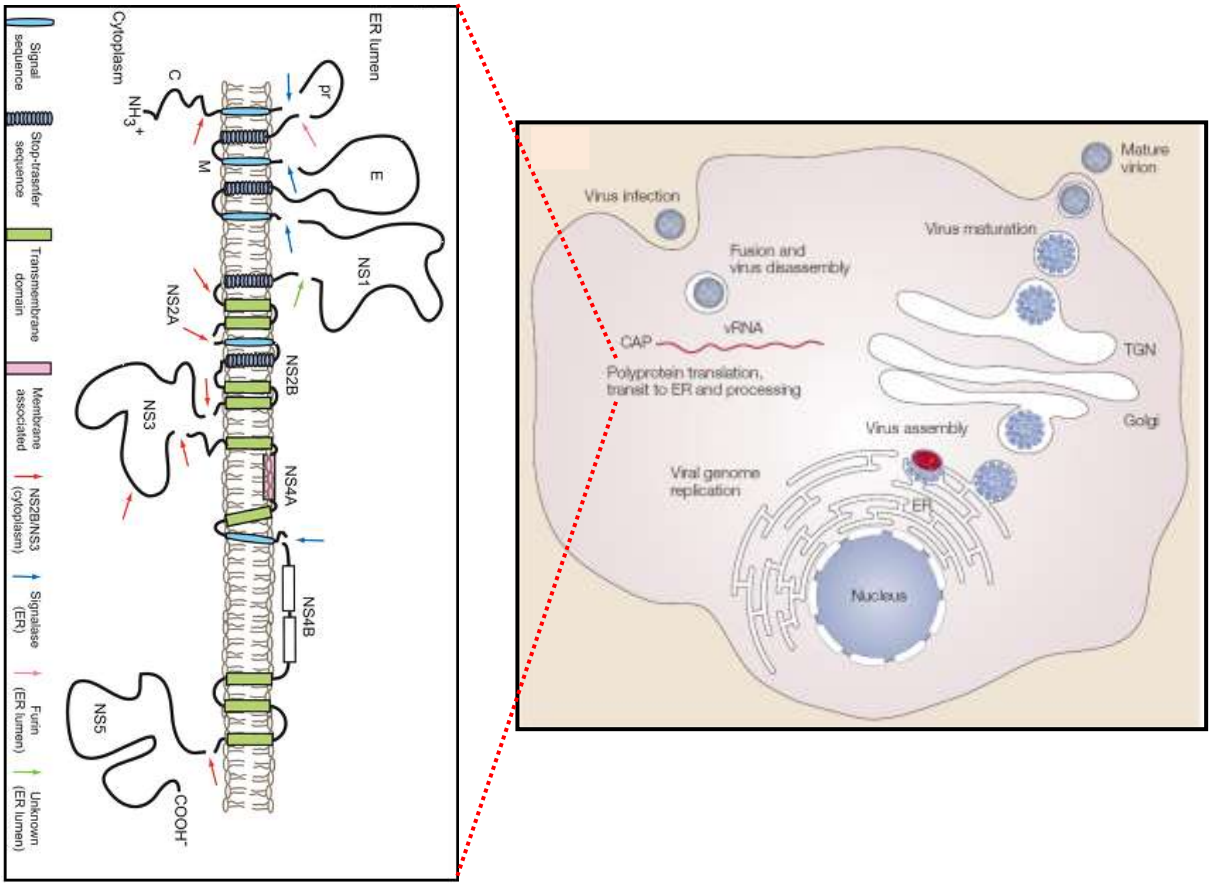

Fig. 1.5: Schematic representation of flavivirus life cycle [adapted from (Mukhopadhyay *et al.*, 2005; Perera & Kuhn, 2008)]. The virion binds to a cell surface receptor and enters the cell by endocytosis. The low pH within the endosome induces membrane fusion and release of nucleocapsid into cytosol where viral RNA (vRNA) is released. The translation of the polyprotein occurs at ER lumen. Host-encoded proteases and virus-encoded proteases cleave the polyprotein to form structural and non-structural proteins (shown in the Inset). Genome replication occurs on intracellular membranes. The structural proteins and the vRNAs then buds into the ER lumen to associate with prM-E heterodimers and forms immature virus particles. The immature virus particles are transported through TGN and cleaved by furin to produce mature, infectious particles. Mature virions are subsequently released by exocytosis.

single minus strand. The synthesis of plus strand RNA is 10 times more efficient than that of minus strand (Brinton, 2002; Chu & Westaway, 1985; Cleaves *et al.*, 1981; Mackenzie *et al.*, 1998). Flavivirus replication occurs in the cytoplasm on virus-induced host cell membranes, which are believed to be derived from ER/Golgi membrane [vesicle pockets (VP)].

Uchil and colleagues (2003) suggested that VPs protect the RF from host defences through a tough double-membrane and protective protein cover. Other virus-induced membranous structures called convoluted membranes (CM) and paracrystalline arrays (PC) are also reported to form near VPs. These virus-induced membranous structures are concentrated in the perinuclear region of host cells, providing a scaffold structure to anchor viral replicative complexes for efficient processing and synthesis (Mackenzie, 2005; Mackenzie *et al.*, 1996; Mackenzie *et al.*, 1998; Mackenzie & Westaway, 2001).

Virion assembly occurs in the lumen of rough ER (Mackenzie & Westaway, 2001). The newly synthesized C protein undergoes oligomerisation (Bhuvanakantham & Ng, 2005; Kiermayr *et al.*, 2004; Ma *et al.*, 2004; Wang *et al.*, 2004) and interacts with flaviviral RNA (Khromykh & Westaway, 1996) to form nucleocapsid and buds into the ER lumen. The nucleocapsid is then packaged into an ER-derived lipid bilayer containing heterodimers of prM and E proteins (Lobigs & Lee, 2004; Lorenz *et al.*, 2003; Mackenzie & Westaway, 2001). This results in the formation of non-infectious, immature virus particles which cannot induce host-cell fusion. Together with immature virus particles, subviral particles are also produced in which nucleocapsid is absent. The

immature and subviral particles are then transported through TGN, where host protease furin cleaves prM protein that is present on the immature virus particles to M protein (Chambers *et al.*, 1990a; Stadler *et al.*, 1997). This produces mature, infectious virus particles or subviral particles where M proteins remain inserted in the envelope of virus particle (Murray *et al.*, 1993; Yu *et al.*, 2008a).

Recently, Yu and colleagues (2008a) showed that the 'pr' portion of prM is also retained on virion to prevent membrane fusion. They also suggested that the 'pr' portion retainment could be a mechanism of flavivirus processing and stabilization in cell secretory pathway. Virions are then transported to the plasma membrane in vesicles and are released from the host cell by exocytosis. The involvement of host proteins in assisting the exocytosis of flaviviruses is largely unknown. The exocyst complex plays an important role in the secretory pathway and vesicular trafficking (Hsu *et al.*, 1999; TerBush *et al.*, 1996) by targeting vesicles to the plasma membrane as well as regulating the later phases of exocytosis process (Zhang *et al.*, 2008b). The exocyst is an octameric protein complex. The subunits are named as EXOC1, EXOC2, EXOC3, EXOC4, EXOC5, EXOC6, EXOC7 and EXOC8. These subunits were also known as Sec3, Sec5, Sec6, Sec8, Sec10, Sec15, Exo70 and Exo84.

In yeast, Sec3 protein (Sec3p) serves as a spatial landmark for polarized secretion through its ability to bind phospholipids and small GTPases (Baek *et al.*, 2010; Finger *et al.*, 1998a; Finger & Novick, 1997; Guo *et al.*, 2001; Hsu *et al.*, 2004; Zhang *et al.*, 2001). In yeast, Sec3p was shown to localize with Exo70 at the growing end of the daughter cell. The polarized localization of Sec3p is

independent of actin assembly although localization of other exocyst components relies on actin cables that serve as tracks for motor-driven vesicle transport to the daughter cell (Boyd *et al.*, 2004; Finger *et al.*, 1998b; Finger & Novick, 1998; Zhang *et al.*, 2005b).

Recently, the structure for the amino-terminal region of yeast Sec3p in complex with Rho1 or by itself was unveiled (Baek *et al.*, 2010; Yamashita *et al.*, 2010). These studies defined a new subclass of pleckstrin homology domains in the exocyst complex and provided the structural insights into how an exocyst subunit might interact with both protein and phospholipid factors on the target membrane.

In contrast to yeast Sec3p, very little is currently known about its mammalian orthologue, human Sec3 protein (hSec3p). Matern and colleague (2001) showed that human Sec3p (hSec3p) interacts with Sec5p and Sec8p, providing further evidence that the identified protein is part of the Sec6/8 exocyst complex Human Sec3p was the last subunit of the mammalian exocyst complex to have been identified (Matern et al., 2001). Unlike yeast Sec3p, hSec3p lacks the Rho binding domain and hence it is unlikely to directly bind GTPases of the Rho family. However, it was shown that hSec3p facilitated the delivery of matrix metalloproteinases to tumor cell invadopodia through an interaction with the polarity protein IQGAP1 that is regulated by RhoA and Cdc42 GTPases (Matern *et al.*, 2001; Sakurai-Yageta *et al.*, 2008). Human Sec3p has also been implicated in the maintenance of desmosomes (Andersen & Yeaman, 2010). A GFP fusion of human Sec3 failed to assemble into exocyst holocomplexes and remained cytosolic when expressed in MDCK cells. This suggested that Sec3p does not

function as a spatial landmark for secretion in mammalian cells (Matern *et al.*, 2001). Moreover, the localization and function of endogenous hSec3p have not been investigated. Because this subunit is important for ensuring correct polarized localization of exocyst complexes in budding yeast, this represents an important gap in our knowledge of the mammalian exocyst complex. Examining the involvement of exocyst components, especially hSec3p, in flavivirus life cycle could shed light on host proteins associated with exocytosis of flaviviruses.

1.8. THE CAPSID PROTEIN

In this literature review, the structural and functional properties of C protein were analyzed in detail since C protein was chosen for studies in the subsequent chapters. The C protein is the first structural protein found in the ORF. The viral polyprotein is cleaved by host signalase and forms anchored C protein that remain anchored on the cytoplasmic side of ER membrane by a conserved hydrophobic signal sequence at its carboxy-termini. The carboxy-termini hydrophobic sequence of anchored C protein is cleaved by NS2B/NS3 protease and forms mature C protein (Chambers *et al.*, 1990a; Markoff, 1989). The C protein is the basic building blocks of nucleocapsid which encapsidates viral RNA (Khromykh & Westaway, 1996; Kiermayr *et al.*, 2004; Kunkel *et al.*, 2001; Patkar *et al.*, 2007).

1.8.1. Alignment of the amino acid sequences of flavivirus capsid protein

As an initial step to examine the genetic relationship of flavivirus C proteins, alignment of the amino acid sequences of various flavivirus C protein was performed with CLUSTALW2 alignment software (Fig. 1.6). Among all the flavivirus proteins, the C protein is the least conserved protein, with less than 35%

sequence identity between most genus members (Table 1.2). Various strains of WNV C proteins (NY, S and KUN) share ~90% sequence identity while C proteins of different serotypes of DENV share ~60-80% sequence identity. The C protein of WNV shares about 60-65% sequence identity with that of JEV C protein. It is not surprising since WNV belongs to Japanese encephalitis serocomplex of flavivirus genus as defined on the basis of cross-neutralization tests using polyclonal sera (Calisher *et al.*, 1989; De Madrid & Porterfield, 1974; Poidinger *et al.*, 1996). The C protein of WNV shares about 25-35% sequence identity with that of DENV. Among the viruses analyzed by multiple sequence alignment, WNV and DENV C protein share the least sequence identity with that of YFV and TBEV. It is not unforeseen since several studies demonstrated that TBEV and YFV are phylogenetically distinct from that of Japanese encephalitis serocomplex and dengue viruses (Gaunt *et al.*, 2001; Kuno *et al.*, 1998).

Phylogenetic trees were also constructed from the aligned amino acid data with a neighbour-joining distance method using CLUSTALW2 and PHYLIP programs (Fig. 1.7). The topology of the tree indicated that all four serotypes of DENV form a cluster with close genetic relationship among the serotypes. As reported earlier, the C protein of KUN is closely associated with WNV(NY) although they form a cluster together with WNV(S) (Li *et al.*, 2006).

Although the amino acid sequences of flavivirus C proteins are poorly conserved, they are structurally and functionally similar. The C protein of flavivirus was shown to be an alpha-helical protein and it functions primarily to package the viral genome (Chambers *et al.*, 1990a; Dokland *et al.*, 2004; Jones *et al.*, 2003; Kofler *et al.*, 2002; Ma *et al.*, 2004).

Fig. 1.6: Multiple amino acid sequence alignment of flavivirus C proteins derived using CLUSTALW software (http://www.ebi.ac.uk/Tools/ clustalw2/index.html). The accession numbers of the viruses are as follows: WNV(NY)-AF260967 (West Nile, New York); KUN-D00246 (Kunjin) WNV(S)-AY688948 (West Nile Sarafend); JEV-U14163 (Japanese encephalitis); DENV1-FN429887 (Dengue type 1); DENV2-FN429895 (Dengue type 2); DENV3-DQ863638 (Dengue type 3); DENV4-M14931 (Dengue type 4); YFV-AF094612 (Yellow fever); TBE-L40361 (Tick borne encephalitis). Red colour: small, hydrophobic or aromatic amino acids. Blue colour: acidic amino acids. Pink colour: basic amino acids. Green colour: amino acids with hydroxyl, amine or amide group. "*": identical. ":": conserved substitutions (same colour group). ".": semi-conserved substitution.

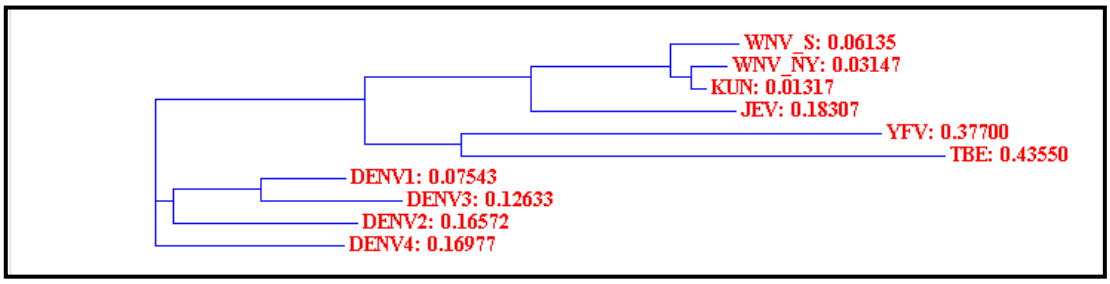

Fig. 1.7: Phylogram generated using CLUSTALW2 and PHYLIP programs.

Table 1.2: Percentage amino acid identities of flavivirus C proteins

Virus	WNV_NY	KUN	WNV_S	JEV	DENV1	DENV2	DENV3	DENV4	YFV	TBEV
WNV_NY		95	90	60	33	31	28	33	17	16
KUN			89	65	34	33	35	33	17	16
WNV_S				65	26	31	28	25	17	20
JEV					30	29	25	32	21	13
DENV1						67	79	66	19	11
DENV2							63	66	13	7
DENV3								57	18	9
DENV4									16	13
YFV										18

1.8.2. Structure of capsid protein

Cryo-electron microscopy (EM) reconstructions of WNV and DENV showed that E protein on the surface is well-ordered. However, EM reconstructions did not show any structure of the inner core. This could be due to the core being disordered or having different symmetry from the envelope (Kuhn *et al.*, 2002; Mukhopadhyay *et al.*, 2003; Zhang *et al.*, 2003b). Characterization of secondary structures in C proteins of DENV and YFV by nuclear magnetic resonance spectroscopy (NMR) revealed that flavivirus C protein is a symmetric dimer in solution. Further analysis of these C proteins with far-UV circular dichroism spectroscopic analyses indicated that flavivirus C protein is an alpha-helical protein (Jones *et al.*, 2003; Ma *et al.*, 2004). The crystal structure of KUNV C protein further confirmed that flavivirus C protein forms dimer and these dimers are organized into tetramers (Dokland *et al.*, 2004).

The secondary structure of DENV C protein is composed of four alpha helices (Fig. 1.8) namely helix I (α1) to helix IV (α4). Helix I (α1) included the amino acids from 26 to 31 of DENV C protein. This is followed by a 14-residue loop, helix II (α2, amino acids 45 to 55 of DENV C protein) and a short loop region (amino acids 56 to 62 of DENV C protein). Following this region are helix III (α3, amino acids 63 to 69 of DENV C protein) and a fourth short loop region (amino acids 70 to 73 of DENV C protein). The conserved internal hydrophobic domain includes helix II (α2), helix III (α3) and the intervening loop. The longest

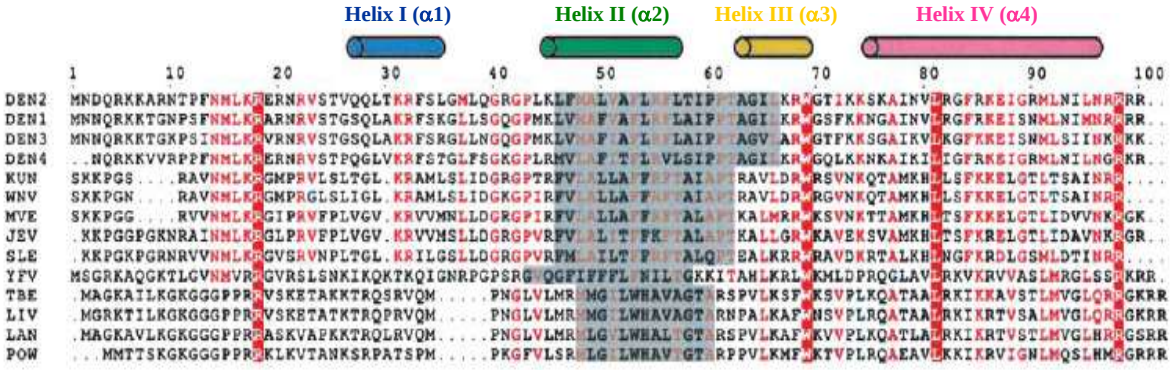

Fig. 1.8: Multiple sequence alignment of flavivirus C protein adapted from Ma and colleagues (2004). The four alpha-helices are shown at the top. The conserved hydrophobic regions are shaded grey. Residues with similarity greater than 50% are in red and the conserved residues are highlighted.

helix in flavivirus C protein is helix IV (α4) that occurs at the C terminus of the protein (amino acids 74 to 96 in case of DENV C protein). The N terminus of C protein (amino acids 1 to 21 of DENV C protein) appeared to be the least structured region of the protein and could be removed without disrupting the structural integrity of the protein (Jones *et al.*, 2003; Ma *et al.*, 2004).

1.8.3. Nucleocapsid formation

Nucleocapsid assembly in general involves the interactions between C-C proteins and C protein-viral RNA. The viral genome is generally protected by multiple copies of C protein and the surrounding lipid envelope. The multiple copies of C proteins, encoded by a relatively short nucleic acid sequence, can encapsidate a relatively large volume of nucleic acid. This strategy reduces the burden of encoding a large protein, but generates a new problem of assembling multimers, in a biologically realistic time frame (Zlotnick, 2005). Moreover, studies suggested that C-C self-association and the eventual formation of a nucleocapsid is a spontaneous process in the presence of nucleic acid (Kiermayr *et al.*, 2004; Kunkel *et al.*, 2001). It is assumed that all the information required for assembly is built into the tertiary structure of C protein.

1.8.3.1. Dimerization of flavivirus capsid protein

The understanding of C protein interactions with itself would provide important data on how the nucleocapsid is organized in flavivirus during assembly. Several studies demonstrated that flavivirus C protein can form homodimers

(Bhuvanakantham & Ng, 2005; Kiermayr *et al.*, 2004; Wang *et al.*, 2004). Self-association of flavivirus C protein was mediated by the first three helices of C protein (Ma *et al.*, 2004). Tryptophan at the amino acid residue 69 in the central hydrophobic region was shown to be a critical determinant in stabilizing the oligomerization of C protein (Bhuvanakantham & Ng, 2005). Studies suggested that dimeric form of C protein is the basic building block of flavivirus nucleocapsid (Kiermayr *et al.*, 2004; Kunkel *et al.*, 2001; Patkar *et al.*, 2007). These observations were supported by structural analysis of KUNV and DENV C protein (Jones *et al.*, 2003; Kuhn *et al.*, 2002; Ma *et al.*, 2004).

1.8.3.2. Flavivirus capsid protein - RNA interaction

The RNA binding properties of flavivirus C protein was first demonstrated with KUNV. The positively-charged clusters in amino- and carboxy-termini of C protein were involved in the recruitment of viral RNA to form nucleocapsid (Khromykh & Westaway, 1996). This was supported by the model proposed based on structural studies (Dokland *et al.*, 2004; Ma *et al.*, 2004). A conformational switch in the disordered N-terminal region caused the order-disorder transition in helix I (α1). As a result, the amino- and carboxy-termini of C protein were brought together. This is significant since the RNA-binding region on C protein was found on both amino- and carboxy-termini (Khromykh & Westaway, 1996). This property can be extended to other flavivirus C proteins since they all have positively-charged clusters. Recently, it was shown that WNV

C protein needs to be dephosphorylated for efficient RNA binding (Cheong & Ng, 2010).

However, the RNA encapsidation signal was not clearly defined although 5' UTR and 3' UTR of KUNV RNA was demonstrated to bind KUNV C protein (Khromykh & Westaway, 1996). Analysis of 5' UTR and 3' UTR of flavivirus genome revealed complex secondary structures such as stem loops and bulges. These structures undergo cyclization whereby the conserved regions on 5'UTR and 3'UTR are paired (Khromykh *et al.*, 2001).

1.8.4. Nuclear phase of flavivirus capsid protein

The C proteins of arthropod-borne flaviviruses such as WNV, DENV, KUNV and JEV were localized in the cytoplasm and nuclei (Bulich & Aaskov, 1992; Chang *et al.*, 2001; Makino *et al.*, 1989; Mori *et al.*, 2005; Oh & Song, 2006; Tadano *et al.*, 1989; Westaway *et al.*, 1997). However, the exact functions of flavivirus C protein in nucleus are unclear since positive-stranded RNA viruses are thought to utilize cellular components in the cytoplasm for replication. Nuclear localization of C protein for positive-stranded RNA viruses is not unusual though. The C protein of coronavirus, another positive-stranded RNA virus, was also shown to localize in the nucleus (Chen *et al.*, 2002; Hiscox *et al.*, 2001; Timani *et al.*, 2005; Wurm *et al.*, 2001). Nuclear localization of flavivirus C protein was shown to be essential for efficient virus replication (Bhuvanakantham *et al.*, 2009; Mori *et al.*, 2005).

1.8.5. Interactions between virus capsid protein and host proteins

Several studies showed that C proteins of RNA viruses functioned as important mediators of virus-host interactions besides serving as building blocks of virions (Beatch & Hobman, 2000; Hunt *et al.*, 2007; Iinuma *et al.*, 1971; Luo *et al.*, 2004a; Luo *et al.*, 2004b; Moriishi *et al.*, 2003; Oh *et al.*, 2006; Ohkawa *et al.*, 2004; Plyusnina & Plyusnin, 2005; Tsukiyama-Kohara *et al.*, 2004; Tyagi *et al.*, 2005; Yang *et al.*, 2008). This is not surprising since it will be beneficial for the viruses to encode multifunctional proteins. Since C protein of several RNA viruses were localized in both cytoplasm and nucleus, C proteins were exposed to a wide variety of host cell proteins in the cytoplasm and nucleus during the replication cycle.

Although C protein is the first viral protein to be synthesized in infected cells, they need not to be incorporated into virions immediately after synthesis. This suggested that there would be a large pool of C protein present within infected cells that could serve other nonstructural functions (Iinuma *et al.*, 1971; Plyusnina & Plyusnin, 2005). For the sake of brevity, this literature review will be limited to C protein of arthropod-borne flaviviruses although C proteins of HCV and coronavirus are referred to on occasions.

1.8.5.1. Interactions between flavivirus capsid protein and importins

Nuclear translocation is generally mediated by a family of transporters or cytosolic receptors known as importins. Proteins containing nuclear localization

signal (NLS) motif bind to importin-α/β to mediate nuclear translocation of the protein (Goldfarb *et al.*, 2004). The mechanism of nuclear translocation necessitates the binding of importin-α to the NLS motif. Importin-α, then acts as an adaptor for the binding of importin-β. Subsequently, importin-β docks the entire complex of NLS-bearing protein and importin-α/β at the nuclear pore complex for nuclear translocation (Gorlich *et al.*, 1996). The C protein of HCV interacted with importins to facilitate its nuclear entry (Suzuki *et al.*, 2005). The C proteins of arthropod-borne flaviviruses were also reported to utilize importins for their nuclear translocation (Bhuvanakantham *et al.*, 2009). Protein kinase C-mediated phosphorylation of arthropod-borne flaviviruses C protein was shown to be essential to mediate efficient nuclear localization (Bhuvanakantham *et al.*, 2010).

1.8.5.2. Interactions between flavivirus capsid protein and nucleolar proteins

Several studies showed that JEV C protein interacted with nucleolar protein B23 and heterogenous nuclear ribonucleoprotein (Mori *et al.*, 2005; Tsuda *et al.*, 2006). It was also shown that nuclear phase of flavivirus C protein was important for efficient viral replication and disruption of nuclear localization was shown to be detrimental for viral replication (Bhuvanakantham *et al.*, 2009; Mori *et al.*, 2005). However, the exact mechanism by which C protein in the nucleus exerts this effect remains to be unveiled. It is likely that being positively charged, C protein might interact with rRNA after entering the nucleolus, thereby regulating ribosome biogenesis necessary for cell division and gene transcription (Gerbi *et*

al., 2003; Hernandez-Verdun & Roussel, 2003; Hernandez-Verdun *et al.*, 2002; Leung *et al.*, 2003; Rubbi & Milner, 2003). This could alter the host cell environment to be more favourable to virus replication/production.

1.8.5.3. Interactions between flavivirus capsid protein and cell cycle-associated proteins

Several studies suggested that flavivirus infection caused cell cycle arrest at various phases for efficient infection and virus production (Helt & Harris, 2005; Oh *et al.*, 2006; Phoolcharoen & Smith, 2004; Su *et al.*, 2001). Oh and colleagues (2006) reported that WNV C protein was able to mediate cell cycle arrest at G2 phase. It is not surprising since the C protein of coronavirus, another positive-stranded RNA virus, was also shown to involve in cell cycle arrest during infection through its interaction with cyclin/cyclin-dependent kinase complex (Li *et al.*, 2007; Surjit *et al.*, 2006). If cell cycle arrest is a virus-induced phenomenon to favour the virus, host should counteract to prevent virus infection. It was shown that C protein-induced cell cycle arrest was prevented when Jab1 protein was over-expressed (Oh & Song, 2006).

1.8.5.4. Interactions between flavivirus capsid protein and apoptosis-related proteins

Apoptosis is a well renowned phenomenon during flavivirus infection (Avirutnan *et al.*, 1998; Catteau *et al.*, 2004; Chu & Ng, 2003; Courageot *et al.*, 2003;

Despres *et al.*, 1996; Diniz *et al.*, 2006; Espina *et al.*, 2003; Jan *et al.*, 2000; Liao *et al.*, 1997; Marianneau *et al.*, 1998; Mongkolsapaya *et al.*, 2003; Myint *et al.*, 2006; Parquet *et al.*, 2001; Prikhod'ko *et al.*, 2002; Samuel *et al.*, 2007; Shrestha *et al.*, 2003; Su *et al.*, 2001; Thongtan *et al.*, 2004). Flaviviral proteins C, prM and NS2B-NS3 were shown to induce apoptosis during flavivirus infection (Catteau *et al.*, 2003a; Catteau *et al.*, 2003b; Prikhod'ko *et al.*, 2002; Ramanathan *et al.*, 2006; Shafee & AbuBakar, 2003; Yang *et al.*, 2002). The C protein of WNV has been implicated in virus-mediated apoptosis *via* the induction of mitochondrial dysfunction and the activation of caspases-9 and -3. It was also capable of inducing apoptosis-mediated inflammation in mouse brain (Yang *et al.*, 2002).

Yang and colleagues (2008) showed that WNV C protein interacted with HDM2 protein and sequestered it into the nucleolus. HDM2 protein participated in negative feedback loop of p53 to inhibit abnormal p53 accumulation under normal conditions (Haupt *et al.*, 1997). Through direct interaction with HDM2, C protein interfered with HDM2-p53 complex formation. This in turn negatively affected p53 stabilization/Bax activation and led to apoptosis (Yang *et al.*, 2008). Dengue virus C protein interacted with death domain-associated protein and induced Fas-mediated apoptosis (Limjindaporn *et al.*, 2007; Netsawang *et al.*, 2010). It was also shown that nuclear localization of flavivirus C protein is important to induce apoptosis (Netsawang *et al.*, 2010; Oh & Song, 2006; Yang *et al.*, 2008).

Certain host proteins have been shown to protect the cells from C-induced cytotoxic effects. Heat shock protein 70 inhibited the nuclear localization of C protein by directly interacting with WNV C protein and protect the host cells against the cytotoxic effects of C protein (Oh & Song, 2006). Another host protein, Jab1 also protected the host cells from C-induced cytotoxic effects by accelerating the nuclear export of C protein and by degrading C protein (Oh *et al.*, 2006).

1.9. PROTEASOME DEGRADATION PATHWAY

Several studies have shown the involvement of proteasome degradation pathway during virus infection (Ashour *et al.*, 2009; Iwatani *et al.*, 2009; Jung *et al.*, 2007; Ko *et al.*; Loureiro & Ploegh, 2006; Mangeat *et al.*, 2009; Marin *et al.*, 2003; Oh *et al.*, 2006; Sato *et al.*, 2009). The majority of virus and host proteins were degraded by 26S proteasome (Rock *et al.*, 1994). The 26S proteasome is a 2.5MDa multisubunit complex that catalyzes ATP-dependent proteolysis of cellular or viral proteins. It is found both in nucleus and cytosol of all eukaryotic cells and is comprised of a single 20S core particle and 19S regulatory particles (Adams, 2002; Baumeister *et al.*, 1998; Pickart & Cohen, 2004; Voges *et al.*, 1999).

The 20S particle is a hollow cylinder composed of four stacked heptameric rings. They are composed of α and β subunits. The α subunits are structural in nature, whereas β subunits are catalytic. The outer two rings in the stack contains seven α

subunits each and serve as docking domains for the regulatory particles. The alpha subunits form a gate to block the unregulated access of substrates to the interior cavity. The inner two rings contain seven β subunits each and contain 3 different proteolytic sites which differ in their specificity (Groll *et al.*, 1997; Nandi *et al.*, 2006). Three major proteolytic activities namely chymotrypsin-like, trypsin-like and caspase-like are contained within 20S core.

The chymotrypsin-like site cleaves peptide bonds after hydrophobic residues, trypsin-like site cuts after basic residues, while caspase-like site cuts preferentially after aspartates (Heinemeyer *et al.*, 1997). All these active sites cleave peptide bonds via a nucleophilic attack on the hydroxyl group of the N-terminal threonine of the catalytic β-subunit (Goldberg, 2000; Heinemeyer *et al.*, 1997; Lowe *et al.*, 1995; Stock *et al.*, 1995). The active subunits are generated from larger precursors that contain a propeptide at their N-terminus, which block the active sites until removed autocatalytically during assembly of 20S particle (Schmidt *et al.*, 1997; Schmidtke *et al.*, 1997). These chymotrypsin-like, trypsin-like and caspase-like activities are responsible for much of the protein degradation required to maintain cellular homeostasis including degradation of critical cell-cycle proteins, tumor suppressors, transcription factors, inhibitory proteins, damaged cellular proteins and viral proteins (Adams, 2002; Glickman & Ciechanover, 2002; Glickman & Maytal, 2002; Heinemeyer *et al.*, 1997; Ko *et al.*; Oh *et al.*, 2006; Rajkumar *et al.*, 2005).

Proteins destined to be degraded by the proteasome are first selectively targeted by the addition of a series of covalently attached ubiquitin molecules (Rajkumar *et al.*, 2005). The 19S regulatory particles are then able to bind and remove the ubiquitin chain. This helps to mediate unfolding and allow the protein to enter into the narrow core of 20S particle, where it is degraded to yield peptides ranging from 3-25 amino acids in length (Nussbaum *et al.*, 1998).

1.10. VACCINE DEVELOPMENT STRATEGY

Although there are licensed vaccines for JEV and YFV, these viruses still claim thousands of life across their vast endemic areas (Gould & Solomon, 2008; Gubler *et al.*, 2007; Oya & Kurane, 2007). There are no approved vaccines available for WNV and DENV. The development of new vaccines or anti-flaviviral drugs is thus of vital importance at this moment.

The capsid gene could be targeted for the development of single-cycle infectious flavivirus mutants. The utility of this approach was first demonstrated by Kofler and colleagues (2004a; 2002; 2004b; 2003). Although large deletions in the internal hydrophobic domain of TBEV C protein impaired the formation of infectious virus particles, it was still capable of secreting significant amounts of sub-viral particles. Impact of removal of entire hydrophobic domain could also be limited by mutating the remaining amino acids to increase the overall hydrophobicity (Kiermayr *et al.*, 2004; Kofler *et al.*, 2004a; Kofler *et al.*, 2002; 2004b; Kofler *et al.*, 2003). Intracranial inoculation of TBEV RNAs containing

these deletions in C gene failed to produce any infectious progeny or disease but significant levels of protective immune responses were elicited in adult mice (Aberle *et al.,* 2005; Kofler *et al.,* 2004a; Kofler *et al.,* 2004b).

Similarly, attenuated DENV carrying deletion of internal stretch of hydrophobic residues were capable of inducing high levels of antibody (Zhu *et al.,* 2007). RepliVAX containing C gene-deleted genome of YFV or WNV were shown to be attenuated in mice (Widman *et al.,* 2008). All these observations demonstrated the potential benefits of this deletion strategy to generate attenuated vaccines against flavivirus.

DNA vaccines encoding C protein of WNV elicited significant immune responses (Forgues *et al.,* 2001; Lazo *et al.,* 2007). The C protein of DENV showed a protective response against infection which was independent of antibody responses. This could eliminate the potential risk of antibody-dependant enhancement associated with the current vaccines under trial (Lazo *et al.,* 2007). The use of chimeric E protein-C protein was also shown to be effective in mice by stimulating both arms of the acquired immune system (Gil *et al.,* 2009; Valdes *et al.,* 2009). Capsid-targeted inactivation of flavivirus was another important anti-viral strategy (Qin & Qin, 2006). Despite the continuous research efforts on vaccine development, the process is faced with difficulties.

1.11. NEED FOR ANTI-VIRALS

Although the development of vaccines offer promises, it is essential to work towards the generation of anti-virals as an alternative approach since arthropod-borne flaviviruses present a growing threat to public health worldwide. Although these viruses account for few hundred million human infections annually, there are no effective therapeutic options currently available. Current treatment measures are largely supportive and involve the use of anti-viral drugs such as ribavirin. Early recognition and prompt supportive treatment can help us to lower the risk of developing severe disease. The most effective protective measures at this moment include vector control program and personal protective measures.

In order to design an appropriate anti-viral drug, it is essential to understand virus morphogenesis and the molecular basis of pathogenesis. The interaction between the virus and host plays an important role during viral replication, virulence and pathogenicity. However, very little has been done in the context of flavivirus-host protein interactions. As far as the C protein of arthropod-borne flavivirus is concerned, the dissected host interacting proteins to date were closely associated with the process of apoptosis (Limjindaporn *et al.*, 2007; Netsawang *et al.*, 2010; Oh & Song, 2006; Yang *et al.*, 2008). Targeting these host proteins might help to develop anti-virals against flavivirus.

1.12. OBJECTIVES

Virus infection and the host cell responses involve a complex interaction between cellular and viral networks. Many viruses attempt to subvert host cell processes to increase the efficiency of virus infection and likewise the cell employs a number of responses to generate an anti-viral state. The interactions between arthropod-borne flavivirus C protein and host proteins are complex and poorly studied. Understanding how cellular proteins interact with viral RNA or viral proteins, as well as the roles of such interactions during virus infection will provide insights for designing novel anti-viral agents. This study aims to characterize the role of flavivirus C protein in contributing to viral pathogenesis.

The specific objectives of this study are as follows:

1) Identify novel host proteins that interact with flavivirus C protein.
2) Examine the effect of identified host proteins on flavivirus life cycle.
3) Determine how flavivirus C protein utilizes/evades the influence of such host proteins

CHAPTER 2

MATERIALS AND METHODS

2.0. MATERIALS AND METHODS

2.1. CELL CULTURE TECHNIQUES

All solutions and media for cell culture were made with sterile ultrapure water (Milipore, USA). All cell culture and media preparation work was performed under aseptic conditions in a Class II Type A2 Bio-safety Cabinet (ESCO Pte Ltd, Singapore). The cells used in this study were grown in 25/75 cm^2 tissue culture flasks (Iwaki Glass, Japan) and 24-/96-well tissue culture plates (Greiner Bio-One, USA). Cells were either cultured in a humidified 37°C incubator with 5% carbon dioxide (CO_2) or a dry incubator (Thermo Electron Corporation, USA). Only the mosquito cell line C6/36 was grown in the 28°C dry incubator.

2.1.1. Cell lines

The cell lines used in this study are listed in Table 2.1. The types of media, passage numbers used for experiments in this project and the origin of cell lines are also included. All cell lines used are adherent cell types.

2.1.2. Media and reagents for cell culture

All cell culture media were supplemented with foetal bovine serum [(FBS), (PAA Laboratories GmbH, Austria)] and their formulations can be found in Appendix 1A to 1D for various cell lines. The heat-inactivated FBS (Appendix 1E) was used for C6/36 and HEK293 cells. The media pH was adjusted to approximately 7.3 with solutions of 1 M hydrochloric acid and 1 M sodium hydroxide (Appendix 1F and 1G).

Table 2.1: Cell lines used and related information

Cell Line	Cell Media	Cell Passage level	Origin
Human Embryonic Kidney cells (HEK293)	DMEM	10-20	American Type Culture Collection, USA
Human Embryonic Kidney cells FT (293FT)	DMEM	10-21	Invitrogen, USA
Mosquito cells derived from *Aedes albopictus* (C6/36)	L-15	50-70	Kind gift from Emeritus Professor Edwin Westaway, Australia
Baby Hamster Kidney Cells 21, clone 13 (BHK)	RPMI	50-60	American Type Culture Collection, USA
hSec3p293OE cells	DMEM supplemented with various components (Appendix 7C)	3-14	Generated in this study
hSec3p293KD cells	DMEM supplemented with various components (Appendix 7C)	3-14	Generated in this study

2.1.3. Cultivation and propagation of cell lines

Flasks of cells were sub-cultured from confluent 75 cm^2 flask monolayer at a ratio of 1:5. The growth medium (Appendix 1A to 1D) was discarded and the monolayer was rinsed with 5 ml of phosphate buffered saline (PBS - Appendix 1H). This was followed by incubation with 2 ml of trypsin (Appendix 1I). The flask was then incubated at 37°C before the cells were dislodged by gentle tapping. The growth media was added to the cell suspension to neutralize the activity of trypsin (Appendix 1I) and the suspended cells were then aliquoted into new 75 cm^2 culture flasks. The cells were incubated at 28°C for C6/36 cells or 37°C for all other cell types.

2.1.4. Cell counting using haemocytometer

A haemocytometer was used for the quantification of cell number in a tissue culture flask or plate. The cell monolayer was first rinsed with PBS (Appendix 1H) following the removal of the growth medium. The cells were then dislodged using trypsin (Appendix 1I). A sample of the cells (neat or undiluted) was mixed at 1:1 ratio with trypan blue (Sigma, USA) to allow differentiation of living and dead cells. The mixture of cells with trypan blue was aliquoted to the counting chamber of the haemocytometer by capillary action. The cells were counted in the four quadrants and averaged out to determine the number of cells in one quadrant. To ensure accuracy, the cells from a sample were counted thrice and averaged out.

2.1.5. Cultivation of cells in tissue culture plates

A confluent cell monolayer of BHK, HEK293 or 293FT cells in a 75 cm^2 tissue culture flask was used to seed four 6-well, 24-well or 96-well plates (Greiner Bio-One, USA). The cell monolayer was treated as previously described (Section 2.1.3) to produce single cell suspension. The cell suspension was then made up to a final volume of 100 ml using appropriate cell culture growth medium. Aliquots of 2 ml, 1 ml or 200 µl of cell suspension were then transferred into each of the 6 wells, 24 wells or 96 wells, respectively. Poly-L-lysine coating (Appendix 1J) was used prior to seeding of HEK293 cells. The plates were then incubated at 37°C in a humidified incubator with 5% CO_2 (Thermo Electron Corporation, USA). The monolayers were confluent in 48 h and ready for use.

2.1.6. Cultivation of cells on coverslips

Individual glass cover slips were aseptically placed in 24-well tissue culture plate. A confluent monolayer of cells from a 75 cm^2 tissue culture flask was used to seed the wells of 24-well plate (Section 2.1.5). Poly-L-lysine coating (Appendix 1J) was used prior to seeding of HEK293 cells. The plates were incubated at 37°C with 5% CO_2 until they were about 80-90% confluent.

2.2. INFECTION OF CELLS

2.2.1. Viruses

The viruses used in this study were WNV (strains Sarafend [WNV(S)], Wengler [WNV(W)] and Kunjin (KUNV)] and DENV serotype 2 (New Guinea C). These

viruses were the kind gifts from Emeritus Professor Edwin Westaway, Australia. The stock viruses were propagated in C6/36 cells for this study.

2.2.2. Infection of cell monolayer for virus propagation

Virus pools were prepared by infecting confluent monolayer of cells in 75 cm^2 tissue culture flask. The cell culture supernatant was discarded and the monolayer was rinsed with 5 ml of PBS (Appendix 1H). About 1 ml of virus suspension was made up to 1.5 ml with virus diluent (Appendix 2A) and used to infect cells in 75 cm^2 at multiplicity of infection (MOI) of 1 or 10. The flask was incubated at 37°C for 1 h and rocked every 15 min to ensure even infection. After 1 h, unabsorbed virus was washed off with 5 ml of maintenance medium (Appendix 2B and 2C) and 10 ml of the same medium was then added after the wash. The infected cells were incubated at 37°C in a humidified incubator with 5% CO_2 (Thermo Electron Corporation, USA) until the appropriate harvesting time. Mock-infected controls used in this study were prepared as mentioned above except that a similar amount of virus diluent (Appendix 2A) was used instead of virus.

2.2.3. Preparation of virus pool

Infection was carried out as described in Section 2.2.2. The virus was harvested when cytopathic effects were pronounced at appropriate timings post infection (p.i.) [18 h - WNV(S); 24 h - WNV(W) and KUNV; 48 h - DENV). To obtain extracellular virus, infected cell culture supernatant was removed from the flask and spun at 1000 x g for 10 min (Sigma, USA) to remove cellular debris.

Intracellluar virus was obtained by harvesting the monolayer of infected cells. The cells were detached from the flask using trypsin (Appendix 1I). The trypsin activity was neutralized with an equal amount of maintenance medium after the cells have detached. The resulting cell suspension was pelleted at 800 x g for 10 min (Sigma. USA) and followed by 3 cycles of freeze-thaw action. The cell debris were removed by spinning (Sigma, USA) at 3000 x g for 15 min. Approximately 500 µl of infected supernatant (extracellular virus) or clarified cell lysate (intracellular virus) was aliquoted into 1 ml sterile cryovials (Nalge Nunc International, Denmark) and immediately snap frozen in -80°C liquid ethanol. The frozen virus stocks were stored at -80°C until further use.

2.2.4. Plaque assay

BHK cells were seeded onto 24-well plates as described in Section 2.1.5. Ten-fold serial dilutions of the virus sample were prepared in virus diluents (Appendix 2A) up to 10^{-8}. Aliquots of 100 µl from each dilution were transferred in triplicates onto confluent cell monolayers in the wells. The plates were incubated at 37°C with 5% CO_2 and rocked every 15 min to ensure even distribution of virus inoculum. The virus inoculum was then removed following one hour incubation and cell monolayers were washed once with PBS (Appendix 1H). One ml of overlay medium (Appendix 2D) was pipetted into each well. The trays were incubated at 37°C for 2 days before the overlay medium was removed for staining. The plaques were visualized by staining the monolayer with 0.5% crystal violet in a 25% formaldehyde solution (Appendix 2E) for at least 2 h at room

temperature (RT) on orbital shaker (Labnet Intl. Inc., USA). The crystal violet solution was removed for proper hazardous chemical disposal and the plate was washed under a running tap to remove residual dye. Plaques were counted and the following equation was used to calculate the number of plaque forming units (PFU) per ml of supernatant: (Average number of plaques from triplicates) x (dilution factor) x 10.

2.2.5. Virus growth kinetics

Appropriate numbers of HEK293, hSec3p293OE and hSec3p293KD cells ($5X10^5$) were infected with WNV/DENV (MOI: 1) or transfected (5-20 μg) with WNV/DENV RNA *in vitro* transcribed from Xbal-linearized full length WNV (Li et al., 2005) or DENV (kind gift from Dr. Andrew Davidson) infectious clones as described by Li and group (2006). The full-length infectious clone of WNV was generated by Li and colleagues (2005) and DENV infectious clone was a generous gift from Dr. Andrew Davidson, Bristol University, United Kingdom. In another experiment, HEK293 cells were first transfected with V5-hSec3pSH2 plasmid followed by infection with WNV/DENV or transfection with RNA *in vitro* transcribed from full length WNV/DENV infectious clone. The cell culture supernatant was collected at the indicated time points for plaque assay.

2.3. MOLECULAR TECHNIQUES

2.3.1. Extraction of viral RNA

Viral RNA extraction was carried out using QIAmp® Viral RNA extraction kit

(Qiagen, USA) following the manufacturer's protocol. Briefly, about 200 µl of virus supernatant was added to AVL buffer and then transferred to the QIAquick spin column. Following centrifugation (Sigma, USA) and subsequent washes, viral RNA was eluted with elution buffer. Quantity and purification of extracted nucleic acids was determined using Nanodrop spectrophotometer (Thermo Scientific, USA). The extracted viral RNA was stored at -80°C until further use.

2.3.2. Complementary DNA (cDNA) synthesis

First strand cDNA was synthesized from viral RNA samples isolated as described in Section 2.3.1. About 500-750 ng of viral RNA was mixed with 1 µl of 10 mM C protein specific primer or random hexamer and 1 µl of 1 mM deoxynucleotide mix [(dNTP) (Promega, USA)]. The mixture was then heated to 65°C for 5 min and placed on ice for 1 min. Subsequently, 4 µl of 5x first strand synthesis buffer (Invitrogen, USA), 2 µl of 0.1 M dithiothreitol (Invitrogen, USA), 1 µl of RNAsin (Promega, USA) and 1 µl of Superscript® III Reverse Transcriptase (Invitrogen, USA) was added to the mixture. The mixture was then heated to 42°C for 30 min and 72°C for 15 min. The resulting cDNA was stored at -20°C until further use.

2.3.3. Polymerase Chain Reaction (PCR)

Polymerase chain reaction was used to amplify specific gene sequences using the appropriate primers. The reaction consisted of a 5 µl of 10x reaction buffer (Fermentas, USA), 1 µl of 10 mM dNTP (Promega, USA), 1 µl each of 10 mM of forward and reverse gene specific primer, 1 µl of Taq polymerase (Fermentas,

USA) and an appropriate amount of template. The reaction was topped up to 50 μl with ultrapure water (Milipore, USA). The primers used in this study were shown in Appendix 3A. All primers were synthesized by Proligo Singapore Pte Ltd. The primers are partially purified through desalting procedures performed by the manufacturers. The mixture was amplified in a PCR thermocycler (Bio-Rad, USA). The PCR mixture was first subjected to initial denaturation step in a thermocycler at 95°C for 4 min. this was followed by 28 cycles of denaturation at 95°C for 2 min, annealing at 55°C for 30 sec and extension at 72°C for 1 min to 10 min. Final extension at 72°C was carried out for 3 min.

2.3.4. DNA purification from PCR reaction and agarose gel electrophoresis

The PCR amplified DNA was purified using QIAquick PCR purification kit (Qiagen, USA) following manufacturer's instructions to remove the buffer and enzymes in the solution. Briefly, the PCR product was mixed with the binding buffer and added to the QIAquick spin column. Following centrifugation (Sigma, USA) and subsequent washes, the PCR amplicons were eluted with elution buffer. The resulting amplicons were analyzed using agarose gel electrophoresis [Appendix 3B(i-iii)]. An appropriate amount of DNA sample was mixed with 10x gel loading buffer [Appendix 3B(iv)] before loading into the well. Approximately 5 μl of 1000 bp or 100 bp DNA markers (Promega, USA) was added in another well to indicate the relative size of the DNA sample. The sample was electrophorized at 120 V for 40 min. The DNA bands were then visualized using

UV transilluminator (Vilber Lourmat, UK) and the gel images were captured using ChemiGenius2 software (Syngene, UK).

2.3.5. Restriction endonuclease (RE) digestion

The purified PCR products were digested with 1 μl of respective restriction enzymes (Appendix 3A, RE sequences were underlined in primer sequence) supplemented with 5 μl of 10x reaction buffer (Promega, USA). The mixture was incubated at 37°C for 4 h. Similarly, 1 μg of various vectors (Appendix 3A) was digested with appropriate restriction enzymes.

2.3.6. Ligation and transformation for plasmid amplification

The RE-digested PCR product and the vector were mixed at the molar ratio of 1:5 together with 1 μl of T4 DNA ligase and 1 μl of 10x ligation buffer (Promega, USA). The mixture was incubated at 4°C overnight. Two microlitres of ligation mixture was added into 100 μl of thawed DH5α competent cells (Invitrogen, USA) and incubated on ice for 20 min. This was followed by heat shock at 42°C for 2 min and incubation at 30°C for 1.5 h. After the recovery of cells, the culture was spun (Sigma, USA) at 4000 x g for 1 min and the supernatant was discarded. The cells were resuspended in 100 μl of LB broth [Appendix 3C(i)] and plated onto agar plate [Appendix 3C(ii)] containing 100 μg/ml of ampicillin or 50 μg/ml of kanamycin (Sigma, USA). The plate was then incubated at 30°C overnight. All bacterial plates were stored at 4°C for future use.

2.3.7. Colony PCR

Several colonies from Section 2.3.6 were picked for PCR colony screening. This method screened for the presence of inserts in transformed bacteria. The bacterial colonies were picked using pipette tips and tapped gently onto a new agar plate containing either ampicillin or kanamycin [Appendix 3C(ii)] before dislodging the remaining cells into a PCR reaction as described in Section 2.3.3 by pipetting up and down. The resulting DNA product was analyzed with gel electrophoresis (Section 2.3.4). Positive colonies were picked from the new agar plates for plasmid extraction (Section 2.3.8).

2.3.8. Plasmid extraction

At least five colonies were selected and inoculated for plasmid extraction. Colonies were picked and inoculated into 2 ml of LB broth containing ampicillin or kanamycin [Appendix 3C(iii)]. The inoculated cultures were allowed to shake for 18 h at 30°C (Sartorius, Germany). This seed culture was diluted and used for plasmid extraction using QIAprep Miniprep or Maxiprep Kits (Qiagen, USA). The resulting plasmids were sequenced (Section 2.3.9) to ensure the correct reading frame.

2.3.9. Sequencing

Approximately 500 ng of plasmid DNA was added to 4 μl of Big-Dye Terminator v3.1 (Applied Biosystems, USA) and 1 μl of the appropriate primer as listed in Appendix 3D. The mixture was topped up to 10 μl with deionised water and

placed in a thermocycler (Bio-Rad, USA). The reaction protocol was as follows: 95°C for 4 min, 30 cycles of 95°C for 30 sec, 55°C for 30 sec, 72°C for 1 min and a final extension for 5 min at 72°C. The product was then purified via ethanol precipitation. Ethanol precipitation was performed by adding 3 M sodium acetate (Promega, USA) and 95% ethanol (Sigma, USA). The resulting mixture was transferred to a 1.5 ml eppendorf tube and incubated on ice for 20 min. The precipitated DNA was then pelleted down at 16000 x g for 30 min at 4°C (Sigma, USA). The supernatant was removed carefully and 500 µl of 70% ethanol [(Appendix 3E(ii)] was added. The precipitate was pelleted down again with similar conditions and the ethanol was discarded. The DNA pellet in the tube was sent to the Microbiology Department sequencing laboratory for electrophoresis (ABI 310 sequencer, Perkin Elmer, USA). Sequences were analyzed using Basic Local Alignment Search Tool (www.ncbi.nlm.nih.gov/blast).

2.3.10. Site-directed mutagenesis

Site-directed mutagenesis was performed using QuickChange Lightning kit (Stratagene, USA). The primer design and reaction assembly were performed according to the manufacturer's recommendation. The primer sequences and the templates used in the mutagenesis study were shown in Appendix 3F. Briefly, the template plasmid was mixed with the appropriate primers, dNTPs and *pfu* polymerase and PCR reaction was carried out. The parental plasmid was then digested with Dpn I enzyme. The resulting mutated plasmids were transformed into XL10 Gold competent cells (Stratagene, USA).

2.3.11. Mutagenesis of the infectious clones of WNV and DENV

Mutations were first introduced on the 1.3 kb carrier plasmid of WNV and DENV as described in Section 2.3.10. The 1.3 kb carrier plasmid contains 5'UTR, C, prM and partial envelope sequences of flavivirus in pBR322 vector. After confirming the presence of introduced mutations by sequencing (Section 2.3.9), the remaining purified plasmids were subjected to RE digestion with 1 µl of *BsiW I* and *Mlu I* (New England Biolabs, USA) each at 37°C for 2 h. The reaction was subjected to agarose gel electrophoresis and the 1.3 kb fragment carrying the mutations was excised from the gel and purified using Gel extraction and purification kits (Qiagen, USA). The full-length infectious clones of WNV/DENV were also RE-digested and subjected to electrophoresis in the same manner and the 11 kb fragment was purified from the gel. Approximately 7.5 µl of the 1.3 kb fragment and 0.5 µl of 11 kb DNA fragments were ligated using 1 µl T4 DNA ligase and transformed into DH5α cells. Positive clones were then sequenced and propagated.

2.3.12. *In vitro* synthesis of infectious RNA

About 5 µg of full-length/mutant infectious clones of WNV and DENV were linearized with *Xba I* (Promega, USA). The linearized DNA was purified by phenol-chloroform extraction and ethanol precipitation and reconstituted in 15 µl of RNase-free water [(Appendix 3E(i)]. The linearized DNA was used for *in vitro* synthesis of infectious RNA using T7 Ribomax^{TM} large scale RNA production system and cap analogue according to the manufacturer's protocol (Promega,

USA). Briefly, the linearized DNA was mixed with T7 reaction components and incubated at 37^{o}C for 4 h. The resulting RNA was purified using phenol:chloroform:isoamyl alcohol (25:24:1, v/v, Invitrogen) and precipitated with isopropanol on ice. The precipitated RNA was then pelleted at 16000 x g for 30 min (Sigma, USA) and washed with 70% ethanol in RNase-free water [Appendix 3E(ii)]. The RNA was resuspended in RNase-free water [Appendix 3E(i)] and quantitated with Nanodrop (Thermo Scientific, USA).

2.3.13. Transfection

HEK293 cells (5X10^{5}) were transfected (single or co-transfection) with various recombinant plasmids or *in vitro* transcribed RNAs from the infectious clones of WNV/DENV using Lipofectamine2000 (Invitrogen, USA). The amount of plasmid DNA, Lipofectamine2000 and Opti-Mem media (Invitrogen, USA) used for 6-well plate, 24-well plate and 96-well plate are listed in Table 2.2.

The appropriate amount of DNA and Lipofectamine2000 (Invitrogen, USA) were diluted separately with an appropriate amount of Opti-Mem media (Invitrogen, USA) and incubated at RT for 5 min. Both the diluted DNA and Lipofectamine2000 solutions were mixed and incubated at RT for 30 min. After incubation, the DNA-liposome complexes were added to the cell monlayers in the culture vessel. The cells were incubated at 37°C for 5 h. The supernatant was removed after 5 h and fresh culture medium containing 2% FBS was added to the cells.

Table 2.2: The amount of DNA and Lipofectamine2000 required to transfect different culture vessels

Culture Vessel (cm^2)	DNA (μg)	Lipofectamine2000 (μl)	Opti-Mem (μl)
6 well (for 1 well)	5	10	500
24 well (for 1 well)	1	2	100
96 well (for 1 well)	0.2	0.5	50

2.3.14. Electroporation

HEK293 cells were rinsed once with PBS (Appendix 1H) and dislodged with trypsin (Appendix 1I). Trypsinization step was neutralized by the addition of DMEM medium (Appendix 2C) and cells were then transferred to 50 ml conical centrifuge tube (BD Bioscience, USA). The cells were spun at 250 x g (Sigma, USA) for 10 min at 4^oC. The supernatant was removed and the cells were resuspended with 10 ml of DEPC-treated PBS (Appendix 3G). The cell suspension was spun (Sigma, USA) again as mentioned above and the supernatant was decanted. The cell pellet was resuspended in 600 μl of DEPC-treated PBS and added to a 1.5 ml microcentrifuge tube (Axygen, USA) containing RNA. The mixture was transferred to a pre-chilled curvette (BTX, USA) and electroporated thrice at 0.85 kV and 25 μF. Following this, the cells were allowed to stand at RT for 10 min before seeding into new tissue culture flasks or plates.

2.3.15. Real-time PCR

Real-time PCR (RT-PCR) was performed using using Taqman probes and ABI prism 7000 (Applied biosystems, USA). HEK293, hSec3p293KD and hSec3p293OE cells were infected with WNV/DENV. At indicated timings, cells were washed with PBS (Appendix 1H), incubated with an alkaline/high-salt solution (1 M NaCl, 50 mM Na bicarbonate, pH 9.5) and washed three times in PBS to remove surface-bound viruses. Total RNA was extracted and analysed by RT-PCR with GAPDH mRNA as the endogenous control. It was shown earlier (Ng *et al.*, 2001) that unlike many of the flaviviruses, WNV (Sarafend) has a relatively short latent period of 4 to 6 h p.i compared to those of other flaviviruses (16 to 24 h p.i.). West Nile virus RNA yields were quantitated at 5 h p.i. to avoid measuring viral RNA from multiple infection rounds. Similarly, at 24 h p.i., prior to significant levels of DENV secretion and spread to neighboring cells (Helt & Harris, 2005), total RNA was harvested. Plus- and minus-strand viral RNA from hSec3p293KD/OE cells was determined relative to that from HEK293 cells as described by Davis and colleagues (2007a). The primers used were shown in Appendix 3H.

2.4. EXPRESSION AND PURIFICATION OF PROTEINS

2.4.1. Expression and purification of proteins in bacteria

Expression and purification of C protein in bacterial system was kindly performed by Mr. Adrian Cheong (Ph.D student, Department of Microbiology). The WNV/DENV C protein was cloned downstream of a histidine tag using pET28a

vector (Novagen, USA). The plasmid encoding the histidine-tagged C (His-C) protein was transformed into the BL21-CodonPlus competent *E. coli* bacteria cells (Stratagene, USA). The cells were grown in LB broth at 30°C until the optical density of culture reached 0.6. The expression of His-C was then induced with 1 mM isopropyl β-D-1-thiogalactopyranoside (Sigma, USA) and purified with immobilized metal ion affinity chromatography (Sartorius, USA).

2.4.2. Expression and purification of C protein in mammalian cells

HEK293 cells transfected with Myc-tagged C protein were harvested at 24 h post-transfection and lysed at RT for 30 min using M-Per mammalian lysis buffer (Thermo Scientific, USA) supplemented with protease and phosphatase inhibitors (Roche, Germany). Cell debris were removed from the supernatant by spinning the cell lysate at 16000 x g (Sigma, USA) for 10 min. Myc-C protein was immuno-purified with 20 μl of sepharose beads conjugated to anti-Myc antibodies (Sigma, USA). The beads were washed thrice in PBS (Appendix 1H) and incubated with cell lysate overnight at 4°C. The beads were spun down at 800 x g (Sigma, USA) for 1 min and washed thrice with PBS. Myc-tagged C protein was eluted from beads by competitive elution using Myc peptide (50 μg/ml) and re-suspended in Tris-HCl buffer, pH 7.4 supplemented with protease and phosphatase inhibitors. The immuno-purified protein was stored at -20°C until further use.

2.4.3. Expression and purification of proteins in rabbit reticulocyte lysates

TNT quick-coupled transcription/translation system was used to *in vitro* transcribe and translate 1 μg of plasmid DNA or RNA following manufacturer's instructions (Promega, USA). The plasmid DNA or RNA was added to the rabbit reticulocyte mixture and incubated at 30^{o}C for 1.5 h. The resulting products were subjected to immunopurification (Section 2.4.2). This system was used to *in vitro* translate V5-hSec3pf1, V5-galactosidase, HAC, HAC5'Δ15, Myc-C, Myc-C5'Δ15, pEF1α plasmids and viral RNA or V5-galactosidase RNA or IRF2 RNA or Importin-α RNA or CAML RNA. The resulting proteins V5-hSec3pf1, HAC, HAC5'Δ15, Myc-C, Myc-C5'Δ15, Importin-α and EF1α were purified using anti-hSec3p, anti-HA, anti-Myc, anti-importin-α or anti-EF1α conjugated sepharose beads as mentioned in Section 2.4.2.

2.5. ANALYSIS OF PROTEIN SAMPLES

2.5.1. Sodium-dodecyl sulphate polyacrylamide gel electrophoresis (SDS-PAGE)

Laemmli discontinuous gel system (Laemmli, 1970) was used for protein separation. To cast 12% separation gel, 4.5 ml of the resolving gel mixture (Appendix 4A) was pipetted into the gel casting apparatus (Bio-Rad, USA) and iso-propanol was layered on top of the mixture. The gel was allowed to polymerize before the isopropanol was decanted. A layer of 5% stacking gel (Appendix 4B) was layered on top of the polymerized resolving gel. Finally, combs were inserted into the stacking gel and the gel was allowed to polymerize.

After polymerization, the comb was removed and the wells were flushed with running buffer (Appendix 4C) before loading the protein samples.

Protein samples were prepared by adding 4x sample loading buffer (Appendix 4D) and boiled at 100°C for 1 min. Each well is loaded with protein samples of up to 20 µl. Pre-stained or unstained molecular weight markers (Promega, USA) were added to one well in each gel. The upper-tank of the gel electrophoresis was filled to the brim with upper-tank running buffer [Appendix 4C(i)] and the lower tank was filled with lower-tank running buffer [Appendix 4C(ii)]. Electrophoresis was carried out using a constant voltage of 100 V for approximately 1.5 h at 4°C. After electrophoresis, the proteins were transferred to a polyvinylidene fluoride (PVDF) membrane (Bio-Rad, USA).

2.5.2. Western blotting

Transfer of proteins onto a blotting paper was accomplished through a dry transfer method. The dry method involved the use of iBlot transfer apparatus (Invitrogen, USA). The gel was placed onto bottom blotting stack and then overlayed with top blotting stack (Invitrogen, USA). The assembly was then placed in the iBlot machine for 7 min. The membrane, which the proteins were transferred to, was removed from the assembly and soaked in Tris-buffered solution containing Tween-20 (TBST, Appendix 4F) with 5% skimmed milk (Appendix 4G) for 1 h at RT. The blot was then washed thrice with TBST for 5 min each. Primary antibodies were prepared in TBST with 5% skimmed milk (Anlene, Australia)

and added to the membrane. The membrane was incubated overnight at 4^{o}C. The primary antibody was removed and washed thrice with TBST for 5 min each. The membrane was then incubated for 1 h at RT with goat anti-rabbit or anti-mouse IgG conjugated with horseradish-peroxidase (Pierce Biotechnology, USA) followed by washing thrice with TBST for 5 min each. Membranes incubated with HRP-conjugated secondary antibodies (Pierce Biotechnology, USA) were developed using SuperSignal Pico system (Pierce Biotechnology, USA). Luminescence was detected with a CL-XPosure film (Thermo Scientific, USA) and the film was processed in an X-ray film developer (Konica Minolta, Japan) after exposure.

2.5.3. Cell-based fluorescence assay

HEK293 cells were seeded onto poly-D-lysine (Sigma, USA) coated 96-well plates (Section 2.1.5) and transfected with various plasmids (Section 2.3.13) or infected with WNV/DENV at MOI of 1. At various timings post-transfection or infection, culture supernatant was removed and the cells were washed with 1 ml of PBS (Appendix 1H). Cells were fixed with 4% paraformeldyhyde (Appendix 4J) for 15 min and permeabilized with 0.2% Triton-X (Appendix 4K) for 5 min at RT. Cells were then blocked with 1% BSA in PBS for 1 h. This was followed by the addition of mouse monoclonal anti-hSec3p (Abnova, USA) and rabbit polyclonal anti-actin (Sigma, USA) antibodies and incubated at 37^{o}C for 2 h.

Following three washes with PBS, the samples were treated with anti-mouse or anti-rabbit Alexa488 or Alexa594 secondary antibodies (Invitrogen, USA) at 37°C for 1 h and washed thrice in PBS before analyzing samples in a microtitre plate reader. The flow chart describing the major steps involved in this assay is shown in Fig. 2.1. Similar assays were developed to detect hSec6p, viral E proteins and HA/Myc-tagged C proteins using anti-hSec6p (Abnova, USA), anti-flaviviral E (4G2, Chemicon, USA), anti-HA and anti-Myc (Clontech, USA) antibodies.

2.5.4. Quantitation of proteins in a sample - Bradford assay

The BSA standards ranging from 10 μg/ml to 1000 μg/ml was prepared and added to the assay reagent (Bio-Rad, USA). Similarly, the protein sample to be measured was also added to the assay reagent and incubated for 3 min. Each concentration of the BSA protein standards and sample were then placed in spectrometer to measure absorbance at 595 nm.

2.5.5. Densitometry

The intensity of the bands on the immunoblot was quantified using GeneTools program and chemigenius documentation system (Syngene).

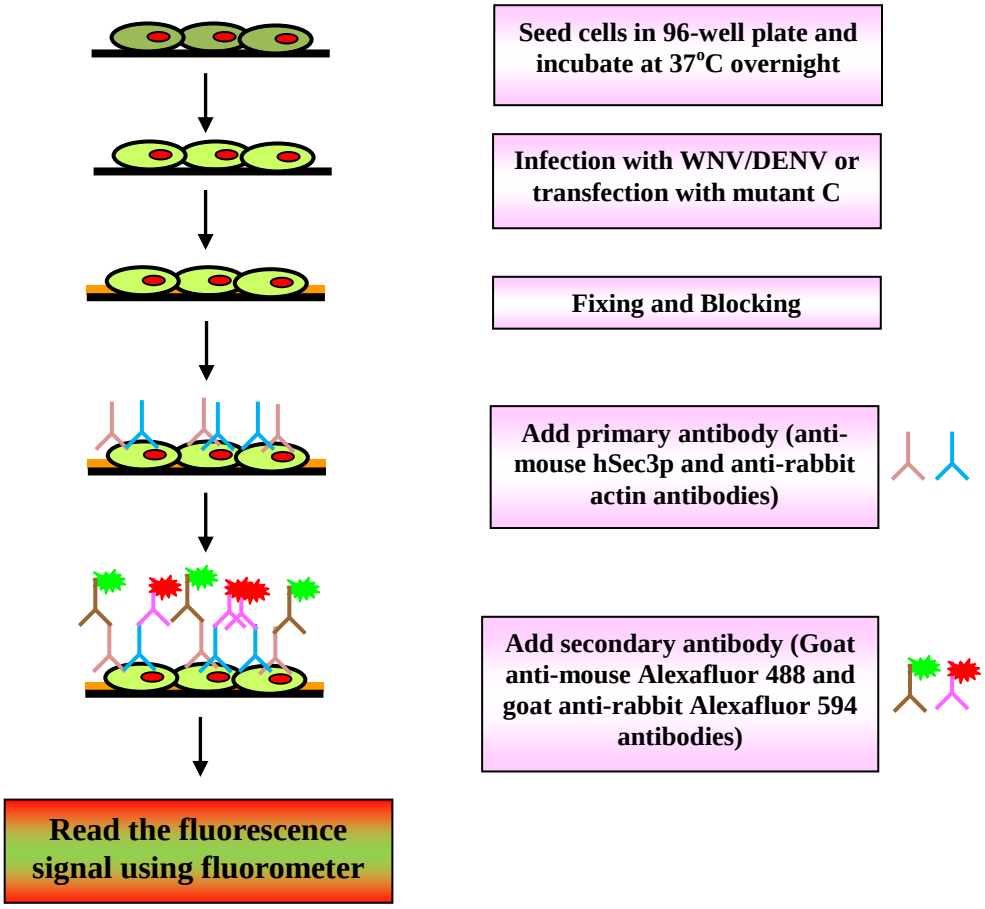

Fig. 2.1: The flow chart showing the major steps involved in cell-based fluorescence assay.

2.6. YEAST TWO-HYBRID ASSAY (Y2H)

Yeast two-hybrid experiments were performed using MATCHMAKER GAL4 Two-Hybrid System 3 kit (Clontech, USA). Yeast mating assays to detect potential human protein interacting partners were performed using Matchmaker Pre-transformed Human brain or liver cDNA library (Clontech, USA).

2.6.1. Preparation of yeast competent cells

An overnight starter culture was prepared by inoculating several (2-3 mm) colonies from a freshly streaked plate of *Saccharomyces cerevisiae*, strain AH109, into 1 ml of YPDA broth (Appendix 5A). This inoculum was then transferred into an Erlenmayer flask containing 50 ml of YPDA and incubated at 30°C for 16-18 h with shaking at 250 rpm (Sartorius, Germany). This starter culture was then used to inoculate a new flask containing 300 ml of fresh YPDA broth to give an initial OD_{600} reading of 0.2-0.3. The culture was then incubated at 30°C for 3 h with shaking at 230-270 rpm until the OD_{600} reading reached 0.5 ± 0.1. Yeast cells from the entire culture were collected by centrifugation (Sigma, USA) at 1000 x g for 5 min at RT. After decanting the supernatant, yeast cells were resuspended in 25-50 ml of sterile water and centrifuged (Sigma, USA) again at 1000 x g for 5 min at RT. The resulting cell pellet was resuspended in freshly prepared 1.5 ml of 1× TE/LiAc solution (Appendix 5B).

2.6.2. Transformation of bait-expressing vectors into yeast host strain AH109

Bait vectors containing WNV and DENV C protein or the prey vectors containing partial/full-length hSec3p were singly- or co-transformed into yeast strain AH109 *via* polyethylene glycol/lithium acetate (PEG/LiAc)-mediated transformation of yeast using YEASTMAKER™ Yeast Transformation System 2 (Clontech, USA). Small-scale yeast transformations were performed as follows: To perform single plasmid transformation, 0.1 μg of plasmid DNA, 0.1 mg of herring testes carrier DNA (Appendix 5C) and 0.1 ml of yeast competent cells were added to a 1.5 ml microfuge tube and mixed by high speed vortexing (Sigma, USA). For simultaneous co-transformation, both bait and prey plasmids should be added. An aliquot of 0.6 ml of sterile PEG/LiAc solution (Appendix 5D) was added to the tube and the contents were vortexed again (Sigma, USA). The tube was incubated at 30°C for 30 min with shaking at 200 rpm (Sartorius, Germany).

After incubation, 70 μl of sterile DMSO (Sigma, USA) was added to the tube and the contents were mixed by gentle inversion. Heat shock was then performed by incubating the tube contents in a 42°C water bath for 15 min. The tube was then removed from the water bath and chilled on ice for 2 min. The contents were then centrifuged at 14000 rpm for 5 sec (Sigma, USA) to collect the cells and 0.5 ml of sterile water was used to resuspend the cells. One hundred μl of the suspension was then plated out on SD-Trp plates (Appendix 5E) and the plates were incubated colony-side down at 30°C for 2-3 days. Ten-fold serial dilutions of the suspension (1:10, 1:100 and 1:1000) were also performed to ensure that at least

one dilution set produces a plate of evenly spaced out colonies. About 100 µl of each dilution was plated onto at least two SD-Trp and SD-Leu (Appendix 5E) plates and the rest were plated onto DDO, TDO and QDO plates (Appendix 5E).

2.6.3. Autoactivation assay

To ensure that the bait itself does not self-activate the Y2H reporter genes, autoactivation assays were performed on AH109 transformed with single bait constructs (WNV or DENV C) as follows: Equal amounts of inocula were taken from a single large (2-3 mm) colony of positive control (AH109 co-transformed with pGBKT7-murine p53 and the pGADT7-SV40 large T-antigen), negative control (AH109 transformed with pGBKT7 or pGBKT7-LaminC) and each of the bait-expressing constructs (AH109 transformed with bait plasmid). Each inoculum was then streaked on a SD-His plate (Appendix 5E) in a gridded fashion. Plates were incubated colony side down at 30°C for 3 days.

2.6.4. Verification of bait expression in pGBKT7 vector

Expression of the bait fusion protein was verified by Western blotting. A single colony of AH109 transformed with bait plasmid was inoculated in SD-Trp broth and incubated overnight at 30°C with shaking at 200 rpm (Sartorius, Germany). The cells were collected by centrifugation at 14000 x *g* for 1 min (Sigma, USA). The cell pellet was washed once with sterile water and collected again by centrifugation (Sigma, USA). Cells were resuspended in 100 µl of sample loading buffer and heated at 95°C for 5 min. The samples were then centrifuged (Sigma,

USA) at 14000 x g for 5 min at 4°C to pellet cell debris. Twenty-five µl of sample was then loaded per lane and resolved on a 12% SDS-PAGE gel and the protein bands detected by Western blotting (Section 2.5.2).

2.6.5. Yeast mating assay

Yeast mating assay was performed as per the manufacturer's protocol as follows: One large (2-3 mm) fresh colony of AH109 transformed with bait was inoculated into 50 ml of SD-Trp broth to maintain selection pressure for the bait transformations. The culture was incubated at 30°C for 16-24 h with shaking at 250-270 rpm (Sartorius, Germany). When the OD_{600} of the culture reached above 0.8, the cells were collected from the entire content of the culture by centrifugation at 1000 x g for 5 min (Sigma, USA). Culture supernatant was decanted and the residual liquid (approximately 5 ml) was used to resuspend the cell pellet by vortexing.

Prior to use, one frozen vial of the pre-transformed yeast (strain Y187) library culture was thawed and mixed by gentle vortexing. The 5 ml inoculum obtained from harvesting the overnight culture was then combined with 1 ml library culture in a 2 L Erlenmeyer flask containing 45 ml of 2 x YPDA/Kan medium (Appendix 5F). Two 1 ml aliquots of 2 x YPDA/Kan medium were used to rinse the cells from the library tube. The total volume of the culture was topped up to 50 ml with 2 x YPDA/Kan medium and incubated at 30°C overnight for 24 h with gentle swirling at 30-50 rpm.

After 24 h of mating, the mating mixture was transferred to a sterile centrifuge tube and the cells were spun down by centrifuging at 1000 x g for 10 min (Sigma, USA). The mating flask was rinsed twice with 50 ml 2 x YPDA/Kan medium. These two rinses were used to resuspend the first pellet and the cell suspension was centrifuged (Sigma, USA) again at 1000 x g for 10 min. The cell pellet was resuspended in 10 ml of 0.5 x YPDA/Kan medium (Appendix 5G) and plated on to SD-Trp, SD-Leu, SD-Trp,Leu (DDO), SD-Trp,Leu,His (TDO) and SD-Trp,Leu,His,Ade (QDO) plates and incubated at 30°C for 3-7 days. All white or light pink colonies growing on TDO or QDO plates with diameters >2 mm were replica plated onto QDO medium containing X-α-Gal (Appendix 5H) and incubated at 30°C for 3-6 days.

2.6.6. Plasmid isolation from yeast

For each yeast co-transformant identified from the yeast mating assay, a single large well-isolated yeast colony grown on QDO plates was used to inoculate 0.5 ml of QDO broth. The cells were thoroughly resuspended by vigorous vortexing. The culture was then incubated at 30°C overnight with shaking at 230-250 rpm (Sartorius, Germany). Cells were harvested by centrifugation (Sigma, USA) at 14000 rpm for 5 min. The supernatant was completely removed by pipetting and the pellet was resuspended in 50 µl of potassium phosphate. Ten µl of lyticase solution (Clontech, USA) was added to each tube, mixed by pipetting and the entire contents were incubated at 37°C for 60 min. Ten µl of 20% SDS was added and subjected to one freeze/thaw cycle (-20°C). The samples were kept at -20°C

until required for use. The bait and prey plasmids from the yeast library were extracted from yeast cotransformants using YEASTMAKER™ Yeast Plasmid Isolation Kit (Clontech, USA) following manufacturer's protocol. Briefly, the yeast cells were incubated with lyticase and SDS. The resulting mixture was loaded onto the spin column and centrifuged (Sigma, USA) and the bait and prey plasmids were eluted using elution buffer.

2.6.7. Isolation of prey expressing plasmids

The samples obtained from Section 2.6.6 contained a mixture of bait and prey plasmids. To separate the prey plasmids from the yeast plasmid solution, 10 µl of yeast plasmid solution (Section 2.6.6) were used to transform chemically competent DH5α *E. coli* cells as described in Section 2.3.6. Selection for prey plasmids were performed by plating the cells on LB-ampicillin [Appendix 3C(ii)] since the library pACT2 plasmid contains ampicillin selection marker. Plasmids were then isolated (Section 2.3.8) and sequenced (Section 2.3.9). The blastn and blastp algorithms were used to analyse the sequence data and to confirm the identity of the library interacting partners.

2.7. PROTEIN-PROTEIN INTERACTION ASSAYS

2.7.1. Co-immunoprecipitation (Co-IP)

HEK293 cells ($5X10^5$) were infected with WNV or DENV (MOI: 1) or co-transfected with 4 µg of GFP/V5/HA/Myc-tagged C (full length, truncated or mutated) and V5-tagged hSec3p (full length or truncated) plasmids using

Lipofectamine2000 (Invitrogen, USA) or electroporated (Bio-Rad, USA) with 20 μg of *in vitro* transcribed RNAs from pWNS plasmid as described in Sections 2.3.13 and 2.3.14. At 14 or 24 h (WNV/DENV) post-infection (p.i.) or 24 h post-transfection, cells were washed with PBS (Appendix 1H) and lysed using lysis buffer (Miltenyi Biotec, Germany) containing protease inhibitors cocktail (Roche, USA).

For NS3 protein interaction assay, cell lysates were pre-treated in the presence and absence of RNaseA/DNase (Promega, USA) at 30^{o}C for 1 h. Cell lysate was pre-mixed with either anti-WNV C (2 μg, gift from E. G. Westaway) or anti-DENV C (2 μg, gift from Dr. Prida Malasit, Mahidol University, Thailand) or anti-GFP (2 μg, Sigma, USA) or anti-V5 (2 μg, Invitrogen, USA) or anti-HA/anti-Myc (2 μg, Clontech, USA) or anti-EF1α (2 μg, Santa Cruz Biotechnology, USA) or anti-importin-α (2 μg, Sigma, USA) antibody-conjugated magnetic microbeads for 30 min on ice and purified using μMACs column (Miltenyi Biotec, Germany). The column was rinsed thrice with wash buffer (Miltenyi Biotec, Germany) and eluted with pre-heated elution buffer (Miltenyi Biotec, Germany). For Western blotting (Section 2.5.2), samples from co-immunoprecipitation assays or co-transfected cell lysates were electrophoresed in 12% SDS-PAGE gels and transferred on to PVDF membrane. The membrane was then incubated with rabbit-polyclonal anti-WNVC (1:200, gift from E.G. Westaway, Australia) or mouse-monoclonal/rabbit-polyclonal anti-V5 (1:1000) or rabbit-polyclonal anti-HA (1:1000) or mouse-monoclonal/rabbit-polyclonal anti-hSec3p (1:300) or

rabbit-polyclonal anti-NS3 (1:300; commercially generated by Sigma, USA) or mouse-monoclonal anti-PTB (1:500; Invitrogen, USA) or mouse-monoclonal/rabbit-polyclonal anti-Myc (1;1000; Sigma, USA) or mouse-monoclonal anti-Sec6 (1:400; Abnova, USA) or mouse-monoclonal anti-actin (1:2000; Millipore, USA) or mouse-polyclonal anti-IRF2 (1:300; Santa Cruz Biotechnology, USA) or mouse-monoclonal/rabbit-polyclonal anti-importin-α (1:400; Sigma, USA) or mouse-monoclonal anti-CAML (1:400; Abnova, USA) or mouse-monoclonal anti-GFP (1:500; Invitrogen, USA) or mouse-polyclonal anti-phosphoserine (1:500; Millipore, USA) antibodies followed by goat anti-rabbit or anti-mouse IgG conjugated with horseradish-peroxidase (1:10000; Pierce Biotechnology, USA) and the immunoreactive bands were developed using SuperSignal Pico system (Pierce Biotechnology, USA).

2.7.2. Mammalian two-hybrid (M2H) assay

The cDNA encoding sequences of full-length/mutated/truncated C proteins were amplified and joined to pSV40-GAL4 50 element and SV40 pA 3' element to create bait proteins of interest. Similarly, the cDNA encoding sequences of hSec3 protein was amplified and joined to pSV40-VP16 5' element and SV40 pA 3' element. The controls used in M2H assay were listed in Appendix 6A. Co-transfection was performed using DNA linear constructs generated from above along with pGAL/*lacZ* plasmid using Lipofectamine2000 (Invitrogen, USA). At 24 h post-transfection, β-galactisodase assay was performed as mentioned earlier (Bhuvanakantham & Ng, 2005) and the specific activity of samples were

calculated using the following formula: nmoles of ortho-nitrophenyl-β-D-galactopyranoside hydrolyzed/incubation time/mg protein.

2.8. KNOCK-DOWN AND OVER-EXPRESSION OF HUMAN Sec3 PROTEIN

2.8.1. Prediction of human Sec3 gene sequence for short hairpin-RNA (shRNA)-targeted gene knock-down

In order to predict unique sites for hSec3 gene knock-down by lentivirus system, the mRNA sequence of hSec3p (Genebank accession number NM_018261) was input into an RNAi designer algorithm, BLOCK-iT RNAi Designer (Invitrogen, USA). It is critical that the shRNA obtained targets only hSec3 mRNA so as to minimise any off-target effects. Putative sites predicted were further validated by aligning them against NCBI nucleotide database using Blast software (http://www.ncbi.nlm.nih.gov/BLAST). Designing of the oligonucleotides containing the required shRNA sequence was done as instructed by the manufacturer's protocol of BLOCK-iT Lentiviral RNAi kit (Invitrogen, USA). A scrambled sequence containing exactly the same number of nuclotides as that of predicted shRNA sequence was obtained by inputting the selected shRNA sequence into nucleotide scrambling algorithm, siRNA Wizard (InvivoGen, USA). On top of containing the same number of nucleotides as the predicted shRNA sequence, the obtained scrambled sequence had no known human homologues to prevent off-target effects. The primers used in lentivector-mediated gene knock-down studies are shown in Appendix 7A.

2.8.2. Insertion of nucleotide containing shRNA sequence into entry vector

Polyacrylamide gel electrophoresis-purified oligonucleotides containing the shRNA sequence and the scrambled sequence for cloning into pENTR™/U6 entry vector (Invitrogen, USA) were commercially obtained (1st Base, Singapore). The oligonucleotides and their respective complementary strands were annealed and diluted according to the manufacturer's protocol. Subsequently, the diluted double-stranded (ds) oligonucleotides encoding hSec3p and scrambled shRNA were ligated with pENTR™/U6 entry vector (Invitrogen, USA) to create a U6 entry clone. After ligation of ds-oligonucleotides with pENTR™/U6 entry vector was complete, the circularised plasmid was introduced into TOP10 competent cells (Invitrogen, USA) for plasmid amplification (Section 2.3.6) and subsequent clone selection (Section 2.3.7). The DNA sequencing reaction was then performed to ensure correct reading frames (Section 2.3.9). The flow chart describing the major steps necessary to produce a pENTR™/U6 entry clone is shown in Fig. 2.2.

2.8.3. Generation of shRNA expression clones for lentivirus production

The shRNA expression clones containing the U6 RNAi cassette of interest were generated by performing a highly specific LR recombination reaction between the entry clone and the pLenti6/BLOCK-iT™-DEST vector using LR clonase (Invitrogen, USA). In order to amplify the resultant plasmid, it was introduced into Stbl3 competent cells (Invitrogen, USA) by transformation (Section 2.3.6). Appropriate clones were then selected using colony PCR (Section 2.3.7). It was

not necessary to confirm the sequence of shRNA-producing sequence as the recombination reaction was highly specific and shRNA-producing sequence had been ascertained previously. The flow chart describing the major steps necessary to produce a pLenti6/BLOCK-iT expression plasmid is shown in Fig. 2.3.

2.8.4. Generation of hSec3p over-expressing plasmid

To generate hSec3p over-expressing construct, hSec3p gene was cloned into pLenti6/V5 Directional TOPO cloning vector (Invitrogen). This resulted in the generation of pLenti6/V5 expression plasmid. The primers used for cloning in lentivectors were shown in Appendix 7B.

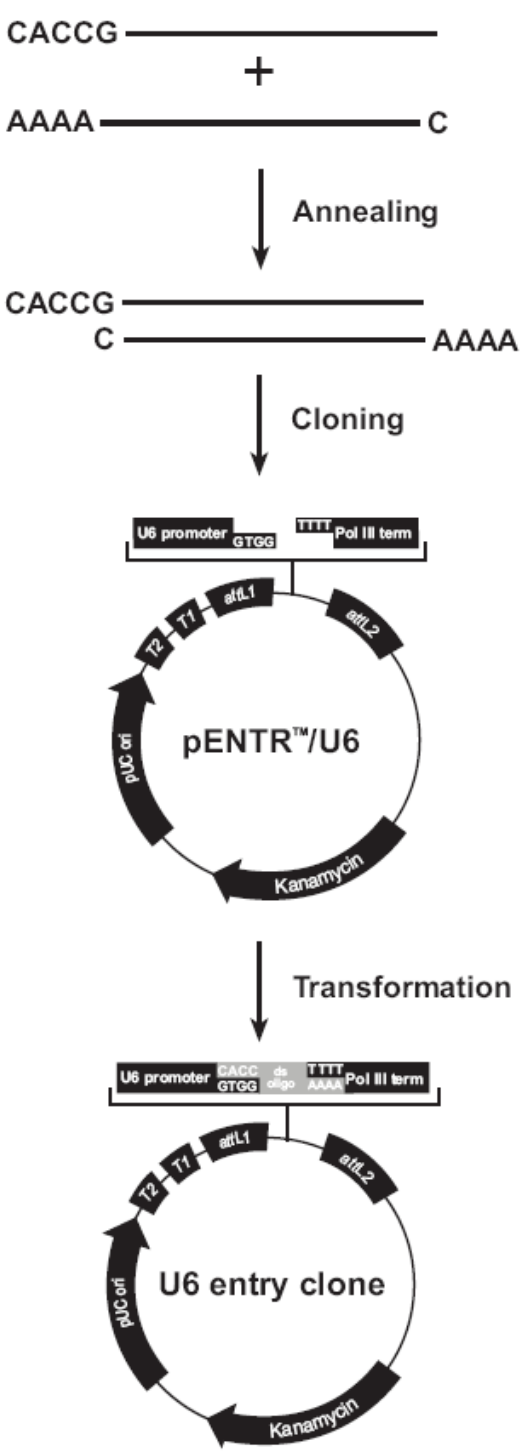

Design and synthesize complementary DNA oligos with each containing 4 nucleotide overhangs

Anneal DNA oligos to generate ds-oligos

Clone ds-oligo into pENTR™/U6 vector using T4 DNA ligase

Transform *E. coli* and analyze colonies for the desired entry clone

Entry clone to recombine with pLenti6/BLOCK-iT-DEST vector to generate an expression plasmid

Fig. 2.2: The flow chart showing the major steps necessary to produce a pENTR™/U6 entry clone (adapted from www.invitrogen.com).

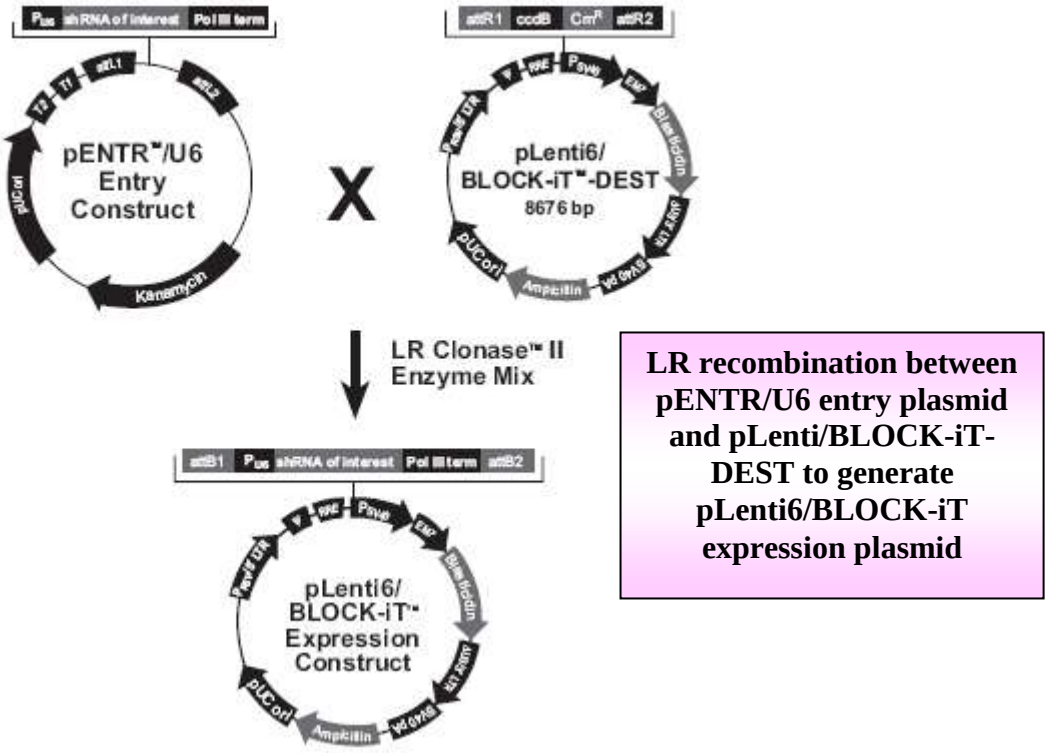

Fig. 2.3: The flow chart showing the generation of a pLenti6/BLOCK-iT expression plasmid (adapted from www.invitrogen.com).

2.8.5. Obtaining lentivirus for transduction of HEK293 cells

The stocks of lentivirus for transduction of HEK293 cells were obtained by following manufacturer's protocol (Invitrogen, USA). Briefly, the shRNA expression clones or hSec3p over-expression clones were co-transfected with ViraPower packaging mix into 293FT cells (Invitrogen, USA) to produce knock-down or over-expression lentiviral stocks. At 24 h post-transfection, the culture supernatant containing the transfection reagent and excess plasmid was removed and fresh complete DMEM (Appendix 1B) was added. At 48 h post-transfection, the culture supernatant containing the lentivirus was aspirated into 50 ml falcon tubes and centrifuged (Sigma, USA) at 1000 x g for 10 min at 4^{o}C to remove cellular debris. One ml of this supernatant was then aliquoted into sterile cryo-vials, sealed and snap-frozen in cold ethanol (-80^{o}C). The flow chart describing the steps necessary to produce lentivirus stocks is shown in Fig. 2.4.

2.8.6. Lentiviral transduction of HEK293 Cells

HEK293 cells grown to about 70% confluency in a 6-well plate (Nunc, Denmark) were transduced using knock-down and over-expression lentivirus obtained from Section 2.8.5. The media was removed and the monolayer was washed once with PBS (Appendix 1H). The frozen vial of knock-down and over-expression lentivirus was quickly thawed at 37^{o}C and added to HEK293 cell monolayer and then incubated at 37^{o}C with 5% CO_2 (Thermo Electron Corporation, USA). The next day, fresh media containing Blasticidin (Invitrogen, USA) was added to select for stably-transduced HEK293 cells.

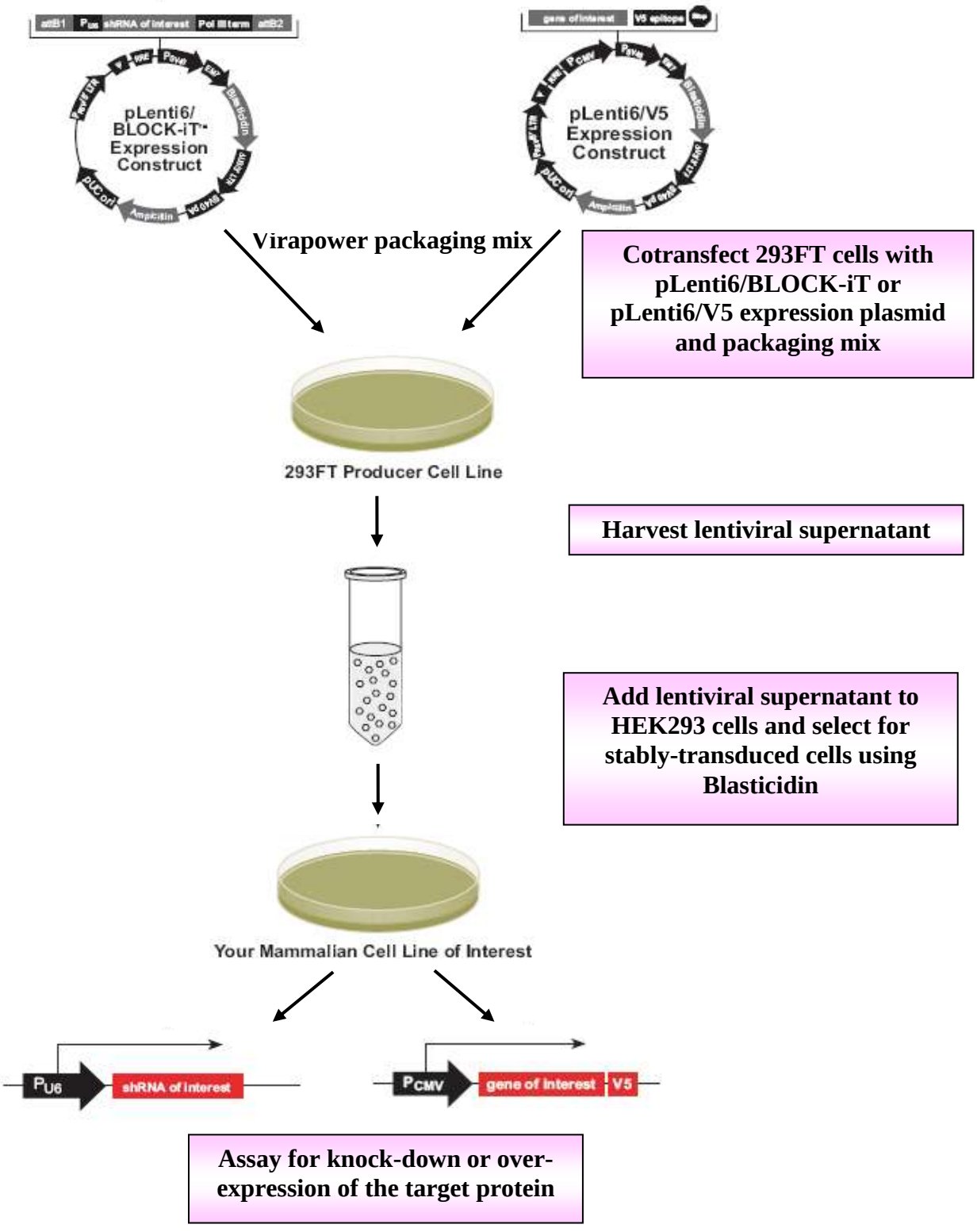

Fig. 2.4: The flow chart describing the steps necessary to produce stably-transduced HEK293 cells (adapted from www.invitrogen.com).

The transduced knock-down and over-expressing cells were named as hSec3p293KD and hSec3p293OE cells, respectively. These transduced cell lines were maintained at 37°C incubator with 5% CO_2 (Thermo Electron Corporation, USA) in DMEM supplemented with various components (Appendix 7C). The flow chart describing the steps necessary to produce stably-transduced HEK293 cells is shown in Fig. 2.4.

2.8.7. Determination of optimal drug concentration for the selection of stable cell lines

Varying concentrations of the selection drug, Blasticidin (Invitrogen, USA) were added to HEK293 cells. The cells were observed for 6 days and fresh media containing respective concentrations of drug was added every day. The fluorescent MultiTox-Fluor Multiplex Cytotoxicity Assay (Promega, USA) was used to determine the cytotoxic effects of varying concentrations of Blasticidin following manufacturer's instructions. The live cell and dead cell substrates were mixed with cytotoxicity reagent and added to HEK293 cells incubated with varying concentrations of Blasticidin. After 1 h of incubation at 37^{o}C, fluorescence relating to cytotoxicity and viability were read as mentioned in the manufacturer's protocol using a fluorescent reader (Tecan, Austria).

2.8.8. Assaying for over-expression and knock-down efficiency

The cell lysate of successfully transduced HEK293 cells were harvested and separated using SDS-PAGE gel (Section 2.5.1). Subsequently, the level of hSec3p

in hSec3p293OE and hSec3p293KD cells was detected by Western blotting (Section 2.5.2) using anti-hSec3p antibody.

2.8.9. Survey of the proliferation capacity of stable cell lines

The fluorescent MultiTox-Fluor Multiplex Cytotoxicity Assay (Promega, USA) was used to determine the proliferation capacity of hSec3p293OE and hSec3p293KD stable cell lines. Approximately 1000 cells in 100 µl of media were seeded into each well of a 96-black well plate (Greiner Bio-One, USA) and incubated overnight at 37°C with 5% CO_2. The next day, 100 µl of sterile assay reagent (Promega, USA) was added to each well. After 1 h of incubation at 37 ^{o}C, fluorescence relating to cytotoxicity and viability were read as mentioned in the manufacturer's protocol using a fluorescent reader (Tecan, Austria).

2.9. PROTEIN-RNA INTERACTION ASSAYS

2.9.1 Preparation of RNA

2.9.1.1. RNA synthesis

The full-length WNV/DENV RNA was synthesised using T7 Ribomax^{TM} large scale RNA production system and cap analogue as described in Section 2.3.12. To synthesize specific regions of viral RNA (WNV/DENV 3'UTR RNA), DNA sequences encoding those regions were amplified by PCR (Section 2.3.3) from WNV/DENV infectious clone and used as templates for RNA synthesis as described in Section 2.3.12.

2.9.1.2 RNA labelling

An appropriate amount of full-length/partial WNV/DENV RNA was labelled with Label^{IT} biotinylation kit (Mirus Bio, USA). Reaction assembly and purification of labelled RNA was performed according to manufacturer's protocol. Briefly, full-length/partial WNV/DENV RNA was mixed with biotin labelling reagent and incubated at 37^{o}C for 2 h. This was followed by ethanol purification (Section 2.3.9). Labelling of RNA was then confirmed by dot blotting the biotinylated RNA on to PVDF membrane and detected with streptavidin conjugated to HRP (Pierce Biotechnology, USA) to ensure that the RNA was labelled.

2.9.2. Viral RNA Immunoprecipitation

HEK293, hSec3p293KD and hSec3p293OE ($5X10^5$) cells were infected with WNV (MOI of 10) or DENV (MOI of 1) or transfected with 4 μg of biotinylated/non-biotinylated WNV/DENV 3'UTR RNA (contains partial NS5 and 3'UTR region). At appropriate timings post-infection (14 h p.i.-WNV; 24 h p.i.-DENV) or 18 h post-transfection, cells were cross-linked with 1% formaldehyde and lysed using lysis buffer (Miltenyi Biotec, USA). Co-immunoprecipitation assay was then performed as described in Section 2.7.1 using anti-EF1α or anti-hSec3p or anti-PTB antibodies. Western blotting (Section 2.5.2) of Co-IP eluents was also performed using anti-hSec3p, anti-EF1α or anti-PTB antibodies. RNA was then isolated from the immunoprecipitated samples using RNeasy kit (Qiagen, USA) and analysed by real-time RT-PCR using Taqman probe as described earlier (Li *et al.*, 2006).

2.9.3. RNA Pull-down assay

HEK293, hSec3p293KD and hSec3p293OE ($5X10^5$) cells were infected with WNV (MOI of 10) or DENV (MOI of 1) or transfected with 4 μg of biotinylated/non-biotinylated WNV/DENV 3'UTR RNA. At appropriate timings post-infection (14 h p.i.-WNV; 24 h p.i.-DENV) or 18 h post-transfection, cells were cross-linked with 1% formaldehyde and lysed using lysis buffer (Miltenyi Biotec, USA). For the pull-down assay, cell lysates were incubated with 100 μl of streptavidin-conjugated DynaL® magnetic beads (Invitrogen, USA) for 4 h at RT. The beads were pulled down using DynaL® magnetic rack (Invitrogen, USA) and the supernatant was removed. The beads were then washed thrice with wash buffer (Appendix 8A). The beads were resuspended in wash buffer and the samples were subjected to Western blot analysis (Section 2.5.2) using anti-hSec3p, anti-EF1α or anti-PTB antibodies.

2.9.4. Competition assay for EF1α-3'UTR complex formation

Equal amounts of biotinylated WNV/DENV 3'UTRs were mixed with recombinant EF1α (Abnova, USA) in the presence or absence of recombinant hSec3p (Abnova, USA) or Sec6p (Abnova, USA). Identical experiments were performed in the presence and absence of non-biotinylated 3'UTRs or tRNAs (Invitrogen, USA). The mixture was incubated overnight at 4^oC before performing pull down assay using streptavidin dynaLbeads as described in Section 2.9.3. The eluents were analyzed by Western blotting (Section 2.5.2) using anti-EF1α or anti-PTB antibodies.

2.10. ANALYSIS OF INTRACELLULAR AND EXTRACELLULAR VIRUS PROTEINS

HEK293, hSec3p293KD and hSec3p293OE cells were infected with WNV/DENV. At indicated time points, cell lysates and culture supernatants were harvested and quantified by Bradford assay (Section 2.5.4). Twenty-five μg of protein from each experimental group was separated by SDS-PAGE (Section 2.5.1) followed by immunoblotting (Section 2.5.2) using anti-WNV E (1:500, H546, Microbix, USA) or anti-DENV E (1:1000, 3H5, Chemicon, USA) antibodies.

2.11. OTHER ASSAYS THAT UTILIZED QUICK-COUPLED TRANSCRIPTION/TRANSLATION (TNT) SYSTEM

2.11.1. hSec3p immunodepletion assay

TNT quick-coupled transcription/translation system (Promega, USA) was used to *in vitro* transcribe and translate 1 μg of V5-hSec3pf1 plasmid following manufacturer's instructions (Promega, USA). The presynthesized V5-hSec3pf1 in the rabbit reticulocyte lysate was incubated with anti-hSec3p-conjugated magnetic beads for 4 h at 4^{o}C and the resulting mixture was loaded onto the Miltenyi column (Miltenyi Biotec, Germany). The column was washed with wash buffer (Miltenyi Biotec, Germany). The flow-through and the eluent from the immunodepleted samples were analyzed for the presence of hSec3p by Western blotting (Section 2.5.2) using anti-hSec3p antibody.

2.11.2. *In vitro* translation assay

TNT quick-coupled transcription/translation system (Promega, USA) was used to *in vitro* transcribe and translate 1 μg of V5-hSec3pf1 plasmids. Ten μg of viral or IRF2 or Importin-α or CAML RNA was generated as described in Section 2.3.12. The presynthesized V5-hSec3pf1 was added to reticulocyte mix containing WNV/DENV RNA in the presence or absence of 10 μM MG132 (Calbiochem). The flow-through from the immunodepleted sample (Section 2.11.1) was mixed with 10 μg WNV, DENV, IRF2, CAML or importin-α RNA in the new reticulocyte reaction. The hSec3p, CAML, IRF2, importin-α and E protein levels were analysed by Western blotting (Section 2.5.2). The EF1α competition assays were then performed using 2- or 5-fold mole excess of EF1α.

2.11.3. Competition assay using C protein

TNT quick-coupled transcription/translation system (Promega, USA) was used to *in vitro* transcribe and translate 1 μg of V5-hSec3pf1, HAC, HAC5'Δ15, Myc-C or Myc-C5'Δ15 plasmids. The presynthesized V5-hSec3pf1, HAC, HAC5'Δ15, Myc-C and Myc-C5'Δ15 proteins were purified using anti-hSec3p, anti-HA or anti-Myc-conjugated magnetic beads as mentioned in Sections 2.4.2 and 2.4.3. Purified hSec3p or EF1α were fractionated on SDS-PAGE gels (Section 2.5.1) and transferred on to PVDF membranes (Section 2.5.2). Blots were blocked in binding buffer (Appendix 8B) for 1.5 h at 4°C, followed by incubation at 4°C overnight in binding buffer containing 20 nM of purified EF1α or hSec3p. Blots were then washed at RT (five times for 15 min; 100 ml/wash) in binding buffer

without BSA (Appendix 8C). The hSec3p-bound EF1α or EF1α-bound hSec3p was detected by incubation with anti-EF1α or anti-hSec3p antibody in phosphate-buffered saline with 5% skimmed milk (Appendix 4G). Primary antibody was removed by washing (four times for 10 min) in TBST (Appendix 4F) and antibody-antigen complexes were detected as described in Section 2.5.2. Competition assays were performed as described above except a 5- or 10-fold mole excess of either HAC/HAC5'Δ15 or Myc-C/Myc-C5'Δ15 proteins was added to the binding reaction mixtures.

2.11.4. *In vitro* translation assay to study hSec3p degradation

The full-length or truncated WNV/DENV C plasmids such as MyCC (WNV), DMycC (DENV), MycC5'Δ15 (WNV) or DMycC5'Δ15 (DENV) were added to the rabbit reticulocyte mix in the TNT quick-coupled transcription/translation system (Promega, USA) together with hSec3p RNA. The *in vitro* translation assay was performed at 30^{o}C for 1.5 h following manufacturer's instructions (Promega, USA). The amount of hSec3p was then analysed by Western blotting using anti-hSec3p antibody (Abnova, USA).

2.12. METHODS RELATED TO PROTEASOME DEGRADATION PATHWAY

2.12.1. Drug inhibition studies

Actinomycin D blocks new RNA synthesis and hence allows the analysis of the fate of the preexisting cellular mRNAs. Host cell transcription was blocked by

incubating HEK293 cells with 2 μg/ml of Actinomycin D (Sigma, USA) for 1 h. This was followed by infection with WNV/DENV. Actinomycin D was included throughout the infection period. MG132 is the reversible cell-permeable proteasome inhibitor. HEK293 cells were treated with 10 μM MG132 (Calbiochem, USA) for 1 h. This was followed by infection with WNV/DENV or transfection with plasmids encoding recombinant WNV/DENV C proteins. MG132 was included throughout the infection or transfection period. Epoxomicin is an irreversible cell-permeable proteasome inhibitor. HEK293 cells were treated with 100 nM epoxomicin (Sigma, USA) for 1.5 h. This was followed by infection with WNV/DENV or transfection with plasmids encoding recombinant WNV/DENV C proteins. HEK293 cells were incubated with various concentrations of inhibitors such as lactacystin (inhibitor of chymotrypsin-like activity) and YU-102 (inhibitor of caspase-like activity) at 37^{o}C for 2 h and observed for cytotoxic effects using the fluorescent MultiTox-Fluor Multiplex Cytotoxicity Assay (Promega, USA).

2.12.2. Titration of various proteolytic activities of 26S proteasome in HEK293 cells

HEK293 cells were serially diluted in a 96-well plate as 100 μl/well samples. Proteasome-Glo cell-based assay kits for for chymotrypsin-like, trypsin-like and caspase-like activities were used following manufacturer's instructions (Promega, USA). Equal volumes of luminescent Proteasome-Glo reagents containing substrates for chymotrypsin-like, trypsin-like, or caspase-like activity were added

to the 96-well plate. Luminescence was then determined 10-15 min after addition using a luminometer. The Proteasome-Glo reagents were prepared as follows: The Proteasome-Glo cell-based buffers were thawed and equilibrated to room temperature together with the lyophilized luciferin detection reagents. The luciferin detection reagents were then reconstituted by adding the appropriate volume of Proteasome-Glo cell-based buffer. The Proteasome-Glo reagents were then prepared by adding the Proteasome-Glo substrates to the reconstituted luciferin detection reagent. For Proteasome-Glo trypsin-like assay, specific inhibitors provided in the kit were added.

2.12.3. Measurement of proteolytic activities of 26S proteasome

HEK293 cells were seeded on to 96-well plate and transfected with various full-length/truncated/mutated WNV/DENV C plasmids or RNAs *in vitro* transcribed from infectious clones of WNV/DENV. At 12 or 24 h post-transfection, Proteasome-Glo cell-based assay kits for for chymotrypsin-like, trypsin-like and caspase-like activities were used to measure the chymotrypsin-like, trypsin-like and caspase-like activities of 26S proteasome as mentioned in Section 2.12.2.

2.13. FLUORESCENCE MICROSCOPY

2.13.1. Preparation of cells

HEK293, hSec3p293OE and hSec3p293KD cells were seeded onto poly-D-lysine (Sigma, USA)-coated coverslips. These cells were either transfected with various plasmids or infected with WNV/DENV. At various timings post-transfection or

infection, culture supernatant was removed and the cells were washed with 1 ml of PBS (Appendix 1H). Cells were fixed with 4% paraformeldyhyde for 15 min and permeabilized with 0.2% Triton-X for 5 min at RT. After fixation, cells were washed thrice with PBS.

2.13.2. Immuno-staining of cells

For hSec3p localization studies, the cells were incubated with anti-hSec3p (Abnova, USA), anti-C (kind gift from E.G. Westaway and Professor Prida Malasit), anti-EF1α (Santa Cruz Biotechnology, USA), anti-NS3 (commercially produced by Sigma, USA) or anti-dsRNA (English & Scientific Consulting, Hungary) antibodies at 37°C for 1 h and washed thrice in PBS (Appendix 1H) for 5 min each. The samples were then treated with anti-mouse or anti-rabbit Alexa488 or Alexa594 secondary antibodies (Invitrogen, USA) at 37°C for 1 h and washed thrice in PBS for 5 min each. Cell nuclei were stained with DAPI (Invitrogen, USA). Finally, the cover slips were mounted onto glass slide (Marienfeld, Germany) with Prolong Gold anti-fade mounting reagent (Invitrogen, USA). Image analysis was performed with Nikon A1Rsi confocal microscope and NIS Elements imaging software (Nikon Imaging Centre, Singapore).

2.14. BIOINFORMATICS SOFTWARE USED IN THIS PROJECT

Various bioinformatics softwares were used in this project for sequence analyses and domain prediction. The major softwares used were listed in Appendix 9.

2.15. STATISTICAL ANALYSIS

Means, standard deviations, *P* values, and 95% confidence intervals were carried out using Microsoft® Office Excel 2003. *P* values were determined by Student's *t* test.

CHAPTER 3

RESULTS

3.0. IDENTIFICATION OF NOVEL HOST PROTEINS INTERACTING WITH FLAVIVIRUS CAPSID PROTEIN AND DOMAIN MAPPING

3.1. INTRODUCTION

Flavivirus capsid (C) protein is a key structural component of virus particles. However, the role of C protein in the pathogenesis of arthropod-borne flaviviruses is poorly understood. Hence, this study sought to identify the potential host proteins interacting with flavivirus C protein using yeast two-hybrid (Y2H) library screening. In this chapter, flavivirus C gene was cloned in yeast vectors encoding GAL4 DNA-binding domain (BD) and expressed in yeast cells as fusion protein. Yeast mating was then performed to isolate the potential cellular proteins that could associate with C protein and have roles in flavivirus replication process. This could aid in the design of novel anti-flaviviral peptides that could disrupt the association between flavivirus C protein and the host proteins.

3.2. YEAST TWO-HYBRID LIBRARY SCREENING

3.2.1. Construction of yeast two-hybrid (Y2H) bait plasmids encoding West Nile and dengue virus capsid proteins

To perform Y2H library screening, it was essential to construct Y2H bait plasmids encoding WNV/DENV C protein with the GAL4 DNA-binding domain to facilitate yeast mating since the prey cDNA inserts used in Y2H library was cloned into yeast vectors encoding GAL4 DNA-activation domain (AD). To construct BD-bait fusion protein expressing plasmids, DNA fragments encoding

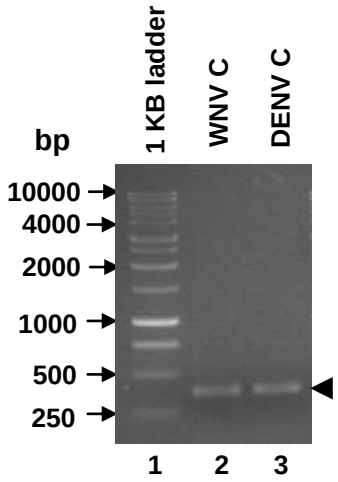

Fig. 3.1: PCR amplification of WNV and DENV C genes. WNV and DENV C genes were amplified by PCR from viral cDNA. Lane 1: 1 KB DNA ladder (Promega); Lane 2: WNV C (arrowhead); Lane 3: DENV C (arrowhead). Arrows at the left indicate positions of 250 to 10000 bp sizes from 1 KB DNA ladder.

WNV and DENV C genes were amplified (Fig. 3.1, primers used were shown in Appendix 3A) from first strand cDNA obtained *via* reverse transcription of extracted WNV and DENV genomic RNA (Sections 2.3.1 to 2.3.3). The resulting DNA fragments were digested with *EcoRI* and *BamHI* (Section 2.3.5) and ligated with T4 ligase into yeast expression vector, pGBKT7 (Section 2.3.6). The pGBKT7 vector had previously been digested with *EcoRI* and *BamHI* (Section 2.3.5). The ligation mixture was transformed into *E. coli* DH5α cells, which were subsequently grown under kanamycin selection (Section 2.3.6). Colony PCR (Section 2.3.7) was performed to identify the putative positive clones (Fig. 3.2). Plasmid DNA was extracted from the putative positive clones and verification of vector-insert junctions as well as the sequence integrity of the inserts were analysed by DNA sequencing (Section 2.3.9). The bait-expressing plasmids were referred as BDC and D-BDC.

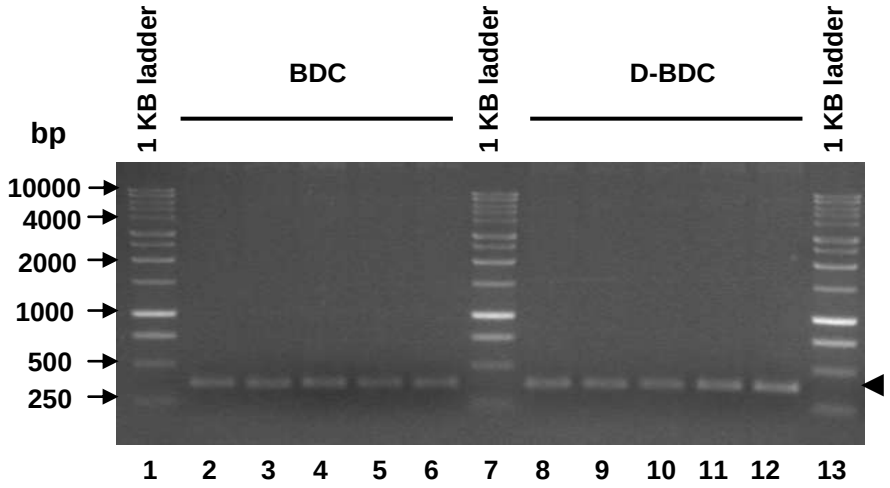

Fig. 3.2: Colony PCR amplification of BDC and D-BDC constructs. WNV and DENV C genes were amplified by PCR from the colonies to identify the putative positive clones. Lane 1: 1 KB DNA ladder; Lanes 2-6: BDC (arrowhead); Lane 7: 1 KB DNA ladder; Lane 8-12: D-BDC (arrowhead); Lane 13: 1 KB DNA ladder. Arrows at the left indicate positions of 250 to 10000 bp sizes from 1 KB DNA ladder.

3.2.2. Expression of West Nile and dengue virus capsid fusion proteins

It is important to transform the bait-expressing plasmids (BDC and D-BDC) into the yeast strain, AH109 before mating with Y182 yeast cells containing prey proteins. Hence, the bait-expressing plasmids (BDC and D-BDC) were transformed individually into AH109 cells (Section 2.6.2). This resulted in the generation of AH109[BDC] and AH109[D-BDC] cells. To test for the expression of fusion protein in AH109[BDC] and AH109[D-BDC] cells, yeast cell lysates were prepared and subjected to Western blotting (Section 2.5.2) using anti-GAL4 DNA binding domain antibody. Both BDC and D-BDC fusion proteins were efficiently expressed in AH109 (Fig. 3.3).

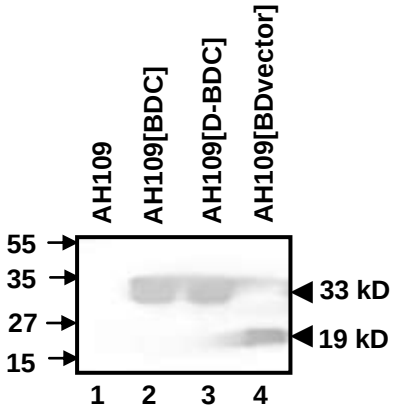

Fig. 3.3: Expression of BDC and D-BDC fusion proteins. AH109 cells were transformed with BDC and D-BDC and pGBKT7 (BD) vector. Cell lysates were subjected to Western blotting. Lane 1: Untransformed AH109; Lane 2: AH109 transformed with BDC; Lane 3: AH109 transformed with D-BDC. Lane 4: AH109 transformed with BD vector. Arrows at the left indicate positions of 15 to 55 kD sizes from pre-stained protein ladder. Arrowheads at the right indicate positions of 19 kD and 33 kD sizes corresponding to the sizes of Gal4 BD domain (BD vector) and WNV/DENV C + Gal4 BD domain (BDC/D-BDC fusions).

3.2.3. Auto-activation assay

The activation of the reporter genes in Y2H system makes use of a transcription event. Hence, the general problem encountered is the activation of transcription by bait proteins non-specifically or in the absence of the interacting partners. It is thus crucial to check if the bait protein of interest is capable of initiating transcription non-specifically. If that is the case, it would seriously affect the successful use of that bait protein in Y2H mating assay.

Auto-activation assay (Section 2.6.3) was thus performed to test for the aberrant activation of reporter genes by BDC and D-BDC in the absence of interacting partners. It is important to ascertain that expression of WNV and DENV C proteins alone in AH109 cells do not lead to the activation of the *HIS3* reporter gene. The bait proteins were singly transformed into AH109 or co-transformed with AD vector and the individual transformants were serially diluted from 10^{-1} to 10^{-6} and plated onto SD-His plates. Auto-activating transformants would activate HIS3 gene and grow on SD-His plates. As indicated in Table 3.1, no intrinsic or non-specific activation for both WNV and DENV C fusions was observed.

Table 3.1: Auto-activation assay for WNV and DENV C fusion proteins

Fusion proteins	Neat	10^{-1}	10^{-2}	10^{-3}	10^{-4}	10^{-5}	10^{-6}
BDC	-	-	-	-	-	-	-
D-BDC	-	-	-	-	-	-	-
BDC + AD vector	-	-	-	-	-	-	-
D-BDC + AD vector	-	-	-	-	-	-	-
p53/T	+++	+++	+++	+++	+++	+++	+++
AH109	-	-	-	-	-	-	-

All serially diluted transformants were plated onto SD-His plates in triplicate. +++, strong growth; -, no growth. AH109 cells co-transformed with pGBKT7-murine p53 and the pGADT7-SV40 large T-antigen (p53/T) served as the positive control while non-transformed AH109 served as negative control.

3.2.4. Yeast mating

To examine whether flavivirus C protein can associate with cellular proteins, WNV/DENV C protein was screened against human brain/liver cDNA yeast two-hybrid library (Section 2.6.5). From 6 x 10^7 cDNA library clones screened, several transformants containing putative WNV/DENV C protein-interacting partners were identified based on the activation of *HIS3* and *ADE2* reporter genes. This was visualized by the growth of the transformants on high stringency QDO selection plates. The authenticity of the interacting partners was further confirmed by plating these transformants on QDO+X-α-Gal plates. True positives obtained from Y2H screening should be able to activate α-galactosidase (α-gal) reporter gene. Such transformants would appear greenish-blue whereas false positives will remain colourless. Several transformants were able to activate α-gal reporter.

3.2.5. Identity of the interacting partners

It is essential to delineate the identity of the interacting partners from the positive transformants (obtained in Section 3.2.4) in order to determine their potential relevance to flavivirus pathogenesis. To achieve this, plasmid DNA was extracted from the putative positive clones (Sections 2.6.6 and 2.6.7) and sequenced (Section 2.3.9) using Matchmaker™ AD insert screening amplimer. The resulting nucleotide sequences were then compared against GenBank non-redundant database using BLASTN and BLASTP algorithms (www.ncbi.nlm.nih.gov/BLAST) with program default parameters. GenBank entries with the highest hit against the library insert sequences were then identified. Host proteins that showed two or more hits in Y2H library screening were listed in Table 3.2 together with their functions. Table 3.3 summarizes the host proteins that showed one hit in Y2H library screening.

Table 3.2: List of identified WNV/DENV C protein-interacting partners with two or more hits in yeast two-hybrid library screening

Library proteins	Flavivirus C protein	No. of clones	Function
Human Sec3 protein (hSec3p, NP_060731.2)	WNV/DENV	6/4	Secretory pathway and vesicular trafficking (Hsu *et al.*, 1999; TerBush *et al.*, 1996)
Calcium-modulating cyclophilin binding ligand (CAML, NP_001736.1)	WNV/DENV	3/4	Involved in Ca signaling pathway and prevents apoptosis (Boya *et al.*, 2004; Edgar *et al.*, 2010; Feng *et al.*, 2002)
Testis-specific protein Y (TSPY, NP_003299.2)	WNV	3	Interacts with EF1a and enhances protein translation (Kido & Lau, 2008)
Protein L-isoaspartyl methyltransferase (PIMT, NP_005380.2)	WNV	3	Repairs isomerized proteins and protects from Bax-induced apoptosis (Huebscher *et al.*, 1999; Shimizu *et al.*, 2005)
Activating transcription factor 6 (ATF6, NP_031374.2)	WNV	3	Unfolded protein response, apoptosis (Manga *et al.*, 2010; Medigeshi *et al.*, 2007; Tanimura *et al.*, 2009)
Vacuolar ATPase (V-ATPase, NP_057025.2)	DENV	2	Acidifies various intracellular organelles and influences low pH dependant-entry and efficient virus egression (Duan *et al.*, 2008; Nishi & Forgac, 2002)
Heat shock protein 27 (HSP 27, NP_001531.1)	DENV	2	Prevents apoptosis (Pasupuleti *et al.*, 2010; Paul *et al.*, 2010)
Heat shock protein 70 (HSP 70, NP_002145.3)	DENV	2	Maintains Ca homeostasis, thereby preventing the initiation of apoptosis (Liu *et al.*, 2006a; Oh & Song, 2006; Tupling *et al.*, 2008)

Table 3.3: List of identified WNV/DENV C protein-interacting partners with only one hit in yeast two-hybrid library screening

Library proteins	Flavivirus C protein	No. of clones	Function
Heat shock protein 90 (HSP 90, NP_002145.3)	WNV/DENV	1	Assists in protein folding, protein degradation and cell signaling (Imai *et al.*, 2003; Jakob *et al.*, 1995; Picard, 2002; Wiech *et al.*, 1992)
Tubulin (NP_1104001.1)	WNV/DENV	1	Trafficking of flavivirus proteins (Chu & Ng, 2002)
Phosphatase Inhibitor (I2PP2A, NP_006232.1)	WNV/DENV	1	Nuclear protein functions as the inhibitor of the serine/threonine phosphatase, PP2A (Hunt *et al.*, 2007)
E3 ubiquitin ligase (dorfin, NP_055063.1)	WNV	1	RING-finger type ubiquitin ligase helps in the formation of ubiquitylated inclusions in neurodegenerative diseases (Hishikawa *et al.*, 2003)
Aquaporin-2 (AQP2, NP_000477.1)	WNV	1	Regulates cAMP-dependent exocytic process and mediates anti-diuretic hormone activity (Szaszak *et al.*, 2008; Takagi *et al.*, 2003)
Human death domain-associated protein (Daxx, NP_001341.1)	DENV	1	Regulates Fas-mediated apoptotic activity (Limjindaporn *et al.*, 2007)

The host proteins, human Sec3 protein (hSec3p) and calcium-modulating cyclophilin binding ligand (CAML) interacted with both WNV and DENV C protein. The known functions of CAML were closely associated with apoptosis (Boya *et al.*, 2004; Edgar *et al.*, 2010; Feng *et al.*, 2002). All the previously identified host interacting proteins of arthropod-borne flavivirus C protein were implicated in the apoptotic function (Lee *et al.*, 2006; Limjindaporn *et al.*, 2007; Netsawang *et al.*, 2010; Oh & Song, 2006; Yang *et al.*, 2008). The hSec3p which is novel and not reported previously was chosen for downstream studies based on its functional relevance (Table 3.2).

From 6 x 10^7 clones screened in the Y2H library, six independent positive clones encoding the carboxy-terminal 72 aa of hSec3p were found to be the binding partner of WNV C protein. Similarly, four clones represented hSec3p as the interacting partner for DENV C protein. The Sec3 protein is one of the eight subunits of the exocyst complex (Lipschutz & Mostov, 2002). In yeast, the exocyst complex plays an important role in the secretory pathway and vesicular trafficking (Hsu *et al.*, 1999; TerBush *et al.*, 1996) by targeting vesicles to the plasma membrane as well as regulating the later phases of exocytosis process (Zhang *et al.*, 2008b). However, the functional role of human Sec3p remains to be defined. Based on the known functions of Sec3p in yeast, it was hypothesized that flavivirus C protein might exploit hSec3p for virus trafficking and release. If the interaction between C protein and hSec3p was disrupted, it could interrupt flavivirus assembly and release.

3.3. VERIFICATION OF CAPSID PROTEIN-hSec3p INTERACTION IDENTIFIED FROM YEAST MATING ASSAY

3.3.1. Yeast two-hybrid (Y2H) assay

The hSec3p isolated from Y2H library screening encoded only the partial hSec3p. Full-length hSec3p was thus cloned in pGADT7 (AD) vector to generate hSec3pf1 plasmid and the resulting plasmid was sequenced (Sections 2.3.4 to 2.3.6). The hSec3p cDNA used in this study showed the exact match with homosapiens Sec3p with accession number NP_060731.2).

To re-affirm the interaction between flavivirus C protein and partial or full-length hSec3p in yeast system, WNV/DENV C protein interacting partners (CIP, i.e. partial hSec3p) or full-length hSec3pf1 were co-transformed into *Saccharomyces cerevisiae* AH109 strain with pGBKT7 (BD) plasmids expressing C proteins (BDC/D-BDC) (Section 2.6.2).

Co-transformants that grew on QDO plates were tested for α-galactosidase production. Strong α-galactosidase signals were obtained for the interaction pairs such as WNV/DENV CIP-BDC/D-BDC and hSec3pf1-BDC/D-BDC pairs (Table 3.4). To eliminate autoactivation (Section 2.6.3), all the BD fusion plasmids were co-transformed with empty AD vector. Likewise, specificity of interaction was tested by co-transforming WNV/DENV CIPs or hSec3pf1 with BD vector containing human lamin-C or empty BD vector. Non-specific interaction or auto-activation was not detected with the isolated library plasmids or with the full-length hSec3pf1 (Table 3.4). This confirmed that the interaction between WNV/DENV C protein and hSec3p was specific and reliable.

Table 3.4: Interaction of WNV/DENV C protein and hSec3p in yeast two-hybrid system, assayed for α-galactosidase activity and *HIS3* autotrophy

AD fusion	BD fusion			
	BDC/D-BDC	Lamin-C	BD vector	p53
WNVCIP3/69/ 77/79/157/342	**+++** (+++)	**-** (-)	**-** (-)	
DENVCIP5/8/88/257	**+++** (+++)	**-** (-)	**-** (-)	
hSec3pf1	**+++** (+++)	**-** (-)	**-** (-)	
AD vector	**-** (-)	**-** (-)	**-** (-)	
SV40 T				**+++** (+++)

WNVCIP or DENVCIP represents WNV/DENV C protein interacting partners. WNVCIP3/69/77/79/157/342 or DENVCIP5/8/88/257 represent the clone numbers (numbers given during Y2H library screening process) showing hSec3p as the interacting partner of C protein. The results obtained from α-galactosidase assay are shown in bold. The relative strength of interaction is determined based on the intensity of the blue phenotype obtained from the positive control after 48 h. Interaction of p53 with SV40 large T-antigen serves as positive control. **+++**, deep blue colonies (strong interaction); **-**, white colonies (no interaction). All the constructs were concurrently assayed for non-specific reporter gene activation by transforming singly or with control BD-Lamin C or BD vector and plated on to SD-His plates. The results obtained from *HIS3* autotrophy are shown in parenthesis. Growth is recorded after 2 days when the positive control shows clear growth. (+++), clear growth (strong interaction); (-), no growth (no interaction). As depicted in the Table, non-specific activation for all the fusions is not observed.

3.3.2. Co-immunoprecipitation

To ensure that the interaction between C protein and hSec3p was not limited by the requirement of nuclear translocation in Y2H system, the hSec3p-C protein interaction was tested in mammalian model (Section 2.7.1). HEK293 cells were infected with WNV/DENV. At 14 h (WNV) and 24 h (DENV) p.i., proteins in cell lysates were precipitated using anti-hSec3p antibody followed by immunoblotting using anti-WNV/DENV C antibody. Lanes 1 and 4 [Fig. 3.4(i)] were loaded with HEK293 cell lysates. Lanes 2 and 5 [Fig. 3.4(i)] were loaded with the mock-infected samples. Lanes 3 and 6 [Fig. 3.4(i)] were loaded with WNV/DENV-infected cell lysates, respectively. The appearance of bands (14 kD) in Lanes 3 and 6 [Fig. 3.4(i)] confirmed the binding between hSec3p and C proteins in HEK293 cells. To ensure the successful precipitation of hSec3p, the precipitated immune complexes were also probed with anti-hSec3p antibody [Fig. 3.4(ii)]. The expression of hSec3p, WNV/DENV C protein and actin loading controls were shown in Fig. 3.4(iii-v). The antibody isotype controls did not pull down the protein of interest [Fig. 3.4(vi)]. No interaction between hSec3p and flavivirus E protein was detected [Fig. 3.5(i)]. These results demonstrated that both WNV and DENV C protein interacted specifically with hSec3p.

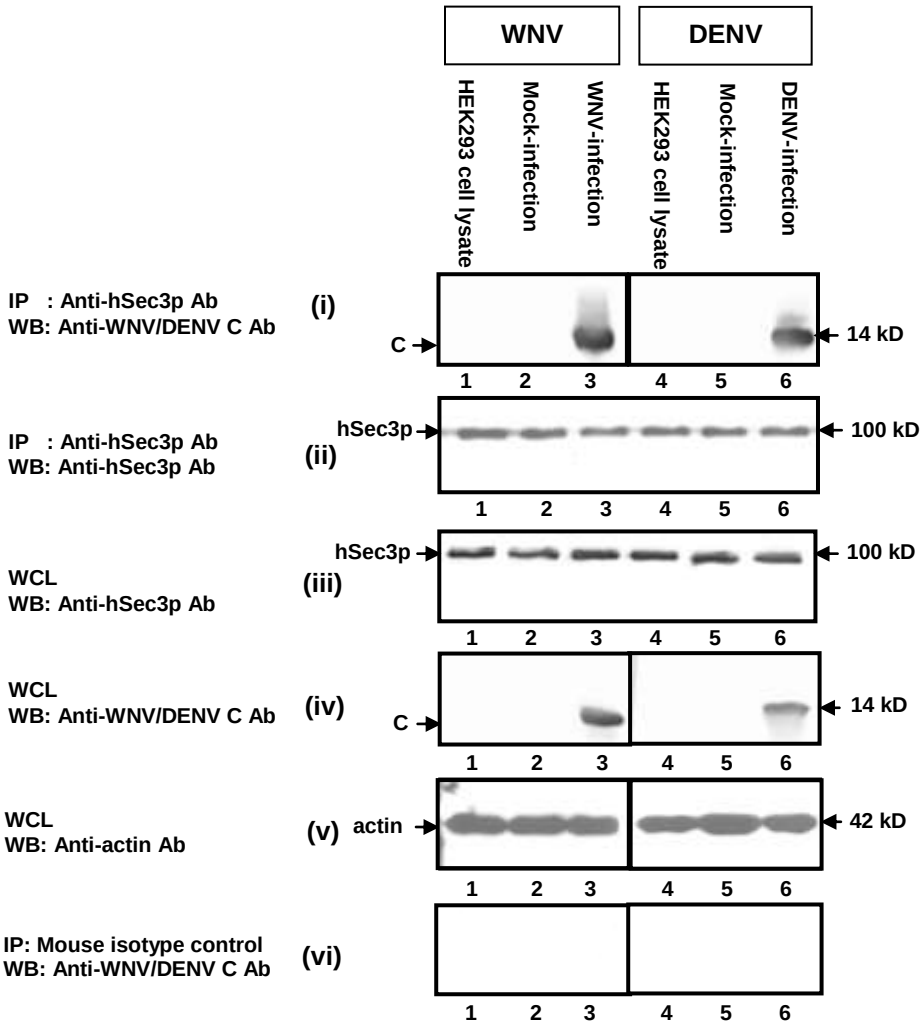

Fig. 3.4: Interaction between WNV/DENV C protein and hSec3p. HEK293 cells were infected with WNV/DENV. (i) Cell lysates were immunoprecipitated with anti-hSec3p mouse antibody and immunoblotted with anti-C rabbit antibody. The presence of bands (14 kD) in Lanes 3 and 6 confirm C protein-hSec3p binding in WNV- and DENV-infected HEK293 cells, respectively. (ii-v) The precipitation efficiency, expression of hSec3p/C protein in cell lysates and actin loading control are detected using anti-hSec3p or anti-WNV/DENV C or anti-actin antibodies. (vi) Antibody isotype control. (IP: Immunoprecipitated sample; WB: Western blot; WCL: Whole cell lysate).

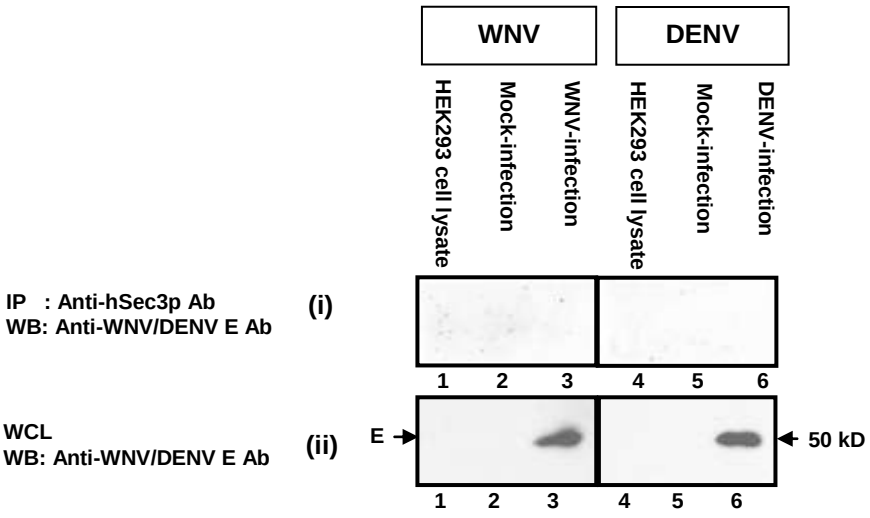

Fig. 3.5: Interaction between WNV/DENV E protein and hSec3p. (i) HEK293 cells were infected with WNV/DENV. (i) Cell lysates were immunoprecipitated with anti-hSec3p antibody and immunoblotted with anti-E antibody. The absence of bands on the immunoblot confirms that there is no interaction between E protein-hSec3p in WNV-/DENV-infected HEK293 cells. (ii) The expression of E protein (50 kD) is detected in WNV-/DENV-infected cells using anti-WNV/DENV E antibody (Lanes 3 & 6). (IP: Immunoprecipitated sample; WB: Western blot; WCL: Whole cell lysate).

3.3.3. Confocal analysis

As further evidence of interaction, WNV/DENV-infected cells were examined for co-localization of the proteins by an immunofluorescence confocal microscopy (Section 2.13). Confocal analysis showed that hSec3p and flavivirus C protein co-localized at the cytoplasmic and perinuclear region (Fig. 3.6). These data supported the physical interaction of WNV/DENV C protein and hSec3p observed with the above biochemical techniques (Sections 3.3.1 and 3.3.2).

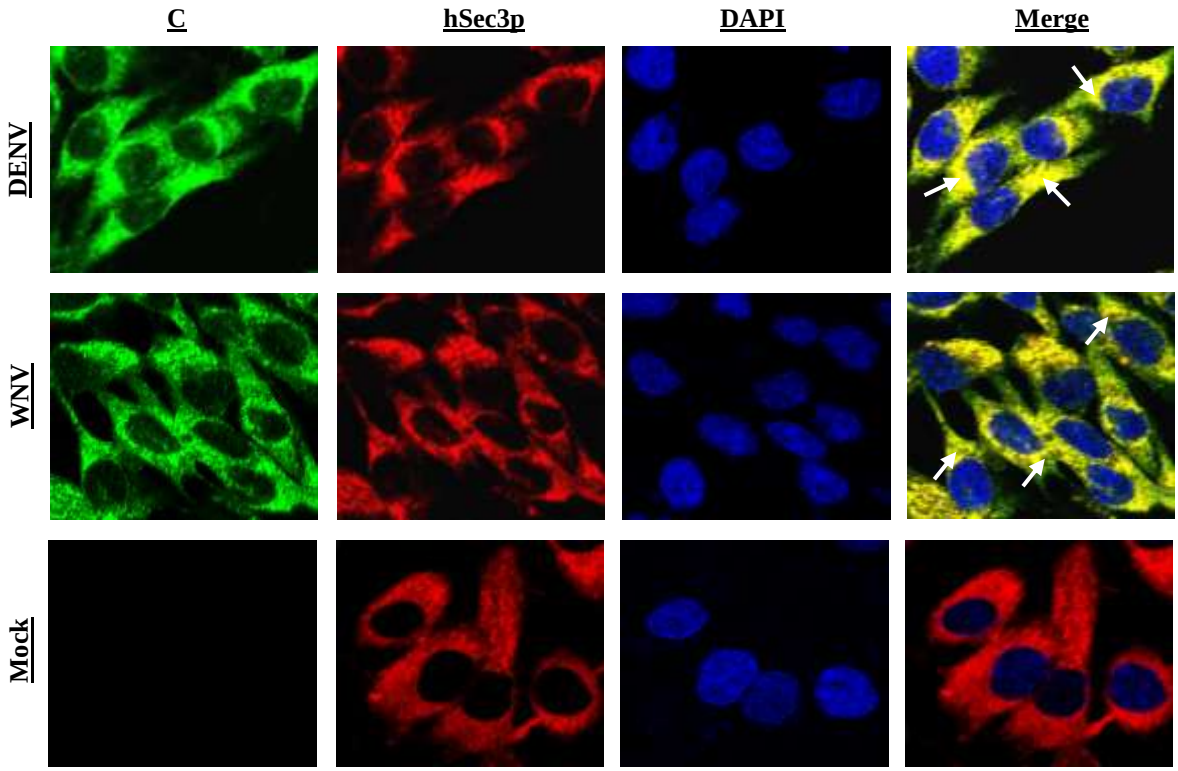

Fig. 3.6: Cellular localization of C protein and hSec3p in WNV-/DENV-infected cells. HEK293 cells were infected with WNV/DENV. The cells were then processed for confocal microscopy using anti-WNV/DENV C or anti-hSec3p antibody together with Alexa488 (green) or Alexa594 (red) secondary antibodies, respectively. Co-localization of hSec3p and C proteins is observed in cytoplasmic and perinuclear regions as depicted in the merged images (arrows). Cell nuclei are stained with DAPI (blue).

3.4. MAPPING THE ASSOCIATION DOMAIN OF FLAVIVIRUS CAPSID PROTEIN AND HUMAN Sec3 PROTEIN

3.4.1. Delineation of flavivirus capsid protein and human Sec3 protein binding domains

In yeast, Sec3p played a crucial role in the secretory pathways and the facilitation of polarized growth (Finger *et al.*, 1998a; Finger & Novick, 1997; Wiederkehr *et al.*, 2003). It was thus hypothesized that flavivirus C protein might exploit hSec3p for virus trafficking and release. Mapping the interacting domains of C protein and hSec3p could aid in the design of novel site-specific peptides that would disrupt the important association between flavivirus C protein and hSec3p.

3.4.2. Delineation of human Sec3 protein-binding domain of flavivirus capsid protein

To define hSec3p binding domain of WNV/DENV C protein, several constructs expressing truncated C proteins were generated (Fig. 3.7). West Nile virus full-length/truncated C proteins were expressed as HA-tagged fusion proteins. The DENV full-length/truncated C proteins were expressed as Myc-tagged fusion proteins as expression of HA-tagged DENV C protein was extremely low.

HEK293 cells were co-transfected with full-length hSec3p (V5-hSec3pf1) and a series of truncated C plasmids. Transfected lysates were precipitated with anti-mouse V5 antibody and immunoblotted with anti-rabbit HA antibody. As shown in Fig. 3.8(i), lysates obtained from mock-transfection (Lane 1) or from co-

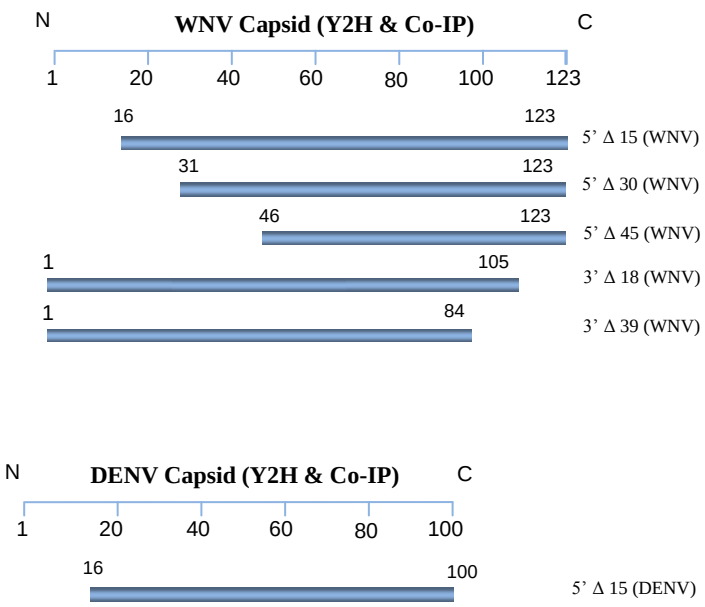

Fig. 3.7: Schematic diagram of 5' and 3' truncated WNV and DENV C mutants. These truncated C plasmids were used for Y2H and Co-IP assays. Truncations were performed by deleting 15 amino acids successively from the N-terminal end of C protein (5'Δ15, 5'Δ30 and 5'Δ45). The cytotoxic motif at the last 18 amino acids (3'Δ18) and the NLS domain together with the cytotoxic motif (3'Δ39) were truncated from the C-terminal end of C protein.

transfection with V5-hSec3pf1 and HAC5'△15, HAC5'△30 or HAC5'△45 (Lanes 3, 4 & 5) did not show any interaction. In contrast, lysates from co-transfection with V5-hSec3pf1 and HAC, HAC3'△18 or HAC3'△39 [Lanes 2, 6 & 7 in Fig. 3.8(i)] showed interactions. To confirm the successful precipitation of hSec3p, the precipitated complexes were also probed with anti-V5 antibody [Fig. 3.8(ii)]. The amount of V5-tagged hSec3p and WNV C protein in whole cell lysates was shown in Fig. 3.8(iii & iv). Actin loading controls were shown in Fig. 3.8(v). Identical hSec3p-binding domain was obtained from DENV C protein [Fig. 3.8(vii-xi)]. The antibody isotype controls did not pull down the protein of interest [Fig. 3.8(vi and xii)]. The reciprocal Co-IP performed showed the same results (Fig. 3.9). This confirmed that the first 15 aa of WNV/DENV C protein were important for hSec3p binding. Similar results were obtained from Y2H assay (Table 3.5).

3.4.3. Delineation of flavivirus capsid protein-binding region of human Sec3 protein

The C protein-binding region of hSec3p was also defined using Y2H (Section 2.6.2) and Co-IP (Section 2.7.1) assays. Several constructs expressing truncated hSec3p were generated (Fig. 3.10). Plasmids encoding full-length or truncated hSec3p were co-transfected with HAC (Fig. 3.11) or Myc-C (Fig. 3.12) in HEK293 cells (Section 2.3.13). As depicted in Figs. 3.11(i) and 3.12(i), lysates from mock-transfection (Lane 1) or from HAC/Myc-C/V5-hSec3pf5 co-transfection (Lane 3) did not show any interaction. In contrast, lysates from co-

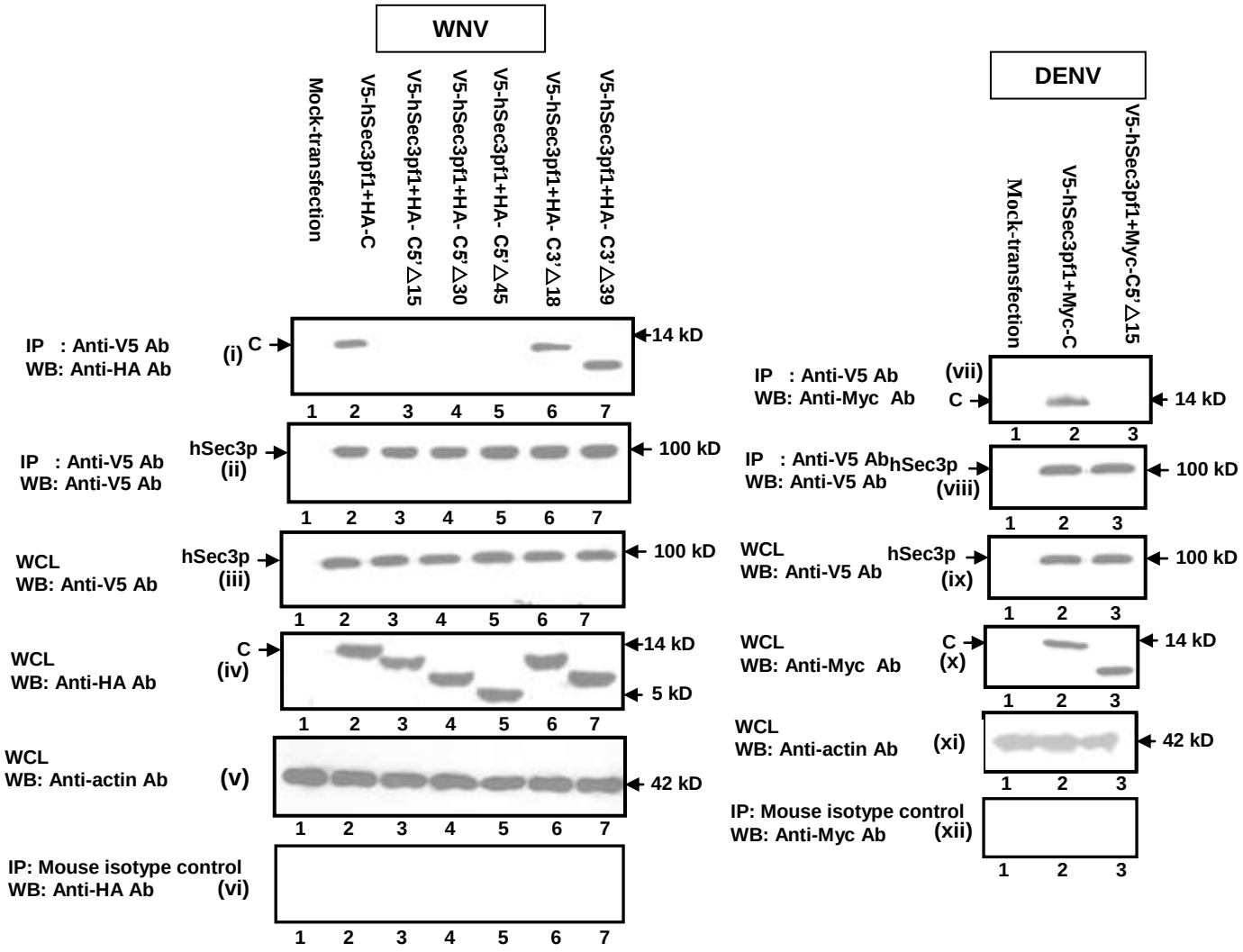

Fig. 3.8: Delineation of hSec3p-associating domain of C protein. (i-vi) Delineation of hSec3p-associating domain of WNV C protein. (i) HEK293 cells were co-transfected with V5-hSec3pf1 and full-length/truncated C plasmids. Cell lysates were immunoprecipitated using anti-V5 mouse antibody and immunoblotted with anti-HA rabbit antibody. The absence of bands in Lanes 3, 4 and 5 indicate that the first 15 aa of WNV C protein are required for hSec3p binding. (ii-vi) Immunoprecipitation control, expression controls, actin loading control and antibody isotype control. (vii-xii) Delineation of hSec3p-associating domain of DENV C protein. (vii) HEK293 cells were co-transfected with V5-hSec3pf1 and full-length/truncated C plasmids. Cell lysates were immunoprecipitated using anti-V5 mouse antibody and immunoblotted using anti-Myc rabbit antibody. The absence of band in Lane 3 indicates that the first 15 aa of DENV C protein are required for association with hSec3p. (viii-xii) Immunoprecipitation control, expression controls, actin loading control and antibody isotype control. (IP: Immunoprecipitated sample; WB: Western blot; WCL: Whole cell lysate).

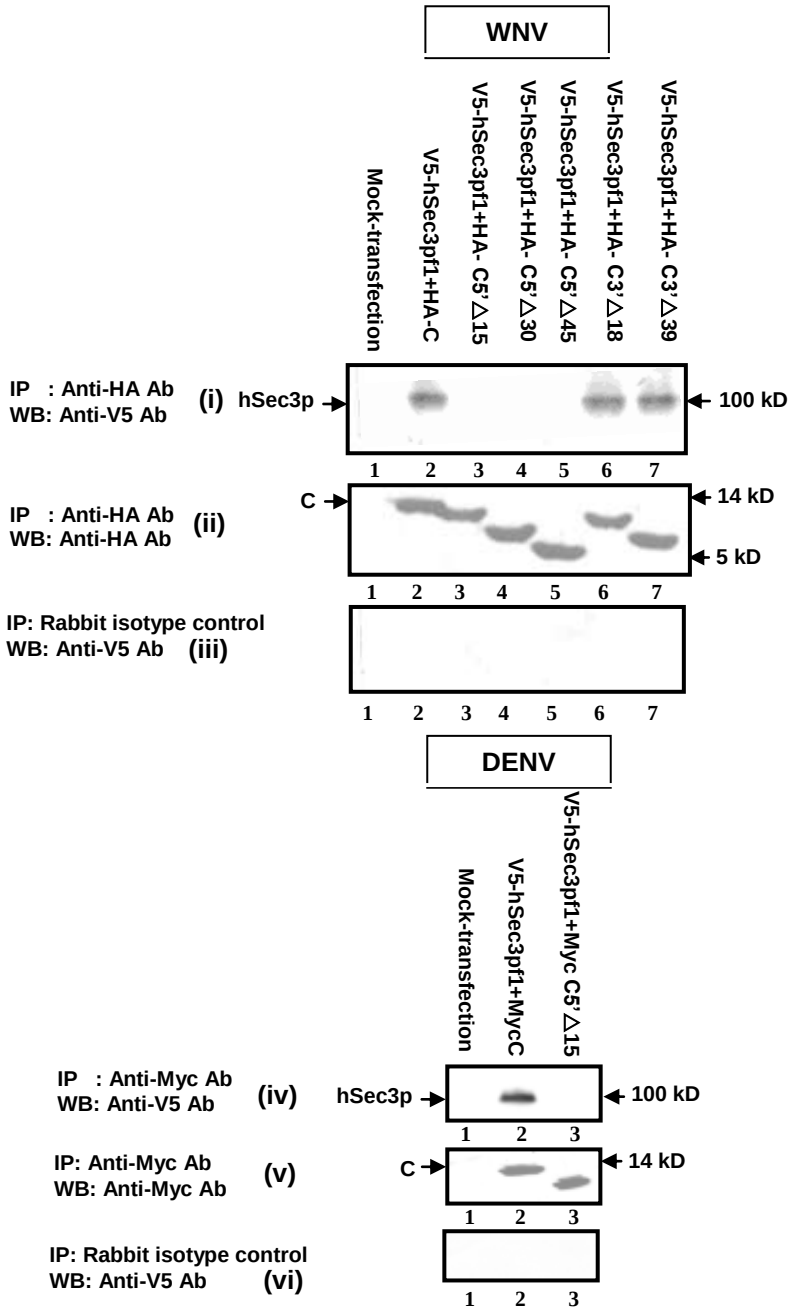

Fig. 3.9: Reciprocal Co-IP to delineate hSec3p-associating domain of C protein. HEK293 cells were co-transfected with V5-hSec3pf1 and full-length/truncated C plasmids. Cell lysates were immunoprecipitated using (i) anti-HA rabbit or (iv) anti-Myc rabbit antibody and analyzed by immunoblotting using anti-V5 mouse antibody. (i) The absence of bands in Lanes 3, 4 & 5 and (iv) Lane 3 indicate that the first 15 aa of WNV/DENV C protein are required for association with hSec3p. (ii & v) Immunoprecipitation using anti-HA/Myc antibody and immunoblotting with anti-HA/Myc antibody to ensure successful immunoprecipitation in all experimental groups. (iii & vi) Reciprocal immunoprecipitation using rabbit antibody isotype control and immunoblotting with anti-V5 antibody. (IP: Immunoprecipitated sample; WB: Western blot; WCL: Whole cell lysate).

Table 3.5: Mapping the hSec3p binding domain of WNV C protein in the yeast two-hybrid system, assayed for α-galactosidase activity and *HIS3* autotrophy.

AD fusion	BD fusion			
	hSec3pf1	**Lamin-C**	**BD vector**	**p53**
C	**+++** (+++)	**-** (-)	**-** (-)	
C5'△15	**-** (-)	**-** (-)	**-** (-)	
C5'△30	**-** (-)	**-** (-)	**-** (-)	
C5'△45	**-** (-)	**-** (-)	**-** (-)	
C3'△18	**+++** (++)	**-** (-)	**-** (-)	
C3'△39	**+++** (++)	**-** (-)	**-** (-)	
AD vector	**-** (-)	**-** (-)	**-** (-)	
SV40 T				**+++** (+++)

The results obtained from α-galactosidase assay are shown in bold. The relative strength of interaction is determined based on the intensity of the blue phenotype obtained from the positive control after 48 h. Interaction of p53 with SV40 large T-antigen serves as positive control. **+++**, deep blue colonies (strong interaction); **-**, white colonies (no interaction). All the constructs were concurrently assayed for non-specific reporter gene activation by transforming singly or with control BD-Lamin C or BD vector and plated on to SD-His plates. The results obtained from *HIS3* autotrophy are shown in parenthesis. Growth is recorded after 2 days when the positive control shows clear growth. (+++), clear growth (strong interaction); (++), moderate growth (moderate interaction); (-), no growth (no interaction). As depicted in the Table, non-specific activation is not observed for all the fusions. All results shown are representatives of at least twelve independent transformants.

transfection with HAC/Myc-C and V5-hSec3pf1 or V5hSec3pf6 [Lanes 2 & 4 in

transfection with HAC/Myc-C and V5-hSec3pf1 or V5hSec3pf6 [Lanes 2 & 4 in

Figs. 3.11(i) and 3.12(i)] showed interactions, confirming that the last 15 aa of hSec3p was crucial for binding. Similar results were obtained from Y2H assay (Table 3.6). To facilitate specific domain identification, the protein sequence of hSec3p was subjected to ELM software analysis (Section 2.14). ELM analysis indicated that the last 15 aa of hSec3p contains putative PDZ and SH2 domains. Mutagenesis studies performed on the putative PDZ [(aa 867 and 869), Lane 5, Figs. 3.11(i) and 3.12(i)] and SH2 [(aa 871), Lane 6, Figs. 3.11(i) and 3.12(i)] binding motifs in the last 15 aa of hSec3p revealed that the aa 871 in the SH2 domain of hSec3p was crucial for this interaction. The reciprocal Co-IP performed showed identical results (Fig. 3.13). This indicated that the SH2 binding motif at the aa residue 871 of hSec3p was crucial for C protein binding.

Overall, yeast two-hybrid library screening performed using WNV/DENV C protein as bait identified several host interacting partners of C protein. Among the new cellular proteins found to interact with WNV/DENV C protein, hSec3p was chosen for further studies due its functions known in yeast. Using a combination of molecular, biochemical and microscopic analyses, the domains mediating the interactions of C protein and hSec3p was delineated and shown that the first 15 amino acids of WNV/DENV C protein is crucial to mediate the interaction between C protein and hSec3p.

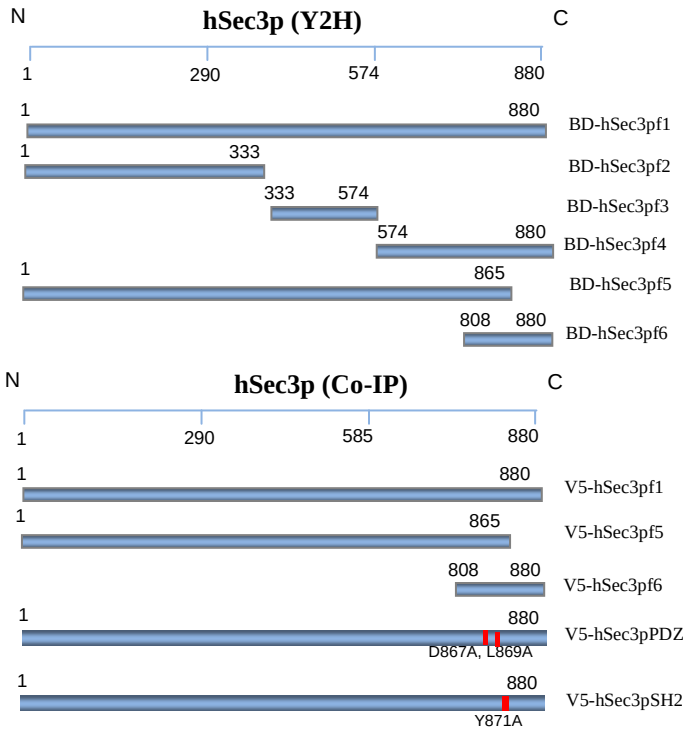

Fig. 3.10: Schematic diagram of 5' and 3' truncated hSec3p mutants. The truncated plasmids of hSec3p were generated at random and were used for Y2H and Co-IP assays.

Table 3.6: Mapping the WNV and DENV C protein binding domain of hSec3p in the yeast two-hybrid system, assayed for α-galactosidase activity and *HIS3* autotrophy.

AD fusion	BD fusion								
	hSec3pf1	hSec3pf2	hSec3pf3	hSec3pf4	hSec3pf5	hSec3pf6	Lamin-C	BD vector	p53
C (WNV and DENV)	**+++** (+++)	**-** (-)	**-** (-)	**+++** (+++)	**-** (-)	**+++** (+++)	**-** (-)	**-** (-)	
AD vector	**-** (-)	**-** (-)	**-** (-)	**-** (-)	**-** (-)	**-** (-)	**-** (-)	**-** (-)	
SV40 T									**+++** (+++)

The results obtained from α-galactosidase assay are shown in bold. The relative strength of interaction is determined based on the intensity of the blue phenotype obtained from the positive control after 48 h. Interaction of p53 with SV40 large T-antigen serves as positive control. **+++,** deep blue colonies (strong interaction); **-**, white colonies (no interaction). All the constructs were concurrently assayed for non-specific reporter gene activation by transforming singly or with control BD-Lamin C or BD vector and plated on to SD-His plates. The results obtained from *HIS3* autotrophy are shown in parenthesis. Growth is recorded after 2 days when the positive control shows clear growth. (+++), clear growth (strong interaction); (++), moderate growth (moderate interaction); (-), no growth (no interaction). As depicted in the Table, non-specific activation is not observed for all the fusions. All results shown are representatives of at least twelve independent transformants.

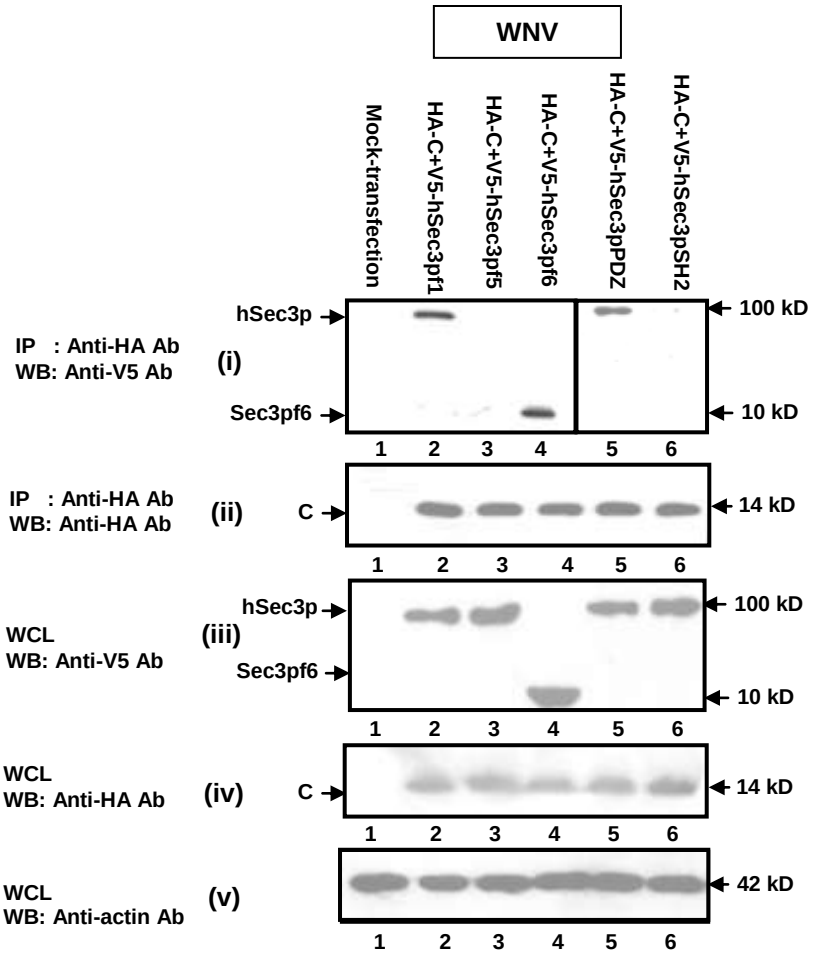

Fig. 3.11: Delineation of WNV C protein-binding domain of hSec3p. (i) HEK293 cells were mock-transfected (Lane 1) or co-transfected with HAC and full-length (Lane 2) or truncated (Lanes 3 & 4) or mutated (Lanes 5 & 6) hSec3p plasmids. Cell lysates were immunoprecipitated using anti-HA antibody and immunoblotted with anti-V5 antibody. The absence of bands in Lanes 3 and 6 show that SH2 binding motif in the last 15 aa of hSec3p is important for binding with WNV C protein. (ii-v) Immunoprecipitation control, expression controls and actin loading controls. (IP: Immunoprecipitated sample; WB: Western blot; WCL: Whole cell lysate).

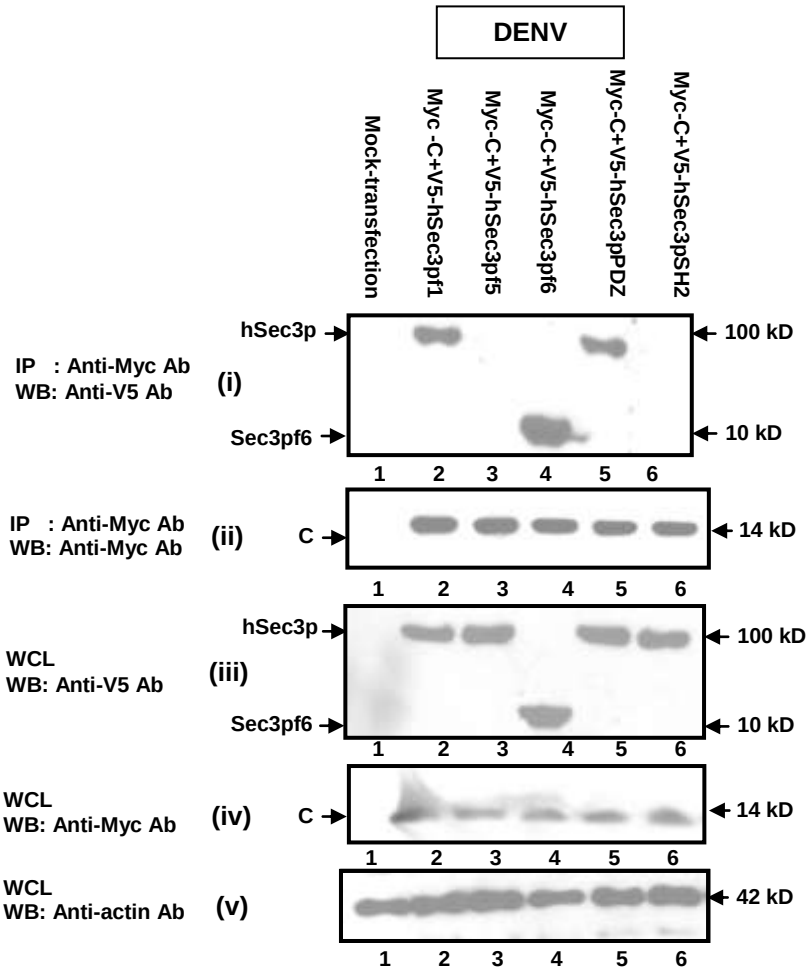

Fig. 3.12: Delineation of DENV C protein-binding domain of hSec3p. (i) HEK293 cells were mock-transfected (Lane 1) or co-transfected with Myc-C and full-length (Lane 2) or truncated (Lanes 3 & 4) or mutated (Lanes 5 & 6) hSec3p plasmids. Cell lysates were immunoprecipitated using anti-Myc antibody and immunoblotted with anti-V5 antibody. The absence of bands in Lanes 3 and 6 show that SH2 binding motif in the last 15 aa of hSec3p is important for binding with DENV C protein. (ii-v) Immunoprecipitation control, expression controls and actin loading controls. (IP: Immunoprecipitated sample; WB: Western blot; WCL: Whole cell lysate).

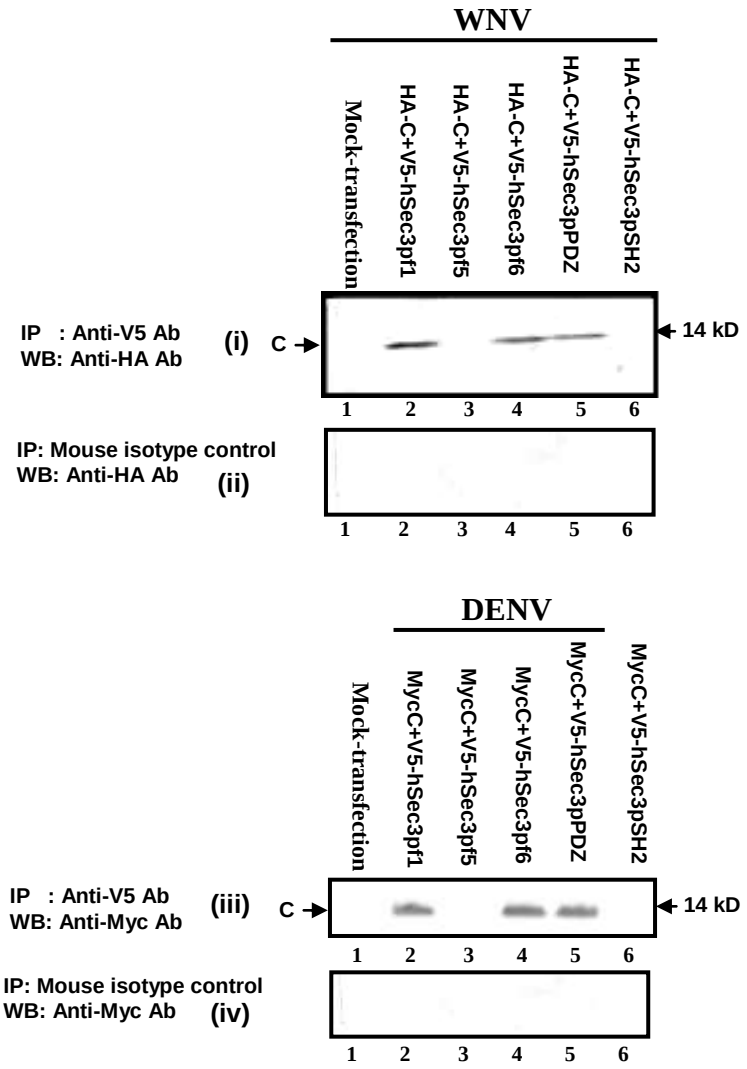

Fig. 3.13: Reciprocal Co-IP to delineate C protein-binding domain of hSec3p. HEK293 cells were mock-transfected (Lane 1) or co-transfected with (i) HAC or (iii) Myc-C and full-length (Lane 2) or truncated (Lanes 3 & 4) or mutated (Lanes 5 & 6) hSec3p plasmids. Cell lysates were immunoprecipitated using anti-V5 antibody and immunoblotted with (i) anti-HA or (iii) anti-Myc antibody. The absence of bands in Lanes 3 and 6 show that SH2 binding motif in the last 15 aa of hSec3p is important for binding with C protein. (ii & iv) Reciprocal immunoprecipitation using mouse antibody isotype control and immunoblotting with (ii) anti-HA or (iv) anti-Myc antibody. (IP: Immunoprecipitated sample; WB: Western blot; WCL: Whole cell lysate).

CHAPTER 4

RESULTS

4.0. INFLUENCE OF HUMAN Sec3 PROTEIN ON FLAVIVIRUS LIFE CYCLE

4.1. INTRODUCTION

Having established the interaction between flavivirus C protein and hSec3p, the next question to address is if hSec3p influences flavivirus production. To investigate the effect of hSec3p on flavivirus life-cycle, it was essential to create a controlled environment whereby the level of hSec3p remained approximately constant. HEK293 cells were thus transduced using lentiviral system either over-expressing hSec3p gene or causing a knock-down of hSec3p gene. To ensure consistent and reproducible experimental outcomes, HEK293 stable cell lines representing hSec3p over-expression or hSec3p knock-down were created (Section 2.8). The effect of hSec3p over-expression and knock-down on flavivirus production was examined. This was followed by investigation on the limiting step(s) which hSec3p targets in flavivirus life-cycle.

4.2. OVER-EXPRESSION AND KNOCK-DOWN OF HUMAN Sec3 GENE USING LENTIVIRUS SYSTEM

4.2.1. Determination of Blasticidin concentration to select stably-transduced HEK293 cells

The vector, pLenti6/BLOCK-iT™-DEST, used to produce lentivirus for transduction of HEK293 cells contained a Blasticidin resistant gene. This permitted for the selection of stably-transduced HEK293 cells using Blasticidin. To allow rapid and efficient selection of cells stably-expressing the desired gene sequences, it was essential to determine the minimum concentration of Blasticidin

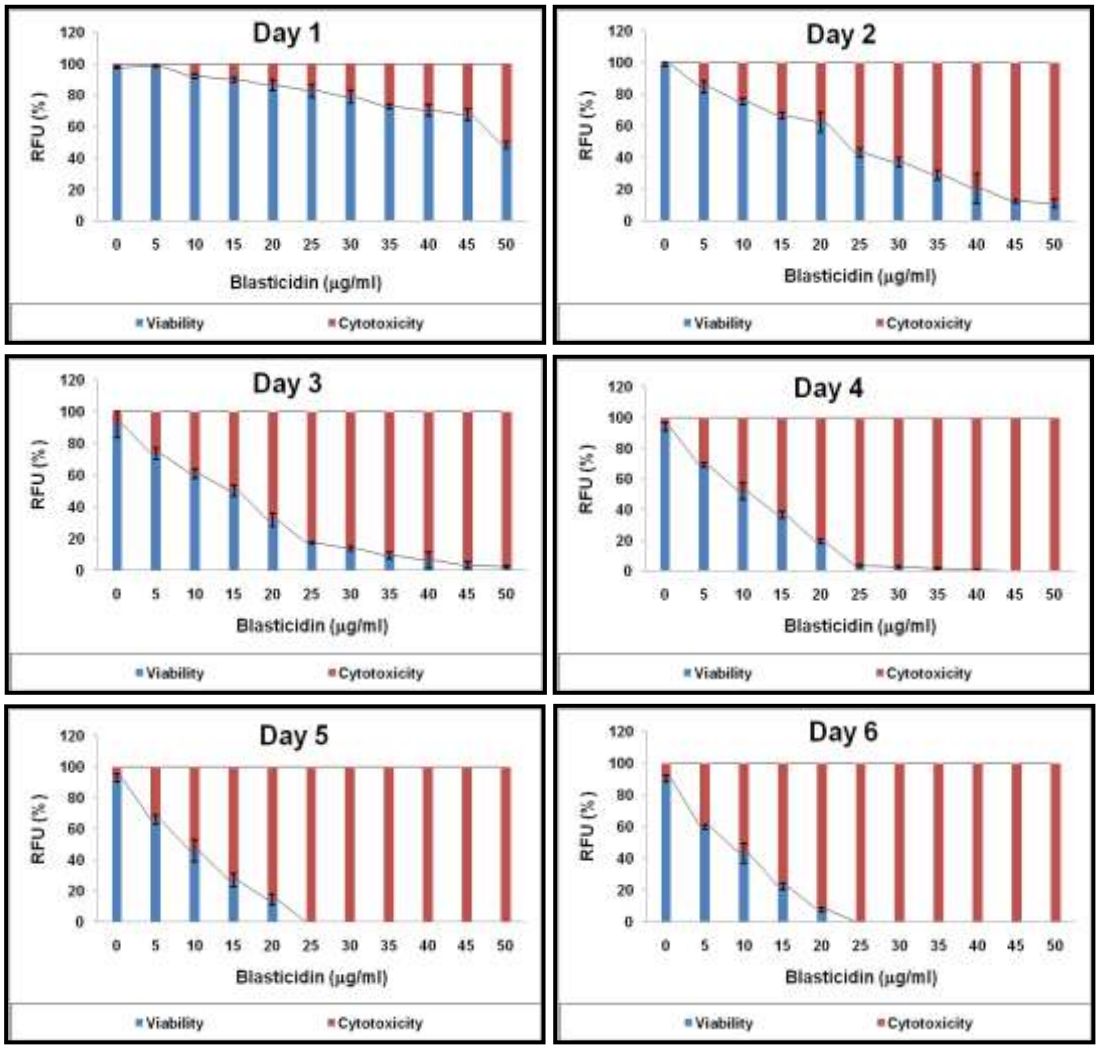

Fig. 4.1: Determination of Blasticidin concentration to select stably-transduced HEK293 cells. Various concentrations of Blasticidin were added to the growth media of HEK293 cells. It is determined that a minimum of 25 µg/ml concentration of Blasticidin is essential to select for stably-transduced cells in the quickest time possible.

necessary to kill off large amounts of non-transduced HEK293 cells in the shortest time possible. Increasing concentrations of Blasticidin (0-50 μg/ml) was added to the growth media of HEK293 cells and observed for cytotoxic effects (Section 2.8.9). It was determined that Blasticidin at 25 μg/ml concentration was adequate to kill significant number of non-transduced cells in 4 days (Fig. 4.1).

4.2.2. Establishment of stably-transduced HEK293 cells

Although 25 μg/ml of Blasticidin was adequate to kill significant number of non-transduced cells (Fig. 4.1), 30 μg/ml of Blasticidin was used to select stably-transduced HEK293 cells to enhance the efficiency of selection. After two weeks of selection, the stably-transduced hSec3p293OE and hSec3p293KD cells were lysed to analyse the hSec3p level (Section 2.8.8) by Western blot [Fig. 4.2(i)]. A highly-expressed protein, β-actin, was used as a loading control [Fig. 4.2(ii)]. Band quantification of the immunoblot revealed that lentivirus-mediated gene knock-down decreased the endogenous hSec3p level by 75% in hSec3p293KD cells. Seventy-one percent increase in hSec3p expression was seen in hSec3p293OE cells [Fig. 4.2(iii)].

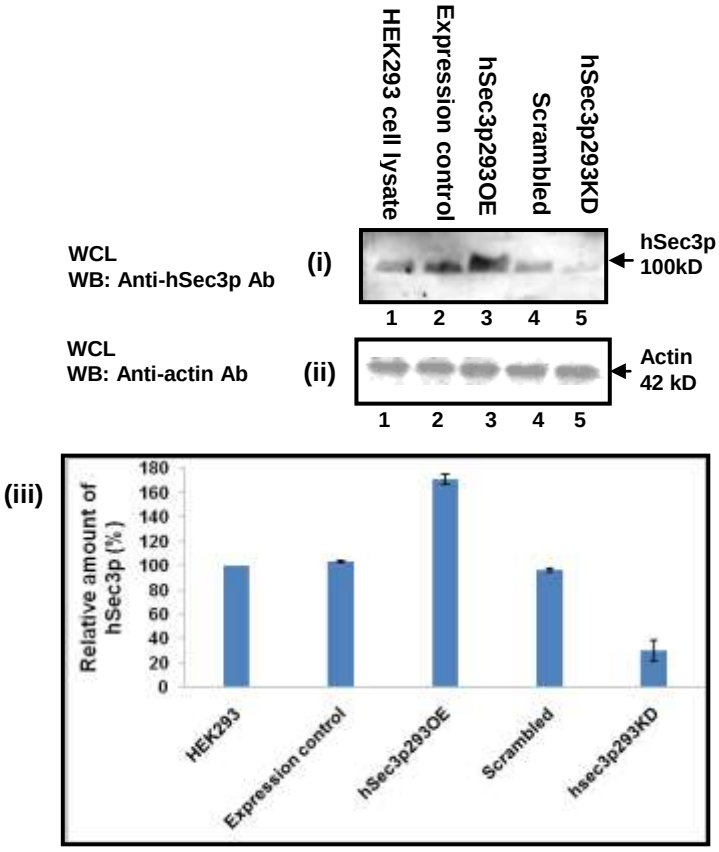

Fig. 4.2: Western blot analysis showing the effect of hSec3p gene silencing and over-expression in HEK293 cells. (i) The lysates from HEK293, Expression control (control plasmid-transduced HEK293 cells), hSec3p293OE, Scrambled (scrambled sequence-transduced HEK293 cells) and hSec3p293KD cells were subjected to Western blotting using anti-hSec3p antibody. Increased hSec3p level is detected in hSec3p293OE cells (Lane 3) and decreased level is observed in hSec3p293KD cells (Lane 5). (ii) The actin loading controls are shown to confirm the equal loading. (iii) The hSec3p bands were quantified using GeneTools program (Syngene). An arbitrary density of 100% is attributed to the endogenous hSec3p level in HEK293 cell lysate. As revealed by the densitometric analysis, lentivirus-mediated gene knock-down decrease the endogenous hSec3p level by 75% in hSec3p293KD cells while 71% increase in hSec3p expression is seen in hSec3p293OE cells.

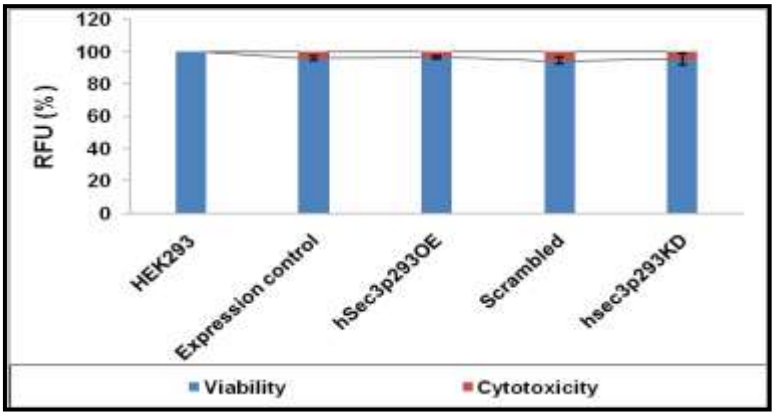

Fig. 4.3: Relative cytotoxicity and viability of transduced-HEK293 cells. The viability and cytotoxicity of HEK293, Expression control, hSec3p293OE, Scrambled and hSec3p293KD cells were tested. The stably-transduced cells are shown to be viable and there is no cytotoxicity related to transduction.

4.2.3. Determination of transduction-related cytotoxicity

To determine whether there was any transduction-associated cytotoxicity, cytotoxicity and viability test was performed on hSec3p293OE and hSec3p293KD cells (Section 2.8.9). The results indicated that the stably-transduced cells had a cytotoxicity and viability profile like that of the non-transduced HEK293 cells. This indicated that there was no transduction-associated cytotoxicity and the transduced cells were highly viable (Fig. 4.3).

4.3. EFFECT OF OVER-EXPRESSION AND KNOCK-DOWN OF HUMAN Sec3 PROTEIN ON THE ABUNDANCE OF PROTEINS INVOLVED IN SECRETORY PATHWAY

Human Sec3 protein is one of the exocyst components involved in secretory pathway. Over-expression and knock-down of hSec3p could therefore affect the abundance of other proteins involved in secretory pathway. It is thus essential to check if differential expression of hSec3p alters the abundance of several proteins involved in secretory pathway. The other components of exocyst complex, Exo70 and human Sec6 protein were chosen to investigate if the abundance of these proteins (involved in secretory pathway) was altered when hSec3p was differentially expressed. Western blotting (Section 2.5.2) of whole cell lysates obtained from HEK293, hSec3p293KD and hSec3p293OE cells were performed using anti-Exo70 and anti-Sec6 antibodies (Fig. 4.4). The results demonstrated that the abundance of host proteins involved in secretory pathway was not affected by the over-expression or knock-down of hSec3p.

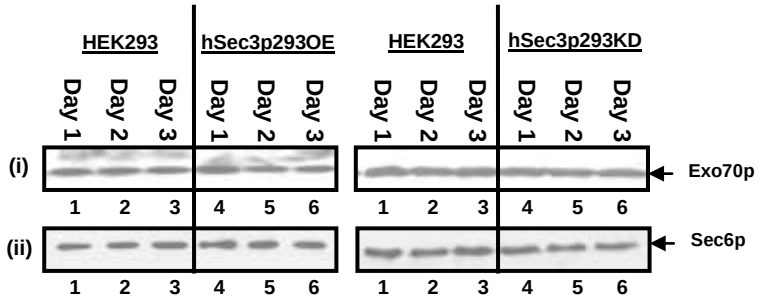

Fig. 4.4: Western blotting of whole cell lysates derived from HEK293, hSec3p293OE and hSec3p293KD cells. Twenty-five micrograms of cell lysate from each experimental group was separated using SDS-PAGE gel and probed with (i) anti-Exo70 or (ii) anti-hSec6 antibodies. There are no observable differences in the levels of proteins involved in the secretory pathway in hSec3p293OE/KD cells compared to HEK293 cells.

4.4. EFFECT OF HUMAN Sec3 PROTEIN OVER-EXPRESSION AND KNOCK-DOWN ON FLAVIVIRUS PRODUCTION

4.4.1. Influence of human Sec3 protein on flavivirus production

After establishing hSec3p293OE and hSec3p293KD cells, the effect of hSec3p on virus production was examined. Based on the known functions of Sec3p in yeast, it was deduced that the knock-down of hSec3p should prevent C protein-exocyst association and disrupt virus production and subsequently virus egression. Similarly, over-expression of hSec3p should facilitate efficient C protein-exocyst association and enhance virus production and transport. This hypothesis was tested by infecting hSec3p293KD and hSec3p293OE cells with WNV or DENV. As shown in Fig. 4.5, an increase in virus titre from as early as 6 h p.i. in WNV(Sarafend) and 15 h p.i. in DENV was detected in hSec3p293KD cells compared to virus-infected HEK293 cells. The maximal increment in virus titre was seen at 18 h and 72 h p.i. for WNV(Sarafend) and DENV, respectively. Following these time points, the differences in virus titres between infected HEK293 and hSec3p293KD cells started to decline. No significant difference in the virus titres was observed in virus-infected control vector/scrambled HEK293 cells. This confirmed that the increase or decrease in virus titres observed in hSec3p293KD or hSec3p293OE cells were specifically due to modulation of hSec3p levels.

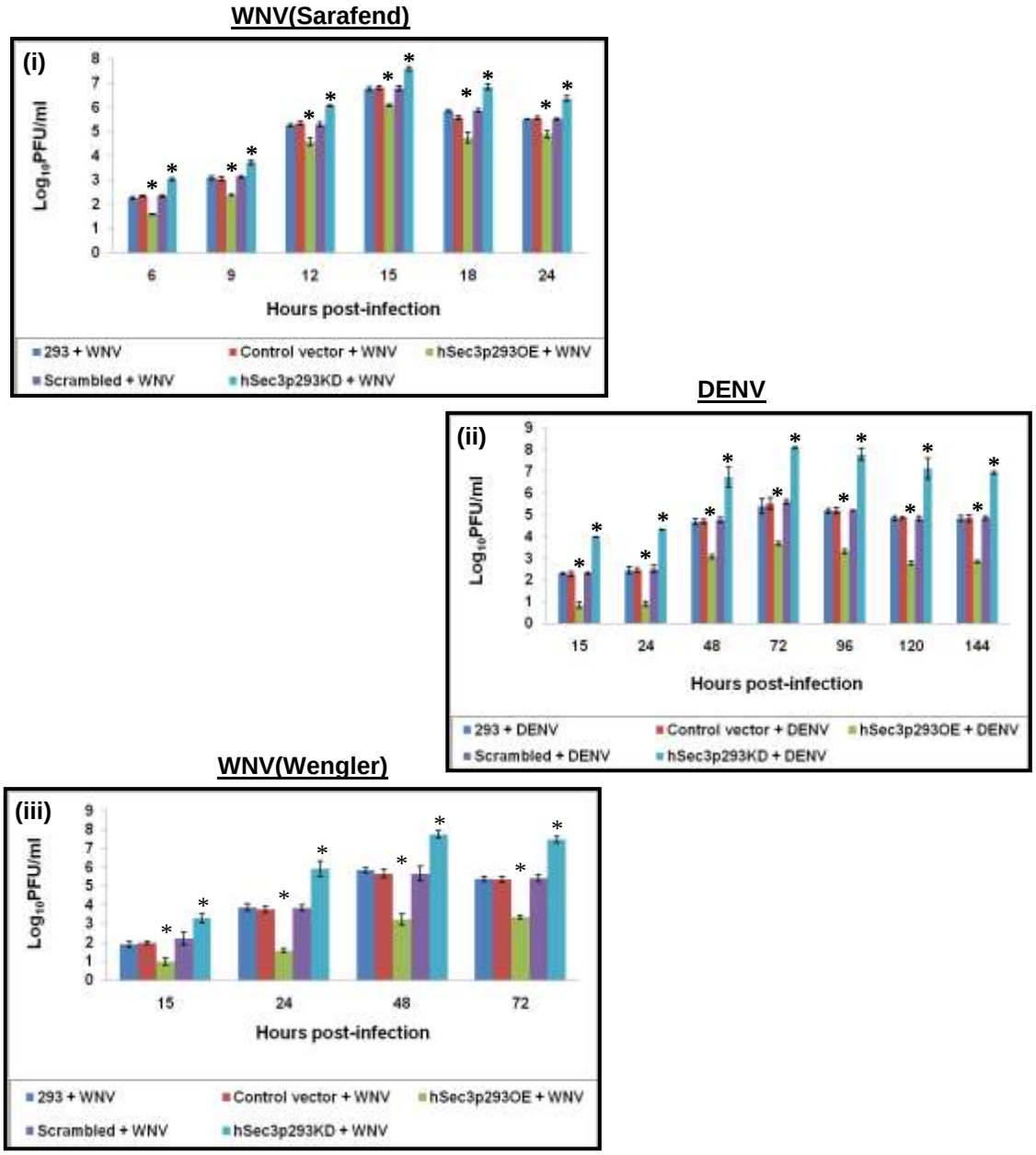

Fig. 4.5: Effect of hSec3p KD/OE on virus titres following virus infection. HEK293, scrambled/control vector + HEK293 and hSec3p293KD/OE cells were infected with (i) WNV(Sarafend) or (ii) DENV or (iii) WNV(Wengler). The supernatants were harvested at the indicated timings to determine virus titres. The results are representatives of 3 independent experiments ± standard deviation. A significant increment or decrement in virus titres is detected in WNV(Sarafend)/DENV/WNV(Wengler)-infected hSec3p293KD/OE cells compared to scrambled/control vector-transduced 293 cells. * indicates $P<0.05$ as compared to (i) 293 + WNV(Sarafend) or (ii) 293 + DENV or (iii) 293 + WNV(Wengler) infections.

The reverse trend was observed in WNV-/DENV-infected hSec3p293OE cells (Fig. 4.5). Reduction in virus titre was observed at as early as 6 h p.i. in WNV(Sarafend) and 15 h p.i. in DENV in hSec3p293OE cells compared to virus-infected HEK293 cells. The maximal decrement in virus titre was seen at 18 h and 120 h p.i. for WNV(Sarafend) and DENV, respectively. Similar to hSec3p293KD cells, the differences in virus titres between infected HEK293 and hSec3p293OE cells were reduced at later timings.

These observations contradicted the initial hypothesis. Instead, hSec3p was shown to be a negative regulator of flavivirus infection. It was also observed that changes in hSec3p expression had a more pronounced effect on DENV compared to WNV(Sarafend). Dengue virus has a relatively longer latent period [(12-24 h) (Helt & Harris, 2005) compared to WNV(Sarafend) which possess a very short latent period [(6 h) (Ng *et al.*, 2001)]. The hSec3p might require longer period to execute its anti-viral effect. Since DENV possess longer latent period, hSec3p might have enough time to fully implement its anti-viral activity compared to WNV(Sarafend).

To test this postulation, WNV(Wengler) was chosen since WNV(Wengler) has a similar length of replication cycle as that of DENV. WNV(Wengler) was used to infect hSec3p293KD and hSec3p293OE cells. Similar to WNV(Sarafend) and DENV, an increase in virus titre was observed in WNV(Wengler) infected-hSec3p293KD cells and a decrease was detected in WNV(Wengler) infected-

hSec3p293OE cells [Fig. 4.5(iii)]. Furthermore, it was also observed that differential expression of hSec3p showed a more pronounced effect on WNV(Wengler) compared to WNV(Sarafend). This demonstrated that the duration of latent period would influence the anti-viral effect of hSec3p.

4.4.2. Effect of capsid protein-binding defective human Sec3 protein mutant on flavivirus production

The effect of C protein-binding defective hSec3p mutant, hSec3pSH2 on flavivirus production was then examined to check if hSec3p needed to physically bind to C protein to negatively influence flavivirus production. The V5-hSec3pSH2 mutant was over-expressed in HEK293, hSecp293OE and hSec3p293KD cells and infected with WNV and DENV. The growth characteristics of both WNV and DENV were determined by plaque assay (Sections 2.2.4 and 2.2.5). When hSec3pSH2 mutant was over-expressed in HEK293, hSec3p293OE and hSec3p293KD cells, the virus titres were decreased in HEK293, hSec3p293OE and hSec3p293KD cells (Fig. 4.6). The inhibitory trend of hSec3pSH2 mutant was surprisingly similar to that observed with full-length V5-hSec3pf1-transfected cells. This indicated that the physical binding between hSec3p and C protein was not essential to influence flavivirus production. The physical binding between hSec3p and C protein might be required to negate the anti-viral activity of hSec3p (Chapter 6). Moreover, there could be other unknown factor(s) mediating the effect of hSec3p on flavivirus production (Chapter 5).

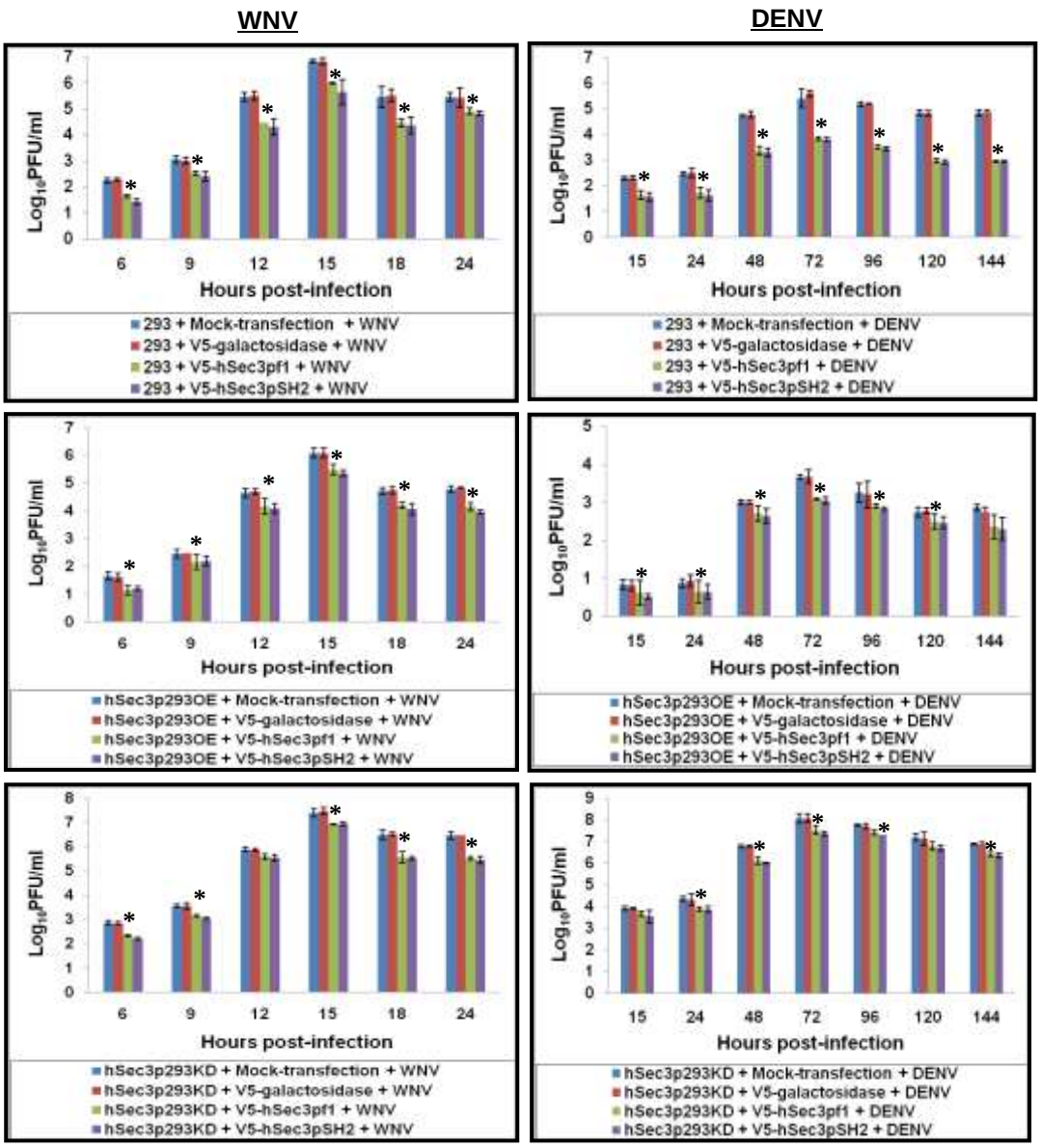

Fig. 4.6: Growth kinetics of WNV/DENV in hSec3pSH2 mutant-over-expressed 293, hSec3p293OE and hSec3p293KD cells. HEK293, hSec3p293OE and hSec3p293KD cells were transfected with V5-hSec3pSH2/V5-hSec3pf1and infected with WNV or DENV. The culture supernatants were harvested over time and virus titres were determined by plaque assay. The results are representatives of 3 independent experiments ± standard deviation. When hSec3pSH2 mutant is over-expressed, a significant decrement in virus titres is detected in WNV/DENV-infected hSec3p293KD/OE cells compared to that of HEK293 cells. * indicates $P<0.05$ as compared to WNV/DENV-infected 293 cells.

4.5. INFLUENCE OF HUMAN Sec3 PROTEIN ON VIRUS ENTRY

Following the observation that hSec3p is a negative regulator of flavivirus production, the first question to address is whether hSec3p-induced fluctuations in virus titres were due to differences in the early events such as viral entry or genome uncoating.

To answer this query, these processes were bypassed by electroporating HEK293, hSec3p293KD and hSec3p293OE cells using WNV/DENV RNA transcribed from full-length infectious clones (Section 2.3.14). At the indicated time points, the titres of infectious virus were then determined by plaque assay (Section 2.2.4). As shown in Fig. 4.7(i), virus titres were higher in WNV RNA-transfected hSec3p293KD cells and lower in WNV RNA-transfected hSec3p293OE cells. Similar trends were observed with DENV RNA transfection [Fig. 4.7(ii)]. No significant difference in the virus titres was observed in viral RNA-transfected control vector/scrambled HEK293 cells. This confirmed that the increase or decrease in virus titres observed in hSec3p293KD or hSec3p293OE cells were specifically due to modulation of hSec3p levels. This indicated that hSec3p-induced effects on virus titres must have occurred after genome uncoating.

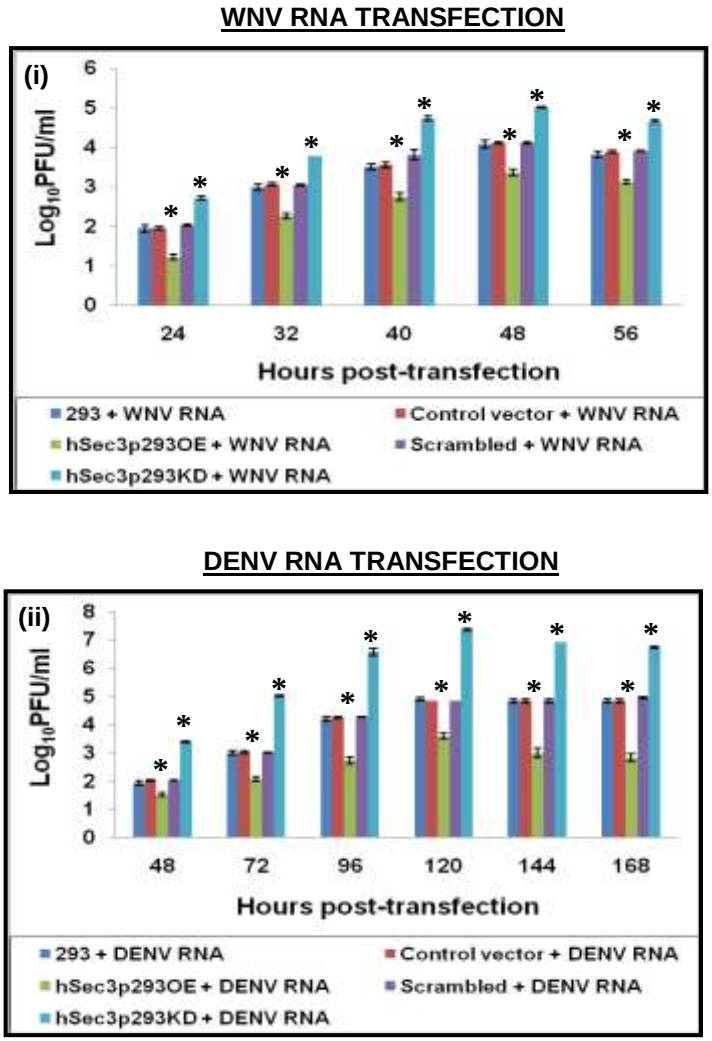

Fig. 4.7: Effect of hSec3p KD/OE on virus titres following viral RNA transfection. HEK293, scrambled/control vector + HEK293 and hSec3p293KD/OE cells were transfected with (i) WNV RNA or (ii) DENV RNA. The supernatants were harvested from RNA-transfected cells to determine virus titres. The results are representatives of three independent experiments ± standard deviation. A significant increment or decrement in virus titres is detected in WNV/DENV RNA-transfected hSec3p293KD/OE cells compared to scrambled/control vector-transduced 293 cells. * indicates $P<0.05$ as compared to (i) 293 + WNV RNA transfection or (ii) 293 + DENV RNA transfection.

4.6. INFLUENCE OF HUMAN Sec3 PROTEIN ON PLUS (+) AND MINUS (-) STRAND RNA SYNTHESIS

To determine if hSec3p-induced effects on virus titres were due to altered viral RNA synthesis, HEK293, hSec3p293KD and hSec3p293OE cells were infected with WNV/DENV. Plus (+) and minus (-) strand viral RNA from WNV/-DENV-infected HEK293, hSec3p293OE and hSec3p293OE cells were then quantitated using real-time PCR (Section 2.3.15). To avoid measuring viral RNA from multiple infection rounds, WNV and DENV RNA levels were quantitated at 5 h and 24 h p.i., respectively.

Interestingly, (+) RNA levels were 8 fold higher in WNV-infected hSec3p293KD cells and 5 fold lower in WNV-infected hSec3p293OE cells [Fig. 4.8(i)]. The levels of (-) RNA were 7.4 fold higher in WNV-infected hSec3p293KD cells and 4.7 fold lower in WNV-infected hSec3p293OE cells [Fig. 4.9(i)]. Similar trends were observed in (+) and (-) RNA levels in DENV-infected hSec3p293KD and hSec3p293OE cells [Figs. 4.8 (ii) & 4.9(ii)]. No significant difference in (+) and (-) RNA levels was observed in virus-infected control vector/scrambled HEK293 cells. This confirmed that the increase or decrease in (+) and (-) RNA levels observed in hSec3p293KD or hSec3p293OE cells were specifically due to modulation of hSec3p levels. These results suggested that differential expression levels of hSec3p can affect viral RNA synthesis of both strands.

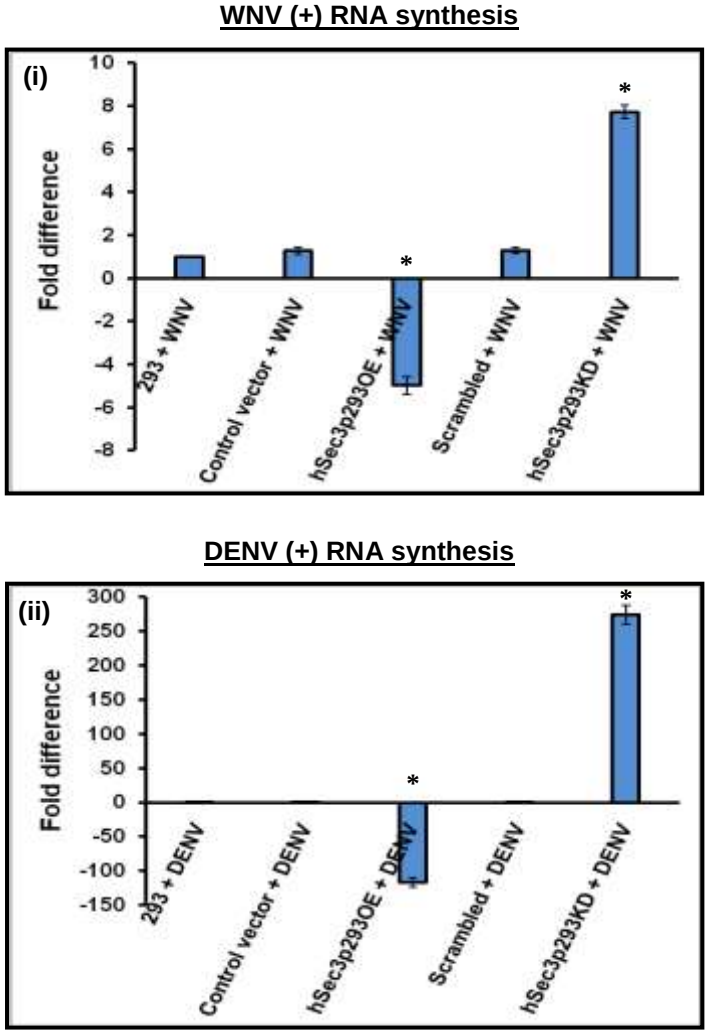

Fig. 4.8: Influence of hSec3p on (+) RNA synthesis. HEK293, hSec3p293OE and hSec3p293KD cells were infected with (i) WNV or (ii) DENV and RNA was extracted and quantified by RT-PCR. The disparity in viral RNA level was expressed as fold difference normalized against the RNA present in WNV-/DENV-infected HEK293 cells. A significant increase [(i) WNV: 8 fold; (ii) DENV: 275 fold] or decrease [(i) WNV: 5 fold; (ii) DENV: 117 fold] in viral (+) strand level is detected in virus-infected hSec3p293KD and hSec3p293OE cells, respectively compared to that of scrambled/control vector-transduced 293 cells. * indicates $P<0.05$ as compared to (i) 293 + WNV infection or (ii) 293 + DENV infection.

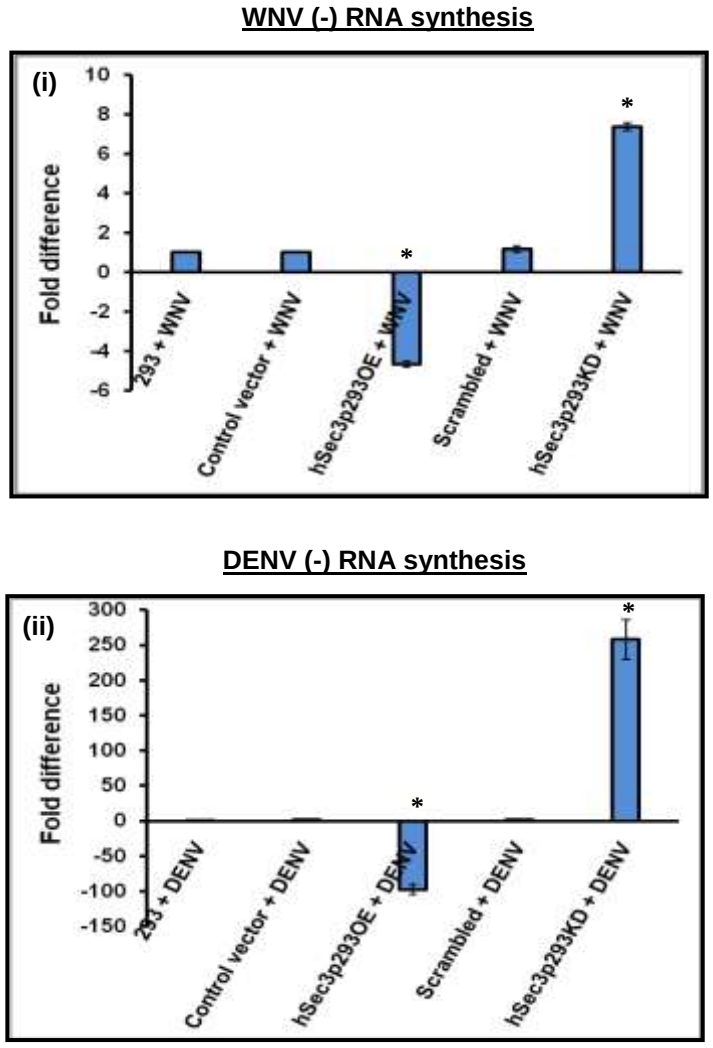

Fig. 4.9: Effect of hSec3p on (-) RNA synthesis. HEK293 and hSec3p293KD/OE cells were infected with (i) WNV or (ii) DENV and RNA was extracted and quantified by RT-PCR. The disparity in viral RNA level was expressed as fold difference normalized against the RNA present in WNV-/DENV-infected HEK293 cells. A significant increase [(i) WNV: 7.4 fold; (ii) DENV: 258 fold] and decrease [(i) WNV: 4.7 fold;(ii) DENV: 98 fold] in viral (-) strand level is detected in hSec3p293KD and hSec3p293OE cells, respectively compared to that of scrambled/control vector-transduced 293 cells. * indicates $P<0.05$ as compared to (i) 293 + WNV infection or (ii) 293 + DENV infection.

4.7. INFLUENCE OF HUMAN Sec3 PROTEIN ON VIRAL PROTEIN PRODUCTION

The above results suggested that viral RNA synthesis was affected by hSec3p expression. To evaluate if hSec3p also influences viral protein production, the level of viral protein synthesized from WNV-/DENV-infected hSec3p293KD/OE cells was analyzed by Western blotting (Section 2.5.2) at various time points using anti-E antibody [Figs. 4.10 and 4.11(i)]. The E protein was used as a surrogate marker for viral protein production. Actin loading controls were included to ensure equal loading [Figs. 4.10 and 4.11(ii)].

Densitometry (semi-quantitative) analysis of the above immunoblots using Syngene program [Figs. 4.10 and 4.11(iii)] revealed that viral E protein synthesis was increased in virus-infected hSec3p293KD cells (WNV: 150-217%; DENV: 249-397%) and decreased in virus-infected hSec3p293OE cells (WNV: 17-38%; DENV: 25-36%) following normalization against the E protein level in HEK293 cells (100%). This trend was similar to that observed with viral RNA synthesis (Section 4.6). This indicated that excess hSec3p has negative effect on viral protein production as well. In addition, it was also observed that differential expression of hSec3p had a greater effect on DENV protein levels compared to that of WNV. This could be due to the differences in the duration of latent period of the virus as observed in Fig. 4.5.

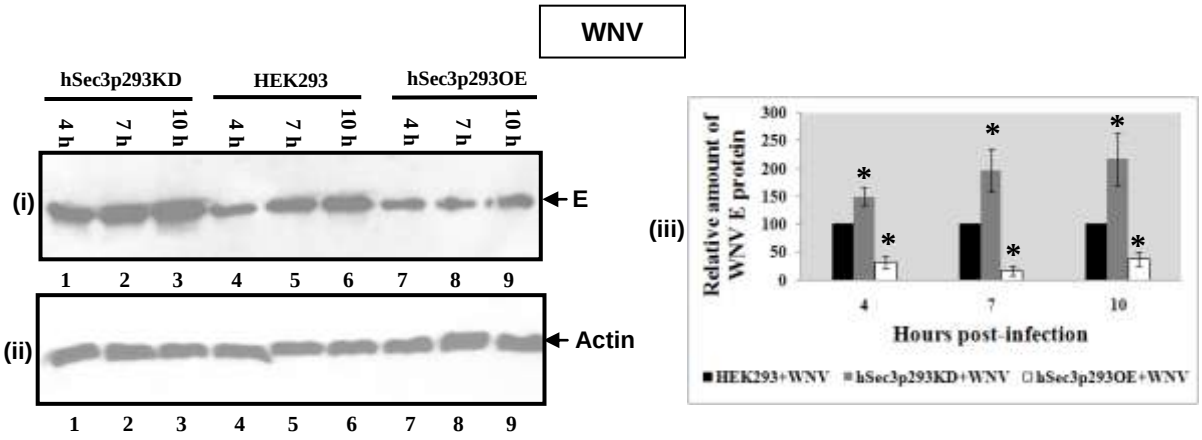

Fig. 4.10: Effect on WNV protein production. HEK293, hSec3p293KD and hSec3p293OE cells were infected with WNV. (i) At the indicated timings, cells were lysed and immunoblotted for E protein. The intracellular viral E proteins increase in hSec3p293KD cells (Lanes 1-3) and decrease in hSec3p293OE cells (Lanes 7-9) compared to HEK293 cells (Lanes 4-6). (ii) Actin loading control to ensure equal loading. (iii) The band intensities of E protein from various experimental groups were quantified using GeneTools program. An arbitrary density of 100% is attributed to the E protein level in WNV-infected HEK293 cells. Results from three independent experiments are averaged for semi-quantitative illustration. Significant changes in the amount of E proteins are observed in WNV-infected hSec3p293KD/OE cells (* indicates $P<0.05$) as compared to HEK293 cells.

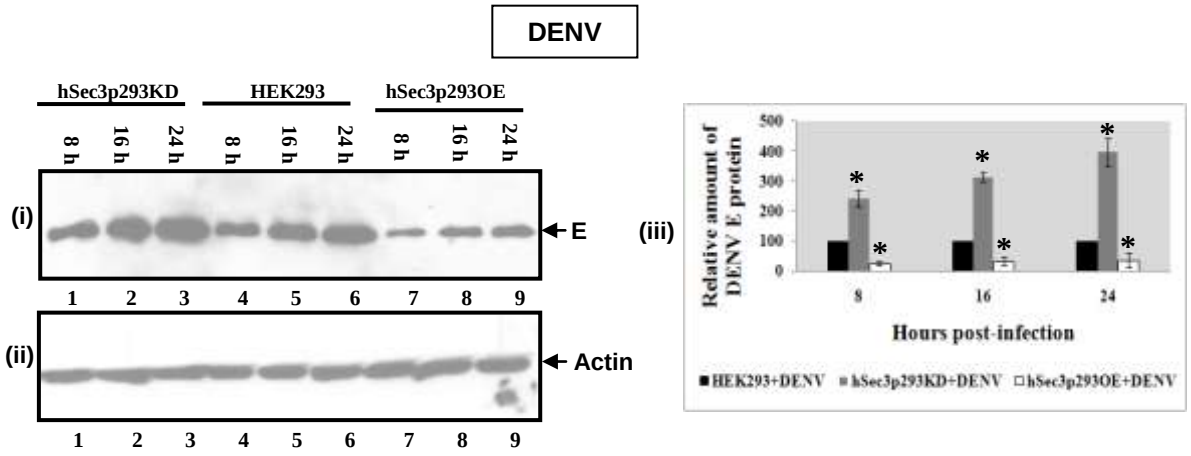

Fig. 4.11: Effect on DENV protein production. HEK293, hSec3p293KD and hSec3p293OE cells were infected with DENV. (i) At the indicated timings, cells were lysed and immunoblotted for E protein. The intracellular viral E proteins increase in hSec3p293KD cells (Lanes 1-3) and decrease in hSec3p293OE cells (Lanes 7-9) compared to HEK293 cells (Lanes 4-6). (ii) Actin loading control to ensure equal loading. (iii) The band intensities of E protein from various experimental groups were quantified using GeneTools program. An arbitrary density of 100% is attributed to the E protein level in DENV-infected HEK293 cells. Results from three independent experiments are averaged for quantitative illustration. Significant changes in the amount of E proteins are observed in DENV-infected hSec3p293KD/OE cells (* indicates $P<0.05$) as compared to HEK293 cells.

4.8. EFFECT OF HUMAN Sec3 PROTEIN ON VIRUS SECRETION

To examine if hSec3p influences virus secretion, HEK293, hSec3p293OE and hSec3p293KD cells were infected with WNV or DENV. At the indicated time points, viral RNAs were extracted from the culture supernatant using QIAamp viral RNA kit (Section 2.3.1) and quantified using real-time RT-PCR [(Section 2.3.15) (Fig. 4.12)]. The viral RNA levels in WNV/DENV-infected HEK293 cell culture supernatants were assigned arbitrarily as one and compared to the viral RNA levels from that of virus-infected hSec3p293KD and hSec3p293OE cell culture supernatants. A significant increase (WNV: 8 fold; DENV: 250 fold) and decrease (WNV: 4 fold; DENV: 100 fold) in viral RNA level was detected in WNV-/DENV-infected hSec3p293KD and hSec3p293OE cell culture supernatants, respectively.

Secreted E protein levels were also quantified by Western blotting (Section 2.5.2) and densitometry [(Section 2.5.5) (Fig. 4.13)]. The amounts of secreted E proteins in WNV/DENV-infected HEK293 cell culture supernatants were assigned as 100% and compared to that from virus-infected hSec3p293KD and hSec3p293OE cell culture supernatants. The level of viral E proteins increased (WNV: 220%; DENV: 600%) in hSec3p293KD cells and decreased (WNV: 45%; DENV: 85%) in hSec3p293OE cell culture supernatants. The observed reduction in secreted viral RNA and protein levels in hSec3p293OE cell culture supernatants correlated with the decreased intracellular viral RNA and protein synthesis reported in Sections 4.6 and 4.7 using quantitative real-time PCR (Section 2.3.15) and semi-quantitative Western blotting (Section 2.5.2).

In this chapter, the effct of hSec3p on flavivirus life cycle was investigated using lentivirus-mediated knock-down and over-expression system. It was shown that hSec3p influences viral RNA transcription and translation.

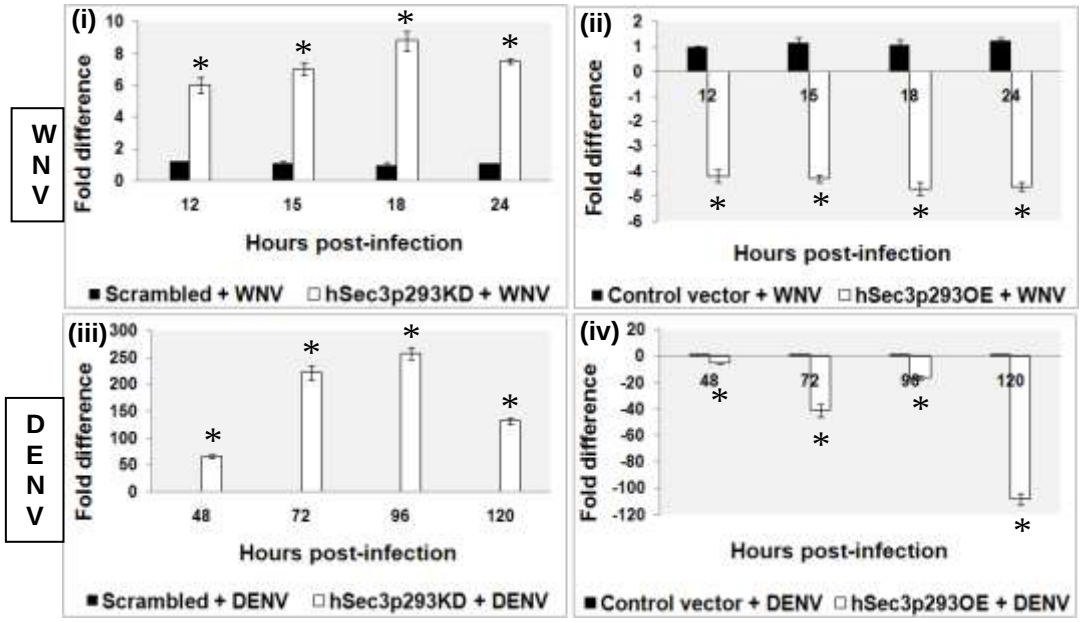

Fig. 4.12: Effect on secreted viral RNA level: HEK293 and hSec3p293KD/OE cells were infected with WNV or DENV and viral RNAs were extracted from the cell culture supernatants and quantified using real-time RT-PCR. A significant increase (WNV: 8 fold; DENV: 250 fold) and decrease (WNV: 4 fold; DENV: 100 fold) in viral RNA level is detected in virus-infected hSec3p293KD and hSec3p293OE cell culture supernatants, respectively (* indicated $P<0.05$).

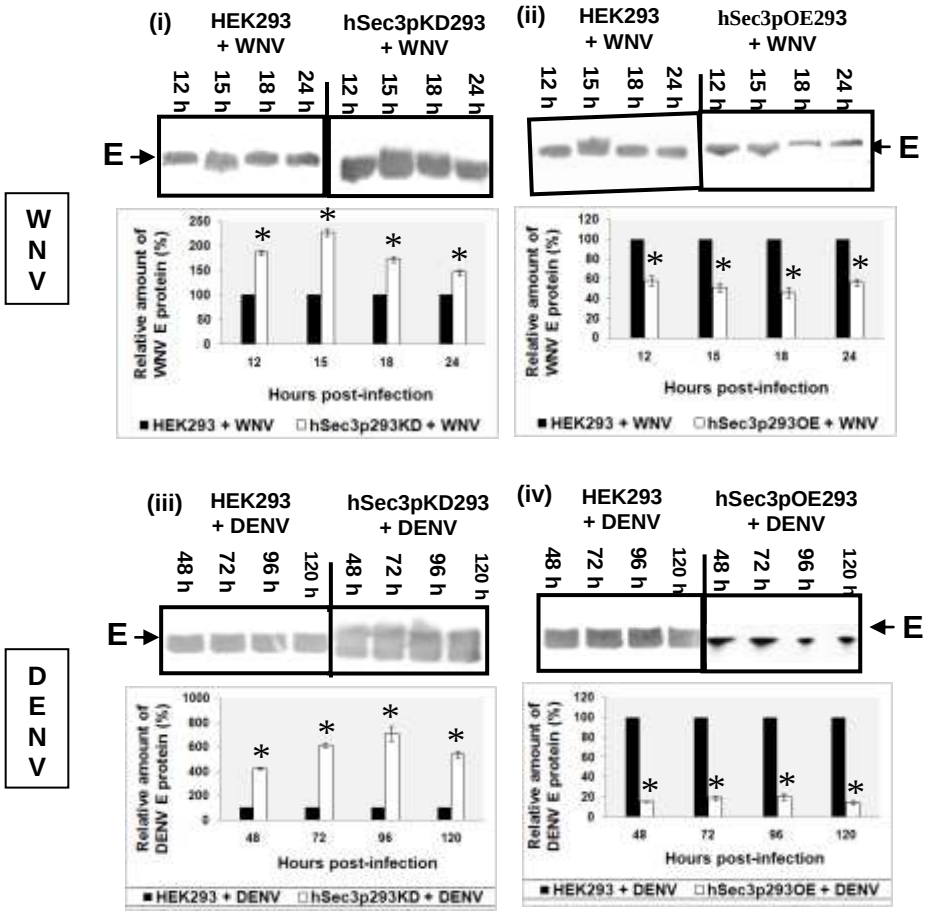

Fig. 4.13: Effect on secreted viral protein level: HEK293 and hSec3p293KD/OE cells were infected with WNV or DENV. At the indicated time points, cell culture supernatants were harvested and the level of secreted E protein was quantified by Western blotting and densitometry. The level of viral E proteins increase in WNV/DENV-infected hSec3p293KD cell culture supernatants and decrease in WNV/DENV-infected hSec3p293OE cell culture supernatants (* indicated $P<0.05$).

CHAPTER 5

RESULTS

5.0. MOLECULAR INSIGHTS INTO THE ANTI-VIRAL ROLE OF HUMAN Sec3 PROTEIN

5.1. INTRODUCTION

The previous two chapters elaborated that hSec3p influenced flavivirus production in a bimodal manner by targeting viral RNA transcription and viral protein production. This chapter sought to address the molecular mechanism underlying the bimodal anti-viral activity of hSec3p using a combination of biochemical, molecular and microscopic techniques.

5.2. MECHANISM BEHIND HUMAN Sec3 PROTEIN-INDUCED REDUCTION IN VIRAL RNA SYNTHESIS

5.2.1. Interaction between elongation factor 1α (EF1α) and human Sec3 protein

Studies have shown that yeast Sec3p was a putative binding partner of EF1α, a key translational regulator (Gavin *et al.*, 2006). Hence, it was investigated if Sec3p-EF1α interaction also occurs in human cells by examining the interaction between EF1α and hSec3p in uninfected, WNV-infected and DENV-infected HEK293, hSec3p293KD or hSec3p293OE cells (Section 2.7.1). The cell lysates were precipitated using anti-hSec3p antibody and immunoblotted with anti-EF1α antibody. As shown in Fig. 5.1[A-C(i)], hSec3p-EF1α interaction was detected in HEK293, hSec3p293KD and hSec3p293OE cells albeit the level of hSec3p-EF1α complexes was higher in hSec3p293OE cells (Lane 3) and lower in hSec3p293KD cells (Lane 5) in both uninfected (A) and virus-infected (B and C) cells.

Fig. 5.1: Influence on the interaction between EF1α and hSec3p. EF1α-hSec3p interaction in (A) uninfected, (B) WNV-infected or (C) DENV-infected HEK293, hSec3p293KD and hSec3p293OE cells were determined by immunoprecipitation using anti-hSec3p antibody and immunoblotted with anti-EF1α antibody. Although the interaction between EF1α and hSec3p is observed in all the experimental groups, more hSec3p-EF1α complexes are detected in hSec3p293OE cells (Lane 3) while much lower level is observed in hSec3p293KD cells (Lane 5). (ii-v) Immunoprecipitation control, expression controls and actin loading control. IP: Immunoprecipitated sample; WB: Western blot; WCL: Whole cell lysate. (D) Densitometry analysis of the bands on the above immunoblots from (A-C) shows that significantly higher level of hSec3p-EF1α complexes are detected in uninfected hSec3p293OE cells while lower levels are observed in uninfected hSec3p293KD cells (** indicates $P<0.05$ as compared to uninfected HEK293 cells). Furthermore, the amount of EF1α-hSec3p complex formation is significantly lowered in the infected cells compared to uninfected cells (* indicates $P<0.05$).

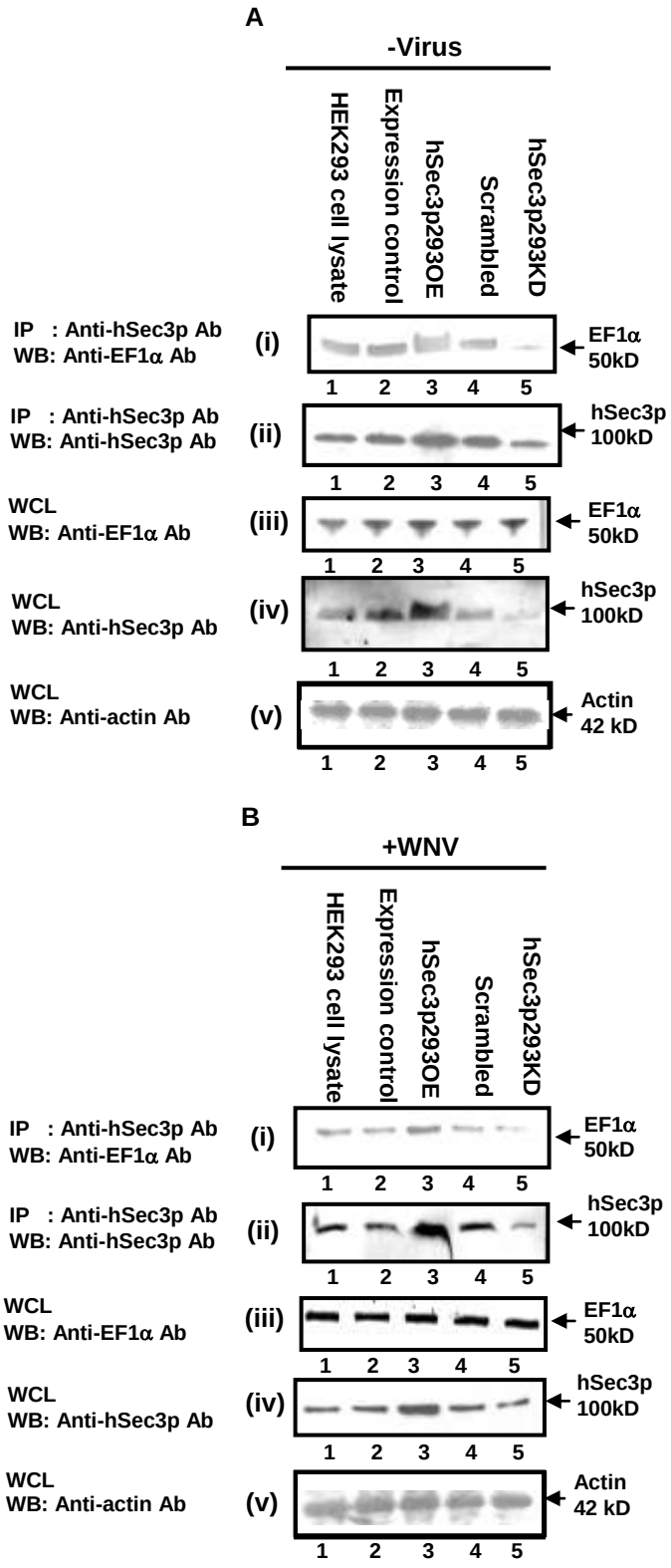
A
-Virus
HEK293 cell lysate
Expression control
hSec3p293OE
Scrambled
hSec3p293KD
IP : Anti-hSec3p Ab
WB: Anti-EF1α Ab
(i)
EF1α
50kD
1 2 3 4 5
IP : Anti-hSec3p Ab
WB: Anti-hSec3p Ab
(ii)
hSec3p
100kD
1 2 3 4 5
WCL
WB: Anti-EF1α Ab
(iii)
EF1α
50kD
1 2 3 4 5
WCL
WB: Anti-hSec3p Ab
(iv)
hSec3p
100kD
1 2 3 4 5
WCL
WB: Anti-actin Ab
(v)
Actin
42 kD
1 2 3 4 5
B
+WNV
HEK293 cell lysate
Expression control
hSec3p293OE
Scrambled
hSec3p293KD
IP : Anti-hSec3p Ab
WB: Anti-EF1α Ab
(i)
EF1α
50kD
1 2 3 4 5
IP : Anti-hSec3p Ab
WB: Anti-hSec3p Ab
(ii)
hSec3p
100kD
1 2 3 4 5
WCL
WB: Anti-EF1α Ab
(iii)
EF1α
50kD
1 2 3 4 5
WCL
WB: Anti-hSec3p Ab
(iv)
hSec3p
100kD
1 2 3 4 5
WCL
WB: Anti-actin Ab
(v)
Actin
42 kD
1 2 3 4 5

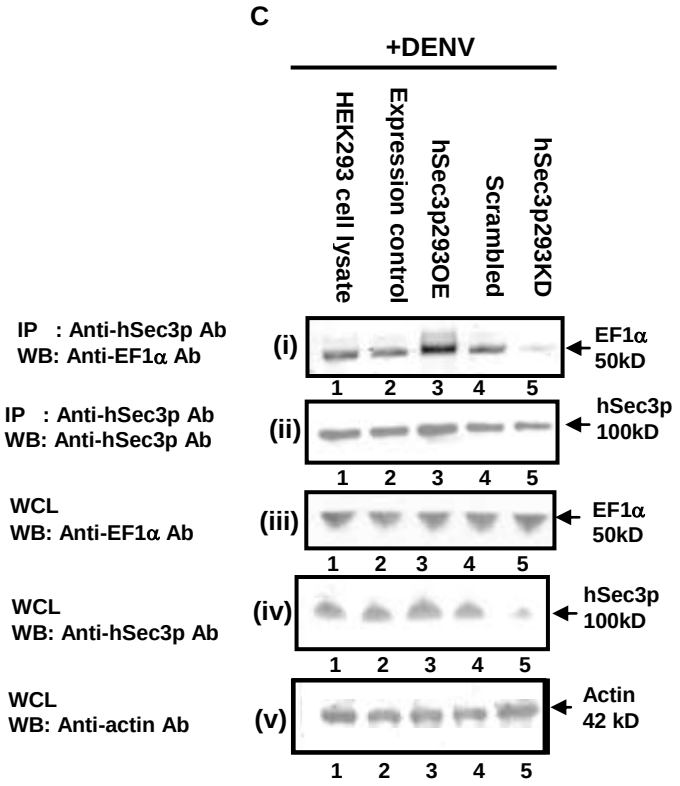
C
+DENV
HEK293 cell lysate
Expression control
hSec3p293OE
Scrambled
hSec3p293KD
IP : Anti-hSec3p Ab
WB: Anti-EF1α Ab
(i)
EF1α
50kD
1 2 3 4 5
IP : Anti-hSec3p Ab
WB: Anti-hSec3p Ab
(ii)
hSec3p
100kD
1 2 3 4 5
WCL
WB: Anti-EF1α Ab
(iii)
EF1α
50kD
1 2 3 4 5
WCL
WB: Anti-hSec3p Ab
(iv)
hSec3p
100kD
1 2 3 4 5
WCL
WB: Anti-actin Ab
(v)
Actin
42 kD
1 2 3 4 5

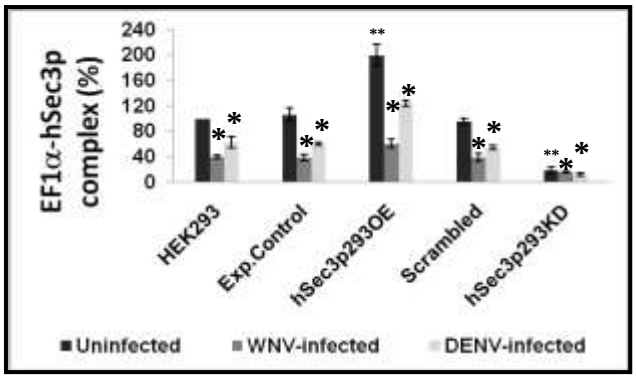
D
EF1α-hSec3p complex (%)
240
200
160
120
80
40
0
HEK293
Exp.Control
hSec3p293OE
Scrambled
hSec3p293KD
Uninfected
WNV-infected
DENV-infected

Densitometry analysis (Section 2.5.5) was performed on the immunoblots obtained from the uninfected and WNV/DENV-infected lysates. In Fig. 5.1(D), the arbitrary value of 100% is given to the formation of EF1α-hSec3p complex in uninfected HEK293 cells. The EF1α-hSec3p complex formation in uninfected expression control, hSec3p293OE, scrambled and hSec3p293KD cells were then compared against the arbitrary value of 100% given to that of HEK293 cells. Similarly, the formation of EF1α-hSec3p complex in WNV/DENV-infected expression control, hSec3p293OE, scrambled and hSec3p293KD cells were compared against the arbitrary value of 100% given to HEK293 cells.

Densitometry analysis showed that there was an increase (~100%) and decrease (~80%) in the formation of EF1α-hSec3p complex in uninfected hSec3p293OE and hSec3p293KD cells, respectively. Similar trend was observed with virus-infected hSec3p293OE and hSec3p293KD cells. It was also noted that the amount of EF1α-hSec3p complex formation was significantly lowered in virus-infected cells (WNV: 60-80%; DENV: 40-90%) compared to uninfected cells regardless of the expression levels of hSec3p. The binding of EF1α to hSec3p correlated with the amount of hSec3p in the lysate of both uninfected and infected cells [Fig. 5.1A-C(iv)]. This indicated that WNV/DENV infection interfered with EF1α-hSec3p complex formation.

5.2.2. Interaction between elongation factor 1α and hSec3p flavivirus C protein-binding defective mutant

The study was extended to examine if hSec3p flavivirus C protein-binding defective mutant, hSec3pSH2 is still capable of interacting with EF1α. HEK293 cells were transfected with V5-tagged galactosidase, full-length hSec3p and hSec3pSH2 mutant and co-immunoprecipitation was performed using anti-V5 antibody. The resulting eluents were subjected to SDS-PAGE analysis followed by immunoblotting with anti-EF1α antibody. As shown in Fig. 5.2(i), the interaction between hSec3p/hSec3pSH2 and EF1α was detected in V5-hSec3pf1 (Lane 3) and V5-hsec3pSH2 mutant (Lane 4) transfected HEK293 cells. This indicated that hSec3pSH2 mutant can still recognize EF1α and form a complex with it.

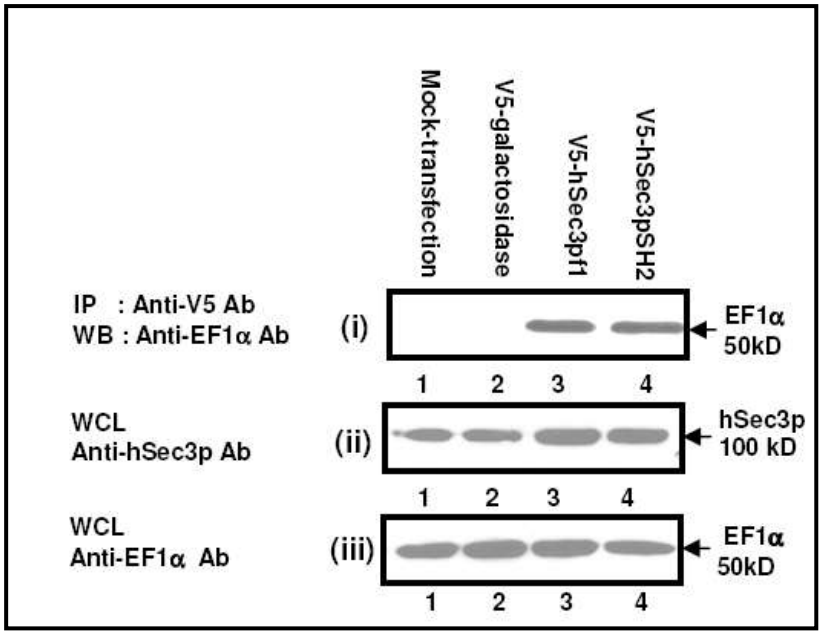

Fig. 5.2: Co-immunoprecipitation of EF1α and hSec3pSH2 mutant. (i) HEK293 cells were transfected with V5-hSec3pf1 (full-length) or V5-hSec3pSH2 mutant. Cell lysates were immunoprecipitated using anti-V5 antibody followed by immunoblotted with anti-EF1α antibody. The results showed that hSec3pSH2 mutant can bind to EF1α (Lane 4). (ii & iii) The expression of hSec3pf1/hSec3pSH2/EF1α was detected using anti-hSec3p/anti-EF1α antibodies. IP: Immunoprecipitated sample; WB: Western blot; WCL: Whole cell lysate.

5.2.3. Influence of human Sec3 protein on the interaction between EF1α and WNV/DENV RNA

Studies have demonstrated that EF1α influenced viral replication by binding to 3'UTR of viral genome (Blackwell & Brinton, 1995; 1997; Davis *et al.*, 2007a; Shi *et al.*, 1996). Following the observation that more hSec3p-EF1α complexes were formed in hSec3p293OE cells, it was explored if this association affects EF1α binding to flavivirus RNA genome. HEK293, hSec3p293OE and hSec3p293KD cells were infected with WNV/DENV or transfected with biotinylated WNV/DENV RNA. At 14 h (WNV)/24 h (DENV) p.i. or 18 h post-transfection, cells were cross-linked and lysed for immunoprecipitation (Section 2.9.2) or pull down assay (Section 2.9.3) using anti-EF1α or anti-hSec3p antibody.

RNA was extracted from the eluents and subjected to RT-PCR (Section 2.3.15) to detect the differences in the level of EF1α-bound RNA in WNV-/DENV-infected or RNA-transfected HEK293 and hSecp293KD/OE cells. In addition, RT-PCR was used to detect if hSec3p directly binds to WNV/DENV RNA. Normalization was performed against mock-transfected samples and GAPDH in all data sets.

As shown in Fig. 5.3(i & ii), EF1α-bound viral RNA levels in WNV-infected/RNA-transfected hSec3p293OE cells were lower by 40% compared to HEK293 cells. Conversely, EF1α-bound viral RNA levels were higher by 40% in WNV-infected/RNA-transfected hSec3p293KD cells. Similar trends were

observed with DENV infection/DENV RNA transfection [Fig. 5.3(i & ii)]. No signal was detected in RT-PCR from the hSec3p-immunoprecipitated samples following WNV/DENV infection or RNA transfection [Fig. 5.3(iii & iv)]. This suggested that hSec3p did not bind to viral RNA directly.

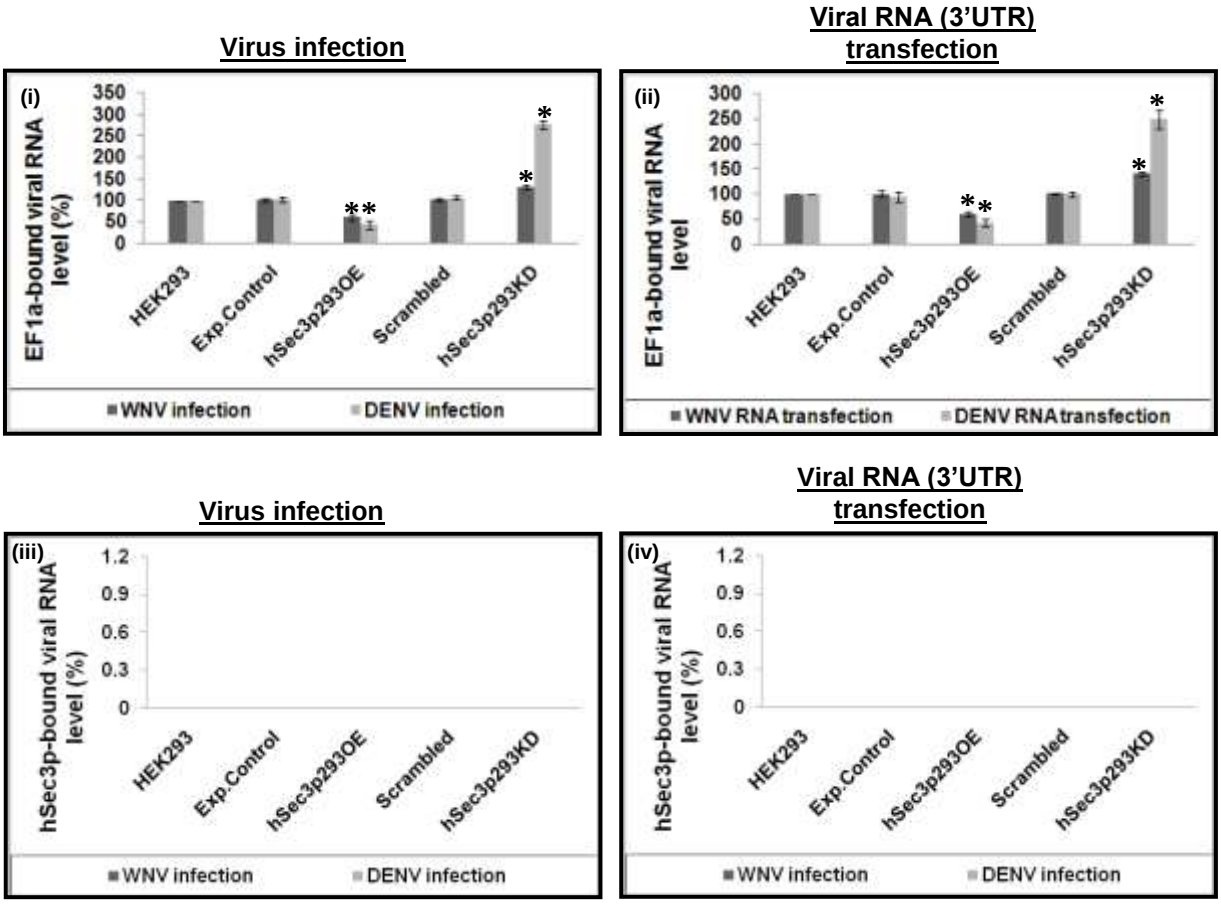

Fig. 5.3: Measurement of EF1α/hSec3p-bound flavivirus RNA. (i) WNV/DENV-infected or (ii) biotinylated WNV/DENV 3'UTR RNA-transfected cells were immunoprecipitated using anti-EF1α antibody. The EF1α-bound RNA was quantitated by RT-PCR. In WNV-infected/RNA-transfected cells, 40% reduction in EF1α-bound viral RNA level is detected in hSec3p293OE cells and 40% increment is detected in hSec3p293KD cells. Similarly, 50% reduction in EF1α-bound viral RNA level is observed in DENV-infected/RNA-transfected hSec3p293OE cells and 250% increment is observed in DENV-infected/RNA-transfected hSec3p293KD cells. * indicates $P<0.05$ as compared to virus-infected/RNA-transfected HEK293 cells. (iii) WNV/DENV-infected or (iv) biotinylated WNV/DENV 3'UTR RNA-transfected cells were immunoprecipitated using anti-hSec3p antibody. The hSec3p-bound RNA was quantitated by RT-PCR. No signal is detected in RT-PCR from the hSec3p-immunoprecipitated samples following WNV/DENV infection or RNA transfection.

To reaffirm that the differential binding of EF1α to viral RNA was hSec3p-specific, the effects of hSec3p over-expression or knock-down were tested on the binding of another RNA-binding host protein [polypyrimidine-tract binding protein, PTB (Anwar *et al.*, 2009, De Nova-Ocampo *et al.*, 2002, Jiang *et al*., 2009, Kim *et al*., 2006)] to viral genome. Polypyrimidine-tract binding protein was reported to affect DENV transcription and not translation (Anwar *et al*., 2009, Jiang *et al*., 2009). In contrast to EF1α, PTB binding to viral RNA was not affected significantly by the over-expression or knock-down of hSec3p (Fig. 5.4). This reaffirmed that the disruption of EF1α-viral RNA complex [Fig. 5.3 (i & ii)] was mediated specifically by hSec3p.

The biotinylated/non-biotinylated RNA-transfected samples were also subjected to pull down assay (Section 2.9.3) using Streptavidin beads followed by immunoblotting using anti-hSec3p/anti-EF1α antibody. Interestingly, (biotinylated) RNA-bound EF1α levels were significantly reduced in viral RNA-transfected hSec3p293OE cells [Fig. 5.5(i & v), Lane 3, WNV: 30%; DENV: 60%) and increased in viral RNA-transfected hSec3p293KD cells [Fig. 5.5(i & v), Lane 5, WNV: 24%; DENV: 40%) compared to viral RNA-transfected HEK293 cells [Fig. 5.5(i & v)], Lane 1, normalized as 100%). The results from RNA-precipitation/pull down study were consistent with EF1α/hSec3p antibody-precipitation assay as described above (Fig. 5.3). In addition, identical experiment was carried out using Streptavidin beads and anti-PTB antibody. In agreement with the results obtained from Fig. 5.4, PTB-viral RNA complex formation was not affected by the over-expression or knock-down of hSec3p (Fig. 5.6).

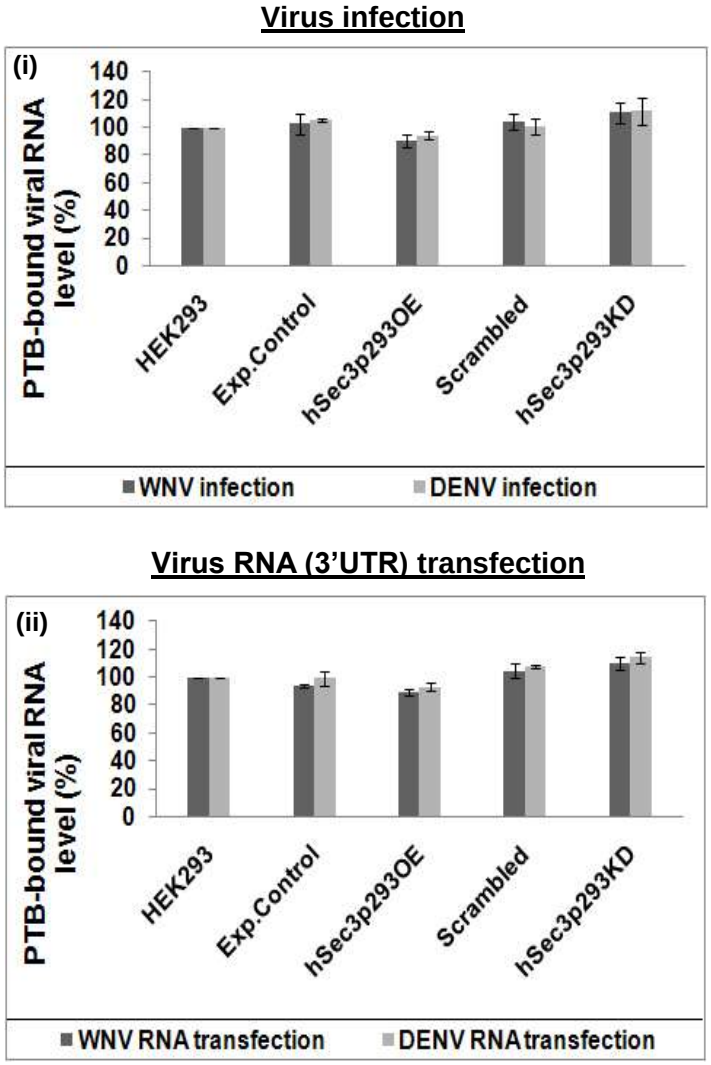

Fig. 5.4: Measurement of PTB-bound flavivirus RNA. (i) WNV/DENV-infected or (ii) biotinylated WNV/DENV 3'UTR RNA-transfected cells were immunoprecipitated using anti-PTB antibody. The PTB-bound RNA were quantitated by RT-PCR. No significant changes ($P>0.05$) are observed in the levels of PTB-bound viral RNA level in both virus-infected and viral RNA-transfected hSec3p293OE/KD cells.

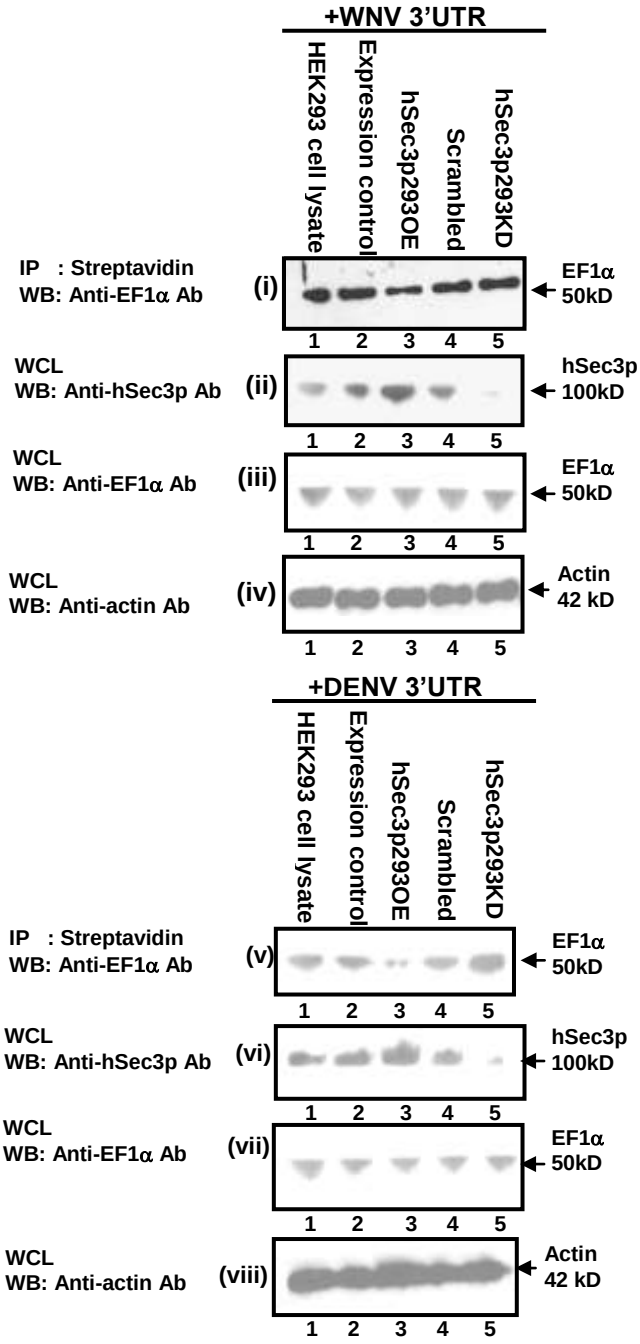

Fig. 5.5: Measurement of RNA-bound EF1α. (i) The biotinylated WNV and (v) DENV 3'UTR RNA-transfected samples were subjected to pull down assay using Streptavidin beads and immunoblotted using anti-EF1α antibody. The interaction between EF1α and 3'UTR [(i) and (v)] is detected in HEK293 (Lane 1), Expression control (Lane 2), hSec3p293OE (Lane 3), Scrambled (Lane 4) and hSec3p293KD (Lane 5) cells. Lower level of EF1α-3'UTR complexes are detected in hSec3p293OE cells (Lane 3) while higher level is observed in hSec3p293KD cells (Lane 5). (ii-iv and vi-viii) The experimental controls are shown. (IP: Pulled down sample; WB: Western blot; WCL: Whole cell lysate).

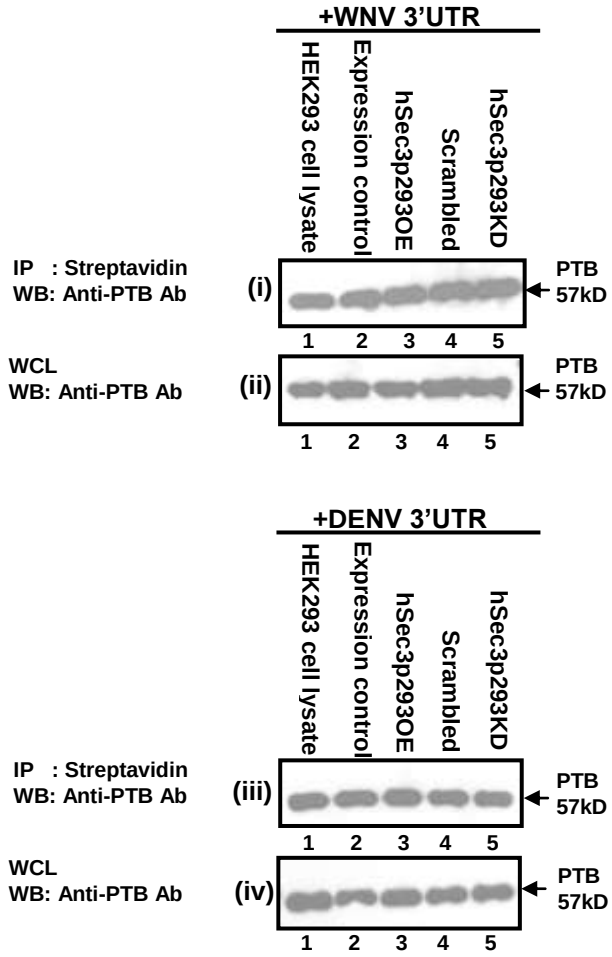

Fig. 5.6. Measurement of RNA-bound PTB. (i) The biotinylated WNV and (iii) DENV 3'UTR RNA-transfected samples were subjected to pull down assay using Streptavidin beads and immunoblotted using anti-PTB antibody. The interaction between PTB and 3'UTR [(i) and (iii)] is not affected when hSec3p is expressed differentially. (ii-iv) The expression of PTB in cell lysate is shown. (IP: Pulled down sample; WB: Western blot; WCL: Whole cell lysate).

To further support the hypothesis that differential level of hSec3p affected the amount of EF1α binding to viral 3'UTR, competition assay (Section 2.9.4) was performed in which different doses of recombinant purified hSec3p was added to fixed amount of EF1α and 3'UTR. As shown in Fig. 5.7(i & ii), the amount of EF1α-3'UTR complexes decreased with increasing concentration of hSec3p. It was also shown that this competition assay was specific as Sec6p (another exocyst component) did not alter the binding of EF1α to 3'UTR [Fig. 5.7(iii & iv)].

The specificity of EF1α binding to viral 3'UTR was also tested by mixing a fixed amount of EF1α and biotinylated WNV/DENV 3'UTR in the presence or absence of non-biotinylated viral 3'UTRs or tRNAs (Section 2.9.4). Pull down assay was then performed using Streptavidin beads followed by immunoblotting using anti-EF1α antibody. As shown in Fig. 5.8(i & ii), the amount of EF1α-(biotinylated)3'UTR complexes decreased in the presence of increasing concentration of non-biotinylated viral 3'UTRs. It was also shown that this competition assay is specific as tRNA did not alter the binding of EF1α to biotinylated 3'UTR [Fig. 5.8(iii & iv)].

Collectively, these observations demonstrated that EF1α binds to viral 3'UTR specifically and hSec3p interfered with EF1α-3'UTR complex formation in a dose-dependent manner. In short, WNV/DENV RNA and hSec3p are competing for binding to EF1α. Reduced binding of EF1α to viral RNA might account for decreased viral RNA synthesis observed in hSec3p293OE cells (Figs. 4.8 and 4.9).

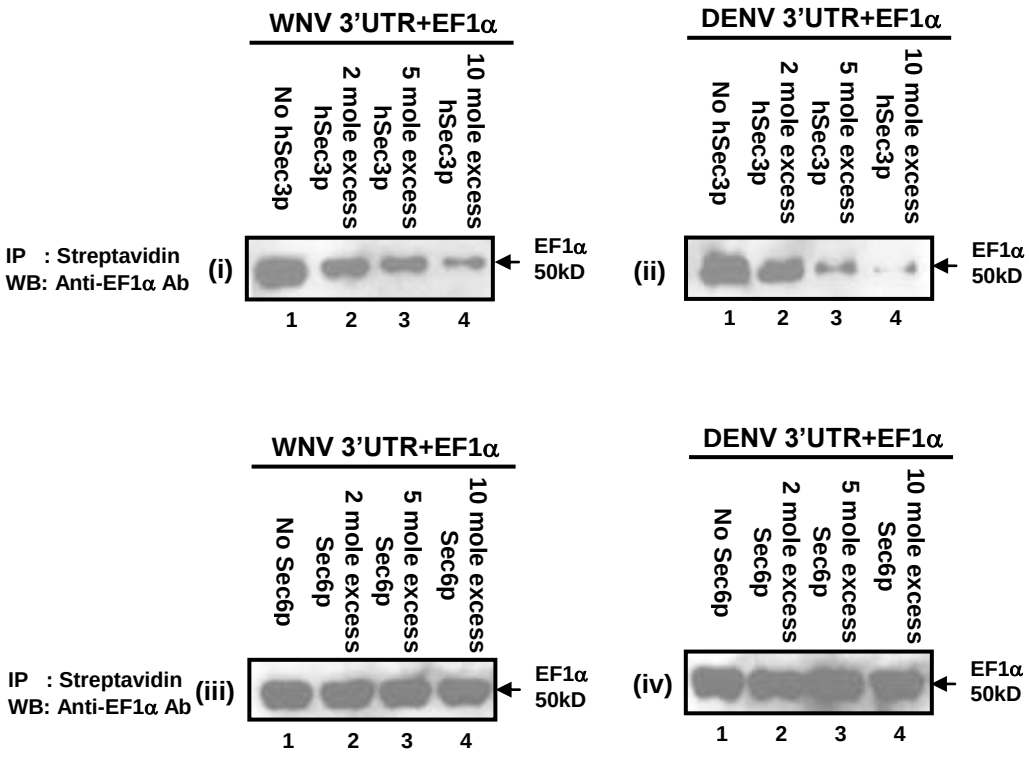

Fig. 5.7: Competition assay. Biotinylated WNV/DENV 3'UTRs, recombinant EF1α were incubated with recombinant (i & ii) hSec3p or (iii & iv) Sec6p and subjected to pull-down assay. This demonstrates that hSec3p interferes with EF1α-3'UTR association specifically. IP: Pulled down sample; WB: Western blot.

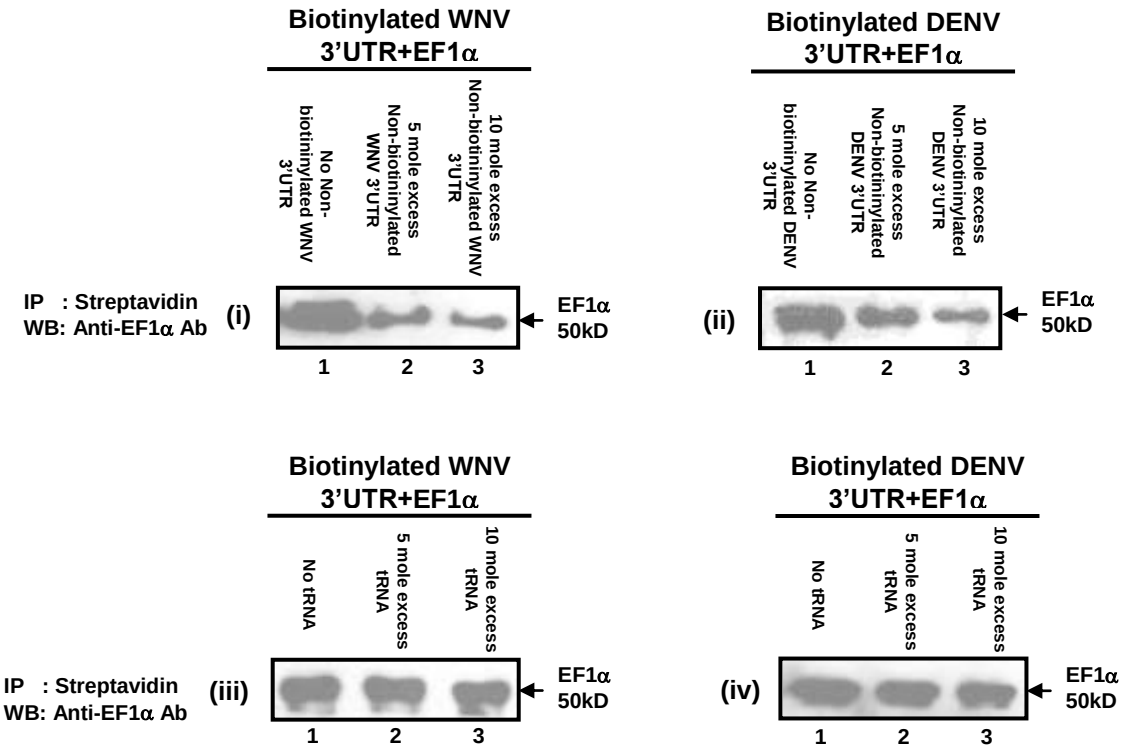

Fig. 5.8: Competition assay. Biotinylated WNV/DENV 3'UTRs, recombinant EF1α were incubated with (i & ii) non-biotinylated 3'UTRs or (iii & iv) tRNAs. Pull down eluents were analyzed by Western blotting. The results show that EF1α binds specifically to viral 3'UTRs. IP: Pulled down sample; WB: Western blot.

5.2.4. Influence of human Sec3 protein on the interaction between elongation factor 1α and viral replicative machinery

Davis and colleagues (2007a) reported that EF1α is capable of interacting with the viral replicative complex. It was thus tested if this interaction is affected in WNV-/DENV-infected hSec3p293KD/OE cells by immunoprecipitating the cell lysates using anti-EF1α antibody and probing for NS3 protein (surrogate marker for viral replicative complex) using anti-NS3 antibody (Section 2.7.1). As shown in Fig. 5.9(i & viii), the level of NS3 protein immunoprecipitated with anti-EF1α antibody was reduced in WNV-/DENV-infected hSec3p293OE cells (Lane 3) and increased in hSec3p293KD cells (Lane 5) compared to wild-type (Lane 1) or expression control plasmid (Lane 2) or scrambled sequence (Lane 4) expressing HEK293 cells. Densitometry analysis (Section 2.5.5) performed on the two representative immunoblots revealed that the level of NS3 protein immunoprecipitated with anti-EF1α antibody is drastically reduced (70%) in WNV-/DENV-infected hSec3p293OE cells and significantly increased (25%) in hSec3p293KD cells. This suggested that the level of hSec3p could modulate the association of EF1α with viral replicative complex.

Next, it was examined if the immunoprecipitation of NS3 protein by EF1α is mediated by an RNA bridge by performing Co-IP assay (Section 2.7.1) in the presence of RNase using anti-EF1α antibody. The membrane was then probed for NS3 protein using anti-NS3 antibody. As shown in Fig. 5.9(ii & ix), NS3 protein

Fig. 5.9: Effect of hSec3p on EF1α-NS3 complex formation. RNase-untreated (i & viii) and treated (ii & ix) cell lysates from WNV-/DENV-infected HEK293 and hSec3p293KD/OE cells were precipitated using anti-EF1α antibody and probed with anti-NS3 antibody. Significantly lower level of EF1α-NS3 complex is detected in hSec3p293OE cells [(i & viii), Lane 3] and higher level of EF1α-NS3 complex is observed in hSec3p293KD cells [(i& viii), Lane 5] compared to HEK293 [(i & viii), Lane 1], expression control [(i & viii), Lane 2] and scrambled control [(i & viii), Lane 4] in RNase-untreated lysates. (ii & ix) The EF1α-NS3 interaction is not observed in RNase-treated samples. [(iii-vii) and (x-xiv)] Precipitation control, expression controls and actin loading control in each experimental group are shown. (IP: Immunoprecipitated sample; WB: Western blot; WCL: Whole cell lysate).

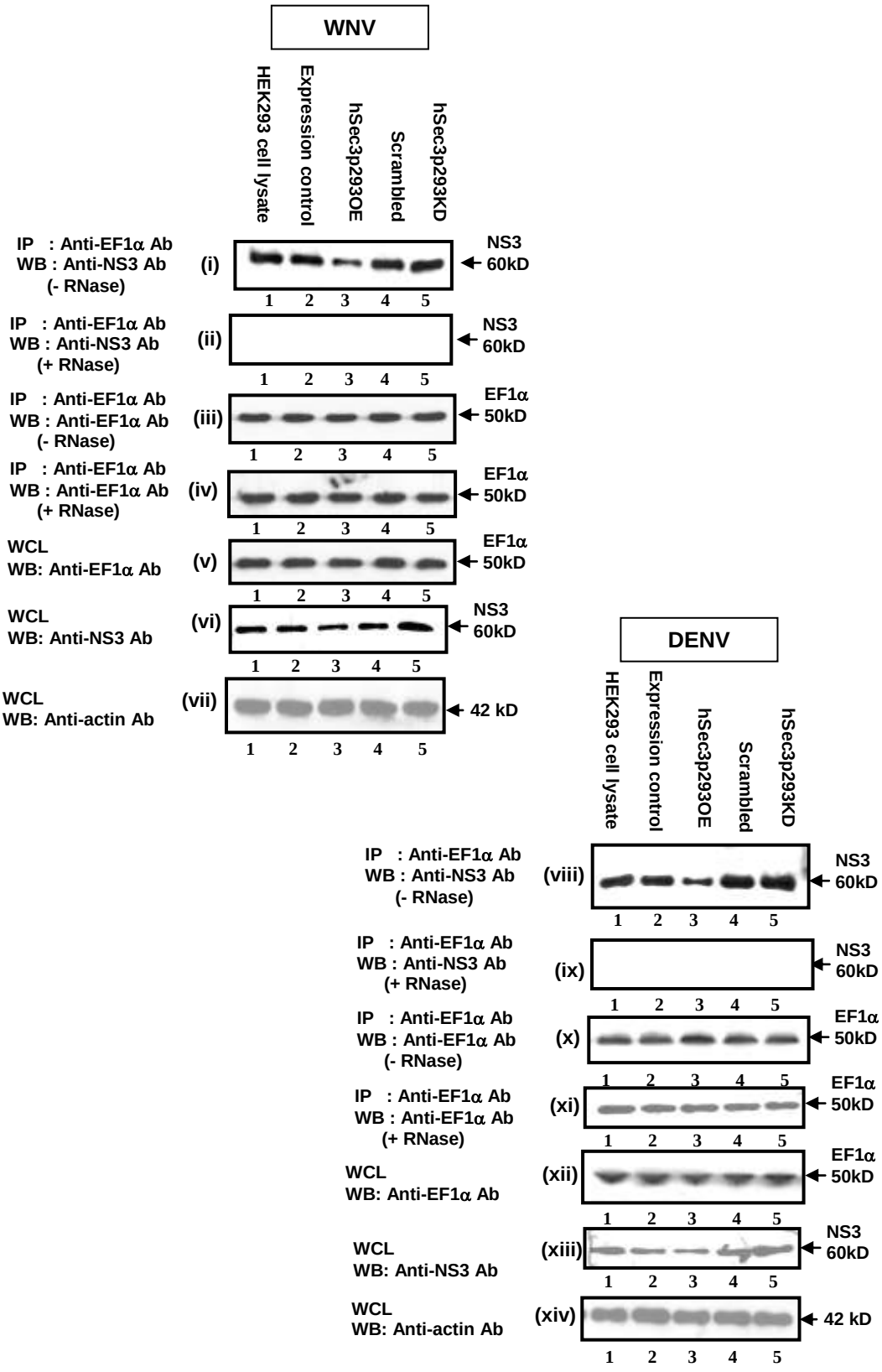
WNV
HEK293 cell lysate
Expression control
hSec3p293OE
Scrambled
hSec3p293KD
IP : Anti-EF1α Ab
WB : Anti-NS3 Ab
(- RNase)
(i)
NS3
60kD
1 2 3 4 5
IP : Anti-EF1α Ab
WB : Anti-NS3 Ab
(+ RNase)
(ii)
NS3
60kD
1 2 3 4 5
IP : Anti-EF1α Ab
WB : Anti-EF1α Ab
(- RNase)
(iii)
EF1α
50kD
1 2 3 4 5
IP : Anti-EF1α Ab
WB : Anti-EF1α Ab
(+ RNase)
(iv)
EF1α
50kD
1 2 3 4 5
WCL
WB: Anti-EF1α Ab
(v)
EF1α
50kD
1 2 3 4 5
WCL
WB: Anti-NS3 Ab
(vi)
NS3
60kD
1 2 3 4 5
WCL
WB: Anti-actin Ab
(vii)
42 kD
1 2 3 4 5
DENV
HEK293 cell lysate
Expression control
hSec3p293OE
Scrambled
hSec3p293KD
IP : Anti-EF1α Ab
WB : Anti-NS3 Ab
(- RNase)
(viii)
NS3
60kD
1 2 3 4 5
IP : Anti-EF1α Ab
WB : Anti-NS3 Ab
(+ RNase)
(ix)
NS3
60kD
1 2 3 4 5
IP : Anti-EF1α Ab
WB : Anti-EF1α Ab
(- RNase)
(x)
EF1α
50kD
1 2 3 4 5
IP : Anti-EF1α Ab
WB : Anti-EF1α Ab
(+ RNase)
(xi)
EF1α
50kD
1 2 3 4 5
WCL
WB: Anti-EF1α Ab
(xii)
EF1α
50kD
1 2 3 4 5
WCL
WB: Anti-NS3 Ab
(xiii)
NS3
60kD
1 2 3 4 5
WCL
WB: Anti-actin Ab
(xiv)
42 kD
1 2 3 4 5

was not precipitated with anti-EF1α antibody following RNase treatment. The successful immunoprecipitation using anti-EF1α antibody was confirmed by probing with anti-EF1α antibody [Fig. 5.9(iii, iv, x & xi)]. Taken together, this showed that the interaction between NS3 protein and EF1α was mediated by an RNA bridge [Fig. 5.9(i, ii, viii & ix)] and the inability of EF1α to associate with RNA (Figs. 5.3 and 5.5) would have prevented the co-immunoprecipitation of EF1α-NS3 complex in hSec3pOE cells [Fig. 5.9(i & viii)].

To assess if hSec3p has an effect on the cellular distribution of EF1α and viral replicative machinery, co-localization studies (Section 2.13) were performed in WNV/DENV-infected HEK293, hSec3p293OE and hSec3p293KD cells. The surrogate markers NS3 (Fig. 5.10) and viral RNA (Fig. 5.11) were used to represent viral replicative machinery. As depicted in Figs. 5.10 and 5.11, NS3, dsRNA and EF1α co-localized predominantly in the perinuclear regions (arrows) regardless of the expression level of hSec3p. This suggested that hSec3p did not alter the cellular localization of EF1α and viral replicative complex.

Fig. 5.10: Association of EF1α with NS3. Cellular localization of EF1α and NS3 in WNV/DENV-infected cells. (i) HEK293, (ii) hSec3p293KD and (iii) hSec3p293OE cells were infected with WNV/DENV. The cells were then processed for confocal microscopy using anti-NS3 and anti-EF1α antibodies together with Alexa488 (green) or Alexa594 (red) secondary antibodies, respectively. Co-localization of NS3 and EF1α proteins are predominantly observed in the perinuclear regions (white arrows) of WNV/DENV-infected HEK293 and hSec3p293KD/OE cells as depicted in the merged images. Cell nuclei are stained with DAPI (blue).

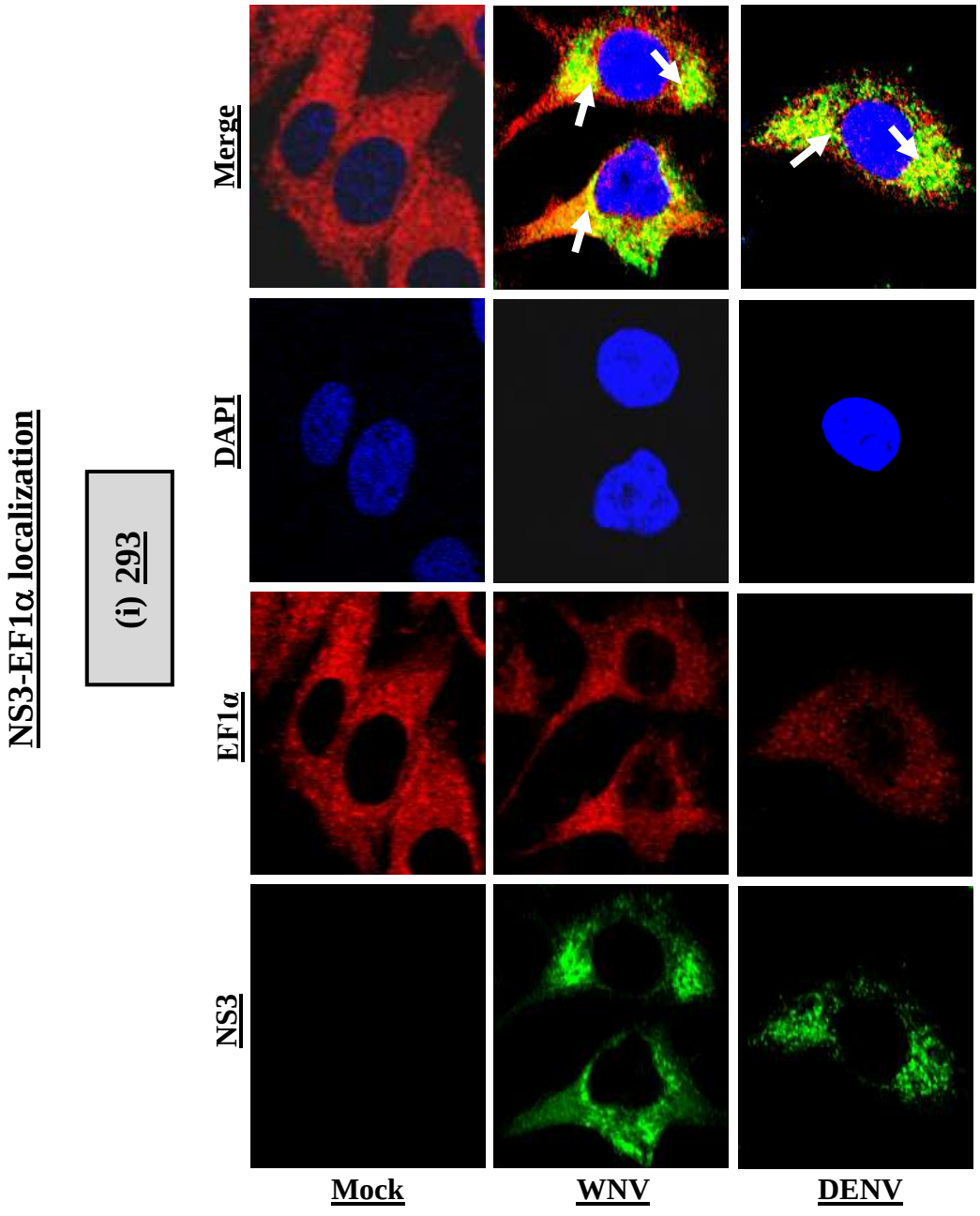
NS3-EF1α localization
(i) 293
Merge
DAPI
EF1α
NS3
Mock
WNV
DENV

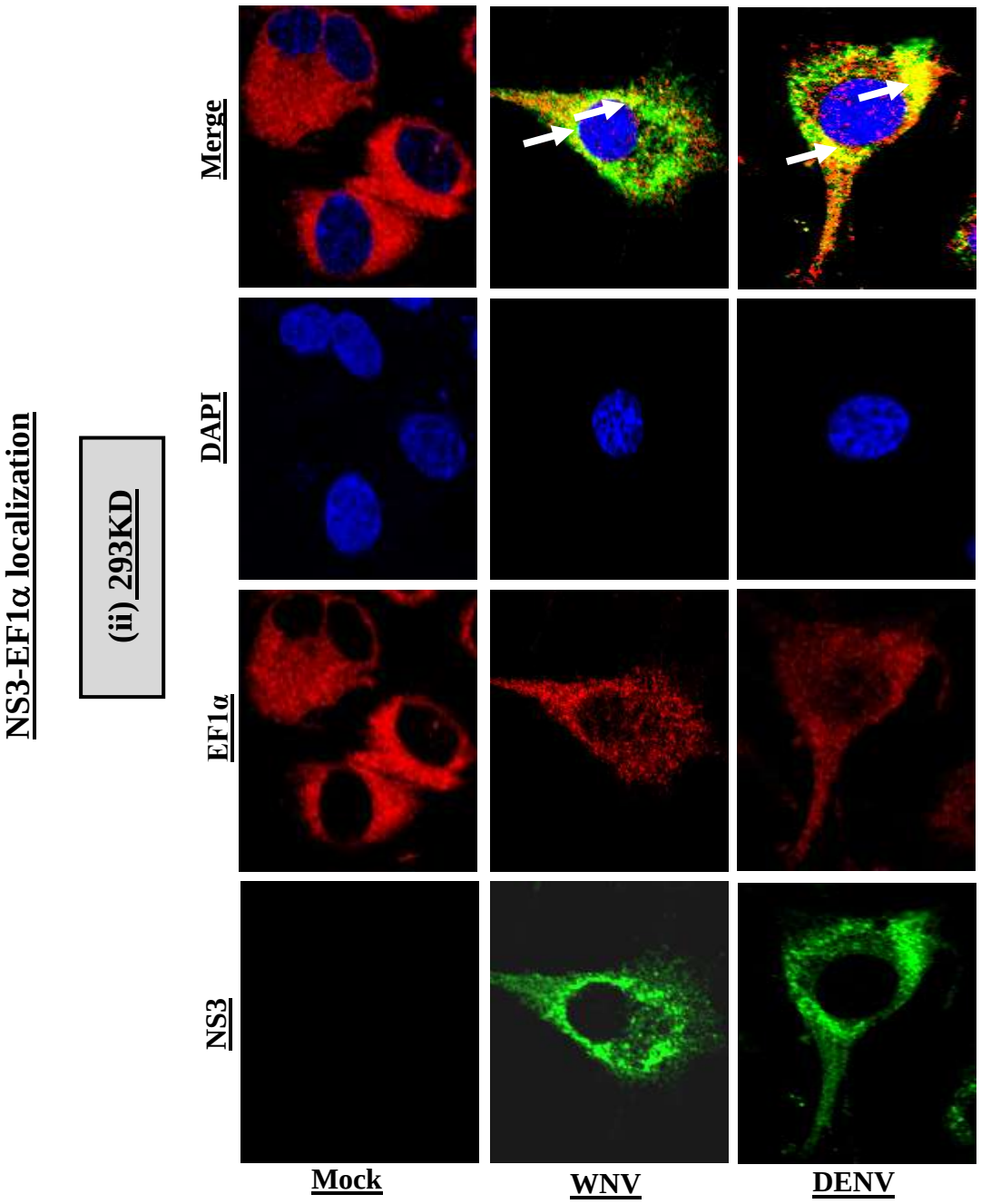
NS3-EF1α localization
(ii) 293KD
Merge
DAPI
EF1α
NS3
Mock
WNV
DENV

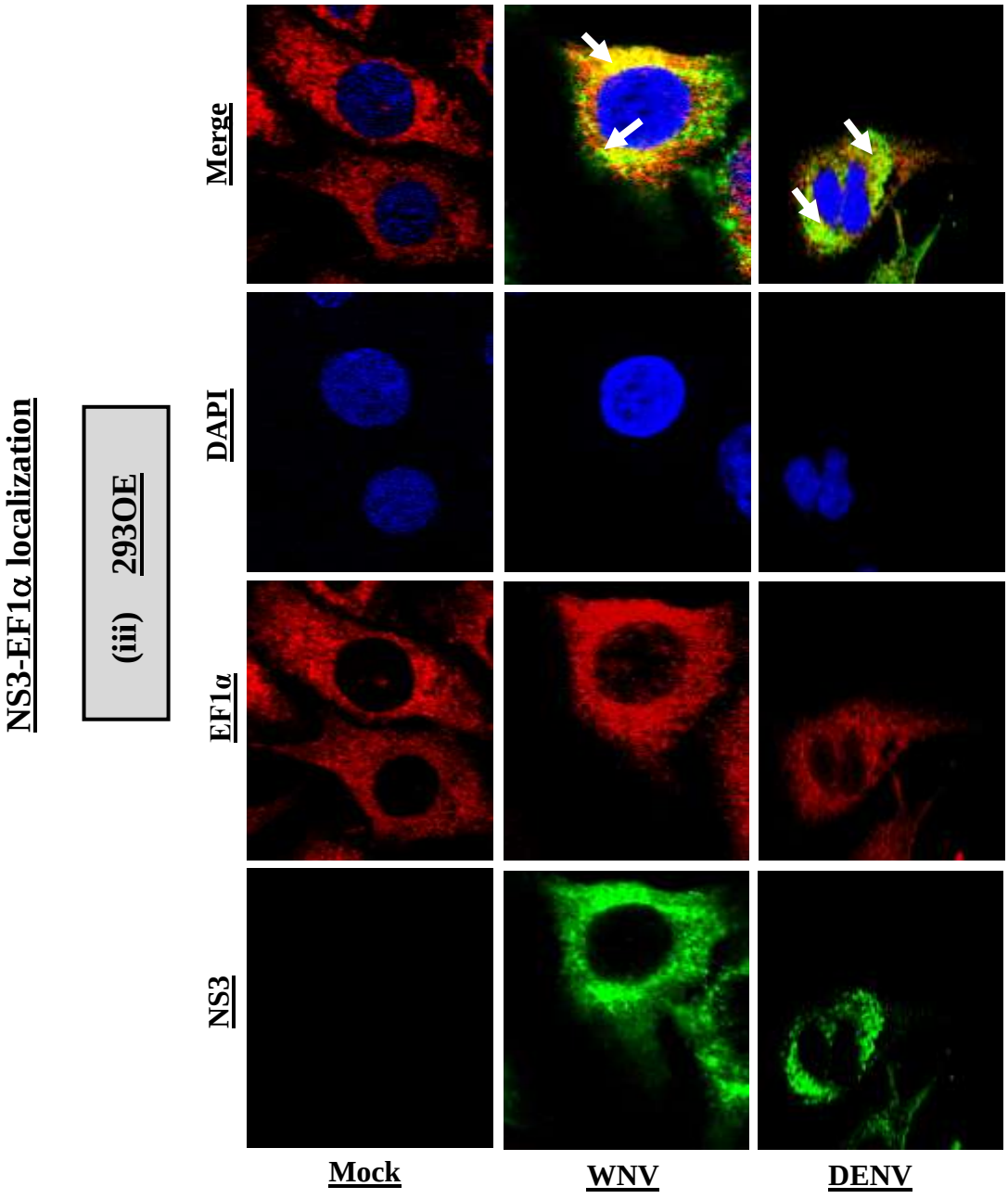
NS3-EF1α localization
(iii) 293OE
Merge
DAPI
EF1α
NS3
Mock
WNV
DENV

Fig. 5.11: Association of EF1α with viral dsRNA. Cellular localization of EF1α and dsRNA in WNV/DENV-infected cells. (i) HEK293, (ii) hSec3p293KD and (iii) hSec3p293OE cells were infected with WNV/DENV. The cells were then processed for confocal microscopy using anti-dsRNA and anti-EF1α antibodies together with Alexa488 (green) or Alexa594 (red) secondary antibodies, respectively. Co-localization of dsRNA and EF1α proteins are predominantly observed in the perinuclear regions (white arrows) of WNV/DENV-infected HEK293 and hSec3p293KD/OE cells as depicted in the merged images. Cell nuclei are stained with DAPI (blue).

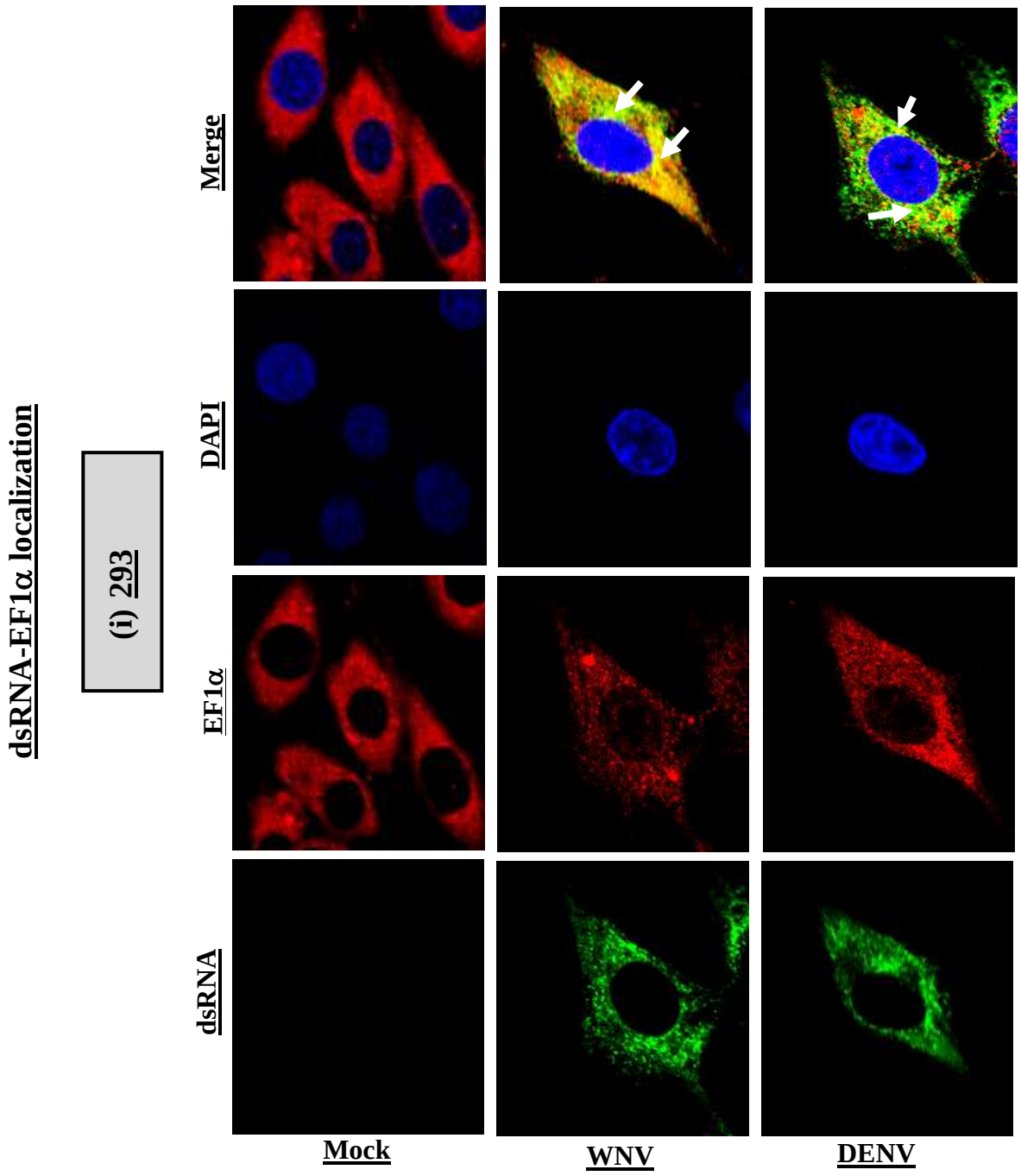
dsRNA-EF1α localization
(i) 293
Merge
DAPI
EF1α
dsRNA
Mock
WNV
DENV

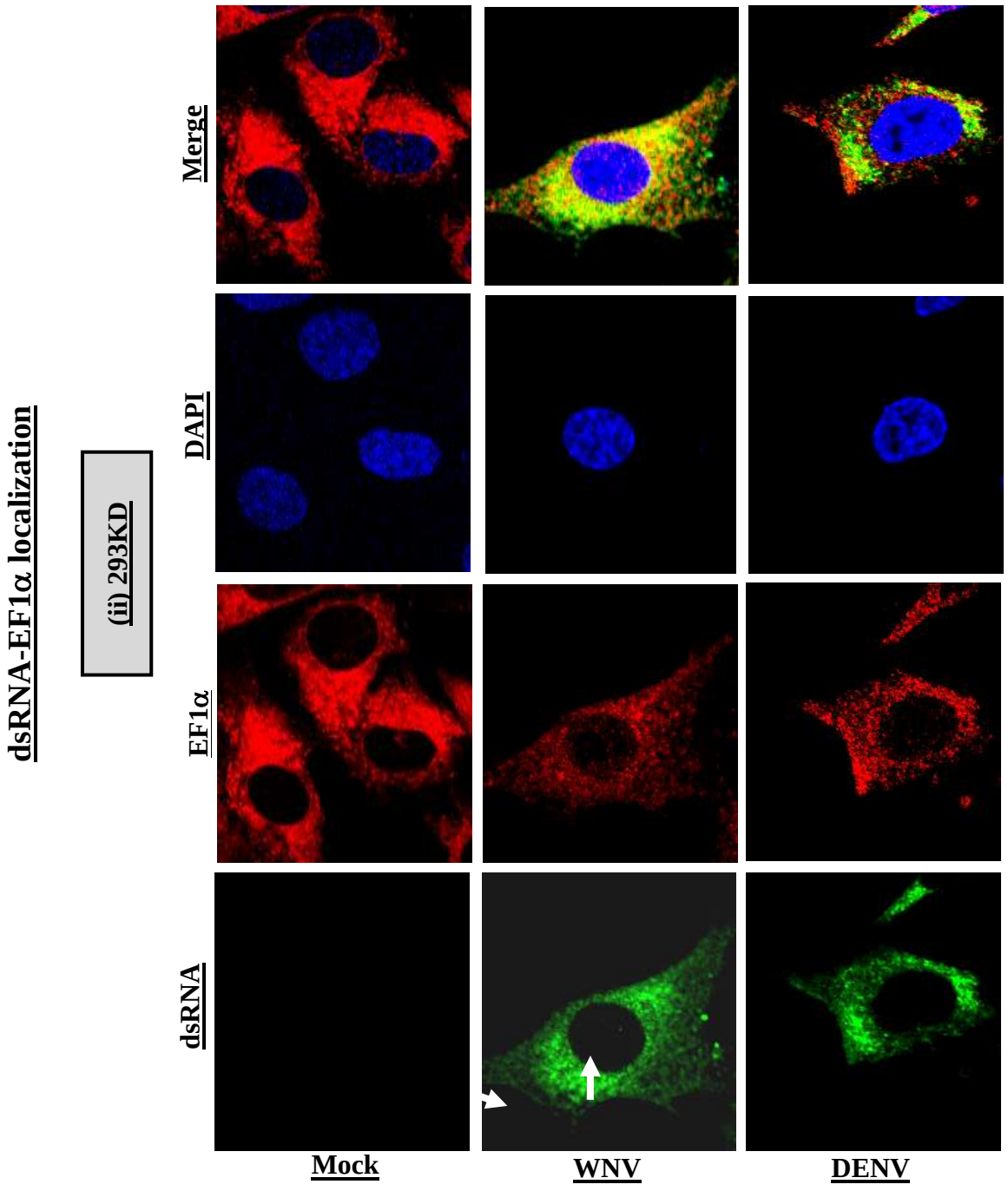
dsRNA-EF1α localization
(ii) 293KD
Merge
DAPI
EF1α
dsRNA
Mock
WNV
DENV

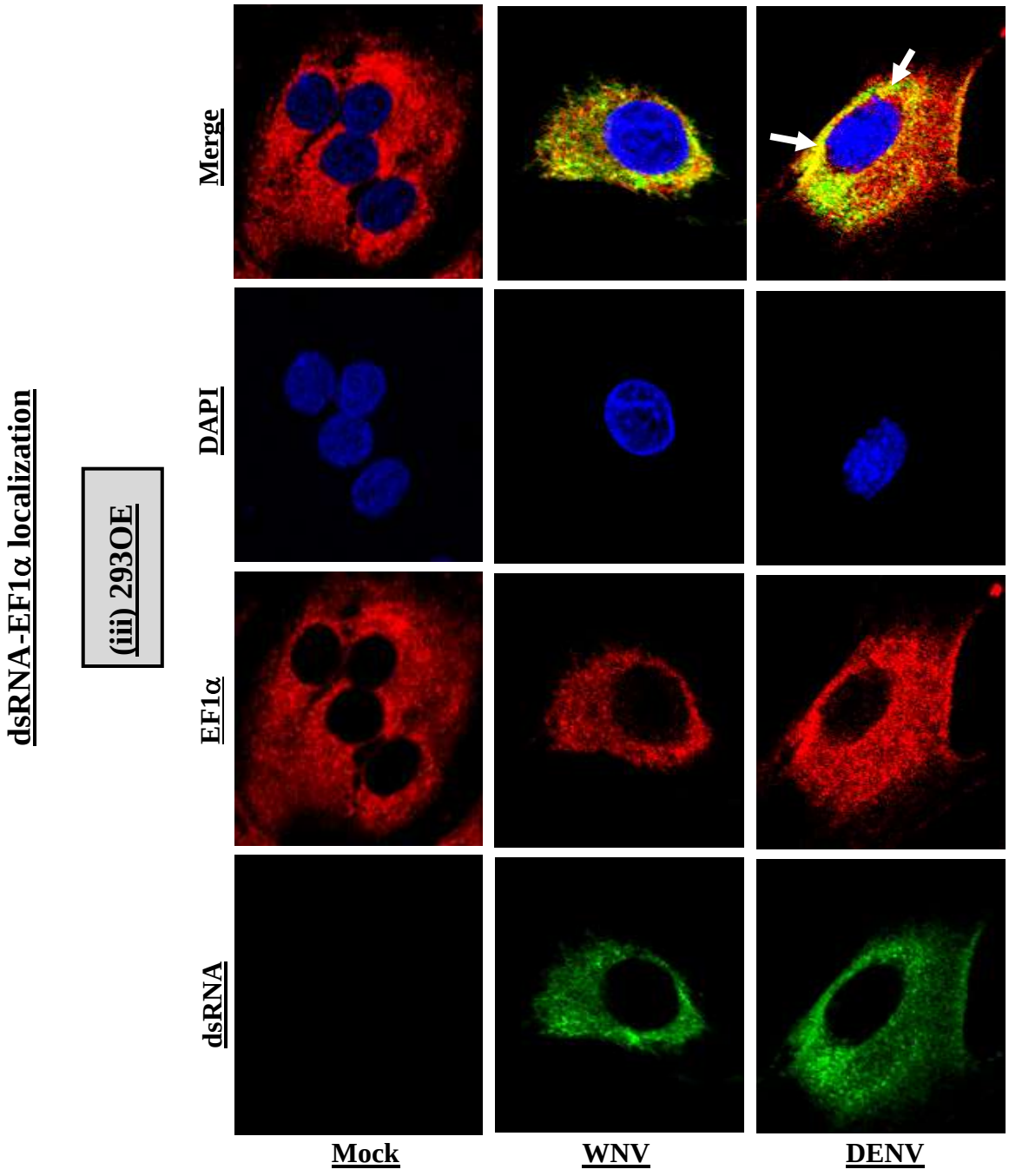
dsRNA-EF1α localization
(iii) 293OE
Merge
DAPI
EF1α
dsRNA
Mock
WNV
DENV

5.3. MECHANISM BEHIND HUMAN Sec3 PROTEIN-INDUCED REDUCTION IN VIRAL PROTEIN SYNTHESIS

5.3.1. Influence of human Sec3 protein on impaired viral RNA translation

The excess hSec3p had negative effect on viral protein expression (Figs. 4.10 and 4.11). The next question to address is if hSec3p has direct effect on viral protein translation. To answer this issue, *in vitro* translation assay (Sections 2.4.3 and 2.11.2) was performed using pre-synthesized full-length V5-hSec3pf1 or V5-galactosidase and WNV/DENV RNA in the absence of MG132, a proteasome inhibitor. The *in vitro* reaction showed that translation of E protein was reduced in the presence of hSec3p [Fig. 5.12(i & ii), Lane 2] and remained unaffected in the absence of hSec3p [Fig. 5.12(i & ii), Lanes 1 & 3]. This indicated that hSec3p had direct influence on viral RNA translation.

Reduced viral protein levels could result from impaired viral RNA translation or accelerated protein degradation. The *in vitro* translation was thus performed in the presence of MG132. If the reduction in viral protein levels was attributed to protein degradation, addition of MG132 should prevent the reduction in viral protein levels. As shown in Fig. 5.12(i & ii), Lane 5], addition of MG132 did not restore the levels of viral protein, indicating that hSec3p directly impaired viral RNA translation rather than accelerating its degradation.

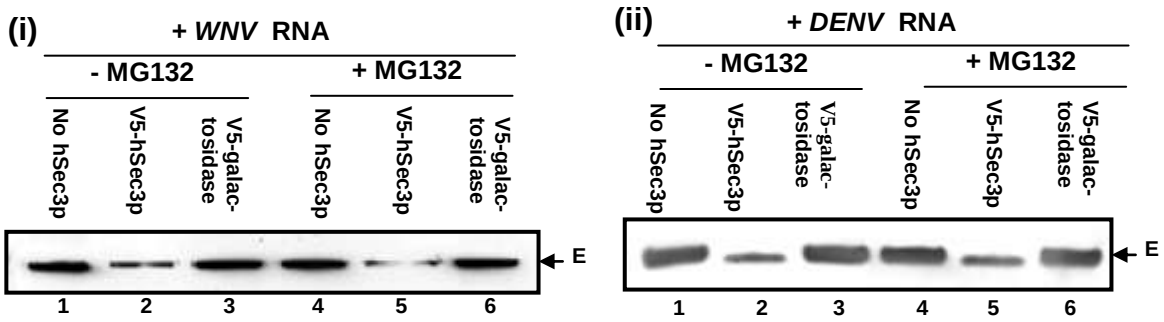

Fig. 5.12: *In vitro* translation assay. (i) WNV RNA or (ii) DENV RNA was translated by adding presynthesized V5-hSec3pf1 or V5-galactosidase in the absence/presence of MG132. The E proteins were analyzed by Western blotting and the band intensities were quantified. The presence of hSec3p results in 60% reduction in WNV/DENV E protein levels (Lane 2) even in the presence of MG132 (Lane 5). * indicates $P<0.05$.

5.3.2. Immunodepletion of human Sec3 protein

To determine if the inhibitory effects of hSec3p were attributed to translation in general or specific to viral translation, immunodepletion assay (Section 2.11.1) was performed where hSec3p was depleted. The *in vitro* translated hSec3p in the reticulocyte mix was immunodepleted using anti-hSec3p antibody and isotype control antibody. The resulting flow-throughs (Fig. 5.13, Lanes 1 & 3) and the eluents (Fig. 5.13, Lanes 2 & 4) were tested for the presence of hSec3p using Western blotting (Section 2.5.2).

Significant amount of hSec3p was immunodepleted in the flow-through fraction of anti-hSec3p antibody-treated samples (Fig. 5.13, Lane 1) and the majority of hSec3p was eluted in the eluent fraction (Fig. 5.13, Lane 2). In contrast, majority of hSec3p was washed off in the flow-through fraction of isotype antibody-treated samples (Fig. 5.13, Lane 3) and there was no hSec3p in the eluent fraction (Fig. 5.13, Lane 4). The flow-through fractions from anti-hSec3p antibody-treated samples (Fig. 5.13, Lane 1) and isotype antibody-treated samples (Fig. 5.13, Lane 3) were used in the subsequent assays to examine the mechanism behind hSec3p-mediated translational repression.

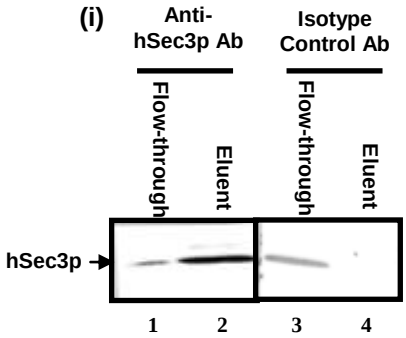

Fig. 5.13: Immunodepletion assay. Presynthesized V5-hSec3pf1 was mixed with either anti-hSec3p antibody or mouse isotype antibody control and subjected to μMACS column purification. The resultant flow-through (Lane 1) and eluent (Lane 2) from anti-hSec3p antibody-treated sample were subjected to immunoblotting using anti-hSec3p antibody. The flow-through (Lane 3) and eluent (Lane 4) from isotype control antibody-treated samples were also subjected to immunoblotting. As shown in Lane 1, significant immunodepletion is achieved in the flow-through fraction.

5.3.2.1. Human Sec3 protein-mediated translational repression is virus-specific

After confirming the significant immunodepletion of hSec3p in the flow-through fraction, it was mixed with a new reticulocyte mixture containing either WNV/DENV or IRF2 or CAML or importin-α RNA (Section 2.11.2). The resulting samples were probed using anti-WNV E, anti-DENV E, anti-IRF2, anti-CAML or anti-importin-α antibodies. The experiments were similarly performed using antibody isotype control.

As shown in Fig. 5.14, the translation of viral E protein (Lanes 1 & 3) was lowered in isotype antibody-treated samples while the translation of viral proteins (Lanes 2 & 4) was unaffected in hSec3p-immunodepleted samples. In contrast, the translation of IRF2, CAML and importin-α were not affected in both hSec3p-immunodepleted and antibody isotype control samples (Fig. 5.14, Lanes 5-10). These *in vitro* experiments in rabbit reticulocyte lysates indicated that the hSec3p-mediated translational repression was virus-specific and it did not affect the translation of selected host genes.

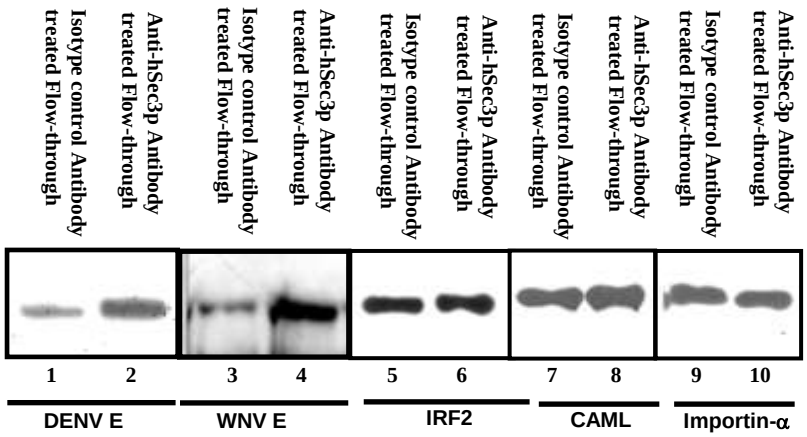

Fig. 5.14: *In vitro* translation assay. The flow-throughs from anti-hSec3p antibody-treated sample and isotype antibody-treated sample were separately mixed with WNV/DENV/IRF2/CAML/importin-α RNA in the *in vitro* translation reaction. WNV/DENV E, IRF2, CAML and importin-α protein levels were detected by Western blotting using anti-E, anti-IRF2, anti-CAML or anti-importin-α antibodies. As shown in Lanes 1 and 3, the translation of WNV/DENV E proteins are reduced in the presence of isotype control antibody-treated reaction mixtures compared to those in the presence of anti-hSec3p antibody-treated flow-through (Lanes 2 and 4). In contrast, the translation of IRF2, CAML and importin-α are not affected in both anti-hSec3p antibody-treated and isotype control antibody-treated flow-throughs (Lanes 5-10). This confirms that hSec3p-mediated translational repression is virus-specific and does not affect the translation of selected host genes.

5.3.2.2. Human Sec3 protein suppressed viral translation by binding to elongation factor 1α

The results so far indicated that hSec3p impaired viral protein translation. Since the capability of hSec3p to bind a key translational enhancer EF1α was demonstrated (Fig. 5.1), it was tempting to investigate if EF1α is the candidate biomolecule targeted by hSec3p for translational suppression. To test this hypothesis, EF1α competition assay was performed (Section 2.11.2).

The flow-through fractions from hSec3p-immunodepleted samples and isotype antibody-treated samples were mixed with an *in vitro* translation reaction containing either WNV/DENV or IRF2 or CAML or importin-α RNA in the presence of 2 and 5 mole excess of EF1α. The resulting samples were probed using anti-WNV E, anti-DENV E, anti-IRF2, anti-CAML or anti-importin-α antibodies.

The negative impact of hSec3p on protein translation was overcome when 2 and 5 mole excess of EF1α was added to the reaction mixture [Fig. 5.15 (i & ii), Lanes 1 & 3]. This further supported that the hSec3p-dependent inhibition of protein translation was mediated by sequestration of EF1α.

In this chapter, the molecular mechanism underlying the anti-viral activity of hSec3p was delineated by unveiling the interrelationship between hSec3p, EF1a and flavivirus replication complex.

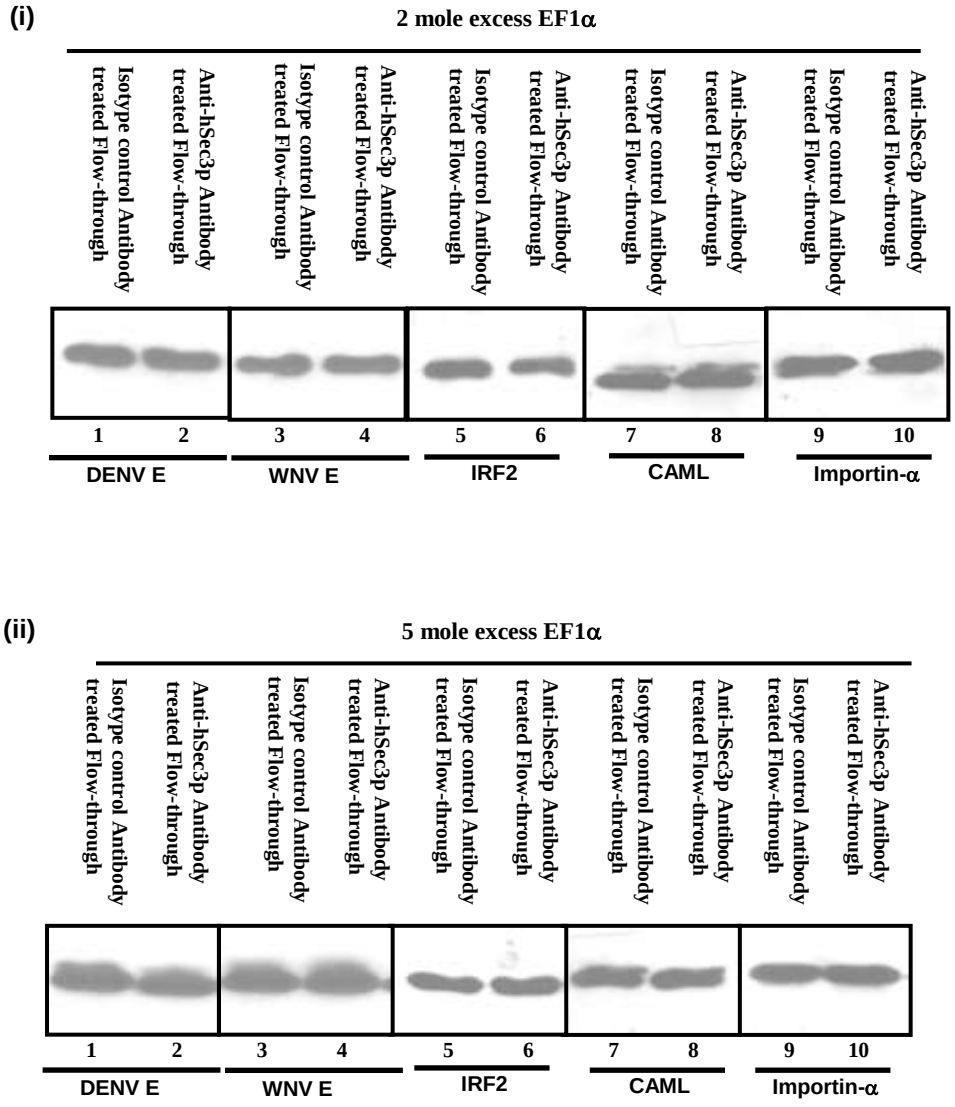

Fig. 5.15: *In vitro* translation assay in the presence of EF1α. The flow-throughs from anti-hSec3p antibody-treated sample and isotype antibody-treated sample were separately mixed with WNV/DENV/IRF2/CAML/importin-α RNA in the rabbit reticulocyte reaction in the presence of (i) 2 or (ii) 5 mole excess of EF1α. The protein levels of WNV/DENV E, IRF2, CAML and importin-α were detected using anti-E, anti-IRF2, anti-CAML or anti-importin-α antibodies. Addition of 2 or 5 mole excess of EF1α circumvent the translational repression mediated by hSec3p.

CHAPTER 6

RESULTS

6.0. MOLECULAR INSIGHTS INTO THE ANTAGONISTIC ACTIVITY OF FLAVIVIRUS CAPSID PROTEIN AGAINST HUMAN Sec3 PROTEIN

6.1. INTRODUCTION

The previous chapters highlighted the anti-flaviviral properties of hSec3p. However, it is unclear how WNV/DENV can still successfully infect the host in the presence of endogenous hSec3p. Can hSec3p-C protein interaction favour flaviviral infection? As described in Section 5.2.1, the amount of EF1α-hSec3p complex formation was significantly lowered in the infected cells compared to uninfected cells. This indicated that WNV/DENV infection could interfere with EF1α-hSec3p complex formation by altering the hSec3p level. This chapter thus sought to investigate the molecular mechanism underlying flavivirus-induced reduction in EF1α-hSec3p complex formation. In this chapter, cell-based fluorescence assay was also developed in-house to quantitate the amount of hSec3p, hSec6p, viral E proteins or HA/Myc-tagged C proteins in high-throughput formats.

6.2. FLAVIVIRUS INFECTION REDUCED THE LEVELS OF HUMAN Sec3 PROTEIN

6.2.1. Effect of flavivirus infection on human Sec3 protein levels

To examine whether flavivirus infection regulated the levels of hSec3p, HEK293 cells were infected with WNV/DENV. At the indicated timings, hSec3p expression was assessed at the protein level in WNV/DENV-infected HEK293 cells using Western blotting. The results showed that hSec3p was down-regulated

in WNV/DENV-infected cells compared to that of un-infected cells [Figs. 6.1A(i) and 6.1B(i)]. The band intensities on the immunoblot were subsequently quantified using GeneTools program and the hSec3p levels were expressed as the percentage difference normalized against the hSec3p levels in the un-infected cell lysate. Densitometry analysis revealed that flavivirus reduced hSec3p level from as early as 4 h p.i. [Figs. 6.1A(iii) and 6.1B(iii)]. This showed that there was active down-regulation of hSec3p in flavivirus-infected cells.

6.2.2. Development of cell-based fluorescence assay (CBF assay)

To examine the levels of hSec3p following virus infection or plasmid transfection in the high-throughput format, CBF assay was developed. HEK293 cells were infected with WNV/DENV. At the indicated timings, cells were stained with anti-hSec3p and anti-actin antibodies followed by incubation with anti-mouse or anti-rabbit Alexa488 or Alexa594 secondary antibodies. The samples were analyzed in a microtitre plate reader. The hSec3p levels in each experimental cohort were normalized against the actin control and the relative levels of hSec3p in virus-infected cells were represented as the percentage difference with respect to that of un-infected HEK293 cells.

Consistent with Fig. 6.1, reduced hSec3p levels were observed in WNV/DENV-infected cells compared to that of un-infected cells (Figs. 6.2A and 6.2B). As shown in Fig. 6.3, the percentage difference of hSec3p levels obtained from Western blotting followed by densitometry (Fig. 6.1) coincided with the data obtained from CBF assay (Fig. 6.2). The data obtained from CBF assay showed slightly lower levels of hSec3p in virus-infected cells compared to that obtained

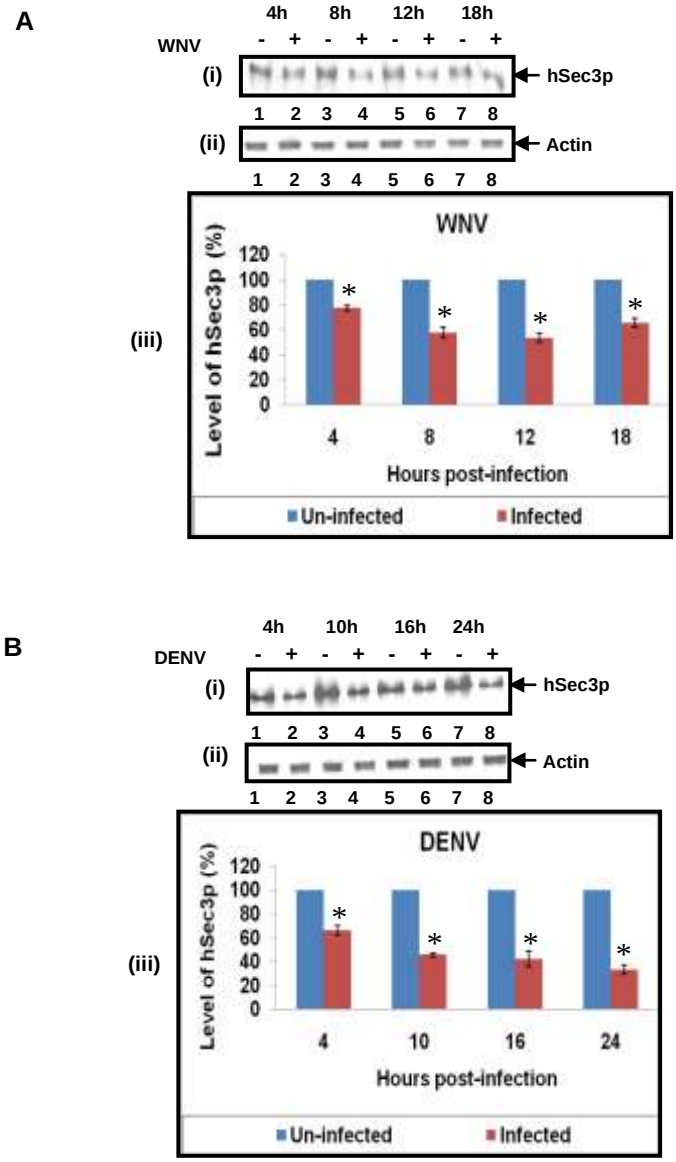

Fig. 6.1: Effect of flavivirus infection on hSec3p expression - Western blotting. HEK293 cells were infected with (A) WNV or (B) DENV. (i) The hSec3p expression level was assessed at the indicated timings by immunoblotting with anti-hSec3p antibody. Reduced hSec3p level is detected in WNV/DENV-infected cells from as early as 4 h p.i. and is sustained up to 24 h p.i. (ii) Actin loading controls are included to ensure equal loading. (iii) Densitometry analysis of the band intensities in the virus-infected cells obtained from the immunoblots [A(i) and B(ii)] after normalization against the band intensities in the un-infected cells. * represents $P<0.05$ compared to un-infected cells.

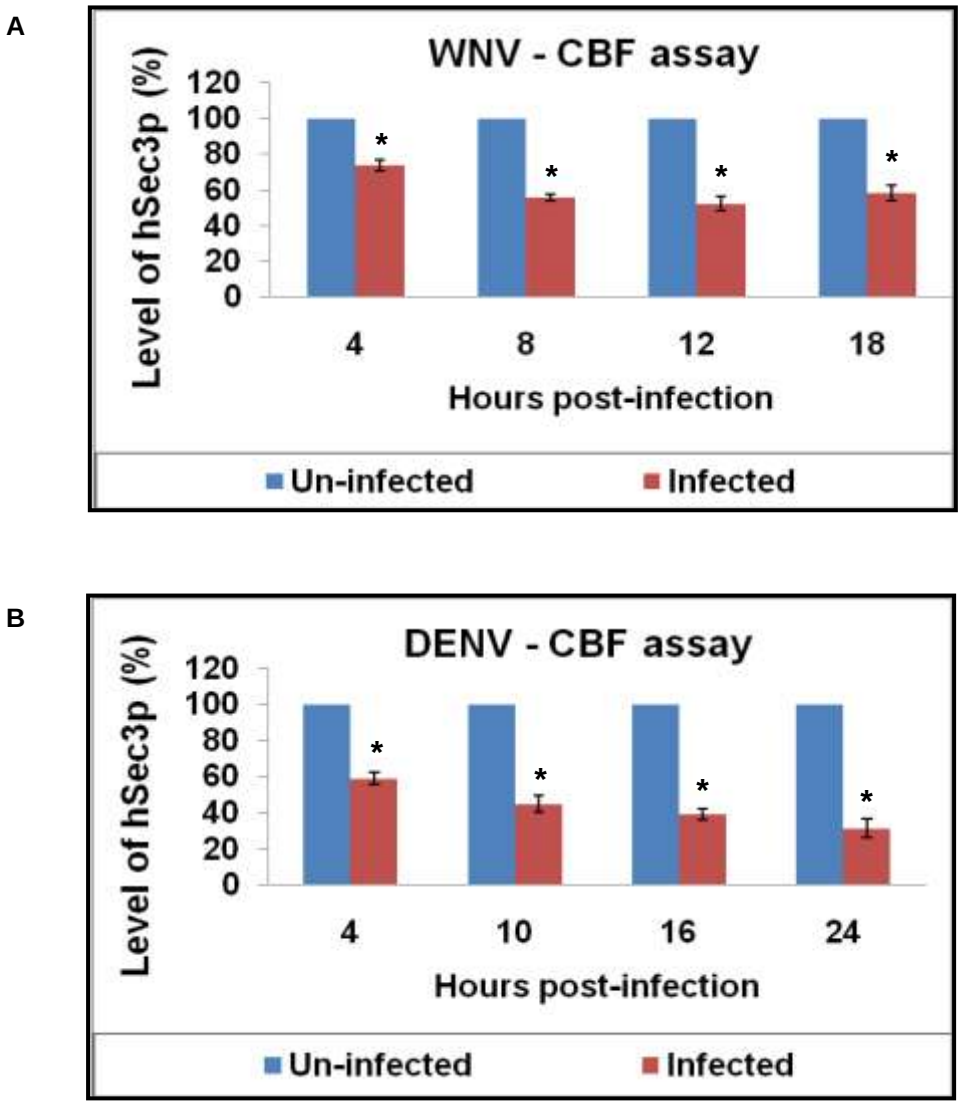

Fig. 6.2: Effect of flavivirus infection on hSec3p expression - CBF assay. HEK293 cells were infected with (A) WNV or (B) DENV. The hSec3p expression level was assessed at the indicated timings by CBF assay using anti-hSec3p and anti-actin antibody. The hSec3p levels are normalized against the actin control and the relative levels of hSec3p in virus-infected cells are shown. Reduced hSec3p level is detected in WNV/DENV-infected cells from as early as 4 h p.i. and is sustained up to 24 h p.i. * represents $P<0.05$ compared to un-infected cells.

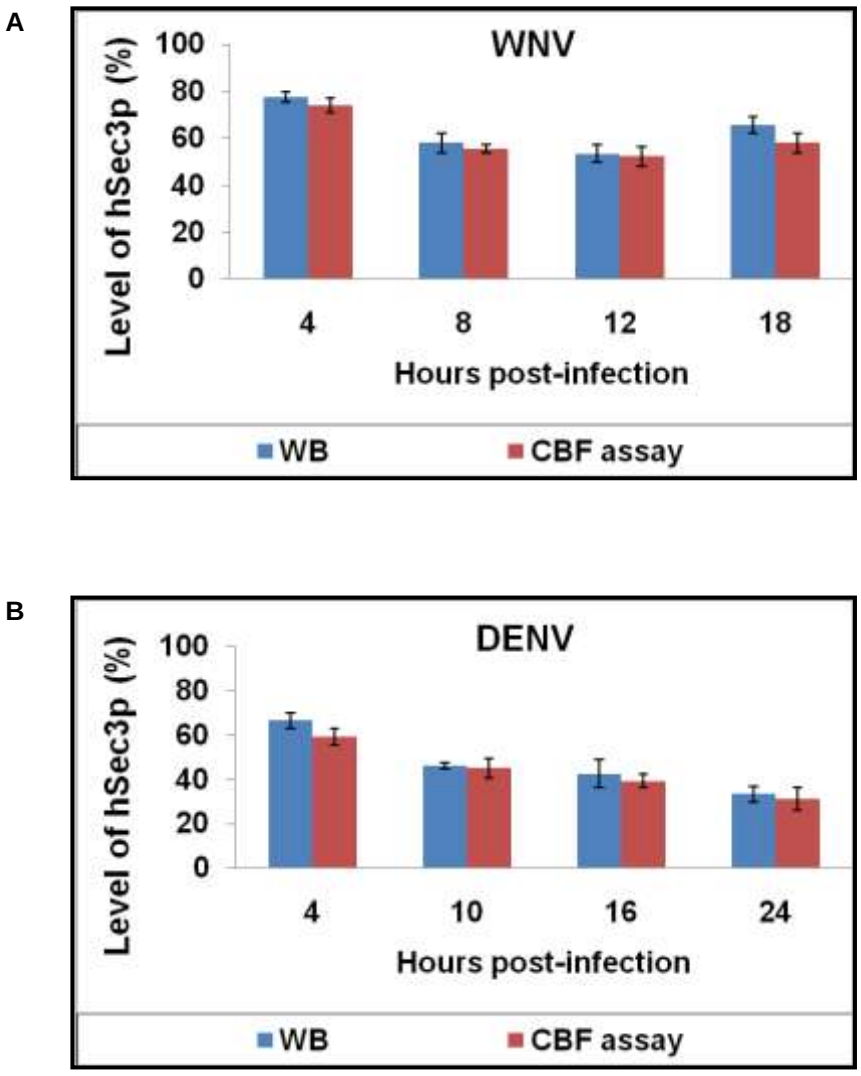

Fig. 6.3: Comparison of hSec3p levels obtained from Western blotting and CBF assay. The hSec3p levels obtained from Western blotting followed by densitometry were compared with that assessed by CBF assay. There is no significant difference in the levels of hSec3p obtained from Western blotting followed by densitometry and CBF assay.

from Western blotting followed by densitometry. However, this difference was not statistically significant (P>0.05) and similar trend was obtained from both assays. This demonstrated that CBF assay developed in this study was reliable and suitable to use in the high-throughput format. The CBF assay was thus utilized in the subsequent experiments to analyze the amount of hSec3p/hSec6p/actin/HA-tagged proteins/Myc-tagged proteins in the cells following various treatments.

The accuracy of the assay could be compromised if the antibody non-specifically detects more than one protein or detects only the denatured protein. To overcome the non-specificity issue, the controls such as mock-infected samples (in case of virus infection) and vector alone-transfected samples (in case of transfection) were included in this study. This would facilitate the normalization to eliminate the non-specific signals contributed by the antibody. It was also confirmed in our laboratory that the antibodies used in this study were able to detect both denatured and non-denatured forms of the protein by performing Western blotting and immuno-fluorescence assay.

6.2.3. Flavivirus infection did not alter the transcription of human *Sec3* gene

To examine if flavivirus-induced changes in hSec3p level were due to altered hSec3p mRNA level, HEK293 cells were infected with WNV/DENV. At the indicated time points, total RNA was extracted and subjected to real-time RT-PCR to detect the differences in the level of hSec3p RNA in flavivirus-infected cells. Normalization was performed against mock-infected samples and GAPDH in all data sets. As shown in Figs. 6.4A and 6.4B, there were no significant changes in the mRNA levels of hSec3p in flavivirus-infected cells (P>0.05). This indicated that flavivirus infection did not alter the transcription of the *hSec3* gene or the stability of the transcribed mRNA.

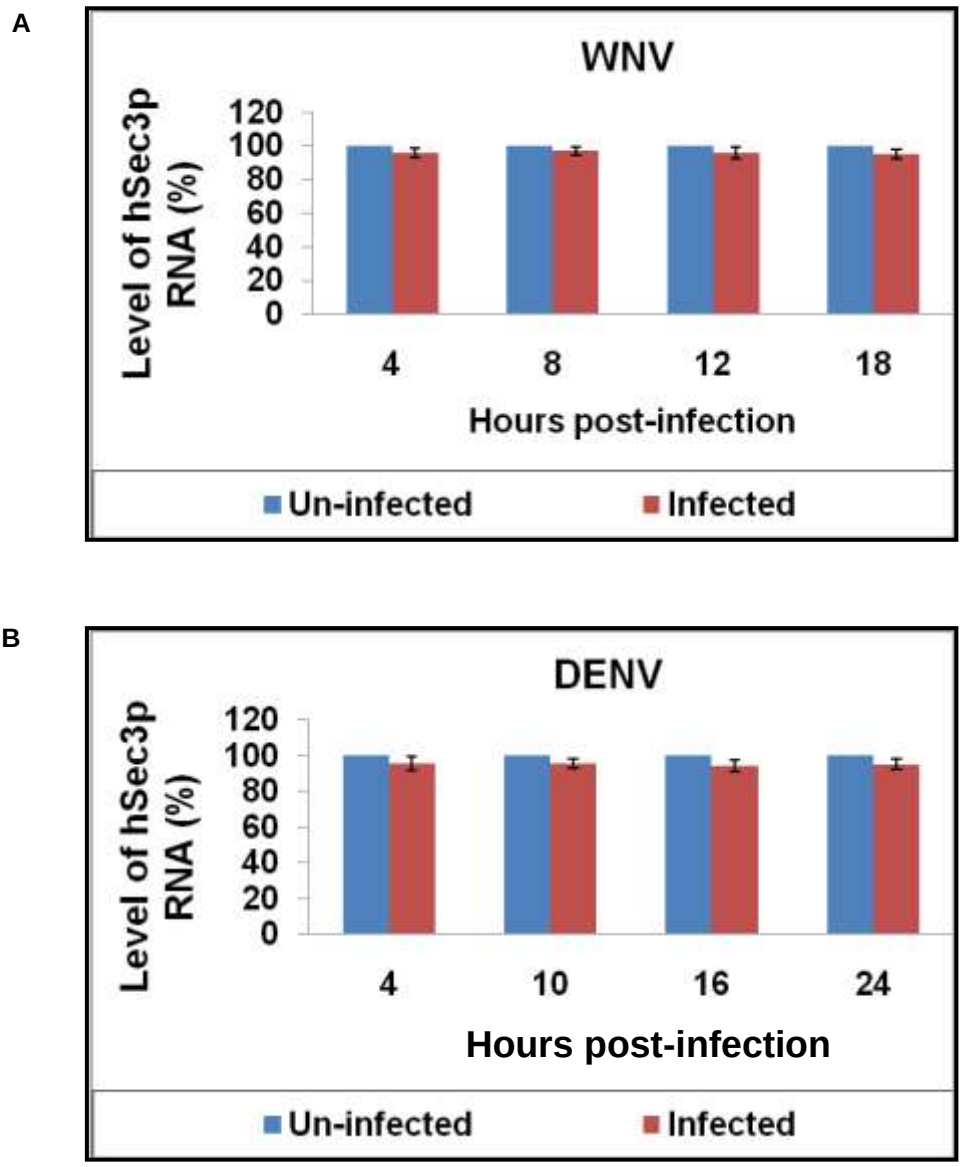

Fig. 6.4: Effect of flavivirus infection on hSec3p mRNA level. HEK293 cells were infected with (A) WNV or (B) DENV. The levels of hSec3p mRNA was measured using real-time PCR. There is no significant difference in the levels of hSec3p mRNA in WNV/DENV-infected cells compared to that of un-infected cells.

6.2.4. Flavivirus infection influenced human Sec3 protein level at the post-transcription level

To investigate if flavivirus infection manipulated the amount of hSec3p at the post-transcription level, cell-based fluorescence (CBF) assay was conducted in the presence of Actinomycin D. Host cell transcription was blocked by incubating HEK293 cells with Actinomycin D. This was followed by infection with WNV/DENV. As shown in Figs. 6.5A and 6.5B, hSec3p level was decreased in WNV/DENV-infected cells even in the presence of Actinomycin D.

To further confirm that this reduction was specific to hSec3p, the expression levels of hSec6p were examined following flavivirus infection. The hSec6p levels were not affected in the presence of WNV/DENV infection (Figs. 6.6A and 6.6B). This indicated that the translation/stability of hSec3p was specifically affected by flavivirus infection.

To investigate if flavivirus infection interfered with hSec3p translation or its stability, the above experiment was performed in the presence of MG132, a proteasomal inhibitor and the level of endogenous hSec3p was monitored. In the presence of MG132, hSec3p levels remained unchanged even after flavivirus infection (Figs. 6.7A and 6.7B). This indicated that intact proteasome activity was required to mediate the reduction of hSec3p levels and the stability of hSec3p was compromised following flavivirus infection.

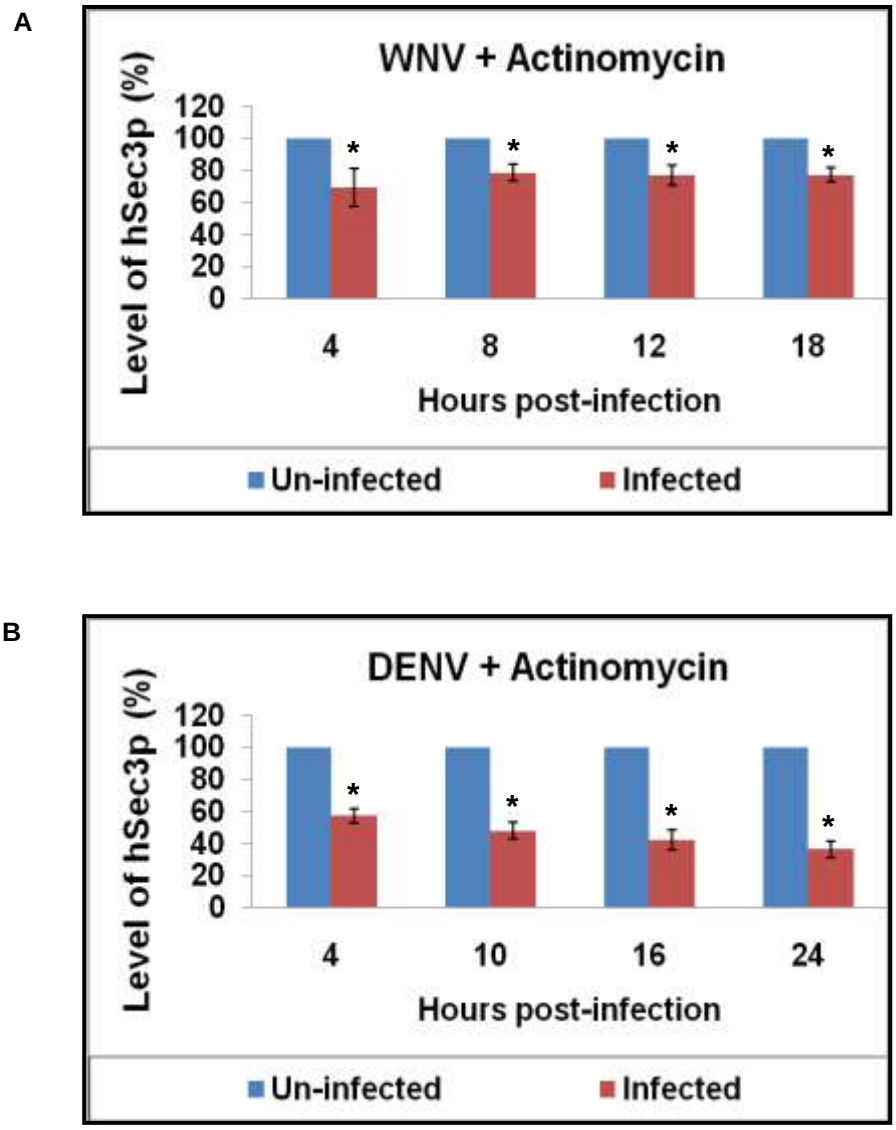

Fig. 6.5: Effect of flavivirus infection on hSec3p expression following Actinomycin treatment. HEK293 cells were treated with Actinomycin D and infected with (A) WNV or (B) DENV. The hSec3p expression level was assessed at the indicated timings by CBF assay using anti-hSec3p and anti-actin antibody. The hSec3p levels are normalized against the actin control and the relative levels of hSec3p in virus-infected cells are shown. Reduced hSec3p level is detected in WNV/DENV-infected cells from as early as 4 h p.i. even in the presence of Actinomycin. * represents $P<0.05$ compared to un-infected cells.

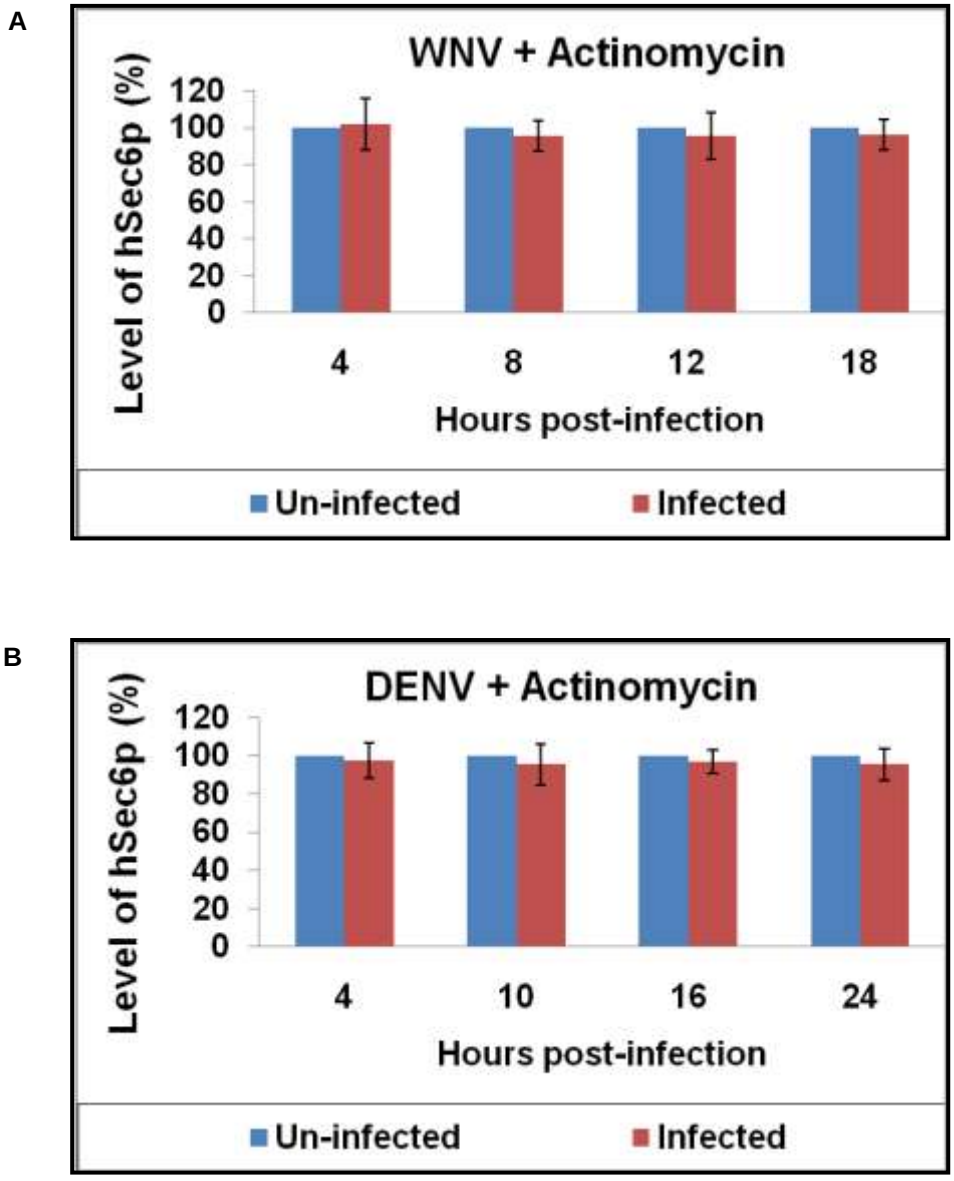

Fig. 6.6: Effect of flavivirus infection on hSec6p expression following Actinomycin treatment. HEK293 cells were treated with Actinomycin D and infected with (A) WNV or (B) DENV. The hSec6p expression level was assessed at the indicated timings by CBF assay using anti-hSec6p and anti-actin antibody. The hSec6p levels are normalized against the actin control and the relative levels of hSec6p in WNV/DENV-infected cells are shown. There are no significant differences ($P>0.05$) in the levels of hSec6p in virus-infected or un-infected cells.

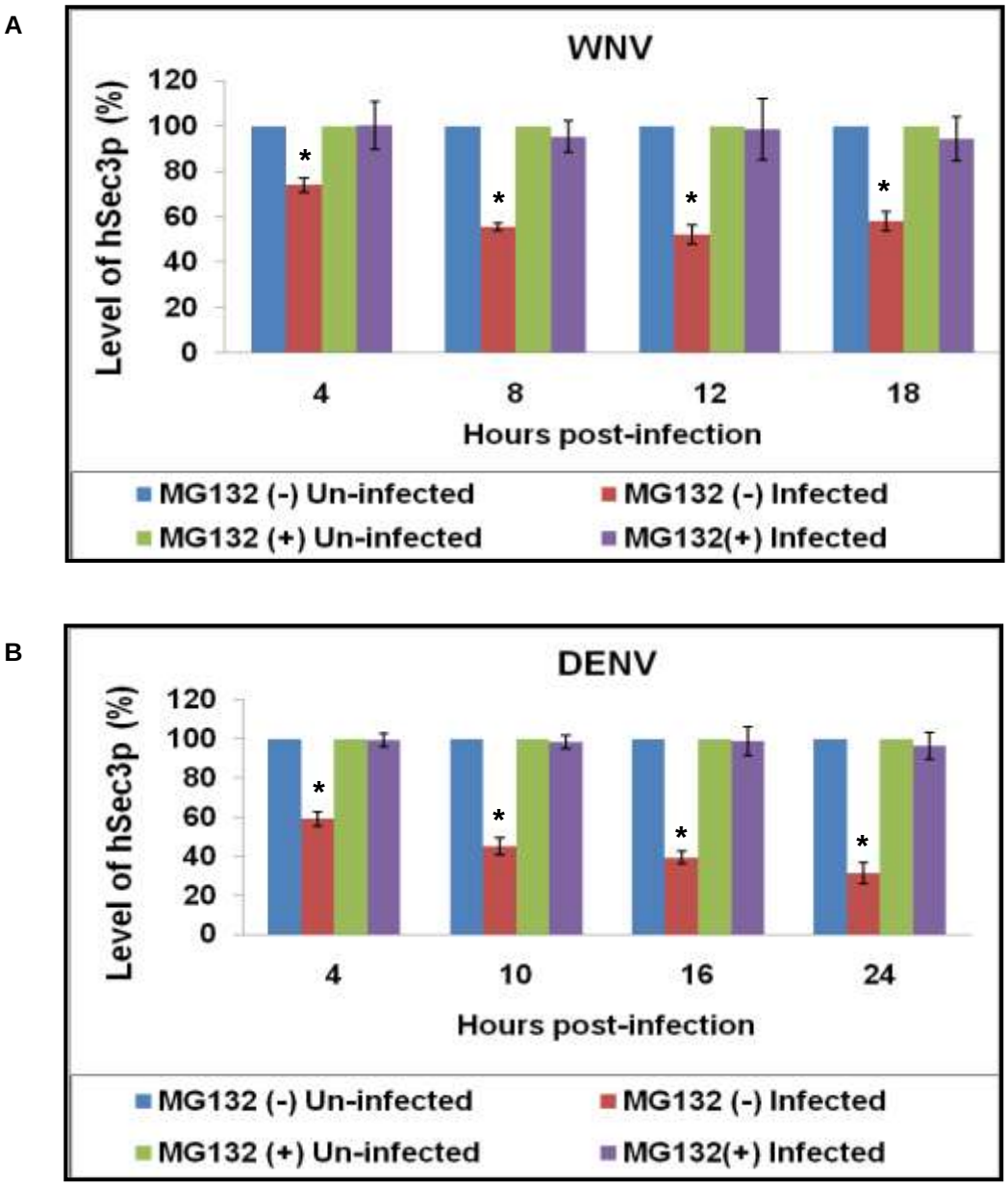

Fig. 6.7: Effect of flavivirus infection on hSec3p expression following MG132 treatment. HEK293 cells were treated with MG132 and infected with (A) WNV or (B) DENV. The hSec3p expression level was assessed at the indicated timings by CBF assay using anti-hSec3p and anti-actin antibody. The hSec3p levels are normalized against the actin control and the relative levels of hSec3p in virus-infected cells are shown. Reduced hSec3p level is detected in WNV/DENV-infected cells from 4 h p.i. in the absence of MG132. In contrast, there are no significant differences in the levels of hSec3p in MG132-treated virus-infected cells. * represents $P<0.05$ compared to un-infected cells.

6.3. FLAVIVIRUS CAPSID PROTEIN REDUCED THE LEVELS OF HUMAN Sec3 PROTEIN

6.3.1. Flavivirus capsid protein down-regulated human Sec3 protein expression

To evaluate the role of flavivirus C protein in reducing hSec3p level, HEK293 cells were transfected with HA-tagged plasmids encoding full-length WNV C gene (WHAC) or Myc-tagged plasmids encoding full-length WNV/DENV C protein (WMycC and DMycC) in the absence or presence of MG132. At 24 h post-transfection, expression of hSec3p and full-length WNV/DENV C proteins were assessed using cell-based fluorescence (CBF) assay.

In the absence of MG132, the hSec3p level was markedly reduced ($P<0.05$) following the transfection with full-length WNV/DENV C protein (Fig. 6.8A). Similar trends were obtained with HA-tagged or Myc-tagged C proteins. This confirmed that HA or Myc tag did not influence the outcome. In contrast, there were no significant differences ($P>0.05$) in the levels of hSec3p in MG132-treated full-length C plasmids-transfected cells (Fig. 6.8A). The expression of full-length WNV/DENV C protein was confirmed using anti-HA/anti-Myc and actin antibodies (Fig. 6.8B). There were no significant changes in the expression levels of hSec6p in the absence or presence of MG132 (Fig. 6.8C). Overall, this demonstrated that flavivirus C protein played an essential role in mediating the proteasome-mediated degradation of hSec3p.

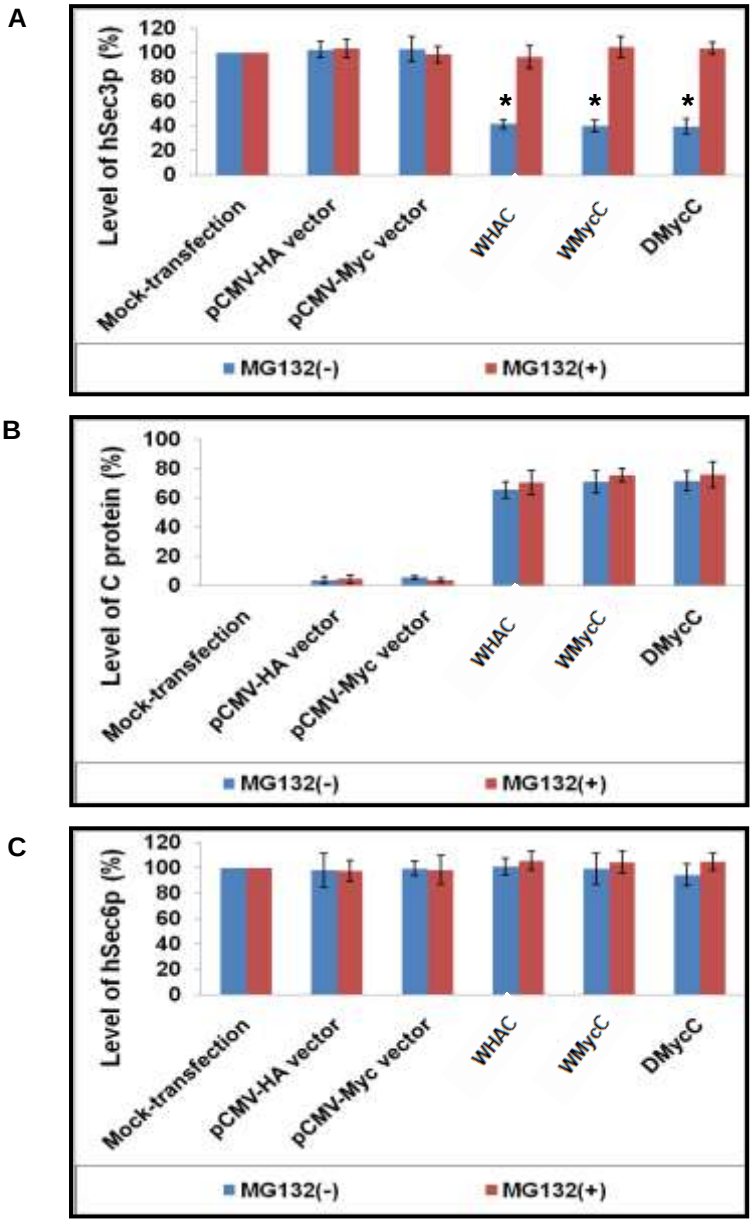

Fig. 6.8: Influence of flavivirus C protein on hSec3p expression. HEK293 cells were transfected with WHAC, WMycC and DMycC in the absence and presence of MG132. (A) The hSec3p expression level was assessed by CBF assay using anti-hSec3p and anti-actin antibody. The hSec3p levels are normalized against the actin control and the relative levels of hSec3p in transfected cells are shown. Reduced hSec3p level is detected in WNV/DENV C-transfected cells in the absence of MG132. In contrast, there are no significant differences in the levels of hSec3p in MG132-treated WNV/DENV C-transfected cells. (B) The expression of C protein is monitored by CBF assay using anti-HA/anti-Myc and anti-actin antibodies. (C) The expression of hSec6p is monitored by CBF assay using anti-hSec6p and anti-actin antibodies. * represents $P<0.05$ compared to mock-transfection.

6.3.2. Flavivirus capsid protein reduced human Sec3 protein expression in a dose-dependent manner

To further determine whether the C protein-mediated reduction in hSec3p levels was dependent on the amount of C protein expression, a dose response experiment was performed. The expression of full-length WNV/DENV C protein was analyzed using CBF assay with anti-Myc and actin antibodies (Fig. 6.9A). Expression of hSec3p was assessed using cell-based fluorescence (CBF) assay. As little as 100 ng of transfected WMycC (WNV) or DMycC (DENV) construct was able to reduce hSec3p level ($P<0.05$), with a maximum reduction reached at 300 ng of WMycC or DMycC plasmids (Fig. 6.9B). When the amount of WMycC or DMycC plasmid was increased, the levels of hSec3p were significantly reduced (Fig. 6.9C). This demonstrated that flavivirus C protein caused the decrement in hSec3p levels in a dose-dependent manner.

6.3.3. Physical binding between capsid protein and human Sec3 protein is critical to reduce human Sec3 protein level

This study was extended to examine whether physical binding flavivirus C protein and hSec3p is essential to mediate the reduction in hSec3p level. HEK293 cells were transfected with WMycC (WNV), WMycC5'Δ15 (WNV), DMycC (DENV) and DMycC5'Δ15 (DENV) plasmids. At 24 h post-transfection, expression of hSec3p and full-length/truncated WNV or DENV C proteins were assessed using cell-based fluorescence (CBF) assay. As mentioned previously, the hSec3p levels

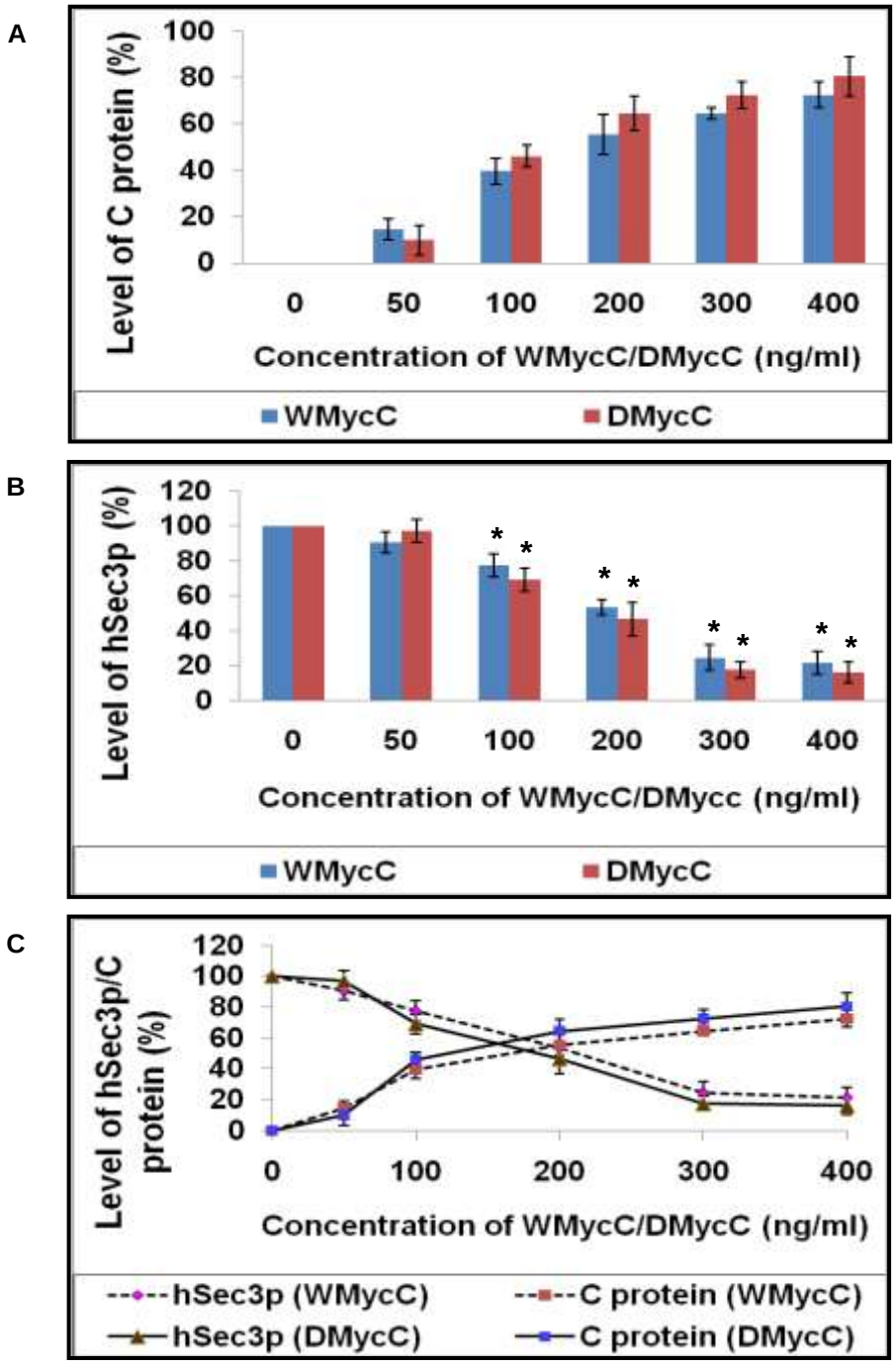

Fig. 6.9: Flavivirus C protein reduced hSec3p level in a dose-dependent manner. HEK293 cells were transfected with various concentrations of WMycC or DMycC. (A) The expression of C protein is monitored by CBF assay using anti-Myc and anti-actin antibodies. (B) The hSec3p expression level is assessed by CBF assay using anti-hSec3p and anti-actin antibody. The levels of hSec3p in WMycC/DMycC-transfected cells are reduced with the increasing concentrations of WMycC/DMycC plasmids. (C) The expression of C proteins negatively correlated with the expression of hSec3p levels. * represents $P<0.05$.

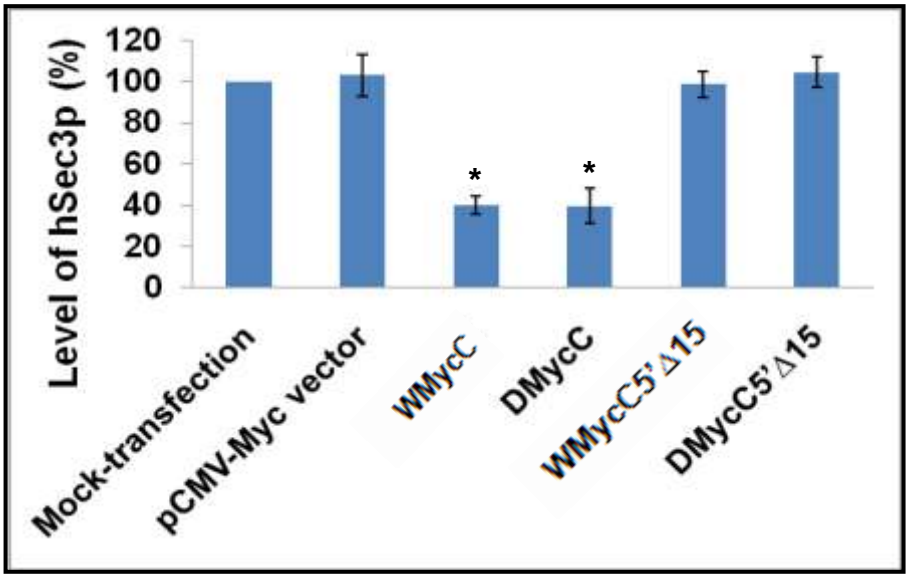

Fig. 6.10: Measurement of hSec3p level in the presence of hSec3p-binding defective C mutants. HEK293 cells were transfected with WMycC, WMycC5'Δ15, DMycC and DMycC5'Δ15 plasmids. The hSec3p expression level was assessed by CBF assay using anti-hSec3p and anti-actin antibody. The hSec3p levels are normalized against the actin control and the relative levels of hSec3p in transfected cells are shown. Reduced hSec3p level is detected in WMycC and DMycC-transfected cells. In contrast, there are no significant differences in the levels of hSec3p in WMycC5'Δ15 and DMycC5'Δ15-transfected cells. * represents $P<0.05$ compared to mock-transfection.

were markedly reduced following the transfection with full-length WNV/DENV C protein (Fig. 6.10). In contrast, equivalent amounts of hSec3p were detected in pCMV-Myc vector and WMycC5'Δ15/DMycC5'Δ15-transfected samples (Fig. 6.10). This indicated that C protein- mediated depletion of hSec3 protein was dependent on the direct binding between C protein and hSec3p.

To further confirm that direct binding between C protein and hSec3p was essential to mediate the decrement in hSec3p level, *in vitro* translation assay was performed by adding WMyCC, DMycC, WMycC5'Δ15 or DMycC5'Δ15 plasmids to the rabbit reticulocyte mix containing hSec3p RNA. As shown in Fig. 6.11A, translation of hSec3p RNA was reduced in the presence of full-length WNV/DENV C protein (Fig. 6.11A, Lanes 2 & 3) and remained unaffected in the presence of hSec3p-binding defective C mutant proteins (Fig. 6.11A, Lanes 4 & 5) as compared to the presence of Myc vector (Fig. 6.11A, Lane 1).

Densitometry analysis revealed that hSec3p level was reduced up to 60% in the presence of full-length WNV/DENV C proteins. There were no significant changes ($P>0.05$) in hSec3p level when hSec3p-binding defective C mutant proteins were added to the *in vitro* translation mix (Fig. 6.11B). This confirmed that flavivirus C protein must physically bind to hSec3p to reduce its level.

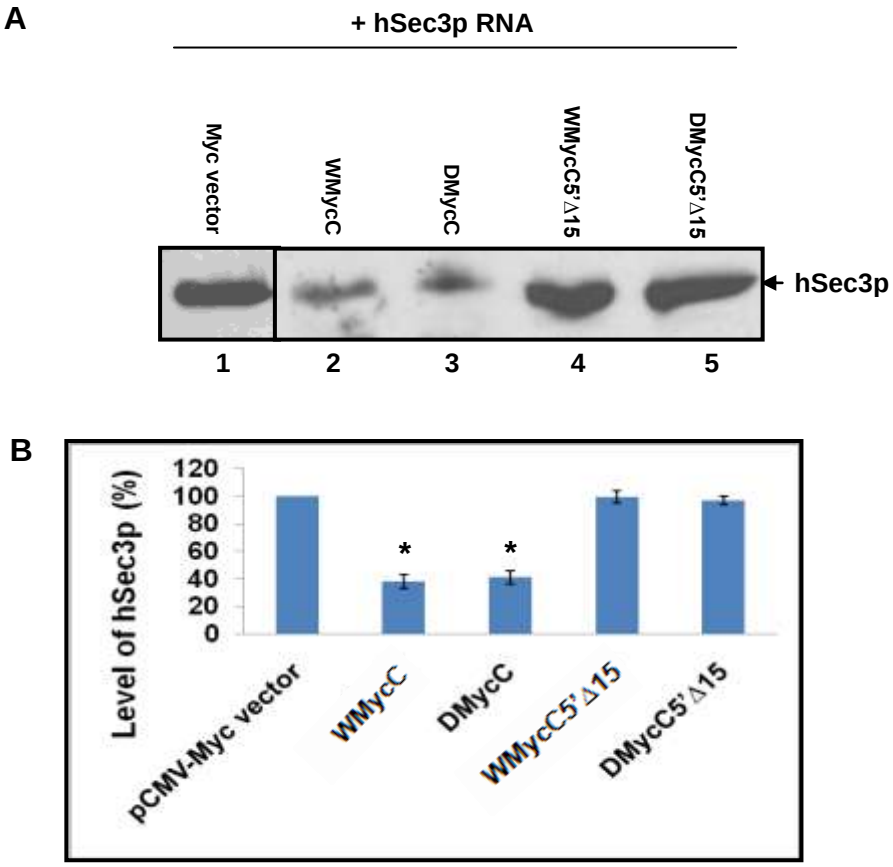

6.11: ***In vitro*** **translation assay**. (A) The plasmids WMycC, DMycC, WMycC5'Δ15 or DMycC5'Δ15 were added to the rabbit reticulocyte mix containing hSec3p RNA and *in vitro* translation assays were performed. The resulting proteins were then subjected to Western blotting using anti-hSec3p antibody. Reduced hSec3p levels are observed in the presence of WMycC/DMycC (Lanes 2 & 3). There are no differences in the hSec3p levels in the presence of WMycC5'Δ15 or DMycC5'Δ15 plasmids (Lanes 4 & 5). (B) The relative intensity of hSec3p bands on the immunoblot from (A) was quantified. Full-length WNV/DENV C protein produces up to 60% reduction in hSec3p levels. In contrast, there are no significant changes in hSec3p levels in the presence of hSec3p-binding defective mutants. * represents $P<0.05$ compared to pCMV-Myc vector.

6.3.4. Influence of flavivirus capsid protein on hSec3p-EF1α complex formation.

The results so far indicated that flavivirus C protein reduced hSec3p level (Sections 6.3.1 to 6.3.3) and the amount of EF1α-hSec3p complex formation was significantly lowered in WNV/DENV-infected cells compared to un-infected cells (Fig. 5.1D). The study was extended to assess if flavivirus C protein played a direct role in reducing hSec3p-EF1α complex formation. HEK293 cells were transfected with WHAC (WNV), WHAC5'△15 (WNV), DMycC (DENV) or DMycC5'△15 (DENV) plasmids. The formation of hSec3p-EF1α complex in WHAC/WHAC5'△15- or DMycC/DMycC5'△15-transfected HEK293 cells were analyzed by immunoprecipitating the cell lysates using anti-hSec3p antibody followed by immunoblotting using anti-EF1α antibody. As depicted in Fig. 6.12(i & vii), the interaction between EF1α and hSec3p was significantly reduced (>80%) in the presence of C protein (Lane 3) and remained unaffected in mock-transfected (Lane 1), vector transfected (Lane 2) and WHAC5'△15-/DMycC5'△15-transfected (Lane 4) cells. The amount of EF1α-hSec3p complex formation (i & vii) correlated with the amount of hSec3p (iv & x) in the cell lysates of various experimental cohorts. Taken together, this indicated that C protein induced the degradation of hSec3p. As a result, the hSec3p level was reduced which subsequently resulted in the decreased formation of EF1α-hSec3p complex.

The formation of C-hSec3p or C-EF1α complex in WHAC/WHAC5'△15- or DMycC/DMycC5'△15-transfected HEK293 cells was also analyzed by

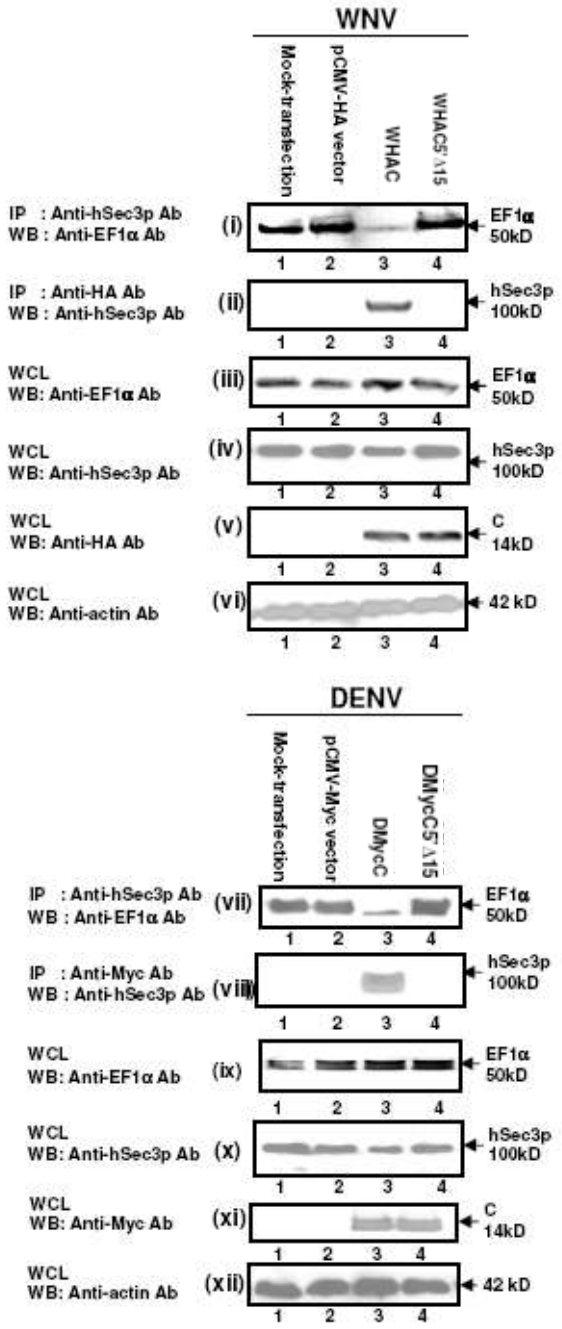

Fig. 6.12: Effect of C protein on hSec3p-EF1α complex formation. HEK293 cells were transfected with WHAC, WHAC5'△15, DMycC or DMycC5'△15 plasmids. Lysates from (i) WHAC/WHAC5'△15 or (vii) DMycC/DMycC5'△15-transfected HEK293 cells were precipitated using anti-hSec3p antibody and immunoblotted with anti-EF1α antibody. The level of hSec3p-EF1α complex is reduced in the presence of C protein (Lane 3) and is unaffected in the absence of C-hSec3p interacting domain (WHAC5'△15/DMycC5'△15, Lane 4). A portion of the same cell lysates was immunoprecipitated using anti-HA (ii)/anti-Myc (viii) antibody and probed with anti-hSec3p antibody. The immunoreactive band is detected only in WHAC/DMycC-transfected samples (Lane 3). [(iii-vi) and (ix-xii)] The loading controls are shown. IP: Immunoprecipitated sample; WB: Western blot; WCL: Whole cell lysate.

immunoprecipitating the cell lysates using anti-HA or anti-Myc antibody followed by immunoblotting using either anti-hSec3p or anti-EF1α antibody. As shown in Fig. 6.12(ii & viii), hSec3p-C association was only detected in the presence of full-length C protein (Lane 3). The reciprocal Co-IP also showed the same results and antibody isotype controls did not pull down the protein of interest (Figs. 6.13A and 6.13B). This demonstrated that the binding between C protein and hSec3p was critical to reduce hSec3p-EF1α complex formation since the complex formation was not affected in the presence of hSec3p-binding defective C proteins (C5'△15).

To further confirm that flavivirus C protein played a direct role in reducing hSec3p-EF1α complex formation, the formation of hSec3p-EF1α complex was analyzed by adding increasing amounts of *in vitro* translated C/C5'△15 proteins. Presynthesized hSec3p [Fig. 6.14(i-iii & v-vii)] was fractionated by SDS-PAGE and blotted to PVDF membrane. Individual lanes were then excised from the blot and incubated with EF1α [Fig. 6.14(i & v)] in combination with 5- or 10-fold mole excess of either *in vitro* translated full length WHAC [Fig. 6.14(i), Lanes 2 & 3] or WHAC5'△15 [Fig. 6.14(i), Lanes 4 & 5] or DMycC [Fig. 6.14(v), Lanes 2 & 3] or DMycC5'△15 [Fig. 6.14(v), Lanes 4 & 5]. No exogenous competitor (C/C5'△15) was added to hSec3p [Fig. 6.14(i & v), Lane 1] to determine 100% control binding to hSec3p.

The formation of hSec3p-EF1α complex was then detected by immunoblotting with anti-EF1α antibody α [Fig. 6.14(i & v)]. The results indicated that flavivirus

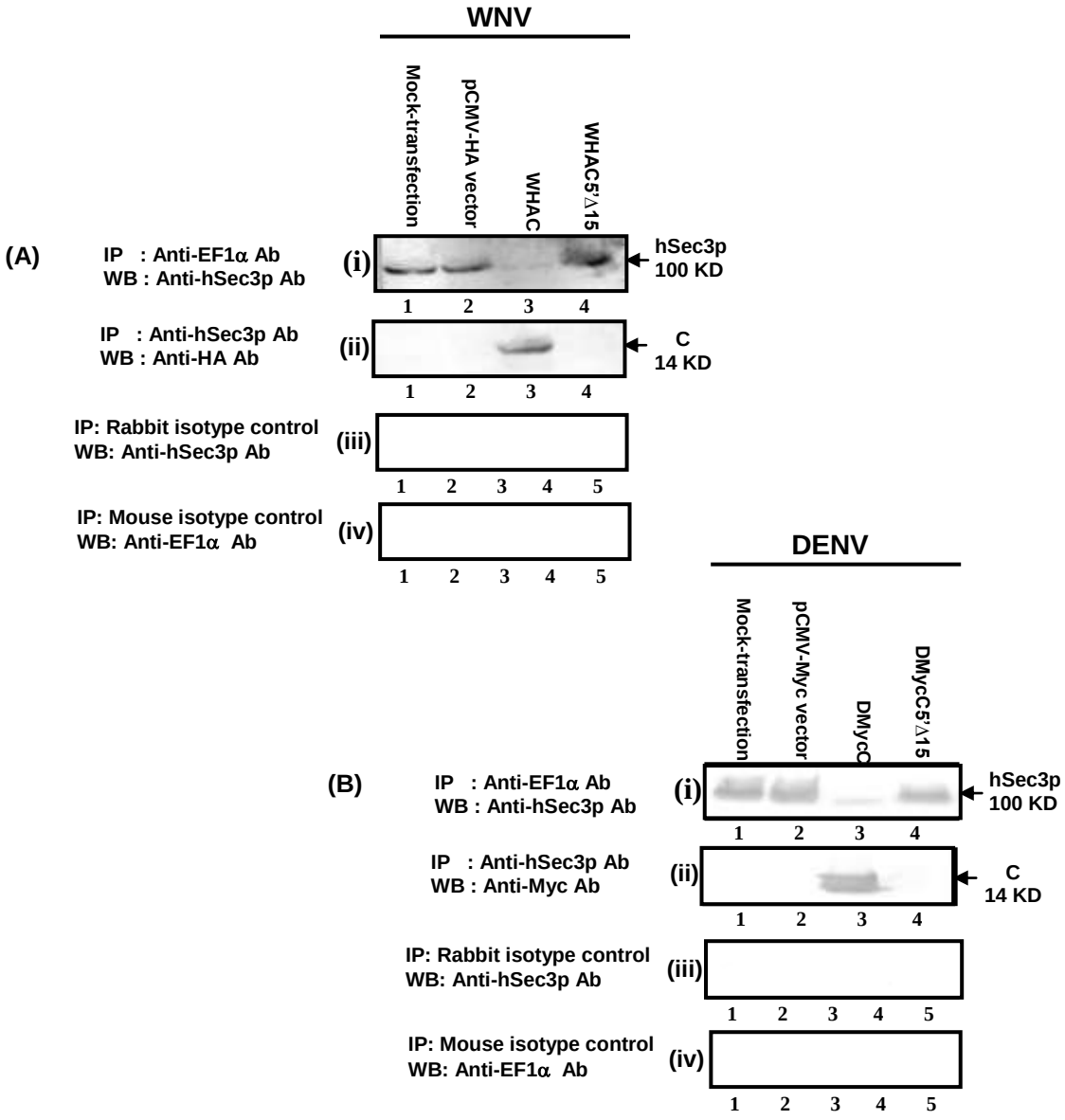

Fig. 6.13: Reciprocal Co-IP to study the effect of flavivirus C protein on hSec3p-EF1α complex formation. [A & B(i)] HEK293 cells were transfected with WHAC, WHAC5'△15, DMycC or DMycC5'△15 plasmids. Lysates from (A) WNV or (B) DENV C/C5'△15-transfected HEK293 cells were immunoprecipitated using anti-EF1α antibody and immunoblotted with anti-hSec3p antibody. The level of hSec3p-EF1α complex is reduced in the presence of C protein (Lane 3) and is unaffected in the absence of C-hSec3p interacting domain (WHAC5'△15/DMycC5'△15, Lane 4). (ii) A portion of the same cell lysates was immunoprecipitated using anti-hSec3p antibody and immunoblotted with anti-HA/anti-Myc antibody. The immunoreactive band is detected only in the WHAC/DMycC-transfected samples (Lane 3). (iii) Immunoprecipitation using rabbit antibody isotype control and immunoblotting with anti-hSec3p antibody. (iv) Reciprocal immunoprecipitation using mouse antibody isotype control and immunoblotting with anti-EF1α antibody. IP: Immunoprecipitated sample; WB: Western blot; WCL: Whole cell lysate.

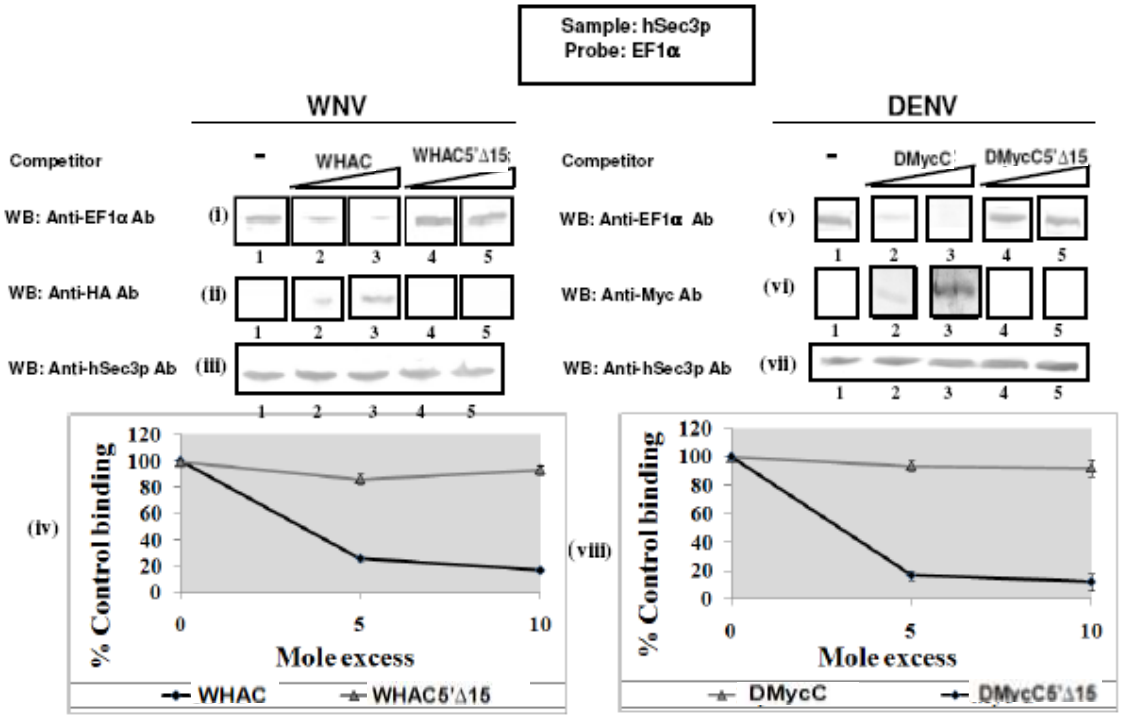

Fig. 6.14: Competition assay. *In vitro* translated hSec3p (i-iii & v-vii) was subjected to Western blotting. Individual lanes were then excised from the blot and incubated with EF1α in combination with 5- or 10-fold mole excess of either *in vitro* translated full length WHAC/DMycC (Lanes 2 & 3)/WHAC5'△15/DMycC5'△15 (Lanes 4 & 5) proteins. No exogenous competitor was added to hSec3p (Lane 1) to determine 100% control binding to hSec3p. (i & v) The formation of hSec3p-EF1α complex is then detected by immunoblotting with anti-EF1α antibody. (ii & vi) The formation of hSec3p-C complex is also examined by immunoblotting with anti-HA or anti-Myc antibody. (iii & vii) The membrane bound hSec3p (input control) is also detected by immunoblotting the membrane with anti-hSec3p antibody. (iv & viii) The EF1α binding is quantitated using three independent assays and plotted relative to its binding in the absence of competitor. WB: Western blot.

C protein interfered with hSec3p-EF1α complex formation in a dose-dependent manner [Fig. 6.14(i & v), Lanes 2 & 3]. In contrast, hSec3p-binding defective C protein, C5'△15 failed to negate hSec3p-EF1α interaction [Fig. 6.14(i & v), Lanes 4 & 5]. The formation of hSec3p-C complex [Fig. 6.14(ii & vi)] was also examined by immunoblotting with anti-HA or anti-Myc antibody. The membrane-bound hSec3p (input control) was also detected by immunoblotting the membrane with anti-hSec3p [Fig. 6.14(iii & vii)] antibody. The EF1α binding to hSec3p was then quantitated by performing densitometry analysis of the band intensities on the immunoblot obtained from [Fig. 6.14(i & v)] and plotted relative to its binding in the absence of competitor [Fig. 6.14(iv & viii)]. Densitometry analysis confirmed that C protein interfered with hSec3p-EF1α complex formation in a dose-dependent manner. Overall, this reaffirmed that the binding between C protein and hSec3p was crucial for reducing hSec3p-EF1α complex formation. Similar results were also obtained from the reciprocal experiment performed using EF1α as sample and hSec3p as probe (Fig. 6.15).

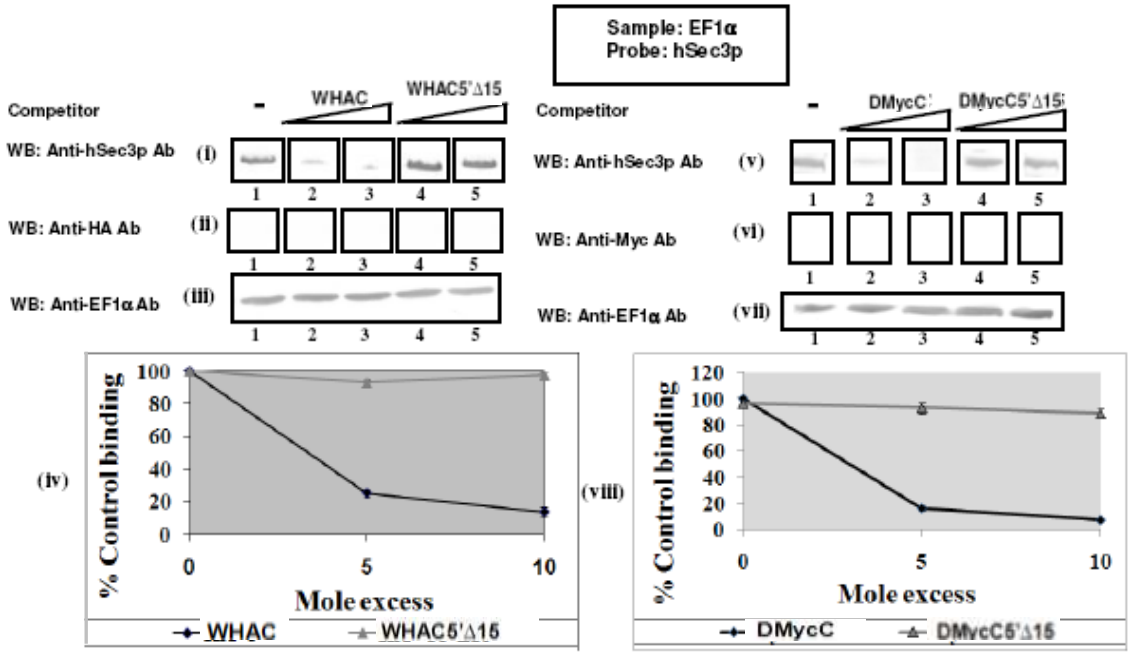

Fig. 6.15: Reciprocal Competition assay. *In vitro* translated EF1α (i-iii & v-vii) was subjected to Western blotting. Individual lanes were then excised from the blot and incubated with hSec3p in combination with 5- or 10-fold mole excess of either *in vitro* translated full length WHAC/DMycC (Lanes 2 & 3)/WHAC5'△15/DMycC5'△15 (Lanes 4 & 5) proteins. No exogenous competitor was added to EF1α (Lane 1) to determine 100% control binding to EF1α. (i & v) The formation of hSec3p-EF1α complex is then detected by immunoblotting with anti-hSec3p antibody. (ii & vi) The formation of EF1α-C complex is also examined by immunoblotting with anti-HA or anti-Myc antibody. (iii & vii) The membrane bound EF1α (input control) is also detected by immunoblotting the membrane with anti-EF1α antibody, respectively. (iv & viii) The hSec3p binding is quantitated and plotted relative to its binding in the absence of competitor. WB: Western blot.

6.3.5. Proteasome-dependent degradation of hSec3p

6.3.5.1. Flavivirus C protein mediated proteasome-dependent degradation of hSec3p

The results obtained from Figs. 6.7 and 6.8 indicated that flavivirus-dependent decrease in hSec3p expression levels was mediated through the proteasome pathway. To further confirm this, HEK293 cells were treated with a more specific inhibitor, epoxomicin and transfected with Myc-tagged plasmids encoding full-length WNV/DENV C gene (WMycC and DMycC). At 24 h post-transfection, expression of hSec3p and full-length WNV/DENV C proteins were assessed using cell-based fluorescence (CBF) assay.

In the absence of epoxomicin, the hSec3p level was markedly reduced following the transfection with full-length WNV/DENV C protein (Fig. 6.16A). In the presence of full-length WNV/DENV C protein, hSec3p expression levels were decreased by 65% ($P<0.05$). In contrast, there were no significant differences ($P>0.05$) in the levels of hSec3p in epoxomicin-treated full-length C plasmids-transfected cells (Fig. 6.16A). In the presence of proteasomal inhibitor, epoxomicin, hSec3p level remained unchanged compared to that of mock-transfection. This suggested that C protein should utilize the proteasomes to decrease the levels of hSec3p. The expression of full-length WNV or DENV C protein was confirmed by CBF assay using anti-Myc and actin antibodies (Fig. 6.16B). There were no significant changes in the expression levels of hSec6p (Fig. 6.16C). Overall, this demonstrated that flavivirus C protein induced the proteasome-mediated degradation of hSec3p.

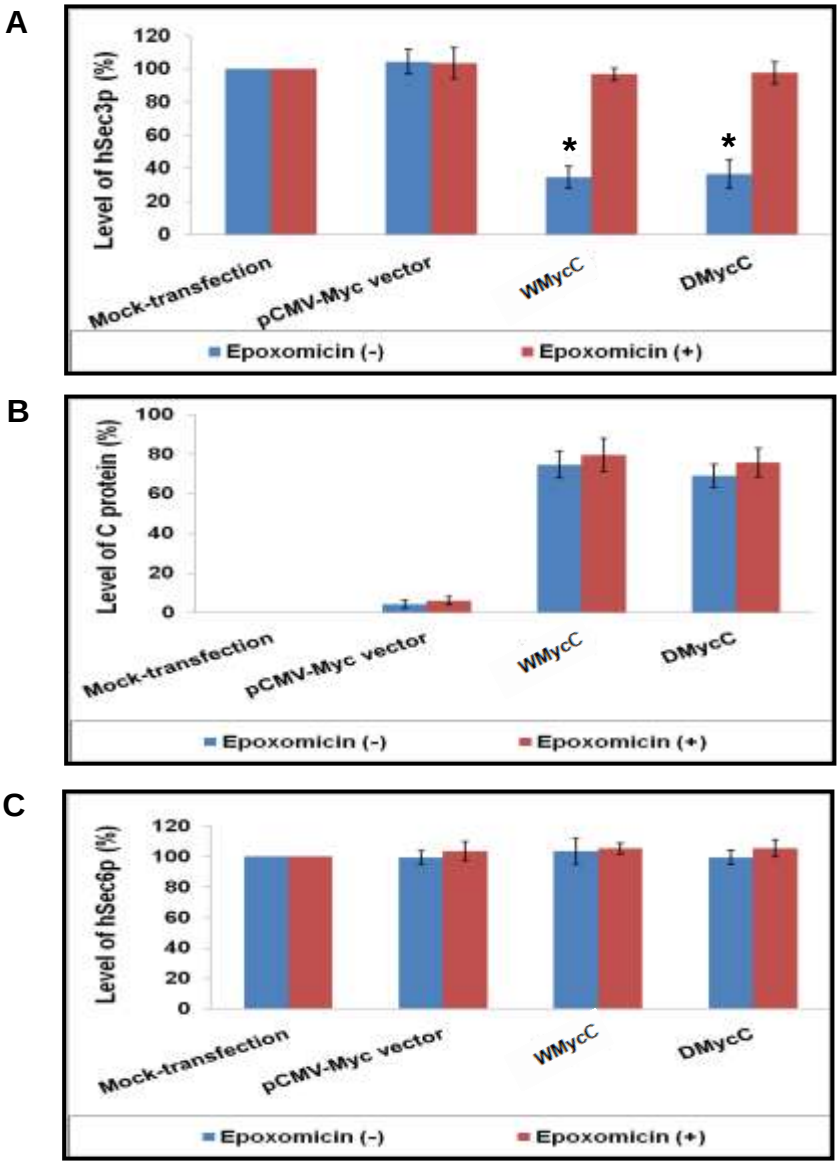

Fig. 6.16: Influence of flavivirus C protein on hSec3p expression in the presence of epoxomicin. HEK293 cells were transfected with WMycC and DMycC in the absence and presence of epoxomicin. (A) The hSec3p expression level was assessed by CBF assay using anti-hSec3p and anti-actin antibody. The levels of hSec3p are normalized against the actin control and the relative levels of hSec3p in transfected cells are shown. Reduced hSec3p level is detected in WNV/DENV C-transfected cells in the absence of epoxomicin. In contrast, there are no significant differences in the levels of hSec3p in epoxomicin-treated WNV/DENV C-transfected cells. (B) The expression of C protein is monitored by CBF assay using anti-Myc and anti-actin antibodies. (C) The expression of hSec6p protein is monitored by CBF assay using anti-hSec6p and anti-actin antibodies. * represents $P<0.05$ compared to mock-transfection.

6.3.5.2. Titration of various proteolytic activities of 26S proteasome in HEK293 cells

The above Sections indicated that flavivirus C protein induced the degradation of hSec3p through proteasome-mediated pathway. Three major proteolytic activities namely chymotrypsin-like, trypsin-like and caspase-like are contained within 26S proteasome. This study was thus extended to investigate which proteolytic activity of 26S proteasome was activated by flavivirus C protein. Prior to measuring the proteolytic activities of 26S proteasome following transfection with WNV/DENV C protein, it is essential to check whether the luminescence signal (representing the proteolytic activity of 26S proteasome) is proportional to the cell number of HEK293. To achieve this, Proteasome-Glo cell-based assay kits for chymotrypsin-like, trypsin-like and caspase-like activities were used. HEK293 cells were serially diluted in a volume of 100 μl/well of a 96-well plate. Newly reconstituted luminescent proteasome reagent containing substrates for chymotrypsin-like, trypsin-like, or caspase-like activity was then added. After 10 min, relative luminescence units (RLU) were determined using a luminometer.

As shown in Fig. 6.17, the results were linear for each of the substrates used (chymotrypsin-like activity R2 = 0.9897; trypsin-like activity R2 = 0.9939; caspase-like activity R2 = 0.9875). For each of the proteasome activities, luminescence was proportional to the cell number, with a linear sample range up to 8000 cells per well in a 96-well plate (Fig. 6.17). In the subsequent assays, HEK293 cells were seeded on to 96-well plate in such a way that the number of

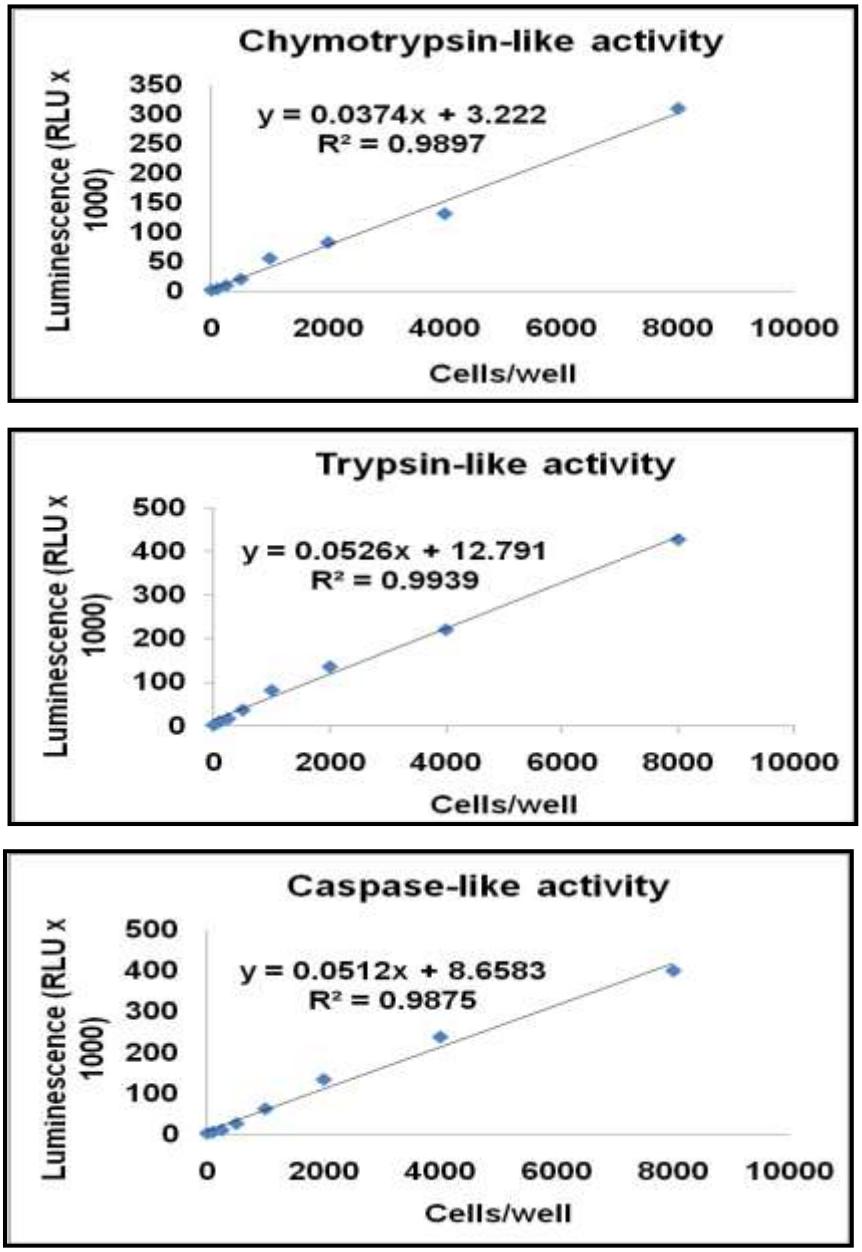

Fig. 6.17: Luminescence is proportional to cell number for each of the proteasome activities. HEK293 cells were serially diluted in a 96-well plate. Following equal volume additions of luminescent proteasome reagent containing substrates for chymotrypsin-like, trypsin-like and caspase-like activity, luminescence was determined using a luminometer. The results are linear for each of the substrates used. The data point at 10000 cells/well is omitted since the relative luminescence signal obtained from 10000 cells/well does not fall within the linear range. Each point represents the average of nine wells.

cells remained as 5000 cells per well. Direct comparison showed that the luminescent signal obtained from chymotrypsin-like proteasome activity varied significantly from that of trypsin-like or caspase-like proteasome activity.

6.3.5.3. Flavivirus C protein activated the chymotrypsin-like and caspase-like activities of 26S proteasome

To demonstrate the specific proteolytic function of 26S proteasome following transfection with WNV/DENV C protein, HEK293 cells were transfected with full-length C protein or hSec3p-binding defective C mutant. At 12 h post-transfection, proteolytic activities of 26S proteasome was examined using Proteasome-Glo cell-based assay kits for chymotrypsin-like, trypsin-like and caspase-like activities.

As shown in Fig. 6.18, full-length C protein of WNV/DENV activated the chymotrypsin-like (A) and caspase-like (C) functions of 26S proteasome ($P<0.05$). In contrast, hSec3p-binding defective C mutant failed to activate the proteolytic activities of 26S proteasome ($P>0.05$). There was no significant difference in the trypsin-like activity (Fig. 6.18B) of 26S proteasome following transfection with full-length C protein or hSec3p-binding defective mutant C protein ($P>0.05$). This suggested that full-length C protein of WNV and DENV triggered the chymotrypsin-like and caspase-like activities of 26S proteasome to degrade hSec3p.

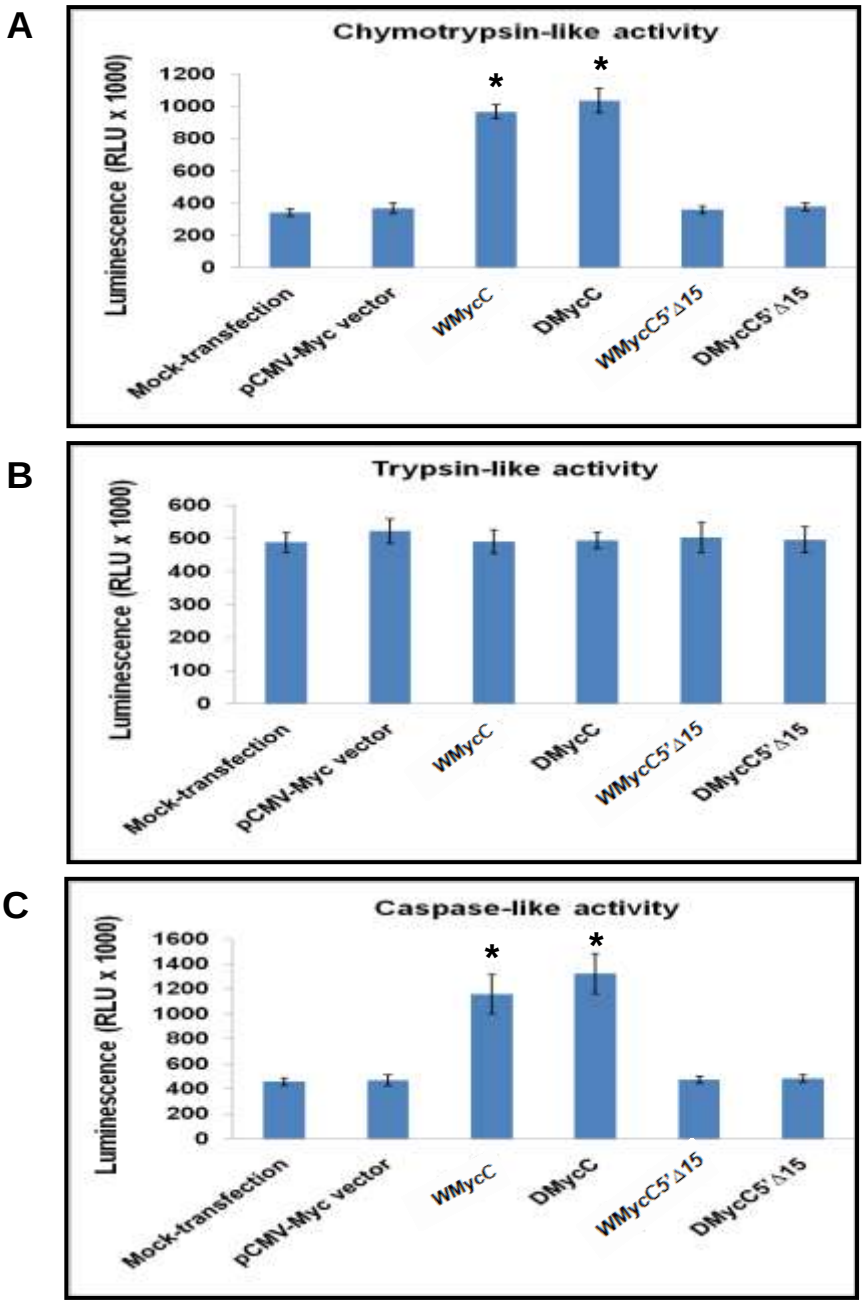

Fig. 6.18: Proteolytic activities of 26S proteasome following transfection with WNV/DENV C protein. HEK293 cells were transfected with full-length C protein (WMycC/DMycC) or hSec3p-binding defective C mutant (WMycC5'Δ15/DMycC5'Δ15) and the proteolytic activities of 26S proteasome was examined. (A) Chymotrypsin-like and (C) caspase-like functions of 26S proteasome are significantly increased following transfection with full-length C protein of WNV/DENV. (B) No significant difference in the trypsin-like activity of 26S proteasome is observed following transfection with WNV/DENV C proteins. * represents $P<0.05$ compared to mock-transfection.

6.3.5.4. Flavivirus C protein activated the chymotrypsin-like activity of 26S proteasome to degrade human Sec3 protein

The above results suggested that flavivirus C protein utilized the chymotrypsin-like and caspase-like functions of 26S proteasome to degrade hSec3p. To confirm whether these two proteolytic activities are essential to execute the degradation of hSec3p, bioassays were performed using proteasome inhibitors. HEK293 cells were incubated with various concentrations of inhibitors such as lactacystin (chymotrypsin-like) and YU-102 (caspase-like) at 37 ^{o}C for 2 h and observed for cytotoxic effects. It was determined that lactacystin and YU-102 up to 5 μM concentration did not induce any cytotoxic effects in HEK293 cells (Fig. 6.19).

After confirming the cytotoxic levels of lactacystin and YU-102, the study was extended to determine the inhibition curves for these inhibitors. Serial dilutions of lactacystin or YU-102 (0-10 μM) were added to the growth media of HEK293 cells. Cells were incubated at 37 ^{o}C for 2 h. The plate was then allowed to equilibrate to 25 ^{o}C before the addition of Proteasome-Glo chymotrypsin-like or caspase-like cell-based reagents to measure the chymotrypsin-like or caspase-like activities, respectively. After 15 min, luminescence was measured. At 5 μM concentration, lactacystin inhibited chymotrypsin-like activity by 92% and YU-102 inhibited caspase-like activity by 93% (Fig. 6.20). Since there was no significant cytotoxicity observed at these concentrations (Fig. 6.19), 5 μM lactacystin/YU-102 was used in the subsequent studies.

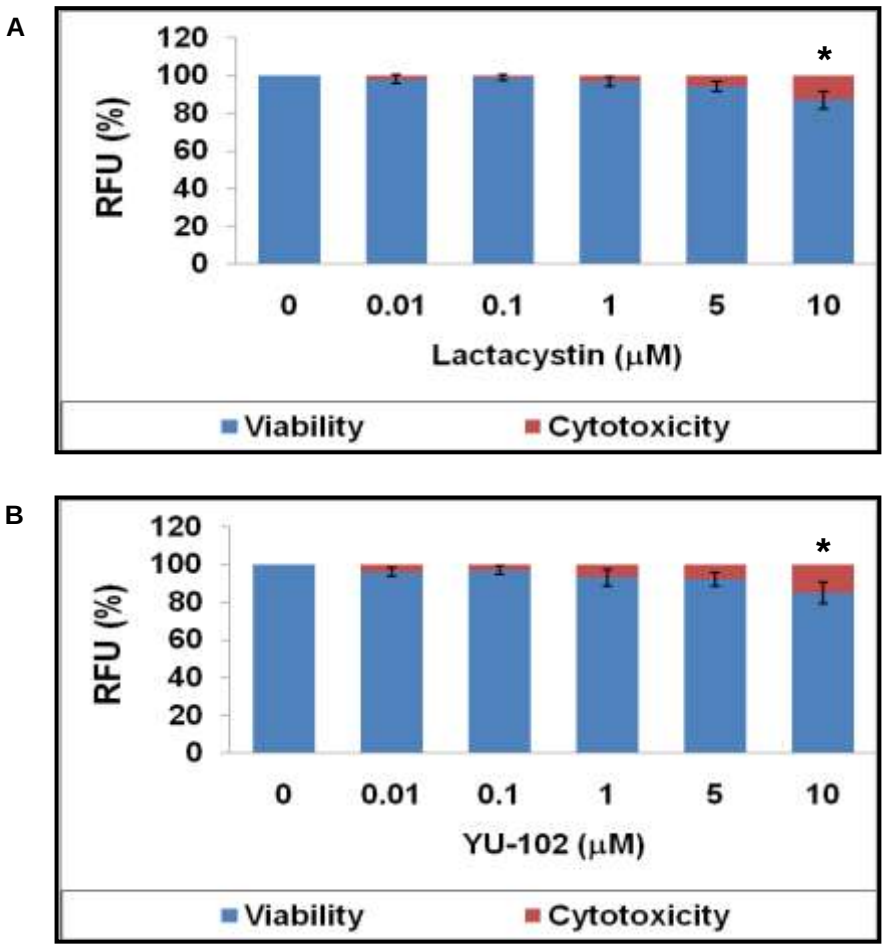

Fig. 6.19: Relative cytotoxicity and viability of lactacystin and YU-102-treated HEK293 cells. The viability and cytotoxicity of lactacystin and YU-102-treated HEK293 cells were tested by incubating HEK293 cells with various concentrations of (A) lactacystin and (B) YU-102. These inhibitors are not shown to induce significant cytotoxicity up to 5 μM concentration ($P>0.05$). At 10 μM concentration, both lactacystin and YU-102 induce significant cytotoxicity. * represents $P<0.05$.

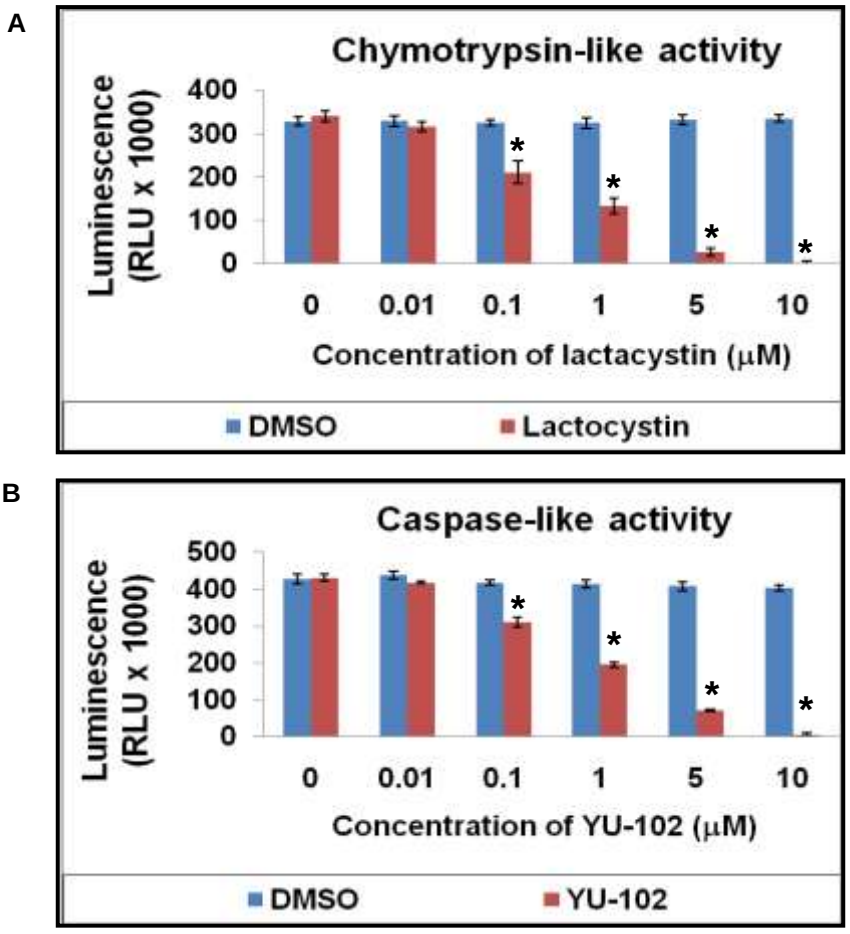

Fig. 6.20: Measurement of chymotrypsin-like and caspase-like activities following inhibitor treatments. (A) HEK293 cells were incubated with various concentrations of lactacystin and chymotrypsin-like activity was measured. (B) HEK293 cells were incubated with various concentrations of YU-102 and caspase-like activity was measured. Both lactacystin and YU-102 efficiently inhibit chymotrypsin-like and caspase-like activities, respectively at 5 μM concentration. * represents $P<0.05$.

To answer whether chymotrypsin-like activity of 26S proteasome was exploited by flavivirus C protein to degrade hSec3p, HEK293 cells were incubated with 5 μM lactacystin (inhibitor of chymotrypsin-like activity) and transfected with Myc-tagged plasmids encoding full-length WNV/DENV C gene (WMycC and DMycC). At 24 h post-transfection, expression of hSec3p and full-length WNV/DENV C proteins were assessed using cell-based fluorescence (CBF) assay.

In the absence of lactacystin, the hSec3p level was markedly reduced following the transfection with full-length WNV/DENV C protein (Fig. 6.21A). In the presence of full-length WNV/DENV C protein, hSec3p expression levels were decreased by 60% ($P<0.05$). In contrast, there were no significant differences ($P>0.05$) in the levels of hSec3p in lactacystin-treated full-length C plasmids-transfected cells (Fig. 6.21A). The expression of full-length WNV or DENV C protein was confirmed by CBF assay using anti-Myc and actin antibodies (Fig. 6.21B). There were no significant changes in the expression levels of hSec6p (Fig. 6.21C). This confirmed that flavivirus C protein induced the chymotrypsin-like proteolytic function of 26S proteasome to mediate the degradation of hSec3p.

To answer whether caspase-like activity of 26S proteasome was also utilized by flavivirus C protein to degrade hSec3p, HEK293 cells were incubated with 5 μM YU-102 (inhibitor of caspase-like activity) and transfected with Myc-tagged

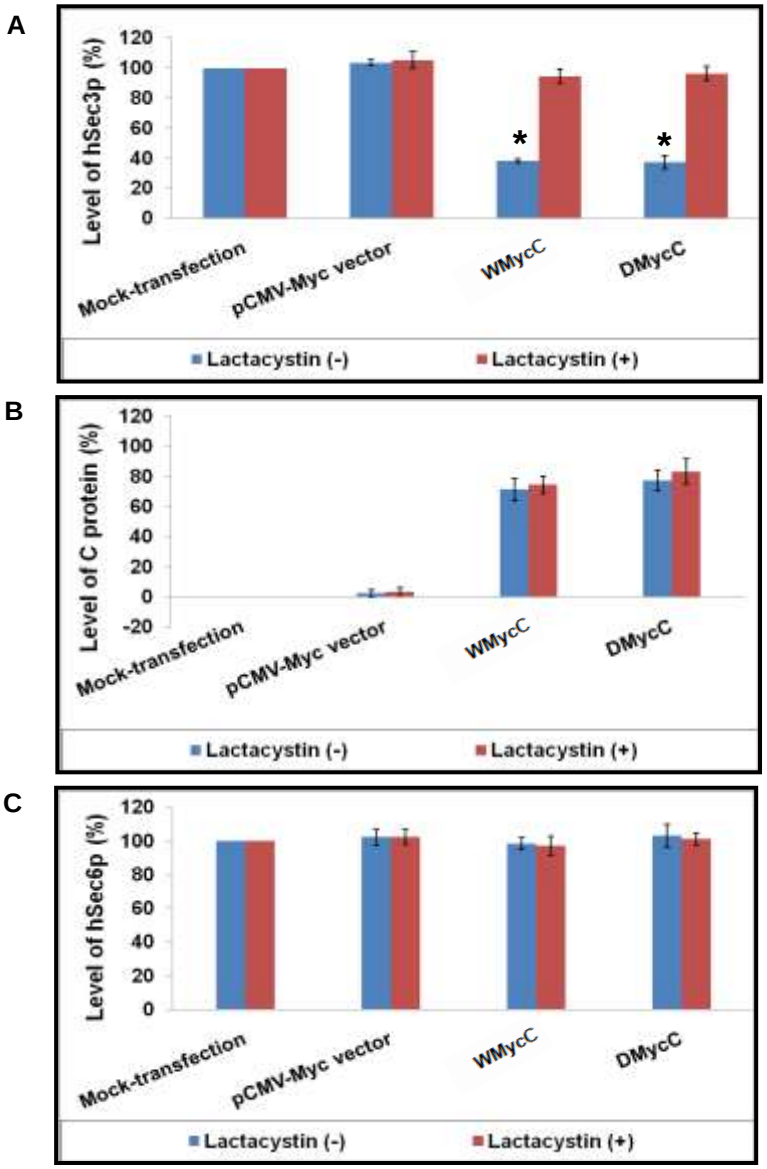

Fig. 6.21: Influence of flavivirus C protein on hSec3p expression in the presence of lactacystin. HEK293 cells were transfected with WMycC and DMycC in the absence and presence of lactacystin. (A) The hSec3p expression level was assessed by CBF assay using anti-hSec3p and anti-actin antibody. The hSec3p levels are normalized against the actin control and the relative levels of hSec3p in transfected cells are shown. Reduced hSec3p level is detected in WNV/DENV C-transfected cells in the absence of lactacystin. In contrast, there are no significant differences in the levels of hSec3p in lactacystin-treated WNV/DENV C-transfected cells. (B) The expression of C protein is monitored by CBF assay using anti-Myc and anti-actin antibodies. (C) The expression of hSec6p protein is monitored by CBF assay using anti-hSec6p and anti-actin antibodies. * represents $P<0.05$ compared to mock-transfection.

plasmids encoding full-length WNV/DENV C gene (WMycC and DMycC). At 24 h post-transfection, the expression of hSec3p and full-length WNV/DENV C proteins were assessed using CBF assay. In the absence or presence of YU102, there was no significant differences in hSec3p level ($P>0.05$) following the transfection with full-length WNV/DENV C protein (Fig. 6.22A). The expression of full-length WNV or DENV C protein was confirmed by CBF assay using anti-Myc and actin antibodies (Fig. 6.22B). There were also no significant changes in the expression levels of hSec6p (Fig. 6.22C). This confirmed that flavivirus C protein did not utilize the caspase-like proteolytic function of 26S proteasome to mediate the degradation of hSec3p. Activation of caspase-like function by flavivirus C protein might be exploited to degrade other host proteins apart from hSec3p to favour the virus.

6.3.5.5. Mapping the domains of flavivirus capsid protein responsible for activating chymotrypsin-like proteolytic function of 26S proteasome

The results obtained from Figs. 6.10 and 6.11 indicated that flavivirus C protein must physically bind to hSec3p to reduce its level as the first 15 amino acids truncated mutant of C protein failed to reduce hSec3p level. To further confirm this, alanine-scanning mutagenesis studies were performed on the first 15 amino acids of C protein. This resulted in the formation of WMycC2-WMycC15 and DMycC12-15 mutants. Oh and colleagues (2006) reported that the last 15 amino acids of WNV C protein contained the cytotoxic and degradation inducing motif. To define the motif on C protein mediating the activation of chymotrypsin-like

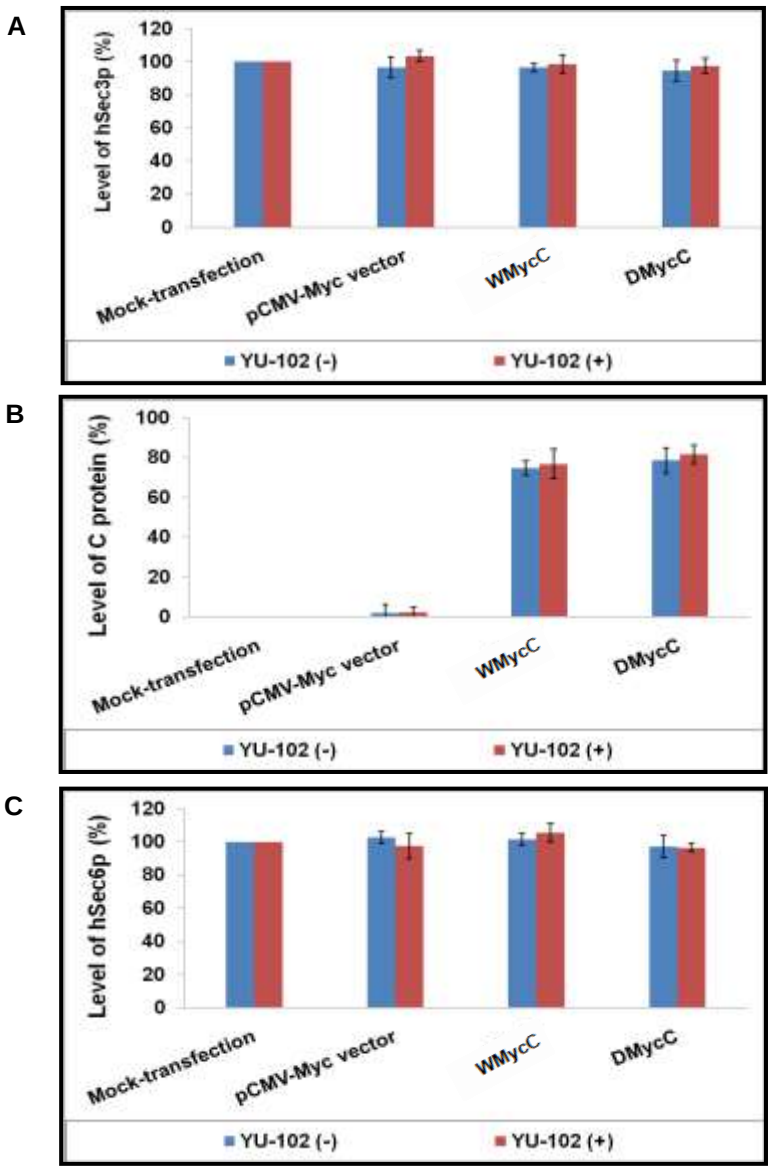

Fig. 6.22: Influence of flavivirus C protein on hSec3p expression in the presence of YU-102. HEK293 cells were transfected with WMycC and DMycC in the absence and presence of YU-102. (A) The hSec3p expression level was assessed by CBF assay using anti-hSec3p and anti-actin antibody. The hSec3p levels are normalized against the actin control and the relative levels of hSec3p in transfected cells are shown. There are no changes in hSec3p level in WNV/DENV C-transfected cells in the absence/presence of YU-102. (B) The expression of C protein is monitored by CBF assay using anti-Myc and anti-actin antibodies. (C) The expression of hSec6p protein is monitored by CBF assay using anti-hSec6p and anti-actin antibodies.

proteolytic function of 26S proteasome, multiple sequence alignment of the amino acid sequences of WNV and DENV C protein was performed using CLUSTALW2 alignment software (Fig. 6.23). Mutations were then introduced on the conserved and semi-conserved regions in the last 15 amino acids (putative degradation motif) of WNV and DENV C protein to produce WMycC109110111, WMycC112113114, WMycC115116117, DMycC102103104, DMycC105106107 and DMycC108109110 mutants.

HEK293 cells were transfected with full-length C protein or various C mutants. At 12 h post-transfection, chymotrypsin-like activity of 26S proteasome was examined using Proteasome-Glo cell-based assay kit. As shown in Fig. 6.24A, similar levels of chymotrypsin-like function was activated following transfection with full-length WNV C protein and all the mutants except WMycC14, WMycC109110111 and WMycC112113114. Similarly, full-length DENV C protein and all the mutants except DMycC13, DMycC102103104 and DMycC105106107 triggered same levels of chymotrypsin-like function (Fig. 6.24B). The mutants WMycC14 and DMycC13 failed to activate any chymotrypsin-like function while the other mutants WMycC109110111, WMycC112113114, DMycC102103104 and DMycC105106107 activated the chymotrypsin-like activity at a much lower level ($P<0.05$) compared to that of full-length C protein. This indicated that the amino acids 14, 109-114 of WNV C protein and 13, 102-107 of DENV C protein played an important role in activating the proteolytic function of 26S proteasome.

```
WNV_S           MSKKPGGPGKNRAVNMLKRGMPRGLSLIGL-KRAMLSLIDGKGPIRFVLALLAFFRFTAI 59
DENV2           -MNNQRKKARNTPFNMLKRERNRVSTVQQLTKRFSLGMLQGRGPLKLFMALVAFLRFLTI 59
                  ::    .:* ..*****   *  ::  * **  *.:::*:**:::.:**:**:** :*

WNV_S           APTRAVLDRWRGVNKQTAMKHLLSFKKELGTLTSAINRRSTKQKKRGGTAGFTILLGLIA 119
DENV2           PPTAGILKRWGTIKKSKAINVLRGFRKEIGRMLNILNRRRR-------TAGIIIMMIPTV 112
                .** .:*.**  ::*..*:: * .*:**:* : . :***         ***: *::   .

WNV_S           CAGA 123
DENV2           MA-- 114
                 *
```

Fig. 6.23: Multiple sequence alignment of WNV/DENV C proteins derived using CLUSTALW software (http://www.ebi.ac.uk/Tools/clustalw2 /index.html). The accession numbers of WNV_S and DENV2 are AY688948 and FN429895, respectively.

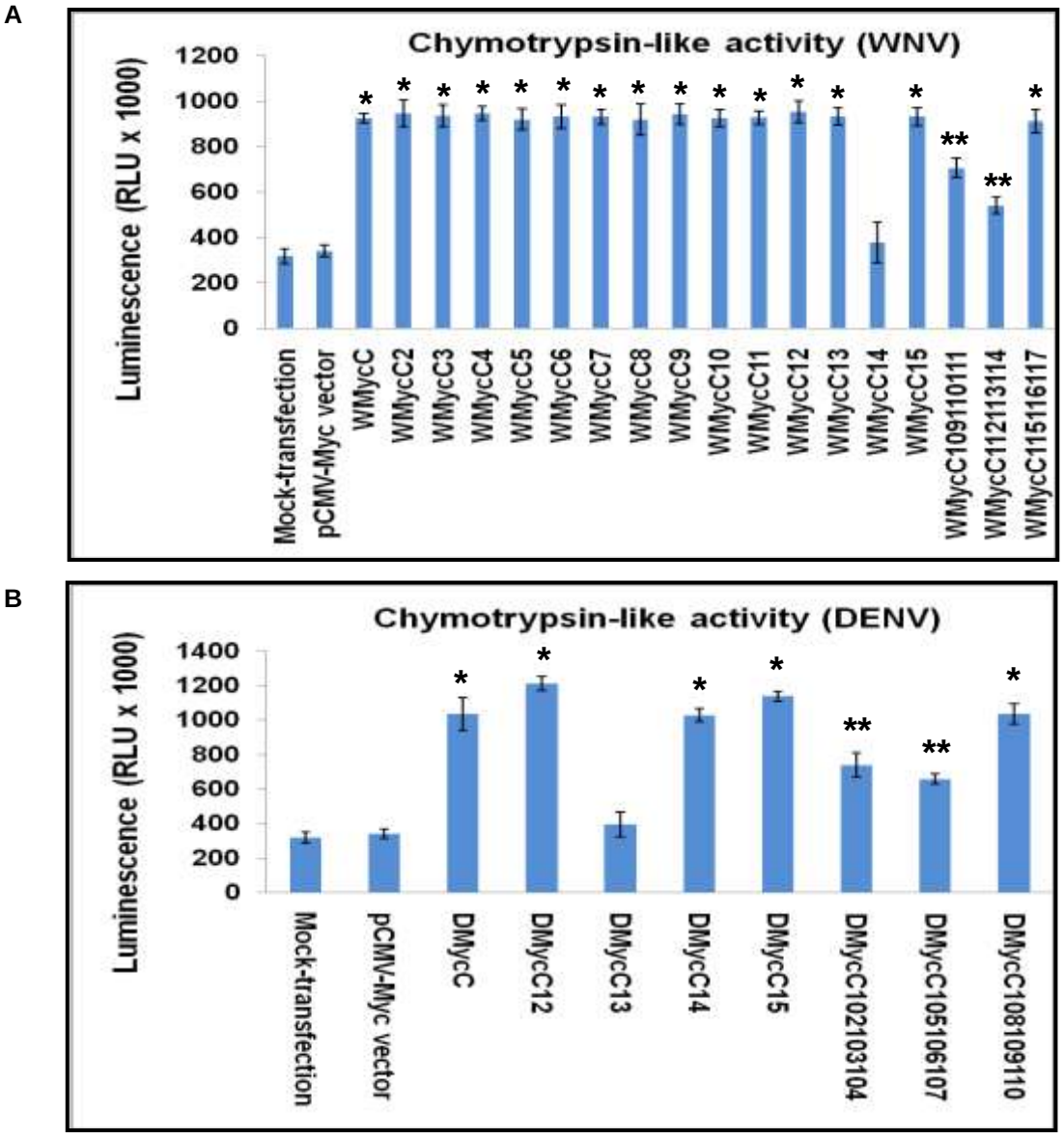

Fig. 6.24: Chymotrypsin-like activity of 26S proteasome following transfection with full-length or mutant C proteins. HEK293 cells were transfected with full-length C protein (WMycC/DMycC) or various C mutants (WMycC2-WMycC15, WMycC109110111, WMycC112113114, WMycC115116117, DMycC12-15, DMycC102103104, DMycC105106107 and DMycC108109110) and the proteolytic activities of 26S proteasome was examined. Chymotrypsin-like functions of 26S proteasome are significantly increased following transfection with full-length C protein and all the mutants of WNV/DENV C protein except WMycC14, WMycC109110111, WMycC112113114, DMycC13, DMycC102103104 and DMycC105106107 mutants. * represents $P<0.05$ compared to mock-transfection. ** represents $P<0.05$ compared to full-length C protein. The results shown here are obtained from three independent experiments with each experiment performed in triplicates.

6.3.5.6. Mapping the domains of flavivirus capsid protein responsible for degrading human Sec3 protein

To investigate if the domains on C protein mediating the activation of chymotrypsin-like functions of 26S proteasome also caused the degradation of hSec3p, HEK293 cells were transfected with full-length C (WMycC/DMycC) or various mutant (WMycC2-WMycC15, WMycC109110111, WMycC112113114, WMycC115116117, DMycC12-15, DMycC102103104, DMycC105106107 and DMycC108109110) plasmids. At 12 h post-transfection, expression of hSec3p and full-length/mutated WNV or DENV C proteins were assessed using cell-based fluorescence (CBF) assay.

The levels of hSec3p were markedly reduced following transfection with full-length WNV/DENV C protein and all the mutants except WMycC14, WMycC109110111, WMycC112113114, DMycC13, DMycC102103104 and DMycC105106107 mutant C proteins (Fig. 6.25). In contrast, equivalent amounts of hSec3p were detected in pCMV-Myc vector, WMycC14 and DMycC13-transfected samples (Fig. 6.25). Although there was a significant reduction in hSec3p levels ($P<0.05$) following transfection with WMycC109110111, WMycC112113114, DMycC102103104 and DMycC105106107 mutants, these reductions were much lower than that observed with full-length C proteins ($P<0.05$). There were no significant differences in the level of C protein expression following various mutations (Fig. 6.26).

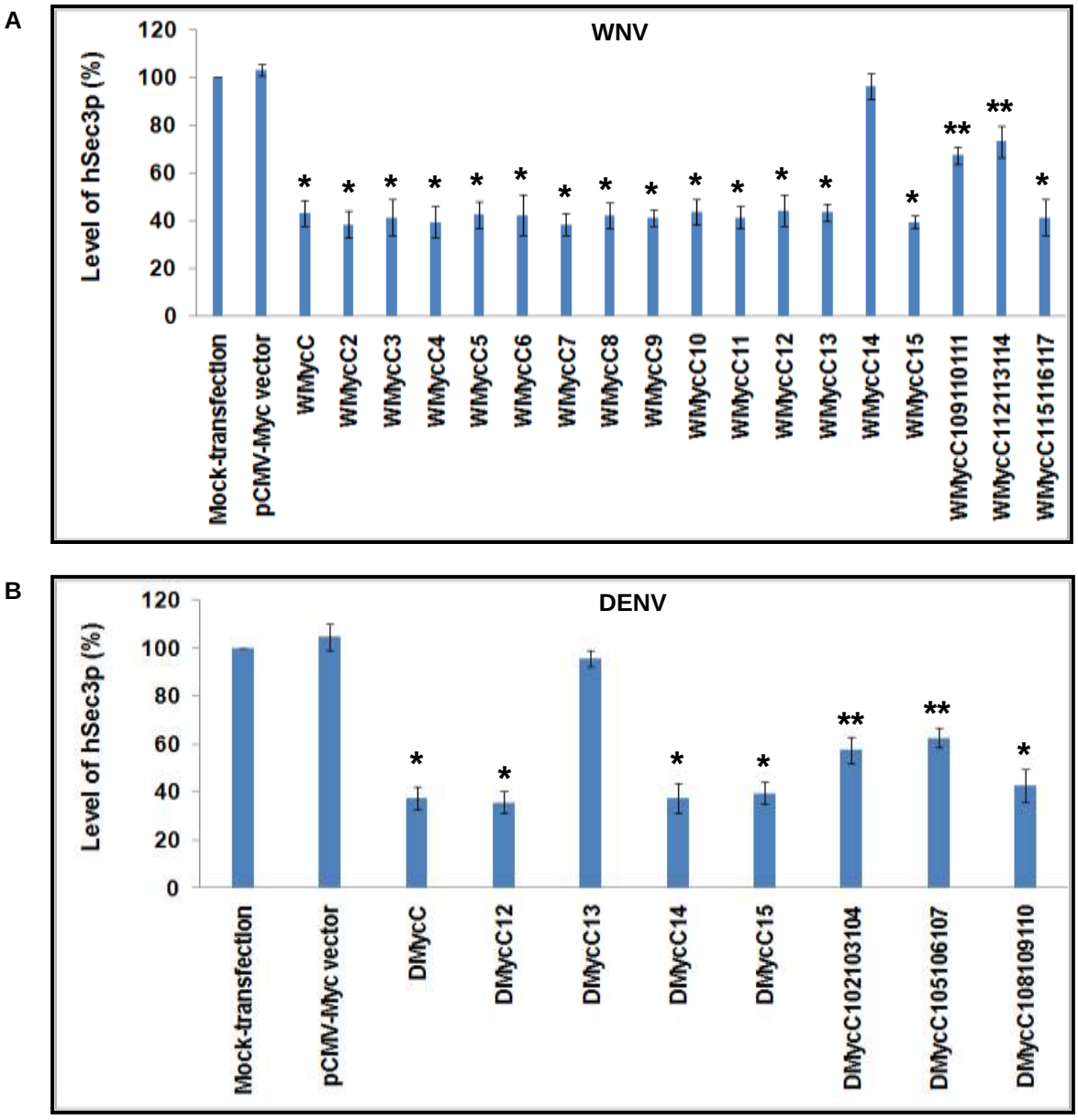

Fig. 6.25: Influence of flavivirus C protein mutants on hSec3p expression. HEK293 cells were transfected with (A) WMycC, WMycC2-WMycC15, WMycC109110111, WMycC112113114, WMycC115116117 or (B) DMycC, DMycC12-15, DMycC102103104, DMycC105106107 and DMycC108109110) plasmids. The hSec3p expression level was assessed by CBF assay using anti-hSec3p and anti-actin antibody. The levels of hSec3p are normalized against the actin control and the relative levels of hSec3p in transfected cells are shown. Similar level of reduction in hSec3p amount is detected in all the C-transfected experimental groups except with WMycC14, WMycC109110111, WMycC112113114, DMycC13, DMycC102103104 and DMycC105106107 mutants. * represents $P<0.05$ compared to mock-transfection. ** represents $P<0.05$ compared to WMycC/DMycC transfection.

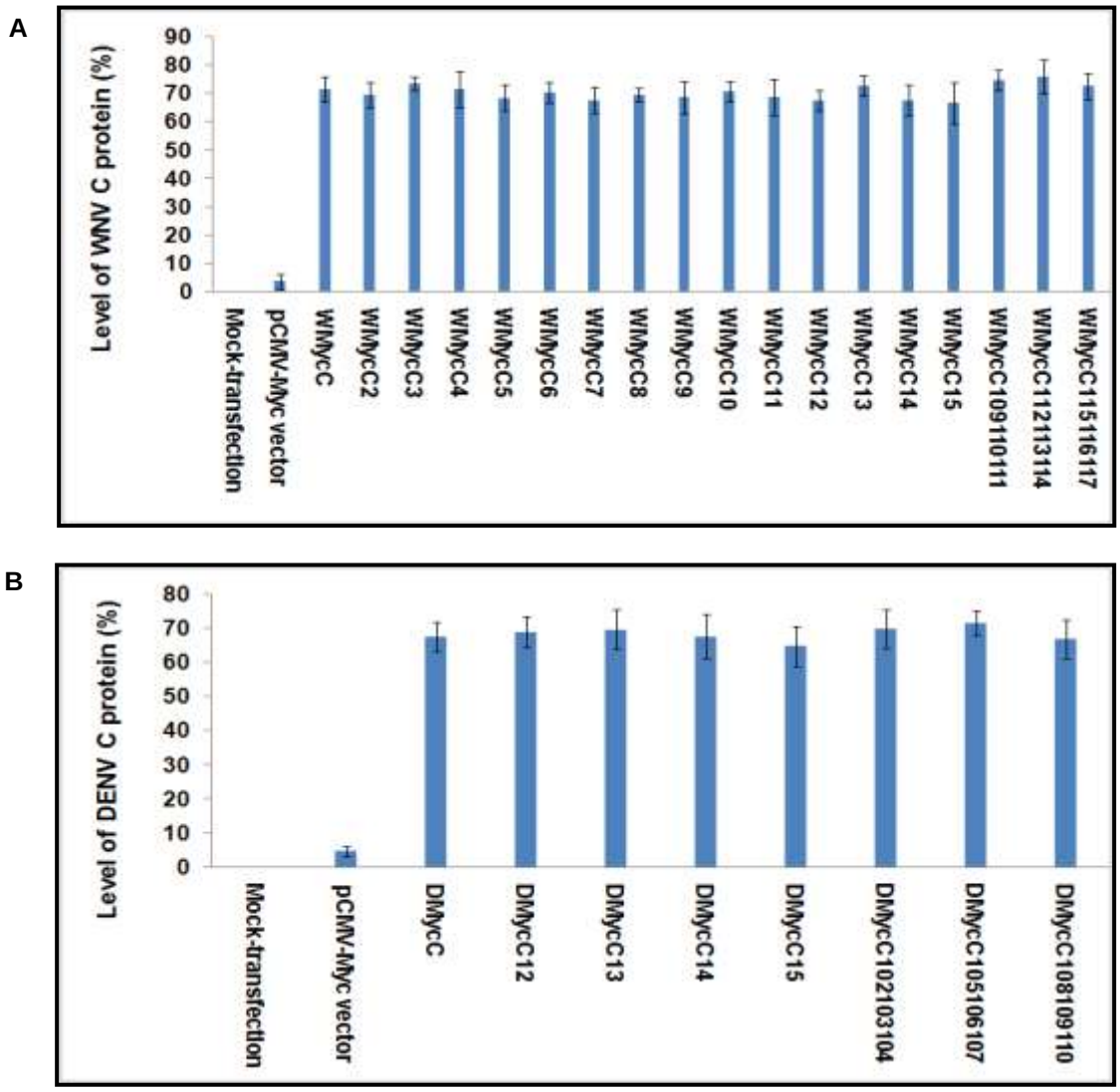

.

Fig. 6.26: Effect of mutations on flavivirus C protein expression. HEK293 cells were transfected with (A) WMycC, WMycC2-WMycC15, WMycC109110111, WMycC112113114, WMycC115116117 or (B) DMycC, DMycC12-15, DMycC102103104, DMycC105106107 and DMycC108109110) plasmids. The expression of C protein is monitored by CBF assay using anti-Myc and anti-actin antibodies. There are no significant differences in the level of C protein expression following various mutations.

Overall, this demonstrated that the amino acids 14, 109-114 of WNV C protein and 13, 102-107 of DENV C protein were essential to mediate the degradation of hSec3p. The degradation motifs important to mediate the degradation of hSec3p resided between the amino acid residues 109-114 of WNV C protein and 102-107 of DENV C protein. The mutations at the amino acid residues 14 of WNV C protein and 13 of DENV C protein falls within the hSec3p-bindng motif on C protein. This suggested that the amino acid residues at 14 of WNV C protein and 15 of DENV C protein could be essential for its binding with hSec3p.

6.3.5.7. Effect of mutations on the interaction between flavivirus capsid protein and human Sec3 protein

To check the interaction status and the strength of interaction between hSec3p and C proteins carrying mutations in the first 15 amino acids, mammalian two-hybrid (M2H) assay was performed. The full-length or the mutated (mutations in the hSec3p interaction domain) WNV/DENV C linear constructs (bait) and the hSec3p linear construct (prey) were co-transfected into HEK293 cells together with the reporter plasmid, pGAL, which encoded for *LacZ* gene. The controls used in M2H assay were listed in Appendix 6A. The interaction between hSec3p and flavivirus full-length/mutated C proteins was then measured by M2H assay.

All negative and background controls did not produce significant β-gal activity and the positive controls activated significant β-gal activity (Fig. 6.27A). In contrast, high levels of β-gal activity were detected from all the co-transfections

except in CW14+hSec3p and CD13+hSec3p pairs (Fig. 6.27B). There was no significant changes ($P>0.05$) in the strength of interaction between hSec3p and flavivirus C mutants other than WC14 and DC13 mutants (Fig. 6.27B). This indicated that the mutations introduced at the amino acid residues 14 of WNV C protein and 13 of DENV C protein affected the interaction between flavivirus C protein and hSec3p. Reduced chymotrypsin-like activity observed from WMycC14 and DMycC13 mutants (Fig. 6.24) could have resulted as a consequence of no interaction between C protein and hSec3p. This further supported the notion that physical binding between C protein and hSec3p was essential to mediate the degradation of hSec3p.

Fig. 6.27: Effect of mutations on the interaction between flavivirus capsid protein and human Sec3 protein. HEK293 cells were transfected with full-length/mutated C (bait) and hSec3p (prey) and subjected to M2H assay. The strength of interaction between C protein and hSec3p was measured by β-galactosidase assay. (A) All the necessary controls are included. (i) Positive controls, negative controls and background controls for WNV full-length/mutated C proteins and hSec3p. (ii) Positive controls, negative controls and background controls for DENV full-length/mutated C proteins and hSec3p. (B) High levels of β-gal activity are detected from all the co-transfections except in (i) CW14+hSec3p and (ii) CD13+hSec3p pairs. There is no significant difference ($P>0.05$) in the binding strength between C protein and hSec3p with other mutants.

A

(i)

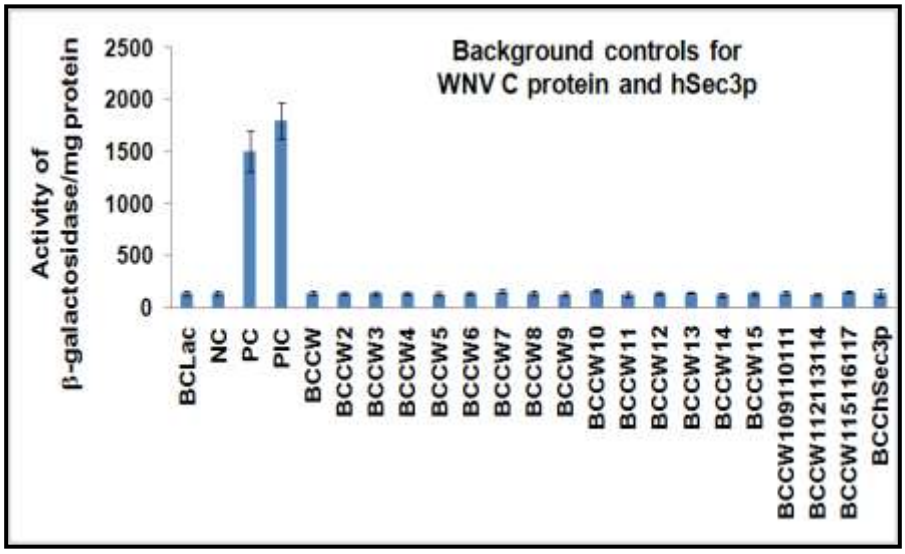
Background controls for
WNV C protein and hSec3p
Activity of
β-galactosidase/mg protein
2500
2000
1500
1000
500
0
BCLac
NC
PC
PIC
BCCW
BCCW2
BCCW3
BCCW4
BCCW5
BCCW6
BCCW7
BCCW8
BCCW9
BCCW10
BCCW11
BCCW12
BCCW13
BCCW14
BCCW15
BCCW109110111
BCCW112113114
BCCW115116117
BCChSec3p

(ii)

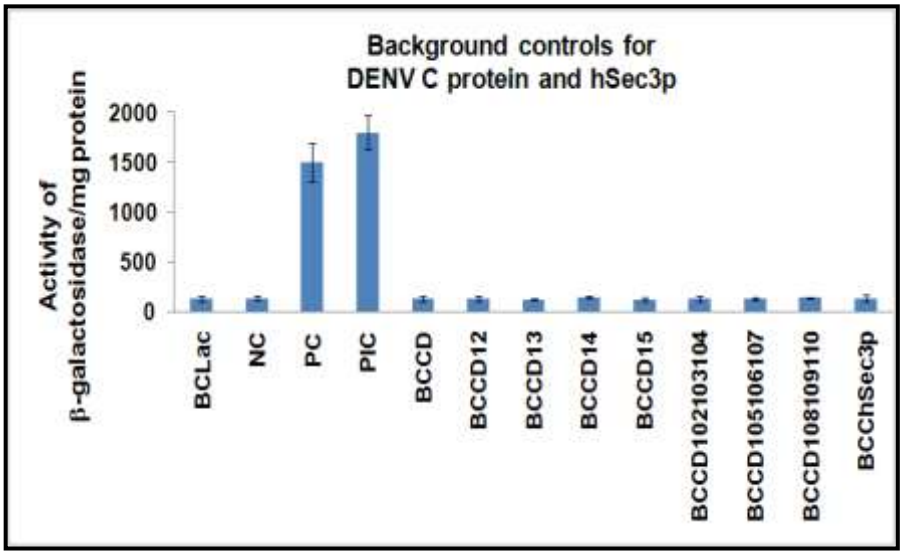
Background controls for
DENV C protein and hSec3p
Activity of
β-galactosidase/mg protein
2000
1500
1000
500
0
BCLac
NC
PC
PIC
BCCD
BCCD12
BCCD13
BCCD14
BCCD15
BCCD102103104
BCCD105106107
BCCD108109110
BCChSec3p

B

(i)

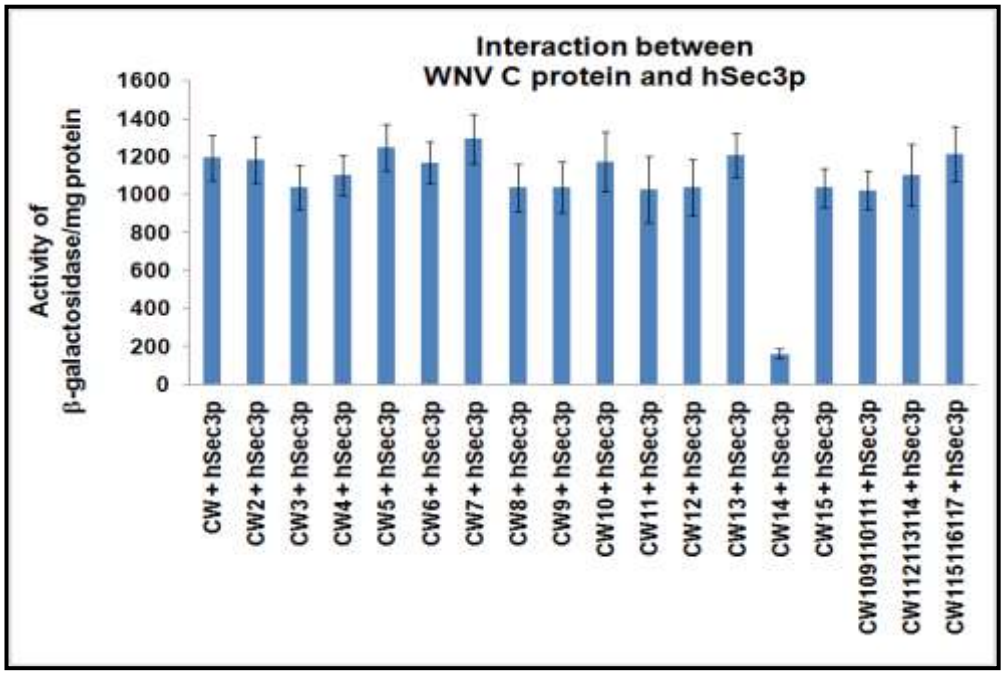
Interaction between
WNV C protein and hSec3p
Activity of
β-galactosidase/mg protein
1600
1400
1200
1000
800
600
400
200
0
CW + hSec3p
CW2 + hSec3p
CW3 + hSec3p
CW4 + hSec3p
CW5 + hSec3p
CW6 + hSec3p
CW7 + hSec3p
CW8 + hSec3p
CW9 + hSec3p
CW10 + hSec3p
CW11 + hSec3p
CW12 + hSec3p
CW13 + hSec3p
CW14 + hSec3p
CW15 + hSec3p
CW109110111 + hSec3p
CW112113114 + hSec3p
CW115116117 + hSec3p

(ii)

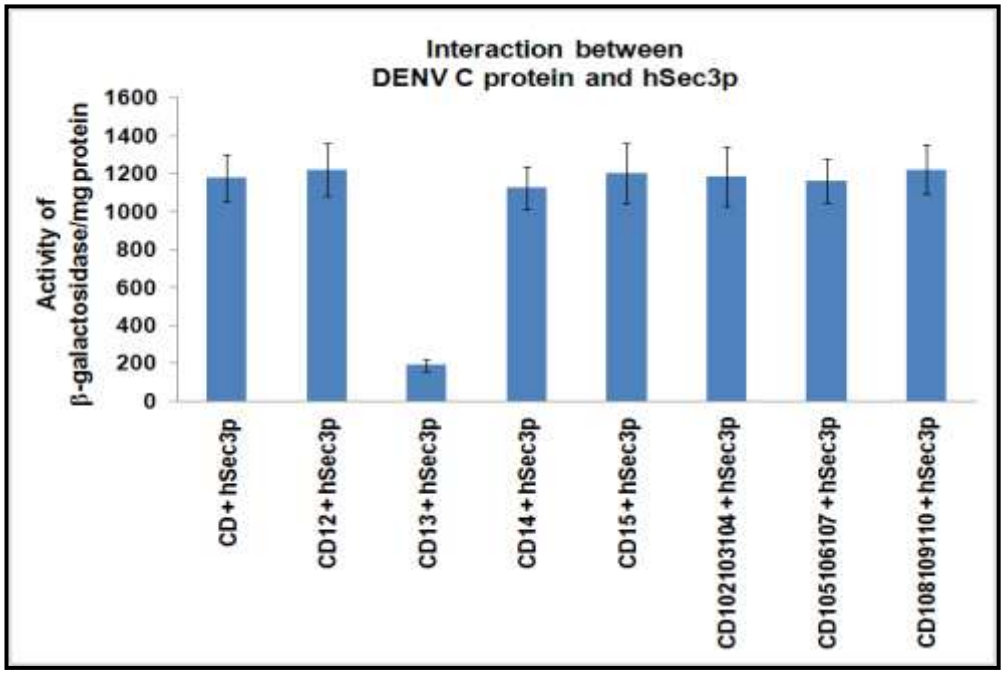
Interaction between
DENV C protein and hSec3p
Activity of
β-galactosidase/mg protein
1600
1400
1200
1000
800
600
400
200
0
CD + hSec3p
CD12 + hSec3p
CD13 + hSec3p
CD14 + hSec3p
CD15 + hSec3p
CD102103104 + hSec3p
CD105106107 + hSec3p
CD108109110 + hSec3p

6.4. REVERSE GENETICS SYSTEM TO ANALYZE THE INFLUENCE OF DEGRADATION MOTIF OF CAPSID PROTEIN ON THE DEGRADATION OF HUMAN SEC3 PROTEIN

To examine the influence of degradation motif of C protein on the degradation of hSec3p, reverse genetics system was utilized. Mutations were introduced on to the degradation motif of C protein in the full-length infectious clones of WNV and DENV. This resulted in the formation of pWNS109110111, pWNS112113114, pWNS115116117, pDENV102103104, pDENV105106107 and pDENV108109110 mutants. To evaluate the role of degradation motif of flavivirus C protein in reducing hSec3p level, HEK293 cells were transfected with the RNAs *in vitro* transcribed from pWNS, pDENV, pWNS109110111, pWNS112113114, pWNS115116117, pDENV102103104, pDENV105106107 and pDENV108109110 plasmids. The expression of hSec3p and hSec6p were then assessed using cell-based fluorescence (CBF) assay at 18 h post-transfection. The chymotrypsin-like activity of 26S proteasome was also measured using Proteasome Glo cell-based kit.

The hSec3p level was markedly reduced following the transfection with RNAs *in vitro* transcribed from pWNS, pDENV, pWNS115116117 and pDENV108109110 [Figs. 6.28A(i) & 6.28B(i)]. In contrast, the reduction in hSec3p level was significantly compromised ($P<0.05$) in pWNS109110111, pWNS112113114, pDENV102103104 and pDENV105106107-RNA-transfected cells compared to that obtained from pWNS and pDENV [Fig. 6.28A(i) & 6.28B(i)]. The amount of

hSec3p in each experimental group inversely correlated well with the level of chymotrypsin-like activity in that particular experimental group ([Fig. 6.28A(ii) & 6.28B(ii)]. In contrast, there were no significant differences ($P>0.05$) in the levels of hSec6p in all the experimental cohorts [Fig. 6.28A(iii) & 6.28B(iii)]. Overall, this demonstrated that the degradation motif present on flavivirus C protein played an essential role in specifically mediating the proteasome-mediated degradation of hSec3p.

This chapter highlighted how flavivirus infection can be successful in the presence of endogenous hSec3p by dissecting the role of WNV/DENV C protein in inducing chymotrypsin-like proteolytic function of 26S proteasome to degrade hSec3p. The experiments conducted in this chapter yielded novel information regarding the functions of C protein during virus replication.

Fig. 6.28: Effect of mutations on degradation motif of C protein on hSec3p expression using reverse genetics system. HEK293 cells were transfected with RNAs *in vitro* transcribed from full-length/mutant infectious clones of (A) WNV and (B) DENV. (i) The hSec3p expression level was assessed by CBF assay using anti-hSec3p and anti-actin antibody. The hSec3p levels are normalized against the actin control and the relative levels of hSec3p in viral RNA-transfected cells are shown. Reduced hSec3p level is detected in [A(i)] pWNS, [A(i)] pWNS115116117, [B(i)] pDENV and [B(i)] pDENV108109110 compared to mock-transfection (* represents $p<0.05$). The hSec3p levels are significantly higher in other mutants compared to that of pWNS or pDENV (** represents $p<0.05$). (ii) Chymotrypsin-like activity of 26S proteasome following viral RNA transfections. Chymotrypsin-like functions of 26S proteasome are significantly increased following transfection with RNA *in vitro* transcribed from in [A(ii)] pWNS, [A(ii)] pWNS115116117, [B(ii)] pDENV and [B(ii)]pDENV108109110 compared to mock-transfection (* represents $p<0.05$). The chymotrypsin-like activity is significantly lower in other mutants compared to that of pWNS or pDENV (** represents $p<0.05$). (iii) The expression of hSec6p protein is monitored by CBF assay using anti-hSec6p and anti-actin antibodies. There is no change in the hSec6p expression levels following RNA transfection.

A

(i)

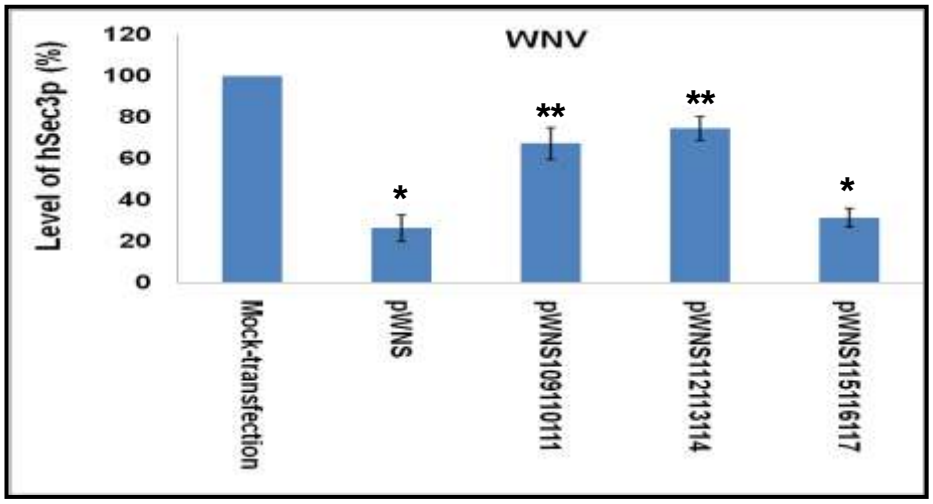
WNV
Level of hSec3p (%)
120
100
80
60
40
20
0
*
**
**
*
Mock-transfection
pWNS
pWNS109110111
pWNS112113114
pWNS115116117

(ii)

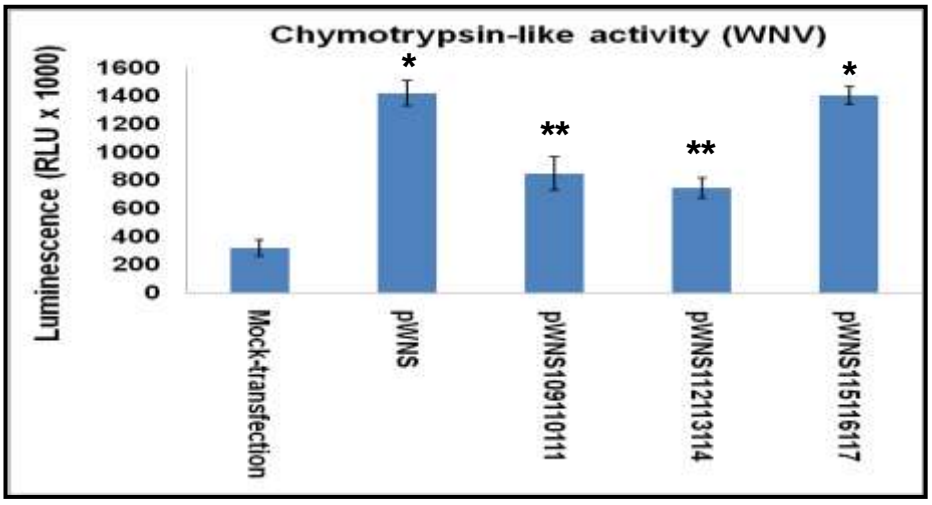
Chymotrypsin-like activity (WNV)
Luminescence (RLU x 1000)
1600
1400
1200
1000
800
600
400
200
0
*
**
**
*
Mock-transfection
pWNS
pWNS109110111
pWNS112113114
pWNS115116117

(iii)

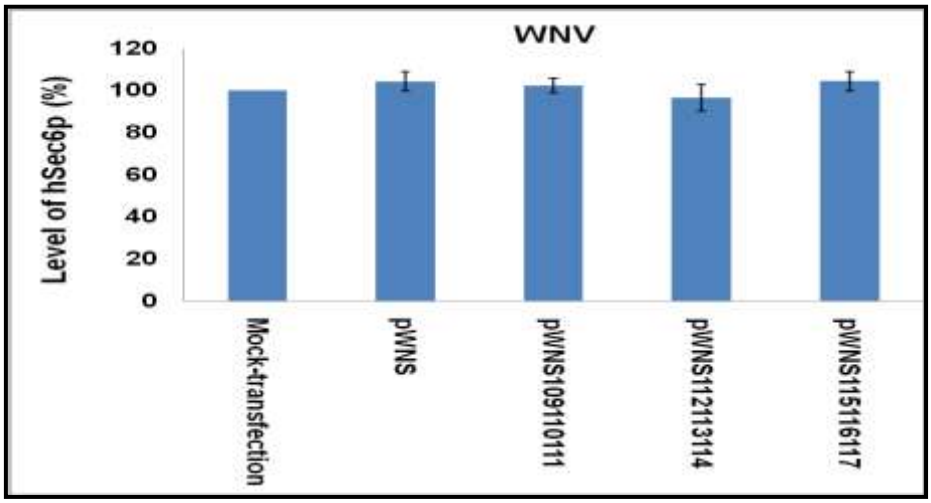
WNV
Level of hSec6p (%)
120
100
80
60
40
20
0
Mock-transfection
pWNS
pWNS109110111
pWNS112113114
pWNS115116117

B

(i)

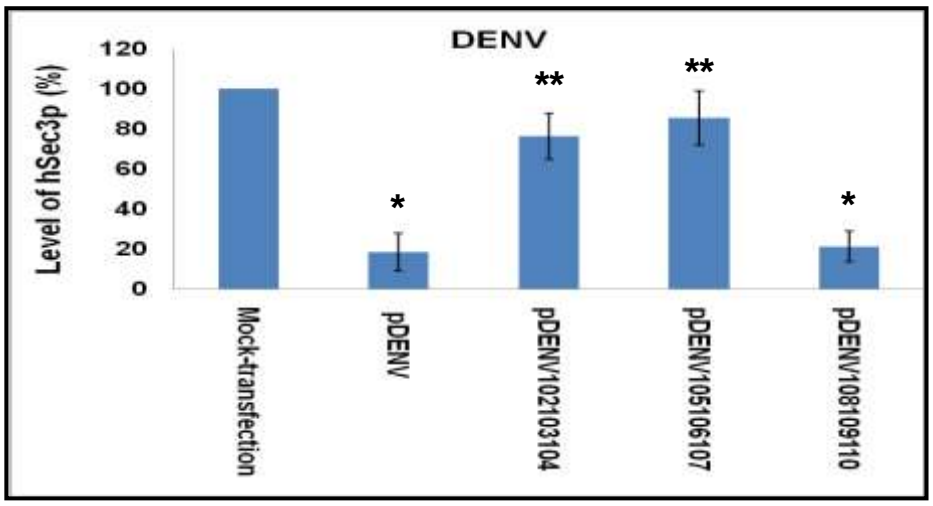
DENV
Level of hSec3p (%)
120
100
80
60
40
20
0
*
**
**
*
Mock-transfection
pDENV
pDENV/102103104
pDENV/105106107
pDENV/108109110

(ii)

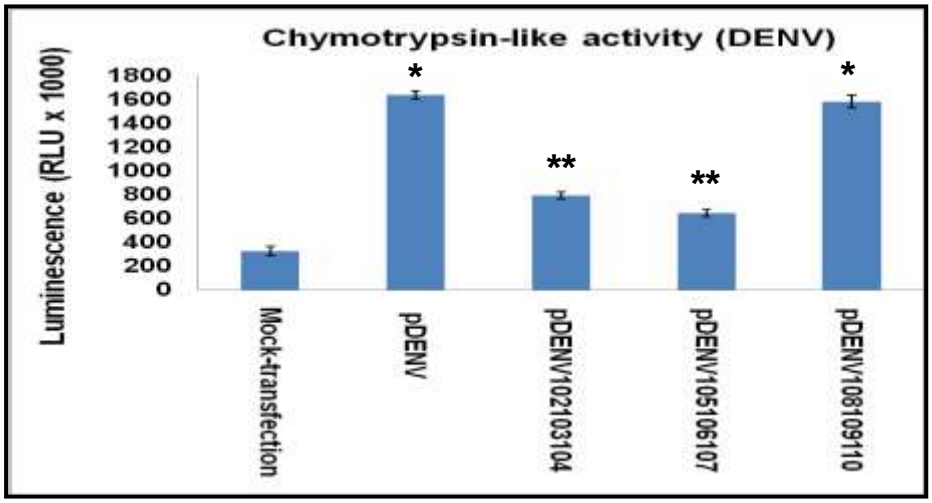
Chymotrypsin-like activity (DENV)
Luminescence (RLU x 1000)
1800
1600
1400
1200
1000
800
600
400
200
0
*
**
**
*
Mock-transfection
pDENV
pDENV/102103104
pDENV/105106107
pDENV/108109110

(iii)

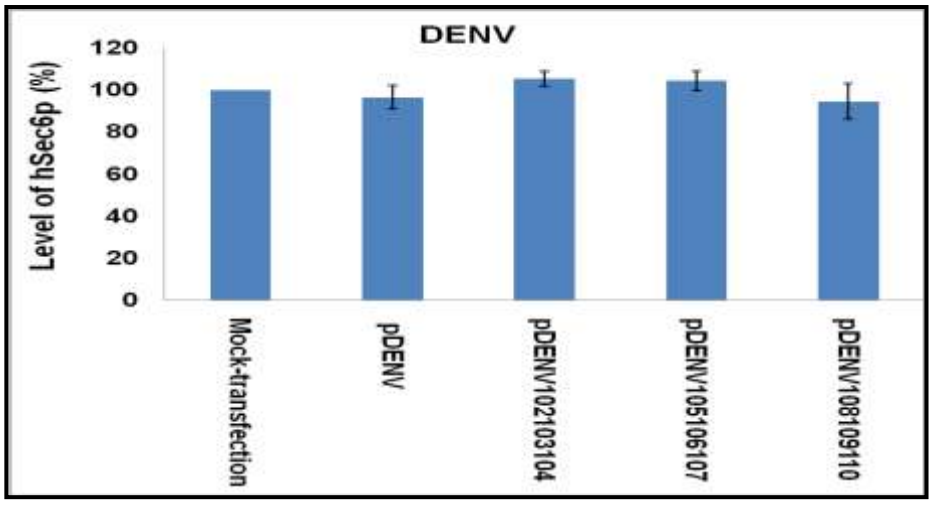
DENV
Level of hSec6p (%)
120
100
80
60
40
20
0
Mock-transfection
pDENV
pDENV/102103104
pDENV/105106107
pDENV/108109110

CHAPTER 7

DISCUSSION

7.0. DISCUSSION

Viruses containing their nucleic acid enclosed in a protein shell are parasites of their host organisms. Although viruses possess simple structures, they employ sophisticated mechanisms to replicate within their hosts. RNA viruses, in general, rely on host cellular components for replication and transcription of their genomic RNAs. They utilize their structural and non-structural proteins to hijack and manipulate the host cell environment to support their life-cycle. These virus-host interactions are complex and dynamic. Understanding this multifaceted bio-molecular process has the potential to yield new and exciting strategies for therapeutic intervention.

The capsid (C) protein of flavivirus is the first viral protein synthesized in an infected cell. The capsid protein is the key structural component of virus particles. They are nucleic acid-binding proteins whose known function is packaging viral genomes into nucleocapsids. However it is not required as a structural component until the later phases of assembly pathway. Growing evidences showed that capsid protein of RNA viruses have non-structural functions in addition to their structural roles (Hunt *et al.*, 2007; Ko *et al.*, 2010; Oh *et al.*, 2006; Yang *et al.*, 2002; Yang *et al.*, 2008). These non-structural functions were achieved by modulating host cell signalling pathways. This is possible since the C protein is the first viral protein to contact host cell proteins in the cytoplasm.

Although flavivirus replication is confined to the cytoplasm of host cells and virus assembly occurs on the endoplasmic reticulum (Mukhopadhyay *et al.*, 2005), the C proteins are observed to have a nuclear phase (Bhuvanakantham *et al.*, 2010; Bhuvanakantham *et al.*, 2009; Bulich & Aaskov, 1992; Chang *et al.*, 2001; Cheong & Ng, 2010; Makino *et al.*, 1989; Mori *et al.*, 2005; Oh & Song, 2006; Tadano *et al.*, 1989; Westaway *et al.*, 1997). As there is no obvious role for nuclear localization of C protein in virus assembly, this nuclear phase may presumably modify the host cell environment in such a way that virus replication and dissemination is enhanced (Bhuvanakantham *et al.*, 2009; Mori *et al.*, 2005). This suggested that the dual cellular distributions (nucleus and cytoplasm) of C proteins place them in a strategic position to act as a modulator of the host cell environment.

Among the flaviviruses, the non-structural functions of capsid protein were well documented in Hepatitis C virus (HCV). They were shown to involve in multiple pathways such as lipid metabolism, T-cell response, cell cycle regulation, transcriptional control, signal transduction, apoptotic pathways, protein degradation and cell transformation (Hosui *et al.*, 2003; Kittlesen *et al.*, 2000; Machida *et al.*, 2010; Ohkawa *et al.*, 2004; Shi *et al.*, 2002; Tu *et al.*, 2010; Yoshida *et al.*, 2002). The cellular functions of C protein in arthropod-borne flaviviruses other than its role as a major structural component are poorly defined. The reported principle non-structural function of C protein in arthropod-borne flaviviruses is mainly associated with apoptosis (Bhuvanakantham *et al.*, 2010;

Lee *et al.*, 2006; Liao *et al.*, 2010; Limjindaporn *et al.*, 2007; Netsawang *et al.*, 2010; Oh *et al.*, 2006; Oh & Song, 2006; Yang *et al.*, 2008). This study aimed to investigate if C protein of WNV and DENV possess any other novel non-structural functions apart from its role in initiating apoptosis. As a starting point, Y2H cDNA library screening was performed to identify the host proteins that could interact with flavivirus C proteins.

The Y2H library screening picked up several proteins associated with apoptosis such as calcium-modulating cyclophilin binding ligand (CAML), protein L-isoaspartyl methyltransferase (PIMT), activating transcription factor 6 (ATF6), heat shock protein 27 (HSP 27), heat shock protein 70 (HSP 70) and human death domain-associated protein (Daxx). This re-affirmed that C proteins of flaviviruses establish a wide network of interactions with the proteins associated with apoptosis. This is consistent with the previous studies that implicated C protein as the inducer of apoptosis (Limjindaporn *et al.*, 2007; Netsawang *et al.*, 2010; Oh *et al.*, 2006; Yang *et al.*, 2002; Yang *et al.*, 2008). It is possible that C protein associates with pro-apoptotic proteins to nullify the anti-viral effects mounted by host cells' defense mechanism in virus-infected cells.

Some of the host proteins that were identified in this study [HSP 70, Daxx and phosphatase Inhibitor (I2PP2A)] were similarly reported as the interacting partners of WNV/DENV C protein (Hunt *et al.*, 2007; Limjindaporn *et al.*, 2007; Netsawang *et al.*, 2010; Oh & Song, 2006). This confirmed the authenticity and

reliability of Y2H library screening performed in this study. The Y2H library screening also isolated several other proteins that were involved in calcium signaling, protein translation, pH maintenance, protein degradation, trafficking, cell signaling and exocytosis (Tables 3.2 and 3.3). This illustrated that C protein of arthropod-borne flaviviruses do interact with a wide variety of cellular proteins during their replication process to manipulate the host cell environment conducive for virus replication.

This study decided to select a novel host protein, human Sec3 protein (hSec3p) which interacted with both WNV/DENV C proteins and whose function is not widely studied in mammalian system. The hSec3p is a component of the human Sec6/8 exocyst complex. Using a combination of Y2H, M2H, Co-IP and confocal analyses, this study demonstrated a unique interaction between flavivirus C protein and an exocyst component. A combination of computational prediction and biochemical mapping studies revealed that the first 15 amino acids of flavivirus C protein and the SH2 domain binding motif in the last 15 amino acids of hSec3p were crucial for the functional interaction between hSec3p and C proteins. The hSec3p-interacting domain on WNV/DENV C protein coincided with the Jab1-interaction domain on WNV C protein and C-RNA interaction domain (Oh *et al*., 2006, Khromykh & Westaway, 1996; Cheong & Ng, 2010). This highlighted the crucial role played by the first 15 amino acids of flavirus C proein. Structural studies showed that this domain is non-structured in flavivirus C protein (Dokland *et al.*, 2004; Jones *et al.*, 2003; Kofler *et al.*, 2002; Ma *et al.*,

2004) One possible explanation for the existence of this non-strutured domain could allow C protein to interact with a wide variety of host proteins and viral RNA genomes.

In yeast, Sec3p played a crucial role in the secretory pathways and the facilitation of polarized growth (Finger *et al.*, 1998a; Finger & Novick, 1997; Wiederkehr *et al.*, 2003). Recent paper has also shown that N terminus of Sec3p interacted with phosphatidylinositol 4, 5-bisphosphate and Cdc42 to regulate exocytosis (Zhang *et al.*, 2008b). Thus, the initial hypothesis was that flavivirus C protein might exploit hSec3p for virus trafficking and release. However, hSec3p knock-down potentiated virus replication/production in WNV-/DENV-infected hSec3p293KD cells while the reverse phenomenon was observed in hSec3p293OE cells (Fig. 4.5). This contradicted the initial hypothesis and indicated hSec3p as a negative regulator of flavivirus infection. This is the only study to date on the discovery that hSec3p exocyst can act as an anti-flaviviral host protein.

It was observed that changes in hSec3p expression had a more pronounced effect on DENV replication compared to WNV(Sarafend). Dengue virus had a relatively longer latent period [(12-24 h) (Helt & Harris, 2005) compared to WNV(Sarafend) which possessed a very short latent period [(6 h) (Ng *et al.*, 2001)]. The hSec3p might require longer period to effectively execute its anti-viral function. With the longer latent period for DENV replication, hSec3p might have sufficient time to fully implement its anti-viral activity unlike in WNV

(Sarafend) replication. This hypothesis was substantiated when WNV(Wengler) which had a growth cycle similar to that of DENV showed same pronounced effect when hSec3p was differentially expressed [Fig. 4.5(iii)]. This demonstrated that the duration of latent period could influence the efficacy of the anti-viral effects of hSec3p.

Viruses utilize hundreds of host cell machineries in a concerted manner to favour each step of their life cycles and identifying these host functions will be of great interest in virology to further the understanding of precise mechanisms of flaviviral life cycle. This study thus aimed to pinpoint which step in flavivirus life-cycle was targeted by hSec3p, i.e., virus entry, viral RNA transcription, viral protein translation and virus secretion. A combination of reverse genetics system, real-time PCR, Western blotting, densitometry, *in vitro* translation assay, Co-IP, pull down assay, competition assay and confocal analyses were employed to elucidate the critical step(s) in flavivirus life-cycle targeted by hSec3p.

Molecular dissection of the mechanism underlying hSec3p-C protein interaction revealed that hSec3p functioned as an anti-viral host factor through a bimodal inhibitory pathway. The expression levels of hSec3p affected both viral transcription and translation processes, in that it significantly reduced the biosynthesis of both viral RNA and proteins (Figs.4.8 - 4.11). Although host proteins such as Interferon regulatory factor 3 and CCR5 receptor (Fredericksen *et al.*, 2004; Lim *et al.*, 2006) can influence WNV infection, to our knowledge,

this is the only report that implicated human exocyst component (hSec3p) as an anti-flavivirus factor. This study further showed that enhanced virus production in hSec3p293KD cells was not attributed to altered virus entry or genome uncoating (Fig. 4.7).

Efforts to verify if physical binding between hSec3p and C protein was needed to negatively manipulate flavivirus production indicated that the physical binding between hSec3p and C protein was not essential. This suggested that there could be other unknown factor(s) mediating the effect of hSec3p on flavivirus production. Delineating the molecular mechanism by which hSec3p exerted its anti-viral effects discovered the translational enhancer, EF1α as the binding partner of hSec3p. Another interesting discovery of this study is the demonstration of the physical interaction between hSec3p and EF1α in mammalian system. The hSec3p sequestered EF1α and reduced the binding opportunity of EF1α with flaviviral RNA genome or RNA-associated replicative complex. It has been reported that EF1α acted as a regulator of (-) RNA synthesis and was a component of the viral transcriptase complex in viruses such as WNV, tobacco mosaic virus, vesicular stomatitis virus and tombusvirus (Davis *et al.*, 2007b; Li *et al.*, 2009; Matsuda *et al.*, 2004; Qanungo *et al.*, 2004). It was also shown that EF1α interacted with 3'UTR of WNV and DENV genome (Blackwell & Brinton, 1995; 1997; Davis *et al.*, 2007b; De Nova-Ocampo *et al.*, 2002; Shi *et al.*, 1996) and this association was a critical determinant of viral (-) RNA synthesis and replicative efficiency (Davis *et al.*, 2007a). Taken together, the

inability of free EF1α to bind flaviviral RNA genome efficiently due to the formation of hSec3p- EF1α complex could have led to the decrement in viral RNA synthesis (Figs. 4.8 and 4.9).

A combination of *in vitro* translation assay, immunodepletion assay and competition assay demonstrated that hSec3p inhibited viral protein translation by similarly sequestrating the translational enhancer, EF1α. The antagonistic activity of hSec3p on viral translation fitted snugly with the current awareness that the inhibition of viral protein translation is a common host response strategy against infection. Certain host proteins such as translation initiation factor DED1 and Y box-binding protein were also identified as cellular factors that block viral translation in Brome Mosaic virus and DENV (Noueiry *et al.*, 2000; Paranjape & Harris, 2007).

The concerted negative effect of hSec3p over-expression on viral transcription and translation resulted in the reduction of viral RNA and protein synthesis. This subsequently led to a decrease in the levels of secreted RNA and virus protein in the virus-infected cell culture supernatants (Figs. 4.12 and 4.13). This decrease correlated with the significant reduction in the virus yield observed in this study (Fig. 4.5). Overall, by highlighting the anti-viral properties of hSec3p, this study revealed the new functional role of hSec3p exocyst.

Interestingly, flavivirus capsid protein-binding defective mutant, hSec3pSH2 inhibited flavivirus production at the same level as intact hSec3p (Fig. 4.6). Dissecting the underlying mechanism revealed that hSec3pSH2 mutant was also capable of sequestering EF1α (Fig. 5.2). Sequestration of EF1α would interfere with viral RNA transcription and translation as described above. This explained why hSec3pSH2 mutant is capable of impairing flavivirus production. This study also demonstrated that the anti-viral mechanism imposed by hSec3p was specific as it did not affect the binding of PTB to viral RNA (Figs. 5.4 and 5.6). When Sec6p was used in the place of Sec3p, it did not interfere with EF1α-3'UTR association (Fig. 5.7).

Based on the known functions of the other cellular proteins identified in this study, Testis-specific protein Y (TSPY) was known to interact with EF1α to enhance protein translation (Kido & Lau, 2008). It is not clear whether there is any cross-talk between flavivirus C protein, hSec3p and TSPY. It is possible that hSec3p could function together with TSPY to inhibit viral translation or C protein could make use of TSPY to alter cellular translation. This warrants further investigation.

Although one may argue that the hSec3p-dependant sequestration of an abundant cellular protein like EF1α should have minimal impact on cellular or viral processes, several studies had shown that differential levels of EF1α could influence biological functions. Recently, Kobayashi and Yonehara (2009)

reported that down-regulation of EF1α could induce cell death in tetraploids. In addition, the importance of EF1α level was further exemplified by Leclercq and colleagues (2008), who demonstrated the dose-dependent effects of EF1α on sphingosine kinase activity. Thus, it was not inconceivable that sequestration of EF1α by hSec3p could exert similar impact on biogenesis of flavivirus.

Just as the host has evolved a mechanism to counter virus replication, virus proteins also developed the abilities to sequester host proteins to favour a productive infection. Zhou and colleagues (2008) reported that SARS nucleocapsid protein bound to EF1α and inhibited cell cytokinesis to favour virus infection. Similarly, another study showed that the binding of EF1α by HCV NS4A inhibited host translation (Kou *et al.*, 2006). Viruses could also utilize their structural and non-structural proteins to cleave and inactivate the key components of anti-viral signalling pathways (Elliott *et al.*, 2007; Ulane & Horvath, 2002; Wright *et al.*, 2006; Zhang *et al.*, 2002; Zhang *et al.*, 2005a) or to recruit host proteasome system to destabilise the anti-viral host proteins (Ashour *et al.*, 2009; Barro & Patton, 2005; Graff *et al.*, 2009; Kalantari *et al.*, 2008). If hSec3p truly posed a hindrance to flavivirus replication, flaviviruses should have evolved some strategies to circumvent the anti-viral effects of hSec3p in a natural infection.

This study has also unveiled how flavivirus C protein overcome the anti-viral effects of hSec3p. The amount of EF1α-hSec3p complex formation was significantly lowered in virus-infected cells compared to uninfected cells (Section

5.2.1). This indicated that WNV/DENV infection could interfere with EF1α-hSec3p complex formation by altering the hSec3p level. Investigation into the molecular mechanism underlying flavivirus-induced reduction in EF1α-hSec3p complex formation revealed that there was active down-regulation of hSec3p in flavivirus-infected cells (Fig. 6.1). This study also unveiled that flavivirus infection did not alter the transcription or stability of *hSec3* gene but influenced hSec3p concentration at the post-transcription level. Reduced hSec3p level resulted in decreased formation of hSec3p-EF1α complex as observed with hSec3p knock-down cells.

The cell-based fluorescence assay developed during this study was used to quantitate hSec3p, hSec6p and epitope-tagged proteins. The results were highly reproducible after normalization against the internal control, actin. The percentage difference in hSec3p levels obtained from Western blotting followed by densitometry coincided with the data obtained from cell-based fluorescence assay (Fig. 6.3). This assay functioned as an alternative to Western blotting and saved time. This assay platform can easily be extended to measure a wide range of cellular and viral proteins, thus opening an avenue to quantitate the protein level at a faster rate in a high-throughput manner.

The proteasome degradation pathway plays a crucial role in various biological processes in cells such as antigen processing, apoptosis, signal transduction, transcriptional regulation and help to eliminate non-functional, misfolded or

unwanted proteins (Coux *et al.*, 1996; Glickman, 2000; Niedermann, 2002; Pickart, 1997). Several viruses exploited the proteasomal pathway to support efficient virus production such as to escape from the immune system, during release from cells or to suppress apoptosis (Hassink *et al.*, 2006; Kikkert *et al.*, 2001; Lagunas-Martinez *et al.*, 2010; Mack *et al.*, 2008; Raaben *et al.*; Sakurai *et al.*, 2004; Urata *et al.*, 2007).

Analysis of hSec3p stability in the presence of MG132, a proteasomal inhibitor indicated that intact proteasome activity was required to mediate the reduction of hSec3p levels. The stability of hSec3p was compromised following flavivirus infection (Fig. 6.7). This demonstrated that flaviviruses subverted the proteasome degradation pathway for their own advantage. Following the observation that hSec3p levels were reduced during flavivirus infection, this study analysed the role of recombinant C protein in altering hSec3p levels. Results indicated that flavivirus C protein was capable of reducing hSec3p levels in the absence of other viral components in a dose-dependent manner (Figs. 6.8 and 6.9). Studies performed with truncated and point mutants of C protein revealed that this protein must physically bind to hSec3p to execute the degradation of hSec3p via proteasome-mediated pathway (Figs. 6.10 and 6.11). The degradation motifs important to mediate the degradation of hSec3p resided between the amino acid residues 109-114 of WNV C protein and 102-107 of DENV C protein (Figs. 6.25 and 6.28). It will be interesting to examine the influence of these introduced mutations at the cytotoxic motif of C protein on flavivirus replication.

After confirming the involvement of proteasomes in decreasing hSec3p levels using MG132 and epoxomicin, this study was extended to dissect which of the three proteolytic functions of 20S proteasome was activated by flavivirus C protein. Analysis of the specific proteolytic activities of 20S proteasome delineated that chymotrypsin-like and caspase-like activities of 20S proteasome were activated by flavivirus C protein (Fig. 6.18). Further detailed analyses using inhibitors discovered that the chymotrypsin-like proteolytic function of 20S proteasome was activated by C protein to execute the proteasome-mediated degradation of hSec3p and caspase-like function had no effect on modulating endogenous hSec3p levels (Figs. 6.21 and 6.22). This study opened a new avenue for the researchers to look into how flavivirus C protein activates the proteasome pathway. In summary, this study demonstrated that flavivirus C protein induced the degradation of hSec3p by activating the chymotrypsin-like proteolytic function of 20S proteasome. As a result, the hSec3p level was reduced which subsequently resulted in the decreased formation of EF1α-hSec3p complex. This rendered free EF1α readily available to interact with 3'UTR of viral RNA to aid viral RNA transcription and translation.

Consistent with this study, the involvement of proteasomes to favour flavivirus infection have been reported for efficient WNV, DENV, HCV and JEV replication (Dutta *et al.*, 2009; Fink *et al.*, 2007; Gilfoy *et al.*, 2009; Kanlaya *et al.*, 2010; Krishnan *et al.*, 2008; Lin *et al.*, 2005b). Flaviviruses have also utilized proteasome-dependent pathway to invade the host immune system by degrading

STATs (Ashour *et al.*, 2009). It is thus clear that proteasomes' involvement plays an essential role in favouring flavivirus infection. Similar scenario was observed during human immunodeficiency virus (HIV) infection. The deoxycytidine deaminase, APOBEC3G protein functioned as the anti-retroviral agent. One of the viral proteins encoded by HIV, Vif induced the proteasome-dependent pathway to degrade APOBEC3G and nullified the anti-viral function of APOBEC3G (Albin & Harris, 2010; Fourati *et al.*, 2010; Mehle *et al.*, 2004; Ooms *et al.*, 2010; Wissing *et al.*, 2010; Zangari *et al.*, 2010). This showed that viruses are capable of utilizing proteasomal functions to degrade the anti-viral cellular proteins to favour the infection.

Studies have also shown that host proteins such as Jab1, subunit of COP9 signalosome and Makorin ring finger protein 1 induced the degradation of flavivirus C protein in a proteasome-dependent manner (Ko *et al.*, 2010; Oh *et al.*, 2006). This suggested that proteasomal degradation pathway played a dual role during flavivirus infection. The host cell uses it as a tool to defend against the virus and the virus exploits it to support successful infection. This ambivalent behavior of proteasomal system suggested that this could have resulted from the co-evolution of the host and the flavivirus.

By inhibiting proteasomal activity, it is possible to impair several processes such as cell proliferation, inflammatory responses and apoptosis. The proteasome inhibitor, bortezomib has been approved by FDA to use in cancer therapy and

organ transplantation (Everly *et al.*, 2010; Flechner *et al.*, 2010; Kennedy *et al.*, 2010; Zangari *et al.*, 2010). It will therefore be of great interest to target the chymotrypsin-like proteolytic function of 20S proteasome in an effort to strengthen the host anti-viral state against flavivirus. This study indicated that the proteasomal pathway could serve as an attractive and novel therapeutic target for flavivirus infection.

In addition, this study also revealed that although WNV and DENV C protein share only 25-35% sequence identity, they acted in the similar fashion to encounter hSec3p in the host cell. It is not surprising since it was known earlier that flavivirus C proteins are structurally and functionally similar although their amino acid sequences are poorly conserved. The C protein of flavivirus was shown to be an alpha-helical protein and it functions primarily to package the viral genome (Chambers *et al.*, 1990a; Dokland *et al.*, 2004; Jones *et al.*, 2003; Kofler *et al.*, 2002; Ma *et al.*, 2004).

In conclusion, this study identified a novel interaction between hSec3p and flavivirus C protein and also unraveled the biological significance of flavivirus C protein and hSec3p association as portrayed in Fig. 7.1. As shown in Fig. 7.1A, flavivirus enters the cell by receptor-mediated endocytosis and trafficked along an endosomal and lysosomal pathway. Subsequently, nucleocapsid is released into the cytoplasm followed by its dissociation into RNA and C particles (Chu & Ng, 2004a). The RNA is translated into structural and non-structural proteins. The non-structural proteins together with some cellular proteins bind flaviviral RNA and form the viral replicative complex. Free EF1α then interacts with flaviviral

RNA or viral replicative complex and results in efficient negative strand RNA synthesis and subsequently leads to efficient positive strand RNA synthesis and viral protein synthesis. This results in enhanced virus assembly and virus secretion. The hSec3p battles against flavivirus infection by sequestering EF1α and thereby decreasing the amount of free EF1α that can bind with flaviviral RNA/replicative complex (shown using red colour in Fig. 7.1B). In this way, hSec3p negates flaviviral RNA transcription and translation, in an attempt to protect the host.

On the other front, flavivirus C protein forms a complex with hSec3p through a direct physical interaction and activates the chymotrypsin-like proteolytic activity of 20S proteasome (Fig. 7.1B, shown using blue colour). This results in the enhanced degradation of hSec3p. As a result, the endogenous hSec3p is exhausted. By increasing the turnover of endogenous hSec3p in the cytoplasm, C protein disrupts the formation of hSec3p-EF1α complex and renders the free EF1α easily available to interact with flaviviral RNA genome. This results in increased viral RNA and protein synthesis which subsequently enhances virus assembly and virus secretion. In this way, flavivirus C protein nullifies the anti-viral checkpoints imposed by hSec3p and helps the virus to establish a microenvironment that facilitates successful replication and infection. Understanding the molecular mechanism of flavivirus C protein and hSec3p interaction, besides revealing the ground-breaking non-structural function of flavivirus C protein and cellular functions of hSec3p, could possibly provide a new interface for pharmaceutical intervention.

Fig. 7.1: A model depicting the biological consequences of flavivirus C protein-hSec3p interaction. Flavivirions enter the cell by receptor-mediated endocytosis and release the nucleocapsid in the cytoplasm followed by its dissociation into RNA and C proteins. The RNA is translated into a polyprotein which subsequently forms structural and non-structural proteins. The non-structural proteins together with some cellular proteins bind flaviviral RNA and form the viral replicative complex. Free EF1α then interacts with viral replicative complex and results in efficient viral RNA and viral protein synthesis. This results in enhanced virus assembly and virus secretion. (A) The hSec3p battles against flavivirus infection by forming more hSec3p-EF1α complex and decreasing the amount of free EF1α available to bind with replicative complex. As a result, decreased viral RNA and proteins are synthesized, which then leads to decreased virus production. (B) Flavivirus C protein sequesters hSec3p and degrades it. This results in the decreased formation of hSec3p-EF1α complex. Free EF1α readily interacts with flaviviral RNA genome and potentiates flavivirus production. The effects mediated by hSec3p are shown in red (A) and the effects mediated by C protein are shown in blue (B). The broken arrow represents the interference caused by hSec3p (red) or C protein (blue) at particular step(s).

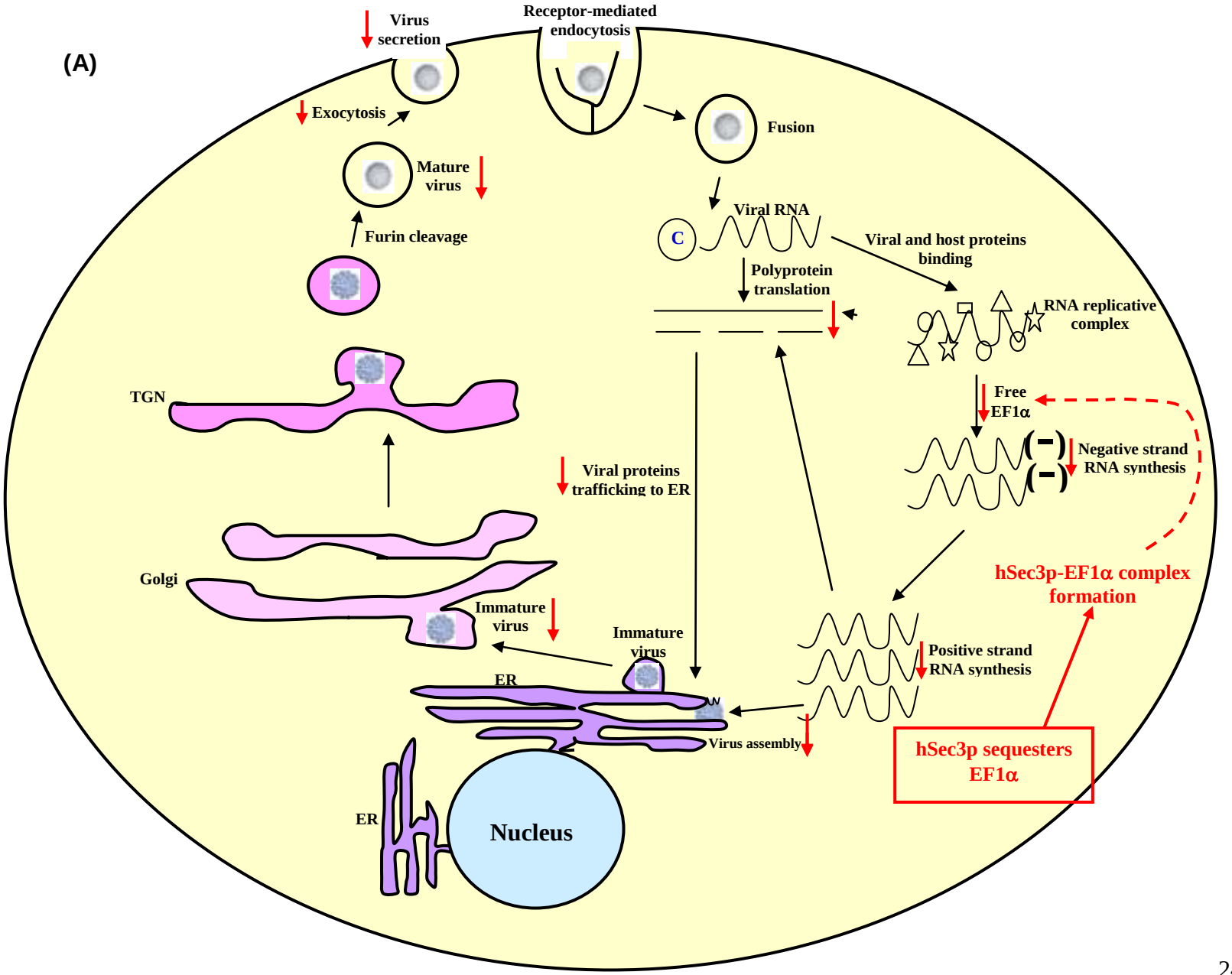
(A)
Virus secretion
Receptor-mediated endocytosis
Exocytosis
Fusion
Mature virus
Furin cleavage
Viral RNA
C
Viral and host proteins binding
Polyprotein translation
RNA replicative complex
TGN
Free EF1α
Negative strand RNA synthesis
Viral proteins trafficking to ER
Golgi
hSec3p-EF1α complex formation
Immature virus
Immature virus
Positive strand RNA synthesis
ER
Virus assembly
hSec3p sequesters EF1α
ER
Nucleus

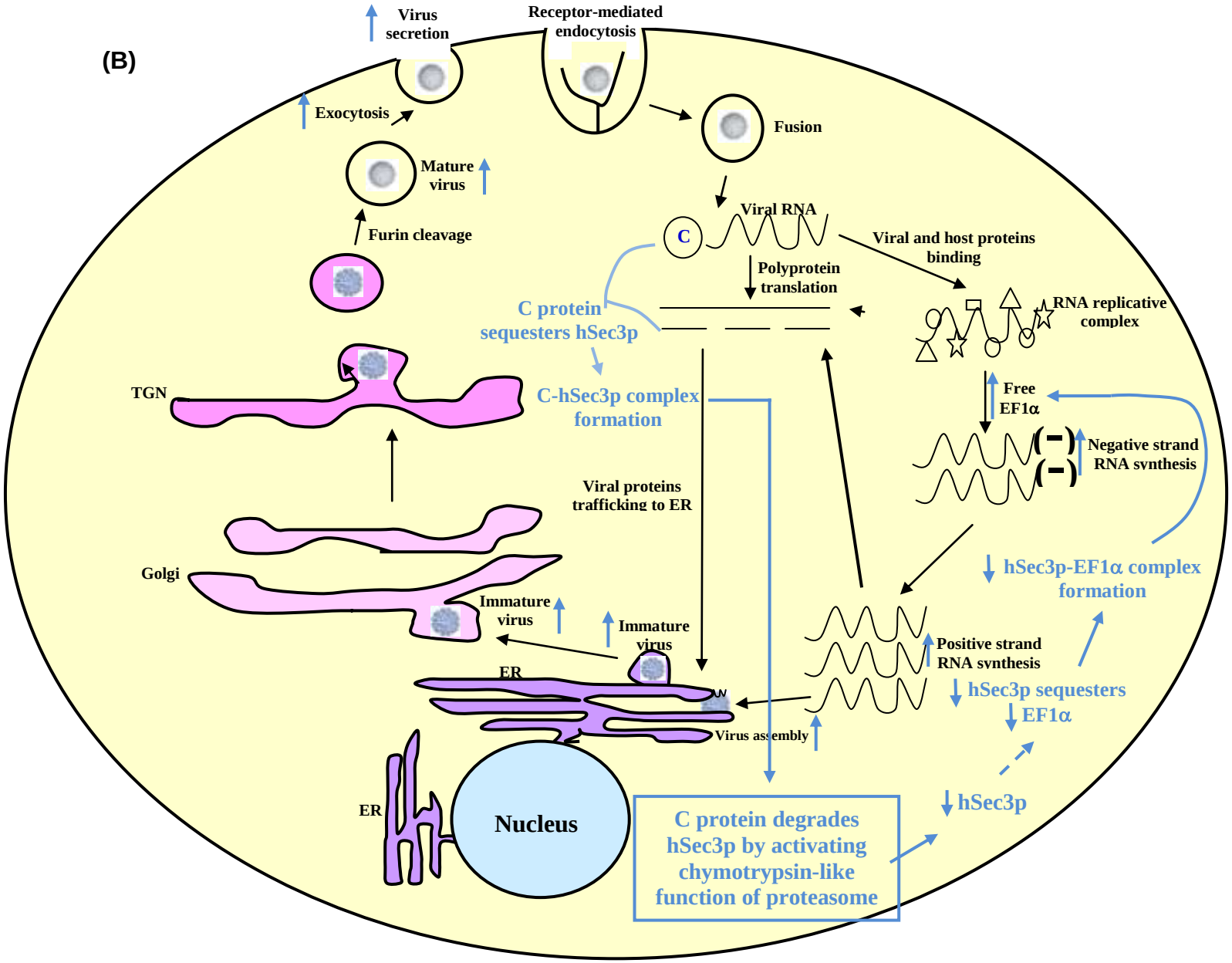
(B)
Virus secretion
Receptor-mediated endocytosis
Exocytosis
Fusion
Mature virus
Viral RNA
Furin cleavage
C
Viral and host proteins binding
Polyprotein translation
C protein sequesters hSec3p
RNA replicative complex
TGN
C-hSec3p complex formation
Free EF1α
Negative strand RNA synthesis
Viral proteins trafficking to ER
Golgi
hSec3p-EF1α complex formation
Immature virus
Immature virus
Positive strand RNA synthesis
ER
hSec3p sequesters EF1α
Virus assembly
ER
Nucleus
hSec3p
C protein degrades hSec3p by activating chymotrypsin-like function of proteasome

REFERENCES

REFERENCES

Aberle, J. H., Aberle, S. W., Kofler, R. M. & Mandl, C. W. (2005). Humoral and cellular immune response to RNA immunization with flavivirus replicons derived from tick-borne encephalitis virus. *J Virol* **79**, 15107-15113.

Acosta, E. G., Castilla, V. & Damonte, E. B. (2008). Functional entry of dengue virus into Aedes albopictus mosquito cells is dependent on clathrin-mediated endocytosis. *J Gen Virol* **89**, 474-484.

Acosta, E. G., Castilla, V. & Damonte, E. B. (2009). Alternative infectious entry pathways for dengue virus serotypes into mammalian cells. *Cell Microbiol* **11**, 1533-1549.

Ada, G. L. & Anderson, S. G. (1959). Yield of infective ribonucleic acid from impure Murray Valley encephalitis virus after different treatments. *Nature* **183**, 799-800.

Adams, J. (2002). Development of the proteasome inhibitor PS-341. *Oncologist* **7**, 9-16.

Albin, J. S. & Harris, R. S. (2010). Interactions of host APOBEC3 restriction factors with HIV-1 in vivo: implications for therapeutics. *Expert Rev Mol Med* **12**, e4.

Allison, S. L., Schalich, J., Stiasny, K., Mandl, C. W. & Heinz, F. X. (2001). Mutational evidence for an internal fusion peptide in flavivirus envelope protein E. *J Virol* **75**, 4268-4275.

Allison, S. L., Schalich, J., Stiasny, K., Mandl, C. W., Kunz, C. & Heinz, F. X. (1995). Oligomeric rearrangement of tick-borne encephalitis virus envelope proteins induced by an acidic pH. *J Virol* **69**, 695-700.

Amberg, S. M. & Rice, C. M. (1999). Mutagenesis of the NS2B-NS3-mediated cleavage site in the flavivirus capsid protein demonstrates a requirement for coordinated processing. *J Virol* **73**, 8083-8094.

Andersen, N. J. & Yeaman, C. (2010). Sec3-containing exocyst complex is required for desmosome assembly in mammalian epithelial cells. *Mol Biol Cell* **21**, 152-164.

Ang, F., Wong, A. P., Ng, M. M. & Chu, J. J. (2010). Small interference RNA profiling reveals the essential role of human membrane trafficking genes in mediating the infectious entry of dengue virus. *Virol J* **7**, 24.

Ashour, J., Laurent-Rolle, M., Shi, P. Y. & Garcia-Sastre, A. (2009). NS5 of dengue virus mediates STAT2 binding and degradation. *J Virol* **83**, 5408-5418.

Avirutnan, P., Malasit, P., Seliger, B., Bhakdi, S. & Husmann, M. (1998). Dengue virus infection of human endothelial cells leads to chemokine production, complement activation, and apoptosis. *J Immunol* **161**, 6338-6346.

Baek, K., Knodler, A., Lee, S. H., Zhang, X., Orlando, K., Zhang, J., Foskett, T. J., Guo, W. & Dominguez, R. (2010). Structure-function study of the N-terminal domain of exocyst subunit Sec3. *J Biol Chem* **285**, 10424-10433.

Barro, M. & Patton, J. T. (2005). Rotavirus nonstructural protein 1 subverts innate immune response by inducing degradation of IFN regulatory factor 3. *Proc Natl Acad Sci U S A* **102**, 4114-4119.

Basurko, C., Carles, G., Youssef, M. & Guindi, W. E. (2009). Maternal and fetal consequences of dengue fever during pregnancy. *Eur J Obstet Gynecol Reprod Biol* **147**, 29-32.

Baumeister, W., Walz, J., Zuhl, F. & Seemuller, E. (1998). The proteasome: paradigm of a self-compartmentalizing protease. *Cell* **92**, 367-380.

Beasley, D. W. (2005). Recent advances in the molecular biology of west nile virus. *Curr Mol Med* **5**, 835-850.

Beatch, M. D. & Hobman, T. C. (2000). Rubella virus capsid associates with host cell protein p32 and localizes to mitochondria. *J Virol* **74**, 5569-5576.

Benarroch, D., Selisko, B., Locatelli, G. A., Maga, G., Romette, J. L. & Canard, B. (2004). The RNA helicase, nucleotide 5'-triphosphatase, and RNA 5'-triphosphatase activities of Dengue virus protein NS3 are Mg2+-dependent and require a functional Walker B motif in the helicase catalytic core. *Virology* **328**, 208-218.

Bhuvanakantham, R., Cheong, Y. K. & Ng, M. L. (2010). West Nile virus capsid protein interaction with importin and HDM2 protein is regulated by protein kinase C-mediated phosphorylation. *Microbes Infect* **12**, 615-625.

Bhuvanakantham, R., Chong, M. K. & Ng, M. L. (2009). Specific interaction of capsid protein and importin-alpha/beta influences West Nile virus production. *Biochem Biophys Res Commun* **389**, 63-69.

Bhuvanakantham, R. & Ng, M. L. (2005). Analysis of self-association of West Nile virus capsid protein and the crucial role played by Trp 69 in homodimerization. *Biochem Biophys Res Commun* **329**, 246-255.

Blackwell, J. & Brinton, M. (1995). BHK cell proteins that bind to the 3' stem-loop structure of the West Nile virus genome RNA. *J Virol* **69**, 5650-5658.

Blackwell, J. & Brinton, M. (1997). Translation elongation factor-1 alpha interacts with the 3' stem-loop region of West Nile virus genomic RNA. *J Virol* **71**, 6433-6444.

Boya, P., Pauleau, A. L., Poncet, D., Gonzalez-Polo, R. A., Zamzami, N. & Kroemer, G. (2004). Viral proteins targeting mitochondria: controlling cell death. *Biochim Biophys Acta* **1659**, 178-189.

Boyd, C., Hughes, T., Pypaert, M. & Novick, P. (2004). Vesicles carry most exocyst subunits to exocytic sites marked by the remaining two subunits, Sec3p and Exo70p. *J Cell Biol* **167**, 889-901.

Bressanelli, S., Stiasny, K., Allison, S. L., Stura, E. A., Duquerroy, S., Lescar, J., Heinz, F. X. & Rey, F. A. (2004). Structure of a flavivirus envelope glycoprotein in its low-pH-induced membrane fusion conformation. *EMBO J* **23**, 728-738.

Brinton, M. A. (2002). The molecular biology of West Nile Virus: a new invader of the western hemisphere. *Annu Rev Microbiol* **56**, 371-402.

Brinton, M. A., Fernandez, A. V. & Dispoto, J. H. (1986). The 3'-nucleotides of flavivirus genomic RNA form a conserved secondary structure. *Virology* **153**, 113-121.

Bulich, R. & Aaskov, J. G. (1992). Nuclear localization of dengue 2 virus core protein detected with monoclonal antibodies. *J Gen Virol* **73 (Pt 11)**, 2999-3003.

Calisher, C. H., Karabatsos, N., Dalrymple, J. M., Shope, R. E., Porterfield, J. S., Westaway, E. G. & Brandt, W. E. (1989). Antigenic relationships between flaviviruses as determined by cross-neutralization tests with polyclonal antisera. *J Gen Virol* **70 (Pt 1)**, 37-43.

Catteau, A., Courageot, M. P. & Despres, P. (2004). Flaviviruses and apoptosis regulation. *Prog Mol Subcell Biol* **36**, 171-189.

Catteau, A., Kalinina, O., Wagner, M. C., Deubel, V., Courageot, M. P. & Despres, P. (2003a). Dengue virus M protein contains a proapoptotic sequence referred to as ApoptoM. *J Gen Virol* **84**, 2781-2793.

Catteau, A., Roue, G., Yuste, V. J., Susin, S. A. & Despres, P. (2003b). Expression of dengue ApoptoM sequence results in disruption of mitochondrial potential and caspase activation. *Biochimie* **85**, 789-793.

Chambers, T. J., Hahn, C. S., Galler, R. & Rice, C. M. (1990a). Flavivirus genome organization, expression, and replication. *Annu Rev Microbiol* **44**, 649-688.

Chambers, T. J., McCourt, D. W. & Rice, C. M. (1990b). Production of yellow fever virus proteins in infected cells: identification of discrete polyprotein species and analysis of cleavage kinetics using region-specific polyclonal antisera. *Virology* **177**, 159-174.

Chambers, T. J., Nestorowicz, A., Amberg, S. M. & Rice, C. M. (1993). Mutagenesis of the yellow fever virus NS2B protein: effects on proteolytic processing, NS2B-NS3 complex formation, and viral replication. *J Virol* **67**, 6797-6807.

Chambers, T. J. & Rice, C. M. (1987). Molecular biology of the flaviviruses. *Microbiol Sci* **4**, 219-223.

Chang, C. J., Luh, H. W., Wang, S. H., Lin, H. J., Lee, S. C. & Hu, S. T. (2001). The heterogeneous nuclear ribonucleoprotein K (hnRNP K) interacts with dengue virus core protein. *DNA Cell Biol* **20**, 569-577.

Chang, H. H., Shyu, H. F., Wang, Y. M., Sun, D. S., Shyu, R. H., Tang, S. S. & Huang, Y. S. (2002). Facilitation of cell adhesion by immobilized dengue viral nonstructural protein 1 (NS1): arginine-glycine-aspartic acid structural mimicry within the dengue viral NS1 antigen. *J Infect Dis* **186**, 743-751.

Chang, Y. S., Liao, C. L., Tsao, C. H., Chen, M. C., Liu, C. I., Chen, L. K. & Lin, Y. L. (1999). Membrane permeabilization by small hydrophobic nonstructural proteins of Japanese encephalitis virus. *J Virol* **73**, 6257-6264.

Chen, C. J., Kuo, M. D., Chien, L. J., Hsu, S. L., Wang, Y. M. & Lin, J. H. (1997a). RNA-protein interactions: involvement of NS3, NS5, and 3' noncoding regions of Japanese encephalitis virus genomic RNA. *J Virol* **71**, 3466-3473.

Chen, H., Wurm, T., Britton, P., Brooks, G. & Hiscox, J. A. (2002). Interaction of the coronavirus nucleoprotein with nucleolar antigens and the host cell. *J Virol* **76**, 5233-5250.

Chen, Y., Maguire, T., Hileman, R. E., Fromm, J. R., Esko, J. D., Linhardt, R. J. & Marks, R. M. (1997b). Dengue virus infectivity depends on envelope protein binding to target cell heparan sulfate. *Nat Med* **3**, 866-871.

Cheong, Y. K. & Ng, M. L. (2010). Dephosphorylation of West Nile virus capsid protein enhances the processes of nucleocapsid assembly. *Microbes Infect*.

Chu, J. & Ng, M. (2004a). Infectious entry of West Nile virus occurs through a clathrin-mediated endocytic pathway. *J Virol* **78**, 10543-10555.

Chu, J. J. & Ng, M. L. (2002). Trafficking mechanism of West Nile (Sarafend) virus structural proteins. *J Med Virol* **67**, 127-136.

Chu, J. J. & Ng, M. L. (2003). The mechanism of cell death during West Nile virus infection is dependent on initial infectious dose. *J Gen Virol* **84**, 3305-3314.

Chu, J. J. & Ng, M. L. (2004b). Infectious entry of West Nile virus occurs through a clathrin-mediated endocytic pathway. *J Virol* **78**, 10543-10555.

Chu, J. J. & Ng, M. L. (2004c). Interaction of West Nile virus with alpha v beta 3 integrin mediates virus entry into cells. *J Biol Chem* **279**, 54533-54541.

Chu, P. W. & Westaway, E. G. (1985). Replication strategy of Kunjin virus: evidence for recycling role of replicative form RNA as template in semiconservative and asymmetric replication. *Virology* **140**, 68-79.

Chung, K. M., Liszewski, M. K., Nybakken, G., Davis, A. E., Townsend, R. R., Fremont, D. H., Atkinson, J. P. & Diamond, M. S. (2006). West Nile virus nonstructural protein NS1 inhibits complement activation by binding the regulatory protein factor H. *Proc Natl Acad Sci U S A* **103**, 19111-19116.

Cleaves, G. R., Ryan, T. E. & Schlesinger, R. W. (1981). Identification and characterization of type 2 dengue virus replicative intermediate and replicative form RNAs. *Virology* **111**, 73-83.

Courageot, M. P., Catteau, A. & Despres, P. (2003). Mechanisms of dengue virus-induced cell death. *Adv Virus Res* **60**, 157-186.

Coux, O., Tanaka, K. & Goldberg, A. L. (1996). Structure and functions of the 20S and 26S proteasomes. *Annu Rev Biochem* **65**, 801-847.

Davis, W., Blackwell, J., Shi, P. & Brinton, M. (2007a). Interaction between the cellular protein eEF1A and the 3'-terminal stem-loop of West Nile virus genomic RNA facilitates viral minus-strand RNA synthesis. *J Virol* **81**, 10172-10187.

Davis, W. G., Blackwell, J. L., Shi, P. Y. & Brinton, M. A. (2007b). Interaction between the cellular protein eEF1A and the 3'-terminal stem-loop of West Nile virus genomic RNA facilitates viral minus-strand RNA synthesis. *J Virol* **81**, 10172-10187.

De Madrid, A. T. & Porterfield, J. S. (1974). The flaviviruses (group B arboviruses): a cross-neutralization study. *J Gen Virol* **23**, 91-96.

De Nova-Ocampo, M., Villegas-Sepulveda, N. & del Angel, R. M. (2002). Translation elongation factor-1alpha, La, and PTB interact with the 3' untranslated region of dengue 4 virus RNA. *Virology* **295**, 337-347.

DeSalvo, D., Roy-Chaudhury, P., Peddi, R., Merchen, T., Konijetti, K., Gupta, M., Boardman, R., Rogers, C., Buell, J., Hanaway, M., Broderick, J., Smith, R. & Woodle, E. S. (2004). West Nile virus encephalitis in organ transplant recipients: another high-risk group for meningoencephalitis and death. *Transplantation* **77**, 466-469.

Despres, P., Flamand, M., Ceccaldi, P. E. & Deubel, V. (1996). Human isolates of dengue type 1 virus induce apoptosis in mouse neuroblastoma cells. *J Virol* **70**, 4090-4096.

Diniz, J. A., Da Rosa, A. P., Guzman, H., Xu, F., Xiao, S. Y., Popov, V. L., Vasconcelos, P. F. & Tesh, R. B. (2006). West Nile virus infection of primary mouse neuronal and neuroglial cells: the role of astrocytes in chronic infection. *Am J Trop Med Hyg* **75**, 691-696.

Dokland, T., Walsh, M., Mackenzie, J. M., Khromykh, A. A., Ee, K. H. & Wang, S. (2004). West Nile virus core protein; tetramer structure and ribbon formation. *Structure* **12**, 1157-1163.

Duan, X., Lu, X., Li, J. & Liu, Y. (2008). Novel binding between pre-membrane protein and vacuolar ATPase is required for efficient dengue virus secretion. *Biochem Biophys Res Commun* **373**, 319-324.

Dutta, K., Ghosh, D. & Basu, A. (2009). Curcumin protects neuronal cells from Japanese encephalitis virus-mediated cell death and also inhibits infective viral particle formation by dysregulation of ubiquitin-proteasome system. *J Neuroimmune Pharmacol* **4**, 328-337.

Edgar, C. E., Lindquist, L. D., McKean, D. L., Strasser, A. & Bram, R. J. (2010). CAML regulates Bim-dependent thymocyte death. *Cell Death Differ*.

Elliott, J., Lynch, O. T., Suessmuth, Y., Qian, P., Boyd, C. R., Burrows, J. F., Buick, R., Stevenson, N. J., Touzelet, O., Gadina, M., Power, U. F. & Johnston, J. A. (2007). Respiratory syncytial virus NS1 protein degrades STAT2 by using the Elongin-Cullin E3 ligase. *J Virol* **81**, 3428-3436.

Espina, L. M., Valero, N. J., Hernandez, J. M. & Mosquera, J. A. (2003). Increased apoptosis and expression of tumor necrosis factor-alpha caused by infection of cultured human monocytes with dengue virus. *Am J Trop Med Hyg* **68**, 48-53.

Everly, M. J., Terasaki, P. I., Hopfield, J., Trivedi, H. L. & Kaneku, H. (2010). Protective Immunity Remains Intact After Antibody Removal by Means of Proteasome Inhibition. *Transplantation*.

Falconar, A. K. (1997). The dengue virus nonstructural-1 protein (NS1) generates antibodies to common epitopes on human blood clotting, integrin/adhesin proteins and binds to human endothelial cells: potential implications in haemorrhagic fever pathogenesis. *Arch Virol* **142**, 897-916.

Falgout, B., Pethel, M., Zhang, Y. M. & Lai, C. J. (1991). Both nonstructural proteins NS2B and NS3 are required for the proteolytic processing of dengue virus nonstructural proteins. *J Virol* **65**, 2467-2475.

Feng, P., Park, J., Lee, B. S., Lee, S. H., Bram, R. J. & Jung, J. U. (2002). Kaposi's sarcoma-associated herpesvirus mitochondrial K7 protein targets a cellular calcium-modulating cyclophilin ligand to modulate intracellular calcium concentration and inhibit apoptosis. *J Virol* **76**, 11491-11504.

Finger, F., Hughes, T. & Novick, P. (1998a). Sec3p is a spatial landmark for polarized secretion in budding yeast. *Cell* **92**, 559-571.

Finger, F. & Novick, P. (1997). Sec3p is involved in secretion and morphogenesis in Saccharomyces cerevisiae. *Mol Biol Cell* **8**, 647-662.

Finger, F. P., Hughes, T. E. & Novick, P. (1998b). Sec3p is a spatial landmark for polarized secretion in budding yeast. *Cell* **92**, 559-571.

Finger, F. P. & Novick, P. (1998). Spatial regulation of exocytosis: lessons from yeast. *J Cell Biol* **142**, 609-612.

Fink, J., Gu, F., Ling, L., Tolfvenstam, T., Olfat, F., Chin, K. C., Aw, P., George, J., Kuznetsov, V. A., Schreiber, M., Vasudevan, S. G. & Hibberd, M. L. (2007). Host gene expression profiling of dengue virus infection in cell lines and patients. *PLoS Negl Trop Dis* **1**, e86.

Flechner, S. M., Fatica, R., Askar, M., Stephany, B. R., Poggio, E., Koo, A., Banning, S., Chiesa-Vottero, A. & Srinivas, T. (2010). The Role of Proteasome Inhibition With Bortezomib in the Treatment of Antibody-Mediated Rejection After Kidney-Only or Kidney-Combined Organ Transplantation. *Transplantation*.

Forgues, M., Marrogi, A. J., Spillare, E. A., Wu, C. G., Yang, Q., Yoshida, M. & Wang, X. W. (2001). Interaction of the hepatitis B virus X protein with the Crm1-dependent nuclear export pathway. *J Biol Chem* **276**, 22797-22803.

Fourati, S., Malet, I., Binka, M., Boukobza, S., Wirden, M., Sayon, S., Simon, A., Katlama, C., Simon, V., Calvez, V. & Marcelin, A. G. (2010). Partially active HIV-1 Vif alleles facilitate viral escape from specific antiretrovirals. *AIDS* **24**, 2313-2321.

Fredericksen, B., Smith, M., Katze, M., Shi, P. & Gale, M. J. (2004). The host response to West Nile Virus infection limits viral spread through the activation of the interferon regulatory factor 3 pathway. *J Virol* **78**, 7737-7747.

Gao, F., Duan, X., Lu, X., Liu, Y., Zheng, L., Ding, Z. & Li, J. (2010). Novel binding between pre-membrane protein and claudin-1 is required for efficient dengue virus entry. *Biochem Biophys Res Commun* **391**, 952-957.

Gaunt, M. W., Sall, A. A., de Lamballerie, X., Falconar, A. K., Dzhivanian, T. I. & Gould, E. A. (2001). Phylogenetic relationships of flaviviruses correlate with their epidemiology, disease association and biogeography. *J Gen Virol* **82**, 1867-1876.

Gavin, A., Aloy, P., Grandi, P., Krause, R., Boesche, M., Marzioch, M., Rau, C., Jensen, L., Bastuck, S., Dümpelfeld, B., Edelmann, A., Heurtier, M., Hoffman, V., Hoefert, C., Klein, K., Hudak, M., Michon, A.,

Schelder, M., Schirle, M., Remor, M., Rudi, T., Hooper, S., Bauer, A., Bouwmeester, T., Casari, G., Drewes, G., Neubauer, G., Rick, J., Kuster, B., Bork, P., Russell, R. & Superti-Furga, G. (2006). Proteome survey reveals modularity of the yeast cell machinery. *Nature* **440**, 631-636.

Gerbi, S. A., Borovjagin, A. V. & Lange, T. S. (2003). The nucleolus: a site of ribonucleoprotein maturation. *Curr Opin Cell Biol* **15**, 318-325.

Gil, L., Lopez, C., Lazo, L., Valdes, I., Marcos, E., Alonso, R., Gambe, A., Martin, J., Romero, Y., Guzman, M. G., Guillen, G. & Hermida, L. (2009). Recombinant nucleocapsid-like particles from dengue-2 virus induce protective CD4+ and CD8+ cells against viral encephalitis in mice. *Int Immunol* **21**, 1175-1183.

Gilfoy, F., Fayzulin, R. & Mason, P. W. (2009). West Nile virus genome amplification requires the functional activities of the proteasome. *Virology* **385**, 74-84.

Glickman, M. H. (2000). Getting in and out of the proteasome. *Semin Cell Dev Biol* **11**, 149-158.

Glickman, M. H. & Ciechanover, A. (2002). The ubiquitin-proteasome proteolytic pathway: destruction for the sake of construction. *Physiol Rev* **82**, 373-428.

Glickman, M. H. & Maytal, V. (2002). Regulating the 26S proteasome. *Curr Top Microbiol Immunol* **268**, 43-72.

Goldberg, A. L. (2000). Probing the proteasome pathway. *Nat Biotechnol* **18**, 494-496.

Goldfarb, D. S., Corbett, A. H., Mason, D. A., Harreman, M. T. & Adam, S. A. (2004). Importin alpha: a multipurpose nuclear-transport receptor. *Trends Cell Biol* **14**, 505-514.

Gorlich, D., Henklein, P., Laskey, R. A. & Hartmann, E. (1996). A 41 amino acid motif in importin-alpha confers binding to importin-beta and hence transit into the nucleus. *EMBO J* **15**, 1810-1817.

Gould, E. A. & Solomon, T. (2008). Pathogenic flaviviruses. *Lancet* **371**, 500-509.

Graff, J. W., Ettayebi, K. & Hardy, M. E. (2009). Rotavirus NSP1 inhibits NFkappaB activation by inducing proteasome-dependent degradation of beta-TrCP: a novel mechanism of IFN antagonism. *PLoS Pathog* **5**, e1000280.

Groll, M., Ditzel, L., Lowe, J., Stock, D., Bochtler, M., Bartunik, H. D. & Huber, R. (1997). Structure of 20S proteasome from yeast at 2.4 A resolution. *Nature* **386**, 463-471.

Gubler, D. J. (1998). Dengue and dengue hemorrhagic fever. *Clin Microbiol Rev* **11**, 480-496.

Gubler, D. J., Kuno, G. & Markoff, L. (2007). Flaviviruses. In *Field Virology* fifth edn. Edited by H. P. Knipe DM: Lippincott, Williams and Wilkins, Philadelphia

Guirakhoo, F., Bolin, R. A. & Roehrig, J. T. (1992). The Murray Valley encephalitis virus prM protein confers acid resistance to virus particles and

alters the expression of epitopes within the R2 domain of E glycoprotein. *Virology* **191**, 921-931.

Guo, W., Tamanoi, F. & Novick, P. (2001). Spatial regulation of the exocyst complex by Rho1 GTPase. *Nat Cell Biol* **3**, 353-360.

Halstead, S. B. (2007). Dengue. *Lancet* **370**, 1644-1652.

Hamilton, P. K. & Taylor, R. M. (1954). Report of clinical case of West Nile virus infection probably acquired in the laboratory. *Am J Trop Med Hyg* **3**, 51-53.

Hassink, G. C., Barel, M. T., Van Voorden, S. B., Kikkert, M. & Wiertz, E. J. (2006). Ubiquitination of MHC class I heavy chains is essential for dislocation by human cytomegalovirus-encoded US2 but not US11. *J Biol Chem* **281**, 30063-30071.

Haupt, Y., Maya, R., Kazaz, A. & Oren, M. (1997). Mdm2 promotes the rapid degradation of p53. *Nature* **387**, 296-299.

Hayes, E. B. & Gubler, D. J. (2006). West Nile virus: epidemiology and clinical features of an emerging epidemic in the United States. *Annu Rev Med* **57**, 181-194.

Heinemeyer, W., Fischer, M., Krimmer, T., Stachon, U. & Wolf, D. H. (1997). The active sites of the eukaryotic 20 S proteasome and their involvement in subunit precursor processing. *J Biol Chem* **272**, 25200-25209.

Heinz, F. X. & Allison, S. L. (2000). Structures and mechanisms in flavivirus fusion. *Adv Virus Res* **55**, 231-269.

Heinz, F. X. & Allison, S. L. (2003). Flavivirus structure and membrane fusion. *Adv Virus Res* **59**, 63-97.

Heinz, F. X., Stiasny, K., Puschner-Auer, G., Holzmann, H., Allison, S. L., Mandl, C. W. & Kunz, C. (1994). Structural changes and functional control of the tick-borne encephalitis virus glycoprotein E by the heterodimeric association with protein prM. *Virology* **198**, 109-117.

Helt, A. M. & Harris, E. (2005). S-phase-dependent enhancement of dengue virus 2 replication in mosquito cells, but not in human cells. *J Virol* **79**, 13218-13230.

Hernandez-Verdun, D. & Roussel, P. (2003). Regulators of nucleolar functions. *Prog Cell Cycle Res* **5**, 301-308.

Hernandez-Verdun, D., Roussel, P. & Gebrane-Younes, J. (2002). Emerging concepts of nucleolar assembly. *J Cell Sci* **115**, 2265-2270.

Hiscox, J. A., Wurm, T., Wilson, L., Britton, P., Cavanagh, D. & Brooks, G. (2001). The coronavirus infectious bronchitis virus nucleoprotein localizes to the nucleolus. *J Virol* **75**, 506-512.

Hishikawa, N., Niwa, J., Doyu, M., Ito, T., Ishigaki, S., Hashizume, Y. & Sobue, G. (2003). Dorfin localizes to the ubiquitylated inclusions in Parkinson's disease, dementia with Lewy bodies, multiple system atrophy, and amyotrophic lateral sclerosis. *Am J Pathol* **163**, 609-619.

Holbrook, M. R., Wang, H. & Barrett, A. D. (2001). Langat virus M protein is structurally homologous to prM. *J Virol* **75**, 3999-4001.

Hosui, A., Ohkawa, K., Ishida, H., Sato, A., Nakanishi, F., Ueda, K., Takehara, T., Kasahara, A., Sasaki, Y., Hori, M. & Hayashi, N. (2003). Hepatitis C virus core protein differently regulates the JAK-STAT signaling pathway under interleukin-6 and interferon-gamma stimuli. *J Biol Chem* **278**, 28562-28571.

Hsu, S., Hazuka, C., Foletti, D. & Scheller, R. (1999). Targeting vesicles to specific sites on the plasma membrane: the role of the sec6/8 complex. *Trends Cell Biol* **9**, 150-153.

Hsu, S. C., TerBush, D., Abraham, M. & Guo, W. (2004). The exocyst complex in polarized exocytosis. *Int Rev Cytol* **233**, 243-265.

Huebscher, K. J., Lee, J., Rovelli, G., Ludin, B., Matus, A., Stauffer, D. & Furst, P. (1999). Protein isoaspartyl methyltransferase protects from Bax-induced apoptosis. *Gene* **240**, 333-341.

Hunt, T. A., Urbanowski, M. D., Kakani, K., Law, L. M., Brinton, M. A. & Hobman, T. C. (2007). Interactions between the West Nile virus capsid protein and the host cell-encoded phosphatase inhibitor, I2PP2A. *Cell Microbiol* **9**, 2756-2766.

Iinuma, M., Nagai, Y., Maeno, K., Yoshida, T. & Matsumoto, T. (1971). Studies on the assembly of Newcastle disease virus: incorporation of structural proteins into virus particles. *J Gen Virol* **12**, 239-247.

Imai, J., Maruya, M., Yashiroda, H., Yahara, I. & Tanaka, K. (2003). The molecular chaperone Hsp90 plays a role in the assembly and maintenance of the 26S proteasome. *EMBO J* **22**, 3557-3567.

Iwatani, Y., Chan, D. S., Liu, L., Yoshii, H., Shibata, J., Yamamoto, N., Levin, J. G., Gronenborn, A. M. & Sugiura, W. (2009). HIV-1 Vif-mediated ubiquitination/degradation of APOBEC3G involves four critical lysine residues in its C-terminal domain. *Proc Natl Acad Sci U S A* **106**, 19539-19544.

Jain, N., Fisk, D., Sotir, M. & Kehl, K. S. (2007). West Nile encephalitis, status epilepticus and West Nile pneumonia in a renal transplant patient. *Transpl Int* **20**, 800-803.

Jakob, U., Lilie, H., Meyer, I. & Buchner, J. (1995). Transient interaction of Hsp90 with early unfolding intermediates of citrate synthase. Implications for heat shock in vivo. *J Biol Chem* **270**, 7288-7294.

Jamieson, D. J., Ellis, J. E., Jernigan, D. B. & Treadwell, T. A. (2006). Emerging infectious disease outbreaks: old lessons and new challenges for obstetrician-gynecologists. *Am J Obstet Gynecol* **194**, 1546-1555.

Jan, J. T., Chen, B. H., Ma, S. H., Liu, C. I., Tsai, H. P., Wu, H. C., Jiang, S. Y., Yang, K. D. & Shaio, M. F. (2000). Potential dengue virus-triggered apoptotic pathway in human neuroblastoma cells: arachidonic acid, superoxide anion, and NF-kappaB are sequentially involved. *J Virol* **74**, 8680-8691.

Jones, C. T., Ma, L., Burgner, J. W., Groesch, T. D., Post, C. B. & Kuhn, R. J. (2003). Flavivirus capsid is a dimeric alpha-helical protein. *J Virol* **77**, 7143-7149.

Jung, J. K., Kwun, H. J., Lee, J. O., Arora, P. & Jang, K. L. (2007). Hepatitis B virus X protein differentially affects the ubiquitin-mediated proteasomal degradation of beta-catenin depending on the status of cellular p53. *J Gen Virol* **88**, 2144-2154.

Kalantari, P., Harandi, O. F., Hankey, P. A. & Henderson, A. J. (2008). HIV-1 Tat mediates degradation of RON receptor tyrosine kinase, a regulator of inflammation. *J Immunol* **181**, 1548-1555.

Kanlaya, R., Pattanakitsakul, S. N., Sinchaikul, S., Chen, S. T. & Thongboonkerd, V. (2010). The ubiquitin-proteasome pathway is important for dengue virus infection in primary human endothelial cells. *J Proteome Res* **9**, 4960-4971.

Kennedy, B., Gargoum, F., Bystricky, B., Curran, D. R. & O'Connor, T. M. (2010). Novel Agents in the Management of Lung Cancer. *Curr Med Chem*.

Khromykh, A. A., Kenney, M. T. & Westaway, E. G. (1998). trans-Complementation of flavivirus RNA polymerase gene NS5 by using Kunjin virus replicon-expressing BHK cells. *J Virol* **72**, 7270-7279.

Khromykh, A. A., Sedlak, P. L. & Westaway, E. G. (1999). trans-Complementation analysis of the flavivirus Kunjin ns5 gene reveals an essential role for translation of its N-terminal half in RNA replication. *J Virol* **73**, 9247-9255.

Khromykh, A. A., Varnavski, A. N., Sedlak, P. L. & Westaway, E. G. (2001). Coupling between replication and packaging of flavivirus RNA: evidence derived from the use of DNA-based full-length cDNA clones of Kunjin virus. *J Virol* **75**, 4633-4640.

Khromykh, A. A. & Westaway, E. G. (1996). RNA binding properties of core protein of the flavivirus Kunjin. *Arch Virol* **141**, 685-699.

Kido, T. & Lau, Y. F. (2008). The human Y-encoded testis-specific protein interacts functionally with eukaryotic translation elongation factor eEF1A, a putative oncoprotein. *Int J Cancer* **123**, 1573-1585.

Kiermayr, S., Kofler, R. M., Mandl, C. W., Messner, P. & Heinz, F. X. (2004). Isolation of capsid protein dimers from the tick-borne encephalitis flavivirus and in vitro assembly of capsid-like particles. *J Virol* **78**, 8078-8084.

Kikkert, M., Hassink, G., Barel, M., Hirsch, C., van der Wal, F. J. & Wiertz, E. (2001). Ubiquitination is essential for human cytomegalovirus US11-mediated dislocation of MHC class I molecules from the endoplasmic reticulum to the cytosol. *Biochem J* **358**, 369-377.

Kittlesen, D. J., Chianese-Bullock, K. A., Yao, Z. Q., Braciale, T. J. & Hahn, Y. S. (2000). Interaction between complement receptor gC1qR and hepatitis C virus core protein inhibits T-lymphocyte proliferation. *J Clin Invest* **106**, 1239-1249.

Ko, A., Lee, E. W., Yeh, J. Y., Yang, M. R., Oh, W., Moon, J. S. & Song, J. MKRN1 induces degradation of West Nile virus capsid protein by functioning as an E3 ligase. *J Virol* **84**, 426-436.

Ko, A., Lee, E. W., Yeh, J. Y., Yang, M. R., Oh, W., Moon, J. S. & Song, J. (2010). MKRN1 induces degradation of West Nile virus capsid protein by functioning as an E3 ligase. *J Virol* **84**, 426-436.

Kobayashi, Y. & Yonehara, S. (2009). Novel cell death by downregulation of eEF1A1 expression in tetraploids. *Cell Death Differ* **16**, 139-150.

Kofler, R. M., Aberle, J. H., Aberle, S. W., Allison, S. L., Heinz, F. X. & Mandl, C. W. (2004a). Mimicking live flavivirus immunization with a noninfectious RNA vaccine. *Proc Natl Acad Sci U S A* **101**, 1951-1956.

Kofler, R. M., Heinz, F. X. & Mandl, C. W. (2002). Capsid protein C of tick-borne encephalitis virus tolerates large internal deletions and is a favorable target for attenuation of virulence. *J Virol* **76**, 3534-3543.

Kofler, R. M., Heinz, F. X. & Mandl, C. W. (2004b). A novel principle of attenuation for the development of new generation live flavivirus vaccines. *Arch Virol Suppl*, 191-200.

Kofler, R. M., Leitner, A., O'Riordain, G., Heinz, F. X. & Mandl, C. W. (2003). Spontaneous mutations restore the viability of tick-borne encephalitis virus mutants with large deletions in protein C. *J Virol* **77**, 443-451.

Konishi, E. & Mason, P. W. (1993). Proper maturation of the Japanese encephalitis virus envelope glycoprotein requires cosynthesis with the premembrane protein. *J Virol* **67**, 1672-1675.

Koschinski, A., Wengler, G. & Repp, H. (2003). The membrane proteins of flaviviruses form ion-permeable pores in the target membrane after fusion: identification of the pores and analysis of their possible role in virus infection. *J Gen Virol* **84**, 1711-1721.

Kou, Y. H., Chou, S. M., Wang, Y. M., Chang, Y. T., Huang, S. Y., Jung, M. Y., Huang, Y. H., Chen, M. R., Chang, M. F. & Chang, S. C. (2006). Hepatitis C virus NS4A inhibits cap-dependent and the viral IRES-mediated translation through interacting with eukaryotic elongation factor 1A. *J Biomed Sci* **13**, 861-874.

Krishnan, M. N., Ng, A., Sukumaran, B., Gilfoy, F. D., Uchil, P. D., Sultana, H., Brass, A. L., Adametz, R., Tsui, M., Qian, F., Montgomery, R. R., Lev, S., Mason, P. W., Koski, R. A., Elledge, S. J., Xavier, R. J., Agaisse, H. & Fikrig, E. (2008). RNA interference screen for human genes associated with West Nile virus infection. *Nature* **455**, 242-245.

Krishnan, M. N., Sukumaran, B., Pal, U., Agaisse, H., Murray, J. L., Hodge, T. W. & Fikrig, E. (2007). Rab 5 is required for the cellular entry of dengue and West Nile viruses. *J Virol* **81**, 4881-4885.

Kuhn, R. J., Zhang, W., Rossmann, M. G., Pletnev, S. V., Corver, J., Lenches, E., Jones, C. T., Mukhopadhyay, S., Chipman, P. R., Strauss, E. G., Baker, T. S. & Strauss, J. H. (2002). Structure of dengue virus: implications for flavivirus organization, maturation, and fusion. *Cell* **108**, 717-725.

Kumar, D., Drebot, M. A., Wong, S. J., Lim, G., Artsob, H., Buck, P. & Humar, A. (2004). A seroprevalence study of west nile virus infection in solid organ transplant recipients. *Am J Transplant* **4**, 1883-1888.

Kunkel, M., Lorinczi, M., Rijnbrand, R., Lemon, S. M. & Watowich, S. J. (2001). Self-assembly of nucleocapsid-like particles from recombinant hepatitis C virus core protein. *J Virol* **75**, 2119-2129.

Kuno, G., Chang, G. J., Tsuchiya, K. R., Karabatsos, N. & Cropp, C. B. (1998). Phylogeny of the genus Flavivirus. *J Virol* **72**, 73-83.

Laemmli, U. K. (1970). Cleavage of structural proteins during the assembly of the head of bacteriophage T4. *Nature* **227**, 680-685.

Lagunas-Martinez, A., Madrid-Marina, V. & Gariglio, P. (2010). Modulation of apoptosis by early human papillomavirus proteins in cervical cancer. *Biochim Biophys Acta* **1805**, 6-16.

Lazo, L., Hermida, L., Zulueta, A., Sanchez, J., Lopez, C., Silva, R., Guillen, G. & Guzman, M. G. (2007). A recombinant capsid protein from Dengue-2 induces protection in mice against homologous virus. *Vaccine* **25**, 1064-1070.

Leclercq, T. M., Moretti, P. A., Vadas, M. A. & Pitson, S. M. (2008). Eukaryotic elongation factor 1A interacts with sphingosine kinase and directly enhances its catalytic activity. *J Biol Chem* **283**, 9606-9614.

Lee, E. & Lobigs, M. (2000). Substitutions at the putative receptor-binding site of an encephalitic flavivirus alter virulence and host cell tropism and reveal a role for glycosaminoglycans in entry. *J Virol* **74**, 8867-8875.

Lee, E. W., Oh, W. & Song, J. (2006). Jab1 as a mediator of nuclear export and cytoplasmic degradation of p53. *Mol Cells* **22**, 133-140.

Leong, A. S., Wong, K. T., Leong, T. Y., Tan, P. H. & Wannakrairot, P. (2007). The pathology of dengue hemorrhagic fever. *Semin Diagn Pathol* **24**, 227-236.

Leung, A. K., Andersen, J. S., Mann, M. & Lamond, A. I. (2003). Bioinformatic analysis of the nucleolus. *Biochem J* **376**, 553-569.

Li, F. Q., Tam, J. P. & Liu, D. X. (2007). Cell cycle arrest and apoptosis induced by the coronavirus infectious bronchitis virus in the absence of p53. *Virology* **365**, 435-445.

Li, H., Clum, S., You, S., Ebner, K. E. & Padmanabhan, R. (1999). The serine protease and RNA-stimulated nucleoside triphosphatase and RNA helicase functional domains of dengue virus type 2 NS3 converge within a region of 20 amino acids. *J Virol* **73**, 3108-3116.

Li, J., Bhuvanakantham, R., Howe, J. & Ng, M. L. (2005). Identifying the region influencing the cis-mode of maturation of West Nile (Sarafend) virus using chimeric infectious clones. *Biochem Biophys Res Commun* **334**, 714-720.

Li, J., Bhuvanakantham, R., Howe, J. & Ng, M. L. (2006). The glycosylation site in the envelope protein of West Nile virus (Sarafend) plays an important role in replication and maturation processes. *J Gen Virol* **87**, 613-622.

Li, L., Lok, S. M., Yu, I. M., Zhang, Y., Kuhn, R. J., Chen, J. & Rossmann, M. G. (2008). The flavivirus precursor membrane-envelope protein complex: structure and maturation. *Science* **319**, 1830-1834.

Li, Z., Pogany, J., Panavas, T., Xu, K., Esposito, A. M., Kinzy, T. G. & Nagy, P. D. (2009). Translation elongation factor 1A is a component of the tombusvirus replicase complex and affects the stability of the p33 replication co-factor. *Virology*.

Liao, C. L., Lin, Y. L., Wang, J. J., Huang, Y. L., Yeh, C. T., Ma, S. H. & Chen, L. K. (1997). Effect of enforced expression of human bcl-2 on Japanese encephalitis virus-induced apoptosis in cultured cells. *J Virol* **71**, 5963-5971.

Liao, H., Xu, J. & Huang, J. (2010). FasL/Fas pathway is involved in dengue virus induced apoptosis of the vascular endothelial cells. *J Med Virol* **82**, 1392-1399.

Lim, J., Glass, W., McDermott, D. & Murphy, P. (2006). CCR5: no longer a "good for nothing" gene--chemokine control of West Nile virus infection. *Trends Immunol* **27**, 308-312.

Limjindaporn, T., Netsawang, J., Noisakran, S., Thiemmeca, S., Wongwiwat, W., Sudsaward, S., Avirutnan, P., Puttikhunt, C., Kasinrerk, W., Sriburi, R., Sittisombut, N., Yenchitsomanus, P. T. & Malasit, P. (2007). Sensitization to Fas-mediated apoptosis by dengue virus capsid protein. *Biochem Biophys Res Commun* **362**, 334-339.

Lin, C. F., Chiu, S. C., Hsiao, Y. L., Wan, S. W., Lei, H. Y., Shiau, A. L., Liu, H. S., Yeh, T. M., Chen, S. H., Liu, C. C. & Lin, Y. S. (2005a). Expression of cytokine, chemokine, and adhesion molecules during endothelial cell activation induced by antibodies against dengue virus nonstructural protein 1. *J Immunol* **174**, 395-403.

Lin, C. F., Lei, H. Y., Shiau, A. L., Liu, C. C., Liu, H. S., Yeh, T. M., Chen, S. H. & Lin, Y. S. (2003). Antibodies from dengue patient sera cross-react with endothelial cells and induce damage. *J Med Virol* **69**, 82-90.

Lin, C. F., Lei, H. Y., Shiau, A. L., Liu, H. S., Yeh, T. M., Chen, S. H., Liu, C. C., Chiu, S. C. & Lin, Y. S. (2002). Endothelial cell apoptosis induced by antibodies against dengue virus nonstructural protein 1 via production of nitric oxide. *J Immunol* **169**, 657-664.

Lin, W., Choe, W. H., Hiasa, Y., Kamegaya, Y., Blackard, J. T., Schmidt, E. V. & Chung, R. T. (2005b). Hepatitis C virus expression suppresses interferon signaling by degrading STAT1. *Gastroenterology* **128**, 1034-1041.

Lindenbach, B. D. & Rice, C. M. (1999). Genetic interaction of flavivirus nonstructural proteins NS1 and NS4A as a determinant of replicase function. *J Virol* **73**, 4611-4621.

Lindenbach, B. D. & Rice, C. M. (2003). Molecular biology of flaviviruses. *Adv Virus Res* **59**, 23-61.

Lipschutz, J. & Mostov, K. (2002). Exocytosis: the many masters of the exocyst. *Curr Biol* **12**, R212-214.

Liu, H., Chiou, S. S. & Chen, W. J. (2004a). Differential binding efficiency between the envelope protein of Japanese encephalitis virus variants and heparan sulfate on the cell surface. *J Med Virol* **72**, 618-624.

Liu, J., Kam, K. W., Borchert, G. H., Kravtsov, G. M., Ballard, H. J. & Wong, T. M. (2006a). Further study on the role of HSP70 on Ca2+ homeostasis in rat ventricular myocytes subjected to simulated ischemia. *Am J Physiol Cell Physiol* **290**, C583-591.

Liu, W. J., Chen, H. B. & Khromykh, A. A. (2003). Molecular and functional analyses of Kunjin virus infectious cDNA clones demonstrate the essential roles for NS2A in virus assembly and for a nonconservative residue in NS3 in RNA replication. *J Virol* **77**, 7804-7813.

Liu, W. J., Chen, H. B., Wang, X. J., Huang, H. & Khromykh, A. A. (2004b). Analysis of adaptive mutations in Kunjin virus replicon RNA reveals a novel role for the flavivirus nonstructural protein NS2A in inhibition of beta interferon promoter-driven transcription. *J Virol* **78**, 12225-12235.

Liu, W. J., Wang, X. J., Clark, D. C., Lobigs, M., Hall, R. A. & Khromykh, A. A. (2006b). A single amino acid substitution in the West Nile virus nonstructural protein NS2A disables its ability to inhibit alpha/beta interferon induction and attenuates virus virulence in mice. *J Virol* **80**, 2396-2404.

Lobigs, M. & Lee, E. (2004). Inefficient signalase cleavage promotes efficient nucleocapsid incorporation into budding flavivirus membranes. *J Virol* **78**, 178-186.

Lorenz, I. C., Allison, S. L., Heinz, F. X. & Helenius, A. (2002). Folding and dimerization of tick-borne encephalitis virus envelope proteins prM and E in the endoplasmic reticulum. *J Virol* **76**, 5480-5491.

Lorenz, I. C., Kartenbeck, J., Mezzacasa, A., Allison, S. L., Heinz, F. X. & Helenius, A. (2003). Intracellular assembly and secretion of recombinant subviral particles from tick-borne encephalitis virus. *J Virol* **77**, 4370-4382.

Loureiro, J. & Ploegh, H. L. (2006). Antigen presentation and the ubiquitin-proteasome system in host-pathogen interactions. *Adv Immunol* **92**, 225-305.

Lowe, J., Stock, D., Jap, B., Zwickl, P., Baumeister, W. & Huber, R. (1995). Crystal structure of the 20S proteasome from the archaeon T. acidophilum at 3.4 A resolution. *Science* **268**, 533-539.

Luo, C., Luo, H., Zheng, S., Gui, C., Yue, L., Yu, C., Sun, T., He, P., Chen, J., Shen, J., Luo, X., Li, Y., Liu, H., Bai, D., Yang, Y., Li, F., Zuo, J., Hilgenfeld, R., Pei, G., Chen, K., Shen, X. & Jiang, H. (2004a). Nucleocapsid protein of SARS coronavirus tightly binds to human cyclophilin A. *Biochem Biophys Res Commun* **321**, 557-565.

Luo, H., Ye, F., Sun, T., Yue, L., Peng, S., Chen, J., Li, G., Du, Y., Xie, Y., Yang, Y., Shen, J., Wang, Y., Shen, X. & Jiang, H. (2004b). In vitro biochemical and thermodynamic characterization of nucleocapsid protein of SARS. *Biophys Chem* **112**, 15-25.

Ma, L., Jones, C. T., Groesch, T. D., Kuhn, R. J. & Post, C. B. (2004). Solution structure of dengue virus capsid protein reveals another fold. *Proc Natl Acad Sci U S A* **101**, 3414-3419.

Macedo de Oliveira, A., Beecham, B. D., Montgomery, S. P., Lanciotti, R. S., Linnen, J. M., Giachetti, C., Pietrelli, L. A., Stramer, S. L. & Safranek, T. J. (2004). West Nile virus blood transfusion-related infection despite nucleic acid testing. *Transfusion* **44**, 1695-1699.

Machado, C. M., Martins, T. C., Colturato, I., Leite, M. S., Simione, A. J., Souza, M. P., Mauad, M. A. & Colturato, V. R. (2009). Epidemiology of neglected tropical diseases in transplant recipients. Review of the literature and experience of a Brazilian HSCT center. *Rev Inst Med Trop Sao Paulo* **51**, 309-324.

Machida, K., Tsukamoto, H., Liu, J. C., Han, Y. P., Govindarajan, S., Lai, M. M., Akira, S. & Ou, J. H. (2010). c-Jun mediates hepatitis C virus hepatocarcinogenesis through signal transducer and activator of transcription 3 and nitric oxide-dependent impairment of oxidative DNA repair. *Hepatology* **52**, 480-492.

Mack, C., Sickmann, A., Lembo, D. & Brune, W. (2008). Inhibition of proinflammatory and innate immune signaling pathways by a cytomegalovirus RIP1-interacting protein. *Proc Natl Acad Sci U S A* **105**, 3094-3099.

Mackenzie, J. (2005). Wrapping things up about virus RNA replication. *Traffic* **6**, 967-977.

Mackenzie, J. M., Jones, M. K. & Young, P. R. (1996). Immunolocalization of the dengue virus nonstructural glycoprotein NS1 suggests a role in viral RNA replication. *Virology* **220**, 232-240.

Mackenzie, J. M., Khromykh, A. A., Jones, M. K. & Westaway, E. G. (1998). Subcellular localization and some biochemical properties of the flavivirus Kunjin nonstructural proteins NS2A and NS4A. *Virology* **245**, 203-215.

Mackenzie, J. M. & Westaway, E. G. (2001). Assembly and maturation of the flavivirus Kunjin virus appear to occur in the rough endoplasmic reticulum and along the secretory pathway, respectively. *J Virol* **75**, 10787-10799.

Makino, Y., Tadano, M., Anzai, T., Ma, S. P., Yasuda, S. & Fukunaga, T. (1989). Detection of dengue 4 virus core protein in the nucleus. II. Antibody against dengue 4 core protein produced by a recombinant baculovirus reacts with the antigen in the nucleus. *J Gen Virol* **70 (Pt 6)**, 1417-1425.

Manga, P., Bis, S., Knoll, K., Perez, B. & Orlow, S. J. (2010). The unfolded protein response in melanocytes: activation in response to chemical stressors of the endoplasmic reticulum and tyrosinase misfolding. *Pigment Cell Melanoma Res*.

Mangeat, B., Gers-Huber, G., Lehmann, M., Zufferey, M., Luban, J. & Piguet, V. (2009). HIV-1 Vpu neutralizes the antiviral factor Tetherin/BST-2 by binding it and directing its beta-TrCP2-dependent degradation. *PLoS Pathog* **5**, e1000574.

Marianneau, P., Flamand, M., Deubel, V. & Despres, P. (1998). Induction of programmed cell death (apoptosis) by dengue virus in vitro and in vivo. *Acta Cient Venez* **49 Suppl 1**, 13-17.

Marin, M., Rose, K. M., Kozak, S. L. & Kabat, D. (2003). HIV-1 Vif protein binds the editing enzyme APOBEC3G and induces its degradation. *Nat Med* **9**, 1398-1403.

Markoff, L. (1989). In vitro processing of dengue virus structural proteins: cleavage of the pre-membrane protein. *J Virol* **63**, 3345-3352.

Markoff, L., Falgout, B. & Chang, A. (1997). A conserved internal hydrophobic domain mediates the stable membrane integration of the dengue virus capsid protein. *Virology* **233**, 105-117.

Martina, B. E., Koraka, P., van den Doel, P., Rimmelzwaan, G. F., Haagmans, B. L. & Osterhaus, A. D. (2008). DC-SIGN enhances infection of cells with glycosylated West Nile virus in vitro and virus replication in human dendritic cells induces production of IFN-alpha and TNF-alpha. *Virus Res* **135**, 64-71.

Matern, H. T., Yeaman, C., Nelson, W. J. & Scheller, R. H. (2001). The Sec6/8 complex in mammalian cells: characterization of mammalian Sec3, subunit interactions, and expression of subunits in polarized cells. *Proc Natl Acad Sci U S A* **98**, 9648-9653.

Matsuda, D., Yoshinari, S. & Dreher, T. (2004). eEF1A binding to aminoacylated viral RNA represses minus strand synthesis by TYMV RNA-dependent RNA polymerase. *Virology* **321**, 47-56.

Matusan, A. E., Pryor, M. J., Davidson, A. D. & Wright, P. J. (2001). Mutagenesis of the Dengue virus type 2 NS3 protein within and outside helicase motifs: effects on enzyme activity and virus replication. *J Virol* **75**, 9633-9643.

Medigeshi, G. R., Lancaster, A. M., Hirsch, A. J., Briese, T., Lipkin, W. I., Defilippis, V., Fruh, K., Mason, P. W., Nikolich-Zugich, J. & Nelson, J. A. (2007). West Nile virus infection activates the unfolded protein response, leading to CHOP induction and apoptosis. *J Virol* **81**, 10849-10860.

Mehle, A., Strack, B., Ancuta, P., Zhang, C., McPike, M. & Gabuzda, D. (2004). Vif overcomes the innate antiviral activity of APOBEC3G by promoting its degradation in the ubiquitin-proteasome pathway. *J Biol Chem* **279**, 7792-7798.

Miller, J. L., de Wet, B. J., Martinez-Pomares, L., Radcliffe, C. M., Dwek, R. A., Rudd, P. M. & Gordon, S. (2008). The mannose receptor mediates dengue virus infection of macrophages. *PLoS Pathog* **4**, e17.

Miller, S., Kastner, S., Krijnse-Locker, J., Buhler, S. & Bartenschlager, R. (2007). The non-structural protein 4A of dengue virus is an integral membrane protein inducing membrane alterations in a 2K-regulated manner. *J Biol Chem* **282**, 8873-8882.

Modis, Y., Ogata, S., Clements, D. & Harrison, S. C. (2003). A ligand-binding pocket in the dengue virus envelope glycoprotein. *Proc Natl Acad Sci U S A* **100**, 6986-6991.

Modis, Y., Ogata, S., Clements, D. & Harrison, S. C. (2004). Structure of the dengue virus envelope protein after membrane fusion. *Nature* **427**, 313-319.

Modis, Y., Ogata, S., Clements, D. & Harrison, S. C. (2005). Variable surface epitopes in the crystal structure of dengue virus type 3 envelope glycoprotein. *J Virol* **79**, 1223-1231.

Mongkolsapaya, J., Dejnirattisai, W., Xu, X. N., Vasanawathana, S., Tangthawornchaikul, N., Chairunsri, A., Sawasdivorn, S., Duangchinda, T., Dong, T., Rowland-Jones, S., Yenchitsomanus, P. T., McMichael, A., Malasit, P. & Screaton, G. (2003). Original antigenic sin and apoptosis in the pathogenesis of dengue hemorrhagic fever. *Nat Med* **9**, 921-927.

Montgomery, S. P., Brown, J. A., Kuehnert, M., Smith, T. L., Crall, N., Lanciotti, R. S., Macedo de Oliveira, A., Boo, T. & Marfin, A. A. (2006). Transfusion-associated transmission of West Nile virus, United States 2003 through 2005. *Transfusion* **46**, 2038-2046.

Mori, Y., Okabayashi, T., Yamashita, T., Zhao, Z., Wakita, T., Yasui, K., Hasebe, F., Tadano, M., Konishi, E., Moriishi, K. & Matsuura, Y. (2005). Nuclear localization of Japanese encephalitis virus core protein enhances viral replication. *J Virol* **79**, 3448-3458.

Moriishi, K., Okabayashi, T., Nakai, K., Moriya, K., Koike, K., Murata, S., Chiba, T., Tanaka, K., Suzuki, R., Suzuki, T., Miyamura, T. & Matsuura, Y. (2003). Proteasome activator PA28gamma-dependent nuclear retention and degradation of hepatitis C virus core protein. *J Virol* **77**, 10237-10249.

Mukhopadhyay, S., Kim, B. S., Chipman, P. R., Rossmann, M. G. & Kuhn, R. J. (2003). Structure of West Nile virus. *Science* **302**, 248.

Mukhopadhyay, S., Kuhn, R. J. & Rossmann, M. G. (2005). A structural perspective of the flavivirus life cycle. *Nat Rev Microbiol* **3**, 13-22.

Munoz-Jordan, J. L., Laurent-Rolle, M., Ashour, J., Martinez-Sobrido, L., Ashok, M., Lipkin, W. I. & Garcia-Sastre, A. (2005). Inhibition of alpha/beta interferon signaling by the NS4B protein of flaviviruses. *J Virol* **79**, 8004-8013.

Munoz-Jordan, J. L., Sanchez-Burgos, G. G., Laurent-Rolle, M. & Garcia-Sastre, A. (2003). Inhibition of interferon signaling by dengue virus. *Proc Natl Acad Sci U S A* **100**, 14333-14338.

Murray, J. M., Aaskov, J. G. & Wright, P. J. (1993). Processing of the dengue virus type 2 proteins prM and C-prM. *J Gen Virol* **74 (Pt 2)**, 175-182.

Murtagh, B., Wadia, Y., Messner, G., Allison, P., Harati, Y. & Delgado, R. (2005). West Nile virus infection after cardiac transplantation. *J Heart Lung Transplant* **24**, 774-776.

Myint, K. S., Endy, T. P., Mongkolsirichaikul, D., Manomuth, C., Kalayanarooj, S., Vaughn, D. W., Nisalak, A., Green, S., Rothman, A. L., Ennis, F. A. & Libraty, D. H. (2006). Cellular immune activation in children with acute dengue virus infections is modulated by apoptosis. *J Infect Dis* **194**, 600-607.

Nandi, D., Tahiliani, P., Kumar, A. & Chandu, D. (2006). The ubiquitin-proteasome system. *J Biosci* **31**, 137-155.

Nash, D., Mostashari, F., Fine, A., Miller, J., O'Leary, D., Murray, K., Huang, A., Rosenberg, A., Greenberg, A., Sherman, M., Wong, S. & Layton, M. (2001). The outbreak of West Nile virus infection in the New York City area in 1999. *N Engl J Med* **344**, 1807-1814.

Navarro-Sanchez, E., Altmeyer, R., Amara, A., Schwartz, O., Fieschi, F., Virelizier, J. L., Arenzana-Seisdedos, F. & Despres, P. (2003). Dendritic-cell-specific ICAM3-grabbing non-integrin is essential for the productive infection of human dendritic cells by mosquito-cell-derived dengue viruses. *EMBO Rep* **4**, 723-728.

Netsawang, J., Noisakran, S., Puttikhunt, C., Kasinrerk, W., Wongwiwat, W., Malasit, P., Yenchitsomanus, P. T. & Limjindaporn, T. (2010). Nuclear localization of dengue virus capsid protein is required for DAXX interaction and apoptosis. *Virus Res* **147**, 275-283.

Ng, M. L., Tan, S. H. & Chu, J. J. (2001). Transport and budding at two distinct sites of visible nucleocapsids of West Nile (Sarafend) virus. *J Med Virol* **65**, 758-764.

Niedermann, G. (2002). Immunological functions of the proteasome. *Curr Top Microbiol Immunol* **268**, 91-136.

Nishi, T. & Forgac, M. (2002). The vacuolar (H+)-ATPases--nature's most versatile proton pumps. *Nat Rev Mol Cell Biol* **3**, 94-103.

Noueiry, A., Chen, J. & Ahlquist, P. (2000). A mutant allele of essential, general translation initiation factor DED1 selectively inhibits translation of a viral mRNA. *Proc Natl Acad Sci U S A* **97**, 12985-12990.

Nussbaum, A. K., Dick, T. P., Keilholz, W., Schirle, M., Stevanovic, S., Dietz, K., Heinemeyer, W., Groll, M., Wolf, D. H., Huber, R., Rammensee, H. G. & Schild, H. (1998). Cleavage motifs of the yeast 20S proteasome beta subunits deduced from digests of enolase 1. *Proc Natl Acad Sci U S A* **95**, 12504-12509.

O'Leary, D. R., Kuhn, S., Kniss, K. L., Hinckley, A. F., Rasmussen, S. A., Pape, W. J., Kightlinger, L. K., Beecham, B. D., Miller, T. K., Neitzel, D. F., Michaels, S. R., Campbell, G. L., Lanciotti, R. S. & Hayes, E. B. (2006). Birth outcomes following West Nile Virus infection of pregnant women in the United States: 2003-2004. *Pediatrics* **117**, e537-545.

O'Leary, D. R., Nasci, R. S., Campbell, G. L. & Marfin, A. A. (2002). From the Centers for Disease Control and Prevention. West Nile Virus activity--United States, 2001. *JAMA* **288**, 158-159; discussion 159-160.

Oh, W., Yang, M. R., Lee, E. W., Park, K. M., Pyo, S., Yang, J. S., Lee, H. W. & Song, J. (2006). Jab1 mediates cytoplasmic localization and degradation of West Nile virus capsid protein. *J Biol Chem* **281**, 30166-30174.

Oh, W. K. & Song, J. (2006). Hsp70 functions as a negative regulator of West Nile virus capsid protein through direct interaction. *Biochem Biophys Res Commun* **347**, 994-1000.

Ohkawa, K., Ishida, H., Nakanishi, F., Hosui, A., Ueda, K., Takehara, T., Hori, M. & Hayashi, N. (2004). Hepatitis C virus core functions as a

suppressor of cyclin-dependent kinase-activating kinase and impairs cell cycle progression. *J Biol Chem* **279**, 11719-11726.

Ooms, M., Majdak, S., Seibert, C. W., Harari, A. & Simon, V. (2010). The localization of APOBEC3H variants in HIV-1 virions determines their antiviral activity. *J Virol* **84**, 7961-7969.

Oya, A. & Kurane, I. (2007). Japanese encephalitis for a reference to international travelers. *J Travel Med* **14**, 259-268.

Paranjape, S. & Harris, E. (2007). Y box-binding protein-1 binds to the dengue virus 3'-untranslated region and mediates antiviral effects. *J Biol Chem* **282**, 30497-30508.

Paranjape, S. M. & Harris, E. (2010). Control of dengue virus translation and replication. *Curr Top Microbiol Immunol* **338**, 15-34.

Parquet, M. C., Kumatori, A., Hasebe, F., Morita, K. & Igarashi, A. (2001). West Nile virus-induced bax-dependent apoptosis. *FEBS Lett* **500**, 17-24.

Pasupuleti, N., Gangadhariah, M., Padmanabha, S., Santhoshkumar, P. & Nagaraj, R. H. (2010). The role of the cysteine residue in the chaperone and anti-apoptotic functions of human Hsp27. *J Cell Biochem* **110**, 408-419.

Patkar, C. G., Jones, C. T., Chang, Y. H., Warrier, R. & Kuhn, R. J. (2007). Functional requirements of the yellow fever virus capsid protein. *J Virol* **81**, 6471-6481.

Paul, C., Simon, S., Gibert, B., Virot, S., Manero, F. & Arrigo, A. P. (2010). Dynamic processes that reflect anti-apoptotic strategies set up by HspB1 (Hsp27). *Exp Cell Res* **316**, 1535-1552.

Peng, T., Wang, J. L., Chen, W., Zhang, J. L., Gao, N., Chen, Z. T., Xu, X. F., Fan, D. Y. & An, J. (2009). Entry of dengue virus serotype 2 into ECV304 cells depends on clathrin-dependent endocytosis, but not on caveolae-dependent endocytosis. *Can J Microbiol* **55**, 139-145.

Perera, R. & Kuhn, R. J. (2008). Structural proteomics of dengue virus. *Curr Opin Microbiol* **11**, 369-377.

Petersen, L. R. & Marfin, A. A. (2002). West Nile virus: a primer for the clinician. *Ann Intern Med* **137**, 173-179.

Petersen, L. R. & Roehrig, J. T. (2001). West Nile virus: a reemerging global pathogen. *Emerg Infect Dis* **7**, 611-614.

Phoolcharoen, W. & Smith, D. R. (2004). Internalization of the dengue virus is cell cycle modulated in HepG2, but not Vero cells. *J Med Virol* **74**, 434-441.

Picard, D. (2002). Heat-shock protein 90, a chaperone for folding and regulation. *Cell Mol Life Sci* **59**, 1640-1648.

Pickart, C. M. (1997). Targeting of substrates to the 26S proteasome. *FASEB J* **11**, 1055-1066.

Pickart, C. M. & Cohen, R. E. (2004). Proteasomes and their kin: proteases in the machine age. *Nat Rev Mol Cell Biol* **5**, 177-187.

Plyusnina, A. & Plyusnin, A. (2005). Recombinant Tula hantavirus shows reduced fitness but is able to survive in the presence of a parental virus: analysis of consecutive passages in a cell culture. *Virol J* **2**, 12.

Poidinger, M., Hall, R. A. & Mackenzie, J. S. (1996). Molecular characterization of the Japanese encephalitis serocomplex of the flavivirus genus. *Virology* **218**, 417-421.

Preugschat, F., Yao, C. W. & Strauss, J. H. (1990). In vitro processing of dengue virus type 2 nonstructural proteins NS2A, NS2B, and NS3. *J Virol* **64**, 4364-4374.

Prikhod'ko, G. G., Prikhod'ko, E. A., Pletnev, A. G. & Cohen, J. I. (2002). Langat flavivirus protease NS3 binds caspase-8 and induces apoptosis. *J Virol* **76**, 5701-5710.

Qanungo, K., Shaji, D., Mathur, M. & Banerjee, A. (2004). Two RNA polymerase complexes from vesicular stomatitis virus-infected cells that carry out transcription and replication of genome RNA. *Proc Natl Acad Sci U S A* **101**, 5952-5957.

Qin, C. F. & Qin, E. D. (2006). Capsid-targeted viral inactivation can destroy dengue 2 virus from within in vitro. *Arch Virol* **151**, 379-385.

Raaben, M., Posthuma, C. C., Verheije, M. H., te Lintelo, E. G., Kikkert, M., Drijfhout, J. W., Snijder, E. J., Rottier, P. J. & de Haan, C. A. The ubiquitin-proteasome system plays an important role during various stages of the coronavirus infection cycle. *J Virol* **84**, 7869-7879.

Rajkumar, S. V., Richardson, P. G., Hideshima, T. & Anderson, K. C. (2005). Proteasome inhibition as a novel therapeutic target in human cancer. *J Clin Oncol* **23**, 630-639.

Ramanathan, M. P., Chambers, J. A., Pankhong, P., Chattergoon, M., Attatippaholkun, W., Dang, K., Shah, N. & Weiner, D. B. (2006). Host cell killing by the West Nile Virus NS2B-NS3 proteolytic complex: NS3 alone is sufficient to recruit caspase-8-based apoptotic pathway. *Virology* **345**, 56-72.

Ray, D., Shah, A., Tilgner, M., Guo, Y., Zhao, Y., Dong, H., Deas, T. S., Zhou, Y., Li, H. & Shi, P. Y. (2006). West Nile virus 5'-cap structure is formed by sequential guanine N-7 and ribose 2'-O methylations by nonstructural protein 5. *J Virol* **80**, 8362-8370.

Ren, J., Ding, T., Zhang, W., Song, J. & Ma, W. (2007). Does Japanese encephalitis virus share the same cellular receptor with other mosquito-borne flaviviruses on the C6/36 mosquito cells? *Virol J* **4**, 83.

Rey, F. A., Heinz, F. X., Mandl, C., Kunz, C. & Harrison, S. C. (1995). The envelope glycoprotein from tick-borne encephalitis virus at 2 A resolution. *Nature* **375**, 291-298.

Rice, C. M. (1990). Overview of flavivirus molecular biology and future vaccine development via recombinant DNA. *Southeast Asian J Trop Med Public Health* **21**, 670-677.

Rock, K. L., Gramm, C., Rothstein, L., Clark, K., Stein, R., Dick, L., Hwang, D. & Goldberg, A. L. (1994). Inhibitors of the proteasome block the degradation of most cell proteins and the generation of peptides presented on MHC class I molecules. *Cell* **78**, 761-771.

Roosendaal, J., Westaway, E. G., Khromykh, A. & Mackenzie, J. M. (2006). Regulated cleavages at the West Nile virus NS4A-2K-NS4B junctions

play a major role in rearranging cytoplasmic membranes and Golgi trafficking of the NS4A protein. *J Virol* **80**, 4623-4632.

Rubbi, C. P. & Milner, J. (2003). Disruption of the nucleolus mediates stabilization of p53 in response to DNA damage and other stresses. *EMBO J* **22**, 6068-6077.

Sakurai-Yageta, M., Recchi, C., Le Dez, G., Sibarita, J. B., Daviet, L., Camonis, J., D'Souza-Schorey, C. & Chavrier, P. (2008). The interaction of IQGAP1 with the exocyst complex is required for tumor cell invasion downstream of Cdc42 and RhoA. *J Cell Biol* **181**, 985-998.

Sakurai, A., Yasuda, J., Takano, H., Tanaka, Y., Hatakeyama, M. & Shida, H. (2004). Regulation of human T-cell leukemia virus type 1 (HTLV-1) budding by ubiquitin ligase Nedd4. *Microbes Infect* **6**, 150-156.

Samuel, M. A., Morrey, J. D. & Diamond, M. S. (2007). Caspase 3-dependent cell death of neurons contributes to the pathogenesis of West Nile virus encephalitis. *J Virol* **81**, 2614-2623.

Sato, Y., Kamura, T., Shirata, N., Murata, T., Kudoh, A., Iwahori, S., Nakayama, S., Isomura, H., Nishiyama, Y. & Tsurumi, T. (2009). Degradation of phosphorylated p53 by viral protein-ECS E3 ligase complex. *PLoS Pathog* **5**, e1000530.

Schmidt, M., Schmidtke, G. & Kloetzel, P. M. (1997). Structure and structure formation of the 20S proteasome. *Mol Biol Rep* **24**, 103-112.

Schmidtke, G., Schmidt, M. & Kloetzel, P. M. (1997). Maturation of mammalian 20 S proteasome: purification and characterization of 13 S and 16 S proteasome precursor complexes. *J Mol Biol* **268**, 95-106.

Sejvar, J. J., Bode, A. V., Marfin, A. A., Campbell, G. L., Ewing, D., Mazowiecki, M., Pavot, P. V., Schmitt, J., Pape, J., Biggerstaff, B. J. & Petersen, L. R. (2005). West Nile virus-associated flaccid paralysis. *Emerg Infect Dis* **11**, 1021-1027.

Shafee, N. & AbuBakar, S. (2003). Dengue virus type 2 NS3 protease and NS2B-NS3 protease precursor induce apoptosis. *J Gen Virol* **84**, 2191-2195.

Shi, P., Li, W. & Brinton, M. (1996). Cell proteins bind specifically to West Nile virus minus-strand 3' stem-loop RNA. *J Virol* **70**, 6278-6287.

Shi, S. T., Polyak, S. J., Tu, H., Taylor, D. R., Gretch, D. R. & Lai, M. M. (2002). Hepatitis C virus NS5A colocalizes with the core protein on lipid droplets and interacts with apolipoproteins. *Virology* **292**, 198-210.

Shimizu, T., Matsuoka, Y. & Shirasawa, T. (2005). Biological significance of isoaspartate and its repair system. *Biol Pharm Bull* **28**, 1590-1596.

Shrestha, B., Gottlieb, D. & Diamond, M. S. (2003). Infection and injury of neurons by West Nile encephalitis virus. *J Virol* **77**, 13203-13213.

Skupski, D. W., Eglinton, G. S., Fine, A. D., Hayes, E. B. & O'Leary, D. R. (2006). West Nile virus during pregnancy: a case study of early second trimester maternal infection. *Fetal Diagn Ther* **21**, 293-295.

Stadler, K., Allison, S. L., Schalich, J. & Heinz, F. X. (1997). Proteolytic activation of tick-borne encephalitis virus by furin. *J Virol* **71**, 8475-8481.

Stock, D., Ditzel, L., Baumeister, W., Huber, R. & Lowe, J. (1995). Catalytic mechanism of the 20S proteasome of Thermoplasma acidophilum revealed by X-ray crystallography. *Cold Spring Harb Symp Quant Biol* **60**, 525-532.

Stocks, C. E. & Lobigs, M. (1995). Posttranslational signal peptidase cleavage at the flavivirus C-prM junction in vitro. *J Virol* **69**, 8123-8126.

Stocks, C. E. & Lobigs, M. (1998). Signal peptidase cleavage at the flavivirus C-prM junction: dependence on the viral NS2B-3 protease for efficient processing requires determinants in C, the signal peptide, and prM. *J Virol* **72**, 2141-2149.

Su, H. L., Lin, Y. L., Yu, H. P., Tsao, C. H., Chen, L. K., Liu, Y. T. & Liao, C. L. (2001). The effect of human bcl-2 and bcl-X genes on dengue virus-induced apoptosis in cultured cells. *Virology* **282**, 141-153.

Surjit, M., Liu, B., Chow, V. T. & Lal, S. K. (2006). The nucleocapsid protein of severe acute respiratory syndrome-coronavirus inhibits the activity of cyclin-cyclin-dependent kinase complex and blocks S phase progression in mammalian cells. *J Biol Chem* **281**, 10669-10681.

Suzuki, R., Sakamoto, S., Tsutsumi, T., Rikimaru, A., Tanaka, K., Shimoike, T., Moriishi, K., Iwasaki, T., Mizumoto, K., Matsuura, Y., Miyamura, T. & Suzuki, T. (2005). Molecular determinants for subcellular localization of hepatitis C virus core protein. *J Virol* **79**, 1271-1281.

Szaszak, M., Christian, F., Rosenthal, W. & Klussmann, E. (2008). Compartmentalized cAMP signalling in regulated exocytic processes in non-neuronal cells. *Cell Signal* **20**, 590-601.

Tadano, M., Makino, Y., Fukunaga, T., Okuno, Y. & Fukai, K. (1989). Detection of dengue 4 virus core protein in the nucleus. I. A monoclonal antibody to dengue 4 virus reacts with the antigen in the nucleus and cytoplasm. *J Gen Virol* **70 (Pt 6)**, 1409-1415.

Takagi, J., Otake, K., Nakao, N., Takashashi, M. & Hirooka, Y. (2003). Urinary excretion of aquaporin-2 and inappropriate secretion of vasopressin in hyponatremic patients after cerebral infarction. *Horm Metab Res* **35**, 62-66.

Tanimura, A., Yujiri, T., Tanaka, Y., Hatanaka, M., Mitani, N., Nakamura, Y., Mori, K. & Tanizawa, Y. (2009). The anti-apoptotic role of the unfolded protein response in Bcr-Abl-positive leukemia cells. *Leuk Res* **33**, 924-928.

Taxonomy, V. (2000). Virus taxonomy: classification and nomenclature of viruses: seventh report of the International Committee onTaxonomy of Viruses, pp. 859-866. Edited by A. press. San Diego.

Teo, D., Ng, L. C. & Lam, S. (2009). Is dengue a threat to the blood supply? *Transfus Med* **19**, 66-77.

TerBush, D., Maurice, T., Roth, D. & Novick, P. (1996). The Exocyst is a multiprotein complex required for exocytosis in Saccharomyces cerevisiae. *EMBO J* **15**, 6483-6494.

Thongtan, T., Panyim, S. & Smith, D. R. (2004). Apoptosis in dengue virus infected liver cell lines HepG2 and Hep3B. *J Med Virol* **72**, 436-444.

Tilgner, M., Deas, T. S. & Shi, P. Y. (2005). The flavivirus-conserved penta-nucleotide in the 3' stem-loop of the West Nile virus genome requires a specific sequence and structure for RNA synthesis, but not for viral translation. *Virology* **331**, 375-386.

Tilgner, M. & Shi, P. Y. (2004). Structure and function of the 3' terminal six nucleotides of the west nile virus genome in viral replication. *J Virol* **78**, 8159-8171.

Timani, K. A., Liao, Q., Ye, L., Zeng, Y., Liu, J., Zheng, Y., Yang, X., Lingbao, K., Gao, J. & Zhu, Y. (2005). Nuclear/nucleolar localization properties of C-terminal nucleocapsid protein of SARS coronavirus. *Virus Res* **114**, 23-34.

Tsuda, Y., Mori, Y., Abe, T., Yamashita, T., Okamoto, T., Ichimura, T., Moriishi, K. & Matsuura, Y. (2006). Nucleolar protein B23 interacts with Japanese encephalitis virus core protein and participates in viral replication. *Microbiol Immunol* **50**, 225-234.

Tsukiyama-Kohara, K., Tone, S., Maruyama, I., Inoue, K., Katsume, A., Nuriya, H., Ohmori, H., Ohkawa, J., Taira, K., Hoshikawa, Y., Shibasaki, F., Reth, M., Minatogawa, Y. & Kohara, M. (2004). Activation of the CKI-CDK-Rb-E2F pathway in full genome hepatitis C virus-expressing cells. *J Biol Chem* **279**, 14531-14541.

Tu, Z., Pierce, R. H., Kurtis, J., Kuroki, Y., Crispe, I. N. & Orloff, M. S. (2010). Hepatitis C virus core protein subverts the antiviral activities of human Kupffer cells. *Gastroenterology* **138**, 305-314.

Tupling, A. R., Bombardier, E., Vigna, C., Quadrilatero, J. & Fu, M. (2008). Interaction between Hsp70 and the SR Ca2+ pump: a potential mechanism for cytoprotection in heart and skeletal muscle. *Appl Physiol Nutr Metab* **33**, 1023-1032.

Turell, M. J., Dohm, D. J., Sardelis, M. R., Oguinn, M. L., Andreadis, T. G. & Blow, J. A. (2005). An update on the potential of north American mosquitoes (Diptera: Culicidae) to transmit West Nile Virus. *J Med Entomol* **42**, 57-62.

Tyagi, S., Surjit, M. & Lal, S. K. (2005). The 41-amino-acid C-terminal region of the hepatitis E virus ORF3 protein interacts with bikunin, a kunitz-type serine protease inhibitor. *J Virol* **79**, 12081-12087.

Uchil, P. D. & Satchidanandam, V. (2003). Architecture of the flaviviral replication complex. Protease, nuclease, and detergents reveal encasement within double-layered membrane compartments. *J Biol Chem* **278**, 24388-24398.

Ulane, C. M. & Horvath, C. M. (2002). Paramyxoviruses SV5 and HPIV2 assemble STAT protein ubiquitin ligase complexes from cellular components. *Virology* **304**, 160-166.

Umareddy, I., Chao, A., Sampath, A., Gu, F. & Vasudevan, S. G. (2006). Dengue virus NS4B interacts with NS3 and dissociates it from single-stranded RNA. *J Gen Virol* **87**, 2605-2614.

Urata, S., Yokosawa, H. & Yasuda, J. (2007). Regulation of HTLV-1 Gag budding by Vps4A, Vps4B, and AIP1/Alix. *Virol J* **4**, 66.

Valdes, I., Bernardo, L., Gil, L., Pavon, A., Lazo, L., Lopez, C., Romero, Y., Menendez, I., Falcon, V., Betancourt, L., Martin, J., Chinea, G., Silva, R., Guzman, M. G., Guillen, G. & Hermida, L. (2009). A novel fusion protein domain III-capsid from dengue-2, in a highly aggregated form, induces a functional immune response and protection in mice. *Virology* **394**, 249-258.

Villordo, S. M. & Gamarnik, A. V. (2009). Genome cyclization as strategy for flavivirus RNA replication. *Virus Res* **139**, 230-239.

Voges, D., Zwickl, P. & Baumeister, W. (1999). The 26S proteasome: a molecular machine designed for controlled proteolysis. *Annu Rev Biochem* **68**, 1015-1068.

Wadei, H., Alangaden, G. J., Sillix, D. H., El-Amm, J. M., Gruber, S. A., West, M. S., Granger, D. K., Garnick, J., Chandrasekar, P., Migdal, S. D. & Haririan, A. (2004). West Nile virus encephalitis: an emerging disease in renal transplant recipients. *Clin Transplant* **18**, 753-758.

Wang, S. H., Syu, W. J. & Hu, S. T. (2004). Identification of the homotypic interaction domain of the core protein of dengue virus type 2. *J Gen Virol* **85**, 2307-2314.

Watson, J. T., Pertel, P. E., Jones, R. C., Siston, A. M., Paul, W. S., Austin, C. C. & Gerber, S. I. (2004). Clinical characteristics and functional outcomes of West Nile Fever. *Ann Intern Med* **141**, 360-365.

Wei, Y., Qin, C., Jiang, T., Li, X., Zhao, H., Liu, Z., Deng, Y., Liu, R., Chen, S., Yu, M. & Qin, E. (2009). Translational regulation by the 3' untranslated region of the dengue type 2 virus genome. *Am J Trop Med Hyg* **81**, 817-824.

Wengler, G. (1993). The NS 3 nonstructural protein of flaviviruses contains an RNA triphosphatase activity. *Virology* **197**, 265-273.

Westaway, E. G. (1987). Flavivirus replication strategy. *Adv Virus Res* **33**, 45-90.

Westaway, E. G., Khromykh, A. A., Kenney, M. T., Mackenzie, J. M. & Jones, M. K. (1997). Proteins C and NS4B of the flavivirus Kunjin translocate independently into the nucleus. *Virology* **234**, 31-41.

Widman, D. G., Frolov, I. & Mason, P. W. (2008). Third-generation flavivirus vaccines based on single-cycle, encapsidation-defective viruses. *Adv Virus Res* **72**, 77-126.

Wiech, H., Buchner, J., Zimmermann, R. & Jakob, U. (1992). Hsp90 chaperones protein folding in vitro. *Nature* **358**, 169-170.

Wiederkehr, A., Du, Y., Pypaert, M., Ferro-Novick, S. & Novick, P. (2003). Sec3p is needed for the spatial regulation of secretion and for the inheritance of the cortical endoplasmic reticulum. *Mol Biol Cell* **14**, 4770-4782.

Wissing, S., Galloway, N. L. & Greene, W. C. (2010). HIV-1 Vif versus the APOBEC3 cytidine deaminases: an intracellular duel between pathogen and host restriction factors. *Mol Aspects Med* **31**, 383-397.

Wright, P. F., Karron, R. A., Madhi, S. A., Treanor, J. J., King, J. C., O'Shea, A., Ikizler, M. R., Zhu, Y., Collins, P. L., Cutland, C., Randolph, V. B., Deatly, A. M., Hackell, J. G., Gruber, W. C. &

Murphy, B. R. (2006). The interferon antagonist NS2 protein of respiratory syncytial virus is an important virulence determinant for humans. *J Infect Dis* **193**, 573-581.

Wurm, T., Chen, H., Hodgson, T., Britton, P., Brooks, G. & Hiscox, J. A. (2001). Localization to the nucleolus is a common feature of coronavirus nucleoproteins, and the protein may disrupt host cell division. *J Virol* **75**, 9345-9356.

Yamashita, M., Kurokawa, K., Sato, Y., Yamagata, A., Mimura, H., Yoshikawa, A., Sato, K., Nakano, A. & Fukai, S. (2010). Structural basis for the Rho- and phosphoinositide-dependent localization of the exocyst subunit Sec3. *Nat Struct Mol Biol* **17**, 180-186.

Yang, J. S., Ramanathan, M. P., Muthumani, K., Choo, A. Y., Jin, S. H., Yu, Q. C., Hwang, D. S., Choo, D. K., Lee, M. D., Dang, K., Tang, W., Kim, J. J. & Weiner, D. B. (2002). Induction of inflammation by West Nile virus capsid through the caspase-9 apoptotic pathway. *Emerg Infect Dis* **8**, 1379-1384.

Yang, M. R., Lee, S. R., Oh, W., Lee, E. W., Yeh, J. Y., Nah, J. J., Joo, Y. S., Shin, J., Lee, H. W., Pyo, S. & Song, J. (2008). West Nile virus capsid protein induces p53-mediated apoptosis via the sequestration of HDM2 to the nucleolus. *Cell Microbiol* **10**, 165-176.

Yoshida, T., Hanada, T., Tokuhisa, T., Kosai, K., Sata, M., Kohara, M. & Yoshimura, A. (2002). Activation of STAT3 by the hepatitis C virus core protein leads to cellular transformation. *J Exp Med* **196**, 641-653.

Yu, I. M., Zhang, W., Holdaway, H. A., Li, L., Kostyuchenko, V. A., Chipman, P. R., Kuhn, R. J., Rossmann, M. G. & Chen, J. (2008a). Structure of the immature dengue virus at low pH primes proteolytic maturation. *Science* **319**, 1834-1837.

Yu, L., Nomaguchi, M., Padmanabhan, R. & Markoff, L. (2008b). Specific requirements for elements of the 5' and 3' terminal regions in flavivirus RNA synthesis and viral replication. *Virology* **374**, 170-185.

Zangari, M., Yaccoby, S., Pappas, L., Cavallo, F., Kumar, N. S., Ranganathan, S., Suva, L. J., Gruenwald, J. M., Kern, S., Zhan, F., Esseltine, D. L. & Tricot, G. (2010). A prospective evaluation of the biochemical, metabolic, hormonal and structural bone changes associated with bortezomib response in multiple myeloma patients. *Haematologica*.

Zhang, B., Dong, H., Stein, D. A., Iversen, P. L. & Shi, P. Y. (2008a). West Nile virus genome cyclization and RNA replication require two pairs of long-distance RNA interactions. *Virology* **373**, 1-13.

Zhang, L., Peeples, M. E., Boucher, R. C., Collins, P. L. & Pickles, R. J. (2002). Respiratory syncytial virus infection of human airway epithelial cells is polarized, specific to ciliated cells, and without obvious cytopathology. *J Virol* **76**, 5654-5666.

Zhang, W., Chipman, P. R., Corver, J., Johnson, P. R., Zhang, Y., Mukhopadhyay, S., Baker, T. S., Strauss, J. H., Rossmann, M. G. & Kuhn, R. J. (2003a). Visualization of membrane protein domains by cryo-electron microscopy of dengue virus. *Nat Struct Biol* **10**, 907-912.

Zhang, W., Yang, H., Kong, X., Mohapatra, S., San Juan-Vergara, H., Hellermann, G., Behera, S., Singam, R., Lockey, R. F. & Mohapatra, S. S. (2005a). Inhibition of respiratory syncytial virus infection with intranasal siRNA nanoparticles targeting the viral NS1 gene. *Nat Med* **11**, 56-62.

Zhang, X., Bi, E., Novick, P., Du, L., Kozminski, K. G., Lipschutz, J. H. & Guo, W. (2001). Cdc42 interacts with the exocyst and regulates polarized secretion. *J Biol Chem* **276**, 46745-46750.

Zhang, X., Orlando, K., He, B., Xi, F., Zhang, J., Zajac, A. & Guo, W. (2008b). Membrane association and functional regulation of Sec3 by phospholipids and Cdc42. *J Cell Biol* **180**, 145-158.

Zhang, X., Zajac, A., Zhang, J., Wang, P., Li, M., Murray, J., TerBush, D. & Guo, W. (2005b). The critical role of Exo84p in the organization and polarized localization of the exocyst complex. *J Biol Chem* **280**, 20356-20364.

Zhang, Y., Corver, J., Chipman, P. R., Zhang, W., Pletnev, S. V., Sedlak, D., Baker, T. S., Strauss, J. H., Kuhn, R. J. & Rossmann, M. G. (2003b). Structures of immature flavivirus particles. *EMBO J* **22**, 2604-2613.

Zhang, Y., Zhang, W., Ogata, S., Clements, D., Strauss, J. H., Baker, T. S., Kuhn, R. J. & Rossmann, M. G. (2004). Conformational changes of the flavivirus E glycoprotein. *Structure* **12**, 1607-1618.

Zhou, B., Liu, J., Wang, Q., Liu, X., Li, X., Li, P., Ma, Q. & Cao, C. (2008). The nucleocapsid protein of severe acute respiratory syndrome coronavirus inhibits cell cytokinesis and proliferation by interacting with translation elongation factor 1alpha. *J Virol* **82**, 6962-6971.

Zhou, Y., Ray, D., Zhao, Y., Dong, H., Ren, S., Li, Z., Guo, Y., Bernard, K. A., Shi, P. Y. & Li, H. (2007). Structure and function of flavivirus NS5 methyltransferase. *J Virol* **81**, 3891-3903.

Zhu, W., Qin, C., Chen, S., Jiang, T., Yu, M., Yu, X. & Qin, E. (2007). Attenuated dengue 2 viruses with deletions in capsid protein derived from an infectious full-length cDNA clone. *Virus Res* **126**, 226-232.

Zlotnick, A. (2005). Theoretical aspects of virus capsid assembly. *J Mol Recognit* **18**, 479-490.

APPENDICES

APPENDIX 1: REAGENTS FOR CELL CULTURE

The following are formulations for the preparation of media used to grow various cell lines used throughout the project. All contents except foetal bovine serum were warmed to 25^{o}C and added to a glass beaker already containing 90% of the final required volume of water. A magnetic stirrer was used to agitate the contents until all solids were fully dissolved.

A. Growth medium, L15 for C6/36 cells (~pH 7.3)

Items	Amount	Source
L15	1 bottle	Sigma, USA
Foetal bovine serum	100 ml	PAA Laboratories, Austria
Deionised water	900 ml	Millipore, USA

B. Growth medium, Dulbecco's Modified Eagle's Medium (DMEM) for HEK293 cells (~pH 7.3)

Items	Amount	Source
DMEM	1 bottle	Sigma, USA
Foetal bovine serum	100 ml	PAA Laboratories, Austria
$NaHCO_3$	3.7 g	Merck Germany
Deionised water	900 ml	Millipore, USA

C. Growth medium, Dulbecco's Modified Eagle's Medium (DMEM) for 293FT cells (~pH 7.3)

Items	Amount	Source
DMEM	1 bottle	Sigma, USA
Foetal bovine serum	100 ml	PAA Laboratories, Austria
$NaHCO_3$	3.7 g	Merck, Germany
Geneticin	50 mg/ml	Invitrogen, USA
Deionised water	890 ml	Millipore, USA

D. Growth medium, Roswell Park Memorial Institute-1640 (RPMI-1640) for BHK cells (~pH 7.3)

Items	Amount	Source
RPMI-1640	1 bottle	Sigma, USA
$NaHCO_3$	2.0 g	Merck, Germany
Foetal bovine serum	100 ml	PAA Laboratories, Austria
Deionised water	900 ml	Millipore, USA

The pH of the media was then adjusted to approximately 7.3 with a handheld pH meter (Beckman Coulter Inc., USA). The solution was then sterilised by filtration in a sterile environment through a 0.2 µm PES membrane bottle top filter unit (Nalge Nunc International, Denmark). A 20 ml aliquot of filtered media was used for screening of microbial contamination by incubation at 37°C for 3 days before the addition of FBS and antibiotic, geneticin. The serum supplemented media were kept at 4°C until further use. The cell culture media were warmed up in water bath to 37°C before use.

E. Heat-inactivated foetal bovine serum (FBS)

Foetal bovine serum for the L15 and DMEM was heat inactivated at 56°C for 30 min in a pre-warmed water bath before being added into the sterile media.

F. 1 M Hydrochloric acid (1 M HCl)

Hydrochloric acid (37% - Merck, Germany) was diluted by 1:10 in deionised water (Millipore, USA) to create a 1 M solution of hydrochloric acid. This was stored at 25°C and used to adjust the pH of media.

G. 1 M Sodium hydroxide (1 M NaOH)

Sodium hydroxide pellets (BDH Ltd., England) was weighed out to 50 g and mixed into 1 L of deionised water (Millipore, USA) to create a 1 M solution of sodium hydroxide. This was stored at 25°C and used to adjust the pH of media.

H. Phosphate-buffered saline (PBS)

Items	Amount	Source
NaCl	8.0 g	Lab Scan Limited, Ireland
KCl	0.2 g	Merck, Germany
Na_2HPO_4	1.15 g	Merck, Germany
KH_2PO_4	0.2 g	Merck, Germany
Deionised water	900 ml	Millipore, USA

The above materials were dissolved in 1 L of deionised water. The pH was adjusted to 7.4 using either 1 M HCl or 1 M NaOH. The solution was aliquoted and autoclaved (Hirayama Corp., Japan) for 15 min at 121°C and stored at 4°C.

I. Trypsin

Trypsin solution for the dissociation of cells from culture flask or plate was made by diluting 10 ml of sterile porcine pancreas derived 10x trypsin solution (Sigma, USA) in 90 ml PBS. This 1x stock of trypsin was stored at 4°C and warmed to 37°C before use.

J. Poly-L- lysine for coating flasks

Poly-L-lysine was prepared from powder (Sigma, USA) into a stock solution of 10 mg in 5 ml of distilled water (Millipore, USA). The stock was then diluted in 1:100 with distilled water to obtain a working concentration. The resulting solution was sterilized by 0.2 µm syringe filter (Sartorius, Germany). This solution was used to plate the tissue culture flasks, plates or coverslips overnight at RT. The next day, the solution was removed and the surface was washed twice with sterile distilled water. The flasks and coverslips were then left in a laminar flow to dry before the plating of cells.

APPENDIX 2: REAGENTS FOR VIRUS INFECTION, GROWTH OF VIRUS AND PLAQUE ASSAY

A. Virus Diluent, Hanks' balanced salt (pH 7.2 - 7.4)

Items	Amount	Source
Hanks' balanced salt	1 bottle	Sigma, USA
$NaHCO_3$	2.2 g	Merck, Germany
10% Bovine serum albumin	1 ml	CSL, Australia
Deionised water	1000 ml	Millipore, USA

The above materials were dissolved in 900 ml of deionised water. A magnetic stirrer was used to agitate the contents until all solids were fully dissolved. The solution was made up to 1000 ml and the pH was adjusted to 7.3 using a pH meter (Beckman Coulter Inc., USA). The solution was then sterilised by filtration through 0.2 µm PES membrane bottle top filter unit (Nalge Nunc International, USA) and stored at 4°C. Virus diluent was warmed to 37°C before use.

B. Maintenance media, L15 for C6/36 cells

Items	Amount	Source
L15	1 bottle	Sigma, USA
Foetal bovine serum	20 ml	PAA Laboratories, Austria
Deionised water	980 ml	Millipore, USA

C. Maintenance media, DMEM for HEK293 cells

Items	Amount	Source
DMEM	1 bottle	Sigma, USA
Foetal bovine serum	20 ml	PAA Laboratories, Austria
$NaHCO_3$	3.7 g	Merck, Germany
Deionised water	980 ml	Millipore, USA

Maintenance media for all the cell lines were prepared in the same way as the growth media for the same cell line in Appendix 1A to 1D, except for the volume difference of foetal bovine serum and sterile deionised water.

D. Overlay medium (pH 7.2 - 7.4)

a. Double strength growth media

Items	Amount	Source
RPMI-1640	1 bottle	Sigma, USA
$NaHCO_3$	2.0 g	Merck, Germany
Foetal bovine serum	40 ml	PAA Laboratories, Austria
Deionised water	460 ml	Millipore, USA

Double strength growth media was prepared in the same way as the growth media for BHK cells in Appendix 1D, except for the volume difference of foetal bovine serum and sterile deionised water.

b. 2% Carboxy-methyl-cellulose (2% CMC)

To make 200 ml of 2% CMC, 4.0 g of CMC powder (Merck, Germany) was mixed well into 200 ml of sterile deionized water. The solution was then autoclaved for 15 min at 121°C and stored at 4°C until further use.

c. Overlay medium

Two hundred ml of double strength media was added to 200 ml of 2% CMC solution and mixed well and stored at 4°C. Overlay medium was warmed to 37°C before use.

E. 0.5% Crystal violet / 25% formaldehyde solution

Items	Amount	Source
Crystal violet powder	5.0 g	Sigma, USA
37% Formaldehyde solution	270 ml	Merck, Germany
PBS	230 ml	See Appendix 1H

The above materials were mixed together and stored at room temperature.

APPENDIX 3: REAGENTS FOR MOLECULAR WORK

A. Primers used in cloning

Primer name	Nucleotide sequence (5'-3')	Plasmid	Vector
(i) Yeast expression system			
Y2HCF (F)	CGTT**GAATTC**ATGTCTAAGAAACCAGGA	ADC	pGADT7 (Clontech, USA)
		BDC	pGBKT7 (Clontech, USA)
		C3'Δ18	pGADT7 (Clontech, USA)
		C3'Δ39	pGADT7 (Clontech, USA)
Y2HC5'Δ15 (F)	CGTT**GAATTC**ATGCTAAAACGCGGTATGC	C5'Δ15	pGADT7 (Clontech, USA)
Y2HC5'Δ30 (F)	CGTT**GAATTC**AAGAGGGCTATGCTGAGTCTG	C5'Δ30	pGADT7 (Clontech, USA)
Y2HC5'Δ45 (F)	CGTT**GAATTC**TTCGTGTTGGCTCTTCTGG	C5'Δ45	pGADT7 (Clontech, USA)
Y2HC3'Δ18 (R)	CG**GGATCC**TTATCTTTTCTTTTGTTTTGTGC	C3'Δ18	pGADT7 (Clontech, USA)
Y2HC3'Δ39 (R)	CG**GGATCC**TTAGAAACTCAAGAGATGCTTC	C3'Δ39	pGADT7 (Clontech, USA)
YTCREV (R)	CG**GGATCC**TTAAGCTCCAGCACAGGCGA	ADC	pGADT7 (Clontech, USA)
		BDC	pGBKT7 (Clontech, USA)
		C5'Δ15	pGADT7 (Clontech, USA)
		C5'Δ30	pGADT7 (Clontech, USA)
		C5'Δ45	pGADT7 (Clontech, USA)
Y2HSec3(F)	CGTT**CATATG**ATGACAGCAATCAAGCAT	hSec3pf1	pGADT7 (Clontech, USA)
		hSec3pf1	pGBKT7 (Clontech, USA)
		hSec3pf2	pGBKT7 (Clontech, USA)
		hSec3pf5	pGBKT7 (Clontech, USA)
Y2HSec3f3(F)	CGTT**CATATG**CAGCAGCGATTCAGTGAT	hSec3pf3	pGBKT7 (Clontech, USA)
Y2HSec3f4(F)	CGTT**CATATG**GAGAAAGATATGATCCGC	hSec3pf4	pGBKT7 (Clontech, USA)
Y2HSec3f6(F)	CGTT**CATATG**GAACTTCGTAAAGTCATT	hSec3pf6	pGBKT7 (Clontech, USA)
Y2HSec3(R)	CG**GGATCC**TTAGTGGGACTGTGCAAT	hSec3pf1	pGBKT7 (Clontech, USA)
		hSec3pf4	pGBKT7 (Clontech, USA)
		hSec3pf6	pGBKT7 (Clontech, USA)
Y2HSec3pf2(R)	CG**GGATCC**TTATTGCTGTTTGACTGCCAG	hSec3pf2	pGBKT7 (Clontech, USA)
Y2HSec3pf3(R)	CG**GGATCC**TTAAGATGAAACAGGCAGTGG	hSec3pf3	pGBKT7 (Clontech, USA)
Y2HSec3pf5(R)	CG**GGATCC**TTAAGTGAATTCCATTGTAAC	hSec3pf5	pGBKT7 (Clontech, USA)
D-BDC(F)	CGTT**GAATTC**ATGAATAACCAACGAAAA	D-BDC	pGBKT7 (Clontech, USA)
		D-ADC	pGADT7 (Clontech, USA)
D-BDC(R)	CG**GGATCC**TTA CGCCATCACTGTTGGAAT	D-BDC	pGBKT7 (Clontech, USA)
		D-ADC	pGADT7 (Clontech, USA)

Primer name	Nucleotide sequence (5'-3')	Plasmid	Vector
(ii) *Mammalian expression system*			
HACCF (F)	CCG**GAATTC**GGATGTCTAAGAAACCAGGA	HAC (W)MycC HAC3'Δ18 HAC3'Δ39	pCMV-HA (Clontech, USA) pCMV-Myc (Clontech, USA) pCMV-HA (Clontech, USA) pCMV-HA (Clontech, USA)
HACC5'Δ15 (F)	CCG**GAATTC**GGATGCTAAAACGCGGTATGC	HAC5'Δ15	pCMV-HA (Clontech, USA)
HACC5'Δ30 (F)	CCG**GAATTC**GGAAGAGGGCTATGCTGAGT	HAC5'Δ30	pCMV-HA (Clontech, USA)
HACC5'Δ45 (F)	CCG**GAATTC**GGTTCGTGTTGGCTCTTCTG	HAC5'Δ45	pCMV-HA (Clontech, USA)
HACC3'Δ18 (R)	CCG**CTCGAG**TTATCTTTTCTTTTGTTTTGTGC	HAC3'Δ18	pCMV-HA (Clontech, USA)
HACC3'Δ39 (R)	CCG**CTCGAG**TTAGAAACTCAAGAGATGCTTC	HAC3'Δ39	pCMV-HA (Clontech, USA)
HACREV (R)	CCG**CTCGAG**TTAAGCTCCAGCACAGGCGAT	HAC (W)MycC HAC5'Δ15 HAC5'Δ30 HAC5'Δ45	pCMV-HA (Clontech, USA) pCMV-Myc (Clontech, USA) pCMV-HA (Clontech, USA) pCMV-HA (Clontech, USA) pCMV-HA (Clontech, USA)
V5Sec3(F)	***CACCATGG***CAGCAATCAAGC	V5-hSec3pf1 V5-hSec3pf5	pcDNA3.1-TOPO-V5-His (Invitrogrn, USA)
V5-hSec3pf6(F)	***CACCATGG***AACTTCGTAAAGTCATT	V5-hSec3pf6	pcDNA3.1-TOPO-V5-His (Invitrogrn, USA)
V5-Sec3(R)	GTGGGACTGTGCAATGCTGGA	V5-hSec3pf1 V5-hSec3pf6	pcDNA3.1-TOPO-V5-His (Invitrogrn, USA)
V5-hSec3pf5(R)	AGTGAATTCCATTGTAAC	V5-hSec3pf5	pcDNA3.1-TOPO-V5-His (Invitrogrn, USA)
DMycC(F)	CCG**GAATTC**GGATGAATAACCAACGAAAA	(D)MycC	pCMV-Myc (Clontech, USA)
DMycCΔ15(F)	CCG**GAATTC**GG CTGAAACGCGAGAGAAAC	(D)MycCΔ15	pCMV-Myc (Clontech, USA)
DMycC(R)	CCG**CTCGAG**TTA CGCCATCACTGTTGGAAT	(D)MycC (D)MycCΔ15	pCMV-Myc (Clontech, USA) pCMV-Myc (Clontech, USA)

(F) denotes forward primer and (R) denotes reverse primer. Restriction site in each primer used for cloning in (i) yeast and (ii) mammalian expression systems are shown in bold. The overhang sequences were underlined. The Kozak sequence for topoisomerase is shown in bold and italized.

B. Reagents for agarose gel electrophoresis

(i) 50 x Tris-acetate-EDTA (TAE) buffer, pH 8.0

Items	Amount	Source
Tris base	242.0 g	Merck, Germany
Glacial acetic acid	57.1 g	Merck, Germany
0.5 M EDTA pH8.0	100 ml	Merck, Germany
Deionised water	900 ml	Millipore, USA

To prepare 1 x TAE buffer, 50 x stock solution was diluted in the ratio of 1:50 using deionized water

(ii) Ethidium bromide (EtBr)

About 0.2 g of EtBr (Sigma, USA) was dissolved in 20 ml of deionized water (Millipore, USA) by stirring with a magnetic stirrer at RT for several hours. The solution was then stored in dark at 4^{o}C.

(iii) 1% Agarose gel

Items	Amount	Source
Ultra-pure agarose	3.0 g	Invitrogen, USA
10× TAE	300 ml	See Appendix 3B(i)
Ethidium Bromide (10 mg/ml)	10 µl	See Appendix 3B(ii)

To cast 1% DNA agarose gel, 3 g of agarose was mixed with 300 ml 1x TAE buffer in a 500 ml conical flask and heated to a boil in a microwave. The flask of molten agarose was cooled and 10 µl of ethidium bromide solution was added and

mixed. The molten agarose was then poured into a gel casting tray and the gel combs were inserted. The solidified gel was then submerged in the gel electrophoresis tank (Bio-Rad, USA) filled with 1x TAE buffer.

(iv) 10 x Gel loading buffer

Items	Amount	Source
Glycerol	10 ml	Merck, Germany
Bromophenol Blue	83 mg	Sigma, USA
EDTA	10 mM	Merck, Germany
Tris-EDTA, pH 8.0	10 ml	Merck, Germany
Deionised water	top up to 20 ml	Millipore, USA

C. Media for bacterial culture

(i) Luria Bertani (LB) broth, pH 7.0

Items	Amount	Source
Bacto-tryptone	10.0 g	Clontech, USA
Bacto-yeast extract	5.0 g	Clontech, USA
NaCl	10.0 g	Merck, Germany
Deionised water	top up to 1 L	Millipore, USA

All the above components were dissolved in 1 L deionized water and autoclaved at 121°C for 15 min and stored at 4°C until further use.

(ii) Luria- Bertani (LB) agar, pH 7.0

Items	Amount	Source
Bacto-tryptone	10.0 g	Clontech, USA
Bacto-yeast extract	5.0 g	Clontech, USA
NaCl	10.0 g	Merck, Germany
Bacto-agar	20.0 g	Clontech, USA
Deionised water	top up to 1 L	Millipore, USA

All the above components were mixed with 1 L deionized water and autoclaved at 121°C for 15 min. After cooling to 55°C, the appropriate antibody was added and poured into petri dishes. The plates were stored at 4°C until further use.

(iii) Antibiotics

Items	Amount	Source
Ampicillin	100 mg	Sigma, USA
Kanamycin	50 mg	Sigma, USA
Deionised water	1 ml	Millipore, USA

All antibiotic solutions were filter-sterilised through a 0.2 μm filter and stored at -20°C prior to use. The stock concentrations of ampicillin and kanamycin are 100 mg/ml and 50 mg/ml, respectively. Working concentrations of ampicillin and kanamycin are 100 μg/ml and 50 μg/ml, respectively.

D. Sequencing primers

Primer name	Nucleotide sequence (5'-3')
WNVCF	ATGTCTAAGAAACCAGGA
WNVCR	AGCTCCAGCACAGGCGAT
DENVCF	ATGGATAACCAACGAAAA
DENVCR	CGCCATCACTGTTGGAAT
hSec3pF1	ATGACAGCAATCAAGCAT
hSec3pF2	GTTAGCTCACAGCTTTTG
hSec3pF3	AAGCAACCACCTAATTCAT
hSec3pF4	CTAAAGAGTACAGATTAT
hSec3pF5	AACAGGACTTCATAAGTA
hSec3pF6	TTCCATTTGTTGCTGAAT
hSec3pF7	CGTAAAGTCATTAAGGAG
hSec3pR	CATGCAATCTGCCTTTTG
Matchmaker™ AD insert screening amplimer	CLONTECH, USA

E. Reagents used for sequencing

(i) DEPC-treated water

One litre of 0.1% DEPC-treated water was prepared by adding 1 ml of DEPC (Sigma, USA) to 100 ml of deionised water (Millipore, New Hampshire, USA) and mixed well. It was left to stir on a magnetic stirrer/hotplate (Bibby Sterilin, UK) overnight at 25°C. The solution was then autoclaved for 15 min at 121°C.

(ii) 70% ethanol

About 7.0 ml of absolute ethanol (Merck, USA) was mixed with 3.0 ml of DEPC-treated water.

F. Primers used in mutagenesis study

Plasmid	Forward Primer (5'-3')	Reverse primer (5'-3')	Template
V5-hSec3pSH2	CAGGACATTCTGGATGCATGTTCC AGCATTGCA	TGCAATGCTGGAACATGCATCC AGAATGTCCTG	V5-hSec3pf1
V5-hSec3pPDZ	ATGGAATTCACTATTGCGGACAT TGCGGATTATTGTTCCAGC	GCTGGAACAATAATCCGCAATG TCCGCAATAGTGAATTCCAT	V5-hSec3pf1
WMycC2	GCCCGAATTCGGATGGCAAAGAA ACCAGGAGGG	CCCTCCTGGTTTCTTTGCCATCC GAATTCGGGC	WMycC
WMycC3	CGAATTCGGATGTCTGCGAAACC AGGAGGGCCC	GGGCCCTCCTGGTTTCGCAGAC ATCCGAATTCG	WMycC
WMycC4	ATTCGGATGTCTAAGGCACCAG GAGGGCCCGGT	ACCGGGCCCTCCTGGTGCCTTA GACATCCGAAT	WMycC
WMycC5	CGGATGTCTAAGAAAGCTGGA GGGCCCGGTAAA	TTTACCGGGCCCTCCAGCTTT CTTAGACATCCG	WMycC
WMycC6	ATGTCTAAGAAACCAGCTGGG CCCGGTAAAAAC	GTTTTTACCGGGCCCAGCTGG TTTCTTAGACAT	WMycC
WMycC7	TCTAAGAAACCAGGAGCTCCCG GTAAAAACCGG	CCGGTTTTTACCGGGAGCTCCT GGTTTCTTAGA	WMycC
WMycC8	AAGAAACCAGGAGGGGCTGGTAA AAACCGGGCT	AGCCCGGTTTTTACCAGCCC CTCCTGGTTTCTT	WMycC
WMycC9	AAACCAGGAGGGCCCGCAAAAA ACCGGGCTGTC	GACAGCCCGGTTTTTTGCGG GCCCTCCTGGTTT	WMycC
WMycC10	CCAGGAGGGCCCGGTGCAAACC GGGCTGTCAAT	ATTGACAGCCCGGTTTGCAC CGGGCCCTCCTGG	WMycC
WMycC11	GGAGGGCCCGGTAAAGCCCGGG CTGTCAATATG	CATATTGACAGCCCGGGCTT TACCGGGCCCTCC	WMycC
WMycC12	GGGCCCGGTAAAAACGCGGCTGTC AATATGCTA	TAGCATATTGACAGCCGCGT TTTTACCGGGCCC	WMycC
WMycC13	CCCGGTAAAAACCGGGCAGTCAAT ATGCTAAAA	TTTTAGCATATTGACTGCCCG GTTTTTACCGGG	WMycC
WMycC14	GGTAAAAACCGGGCTGCTAATATG CTAAAACGC	GCGTTTTAGCATATTAGCAG CCCGGTTTTTACC	WMycC
WMycC15	AAAAACCGGGCTGTCGCTATGCTA AAACGCGGT	ACCGCGTTTTAGCATAGCGA CAGCCCGGTTTTT	WMycC
DMycC12	AAGGCGAGAAATACCGCATTCAAT ATGCTGAAA	TTTCAGCATATTGAATGCGG TATTTCTCGCCTT	DMycC
DMycC13	GCGAGAAATACCCCTGCCAATATG CTGAAACGC	GCGTTTCAGCATATTGGCAG GGGTATTTCTCGC	DMycC
DMycC14	AGAAATACCCCTTTCGCTATGCTG AAACGCGAG	CTCGCGTTTCAGCATAGCGA AAGGGGTATTTCT	DMycC
DMycC15	AATACCCCTTTCAATGCGCTGAAA CGCGAGAGA	TCTCTCGCGTTTCAGCGCAT TGAAAGGGGTATT	DMycC
WCapIC2	ACGAAGATCTCGATGGCGAAGAA AGCAGGAGGG	CCCTCCTGCTTTCTTCGCCA TCGAGATCTTCGT	pWNS carrier plasmid

WCapIC3	AAGATCTCGATGTCTGCTAAAGCA GGAGGGCCC	GGGCCCTCCTGCTTTAGCAG ACATCGAGATCTT	pWNS carrier plasmid
WCapIC4	ATCTCGATGTCTAAGGCCGCAGGA GGGCCCGGT	ACCGGGCCCTCCTGCGGCCT TAGACATCGAGAT	pWNS carrier plasmid
WCapIC5	TCGATGTCTAAGAAAGCCGGAGG GCCCGGTAAA	TTTACCGGGCCCTCCGGCTT TCTTAGACATCGA	pWNS carrier plasmid
WCapIC6	ATGTCTAAGAAACCAGCCGGGCC CGGTAAAAAC	GTTTTTACCGGGCCCGGCTG GTTTCTTAGACAT	pWNS carrier plasmid
WCapIC7	TCTAAGAAACCAGGAGCTCCCGG TAAAAACCGG	CCGGTTTTTACCGGGAGCTC CTGGTTTCTTAGA	pWNS carrier plasmid
WCapIC8	AAGAAACCAGGAGGGGCAGGTAA AAACCGGGCT	AGCCCGGTTTTTACCTGCCC CTCCTGGTTTCTT	pWNS carrier plasmid
WCapIC9	AAACCAGGAGGGCCCGCGAAAAA CCGGGCTGTC	GACAGCCCGGTTTTTCGCGG GCCCTCCTGGTTT	pWNS carrier plasmid
WCapIC10	CCAGGAGGGCCCGGTGCCAACCG GGCTGTCAAT	ATTGACAGCCCGGTTGGCAC CGGGCCCTCCTGG	pWNS carrier plasmid
WCapIC11	GGAGGGCCCGGTAAAGCACGGGC TGTCAATATG	CATATTGACAGCCCGTGCTT TACCGGGCCCTCC	pWNS carrier plasmid
WCapIC12	GGGCCCGGTAAAAACGCTGCTGTC AATATGCTA	TAGCATATTGACAGCAGCGT TTTTACCGGGCCC	pWNS carrier plasmid
WCapIC13	CCCGGTAAAAACCGGGGTGTCAAT ATGCTAAAA	TTTTAGCATATTGACACCCC GGTTTTTACCGGG	pWNS carrier plasmid
WCapIC14	GGTAAAAACCGGGCTGCAAATAT GCTAAAACGC	GCGTTTTAGCATATTTGCAG CCCGGTTTTTACC	pWNS carrier plasmid
WCapIC15	AAAAACCGGGCTGTCGCGATGCT AAAACGCGGT	ACCGCGTTTTAGCATCGCGA CAGCCCGGTTTTT	pWNS carrier plasmid
DCapIC12	AAGGCGAGAAATACCGCATTCAAT ATGCTGAAA	TTTCAGCATATTGAATGCGG TATTTCTCGCCTT	pDENV carrier plasmid
DCapIC13	GCGAGAAATACCCCTGCCAATATG CTGAAACGC	GCGTTTCAGCATATTGGCAG GGGTATTTCTCGC	pDENV carrier plasmid
DCapIC14	AGAAATACCCCTTTCGCTATGCTG AAACGCGAG	CTCGCGTTTCAGCATAGCGA AAGGGGTATTTCT	pDENV carrier plasmid
DCapIC15	AATACCCCTTTCAATGCGCTGAAA CGCGAGAGA	TCTCTCGCGTTTCAGCGCAT TGAAAGGGGTATT	pDENV carrier plasmid

G. DEPC-treated PBS

One litre of 0.1% DEPC-treated PBS was prepared by adding 1 ml of DEPC (Sigma, USA) to 100 ml of PBS (Appendix 1H) and mixed well. It was left to stir on a magnetic stirrer/hotplate (Bibby Sterilin, UK) overnight at 25°C. The solution was then autoclaved for 15 min at 121°C.

H. Primers used for real-time PCR assay

Primers used in Plus (+) strand RNA synthesis
5’ GGTTCGCCACATCACTACACTT 3’
5’ GATCAGTTCCGTGAAATGGTTTGA 3’
Primers used in Minus (-) strand RNA synthesis
5’ GCGTAATACGACTCACTATA 3’
5’ GATCAGTTCCGTGAAATGGT 3’

Viral RNAs extracted from the culture supernatant as well as from the cell lysates were reverse transcribed with Supercriptase III (Invitrogen, USA) using the primers corresponding to nucleotides 11000 to 11020. The reverse transcripts were applied to a real-time PCR assay using iTaq^{TM} Supermix (BIO-RAD) with specific primers mentioned above. The kinetics of cDNA amplification were monitored with an ABI PRISM 7000 sequence detection system (Applied Biosystems) using a dual labeled probe (5’ TGGAACCTGCTGCCAGTCATACCACC 3’) conjugated with 6-carboxyfluorescein at the 5’ end and 6-carboxy-tetramethylrhodamine at the 3’ end. The *in vitro* transcribed RNAs from the full-length infectious clones of WNV and DENV were used as the standards for quantification. Detection of minus stand viral RNA was performed as mentioned by Davis and colleagues (2007). For the detection of minus-strand RNA level, T7-tagged primer real time RT-PCR was carried out. The minus-strand primer, 5’ gcgtaatacgactcactataGGTTCGCCACATCACTACACTT 3’ (T7 tag sequence in lowercase) was used to reverse transcribe minus

strand RNA. The resulting reverse transcripts with the introduced T7 sequence were then applied to a real-time PCR assay using iTaq™ Supermix (BIO-RAD) with specific primers as mentioned in Section 2.3.15.

APPENDIX 4: REAGENTS FOR PROTEOMIC STUDIES

A. 12% Separation/resolving gel mixture

Items	Amount	Source
30% Acrylamide & 0.8% bis-acrylamide	12.0 ml	BioRad, USA
1 M Tris buffer, pH 8.8	11.25 ml	Merck, Germany
10% SDS	0.3 ml	Merck, Germany
Deionised water	6.35 ml	Millipore, USA
N,N,N',N'-tetramethyl ethylene diamine (TEMED)	40.0 µl	BioRad, USA
10% Ammonium persulphate	80.0 µl	Merck, Germany

B. 5% Stacking gel mixture

Items	Amount	Source
30% Acrylamide & 0.8% bis-acrylamide	1.67 ml	BioRad, USA
0.5 M Tris buffer, pH 6.8	2.5 ml	Merck, Germany
10% SDS	0.1 ml	Merck, Germany
Deionised water	5.7 ml	Millipore, USA
N,N,N',N'-tetramethyl ethylene diamine (TEMED)	20.0 µl	BioRad, USA
10% Ammonium persulphate	50.0 µl	Merck, Germany

C. SDS-PAGE Running Buffer (pH 8.9)

Items	Amount	Source
Tris-base	6.07 g	Merck, Germany
Glycine	28.73 g	Merck, Germany
SDS	2.0 g	Merck, Germany
Deionised water	1 L	Millipore, USA

(i) Upper tank buffer

To prepare 500 ml of upper tank buffer, 250 ml of above SDS-PAGE running buffer was mixed with 250 ml of deionized water.

(ii) Lower tank buffer

To prepare 4 L of lower tank buffer, 750 ml of above SDS-PAGE running buffer was mixed with 3250 ml of deionized water.

D. Sample loading buffer

Items	Amount	Source
1 M Tris, pH 6.8	2.4 ml	Merck, Germany
SDS	0.8 g	Merck, Germany
Glycerol (100%)	4 ml	Analar, USA
Bromophenol Blue	0.01% (Final concentration is 0.02%)	Sigma, USA
β-mercaptoethanol	1 ml	Sigma, USA
Deionised water	2.8 ml	Millipore, USA

E. Transfer buffer

Items	Amount	Source
Glycine	14.4 g	Merck, Germany
Tris-base	3.03 g	Merck, Germany
Methanol	200 ml	Merck, Germany
Deionised water	800 ml	Millipore, USA

Glycine and Tris-base were added and mixed well with 800 ml of deionised water before the addition of methanol. The reagent should be freshly prepared.

F. 1 x Tris-buffered saline with 0.5% Tween-20 (TBST)

Items	Amount	Source
Tris-base	3.0 g	Merck, Germany
KCl	0.2 g	Merck, Germany
NaCl	8.8 g	Merck, Germany
Tween-20	1.0 ml	Merck, Germany
Deionised water	1 L	Millipore, USA

G. 5% Skimmed milk

Items	Amount	Source
Skimed milk	5.0 g	Anlene, Australia
1x TBST	100 ml	See Appendix 4F

H. 1 x Phosphate-buffered saline with 0.05% Tween-20 (PBST)

Items	Amount	Source
PBS	100 ml	See Appendix 1H
Tween-20	0.05 ml	Merck, Germany

I. 1% BSA in PBS

Items	Amount	Source
BSA	1.0 g	Invitrogen, USA
PBS	100 ml	See Appendix 1H

J. 4% Paraformaldehyde

Items	Amount	Source
25% Paraformaldehyde	16 ml	Invitrogen, USA
PBS	84 ml	See Appendix 1H

This reagent was prepared in a glass bottle in the fume hood and stored at 4^{o}C.

K. 0.2% Triton-X

Items	Amount	Source
10% Triton-X	200 µl	ICN, USA
PBS	100 ml	See Appendix 1H

This reagent was prepared in a glass bottle and then filter sterilized using 0.2 µm filter and stored at 4^{o}C

APPENDIX 5: REAGENTS FOR YEAST TWO-HYBRID (Y2H) ASSAY

A. Yeast peptone dextrose adenine (YPDA) medium

Items	Amount	Source
Difco peptone	20 g	Clontech, USA
Yeast extract	10 g	Clontech, USA
Agar (for plates only)	20 g	Clontech, USA
0.2% adenine hemisulphate	15 ml	Sigma, USA

All reagents were dissolved in 950 ml of deionized water. The pH of the medium was adjusted to 6.5 and autoclaved at 121°C for 15 min. The YPDA medium was cooled to ~55°C and 50 ml of sterile 40% dextrose was added and the final volume was adjusted to 1 L.

B. 1 x TE/LiAc solution

Items	Amount	Source
10 x TE buffer	1 ml	Clontech, USA
10 x LiAc	1 ml	Clontech, USA
Deionised water	8 ml	Millipore, USA

The above reagents were mixed together before use.

C. Herring testes carrier DNA (10 mg/ml)

The herring testes carrier DNA in solution was denatured by placing it in a boiling water bath for 20 min and immediately cooling it on ice.

D. PEG/LiAc solution

Items	Amount	Source
PEG 4000	8 ml	Clontech, USA
10 x TE buffer	1 ml	Clontech, USA
10 x LiAc	1 ml	Clontech, USA

The above reagents were mixed together before use.

E. Synthetic drop-out (SD) medium

Items	Amount	Source
Minimal SD base	26.7 g	Clontech, USA
-Trp supplement (-Trp)	0.74 g	Clontech, USA
-Leu supplement (-Leu)	0.69 g	Clontech, USA
-His supplement (-His)	0.77 g	Clontech, USA
-Trp-Leu supplement (DDO)	0.64 g	Clontech, USA
-Trp-Leu-His supplement (TDO)	0.62 g	Clontech, USA
-Trp-Leu-His-Ade supplement (QDO)	0.6 g	Clontech, USA
Bacto-agar (for plates only)	20 g	Clontech, USA
Deionised water	1 L	Millipore, USA

Minimal SD base and one of the supplements were mixed in 1 L of sterile deionized water and the pH of the medium was adjusted to 5.8 and autoclaved at 121°C for 15 min.

F. 2 x YPDA medium containing kanamycin (2 x YPDA/Kan)

Items	Amount	Source
Difco peptone	20 g	Clontech, USA
Yeast extract	10 g	Clontech, USA
Agar (for plates only)	20 g	Clontech, USA
0.2% adenine hemisulphate	15 ml	Sigma, USA

To prepare 2 x YPDA/Kan medium, the above reagents were dissolved in 475 ml of deionized water and the pH of the medium was adjusted to 6.5 and autoclaved at 121°C for 15 min. The YPDA medium was cooled to ~55°C and 25 ml of sterile 40% dextrose and 1.5 ml of 50 mg/ml kanamycin (final concentration 10-15 mg/L) were added.

G. 0.5 x YPDA medium containing kanamycin (0.5 x YPDA/Kan)

Items	Amount	Source
Difco peptone	20 g	Clontech, USA
Yeast extract	10 g	Clontech, USA
Agar (for plates only)	20 g	Clontech, USA
0.2% adenine hemisulphate	15 ml	Sigma, USA

To prepare 0.5 x YPDA/Kan medium, the above reagents were dissolved in 1900 ml of sterile water and the pH of the medium was adjusted to 6.5 and autoclaved at 121°C for 15 min. The YPDA medium was cooled to ~55°C and 100 ml of sterile 40% dextrose and 6 ml of 50 mg/ml kanamycin (final concentration 10-15 mg/L) were added.

H. QDO + X-α-Gal plates

Twenty micrograms of 5-bromo-4-chloro-3-indolyl-β-D-galactopyranoside (Clontech, USA) was dissolved in 1 ml of N, N'-dimethylformamide (Sigma, USA) and store in the dark at -20°C until use. One hundred microlitres of X-α-Gal was spreaded onto the QDO plates and dried before use.

APPENDIX 6: REAGENTS FOR MAMMALIAN TWO-HYBRID (M2H) ASSAY

A. Controls used in M2H assay

Controls	Transfection	Purpose
Negative control **(NC)**	pCR®2.1/VP16-CP negative control plasmid was co-transfected with the reporter plasmid pGAL/lacZ	To detect the levels of false positive interactions
Background LacZ control **(BC_{Lac})**	No transfection	To determine the background β-galactosidase activity in BHK cells
Positive control **(PC)**	pCR®2.1/GAL4-VP16 positive control plasmid was co-transfected with the reporter plasmid pGAL/lacZ	To verify induction of the reporter gene
Positive interaction control **(PIC)**	pCR®2.1/p53 bait control plasmid and pCR®2.1/LgT prey control plasmid were co-transfected with the reporter plasmid pGAL/lacZ	To verify that the cell line and detection are working properly
Background control for the prey protein (importinα/importinβ/C) **(BChSec3p)**	Prey construct was co-transfected with the reporter plasmid pGAL/lacZ in the absence of bait construct	To check if prey protein can function as a transcriptional activator in the absence of bait protein
Background controls for full-length/mutated C proteins (bait) **(BCCW, BCCW2-BCCW15, BCCW109110111, BCCW112113114, BCCW115116117, BCCDMycC12-BCCD, BCCD12-BCCD15, BCCD102103104, BCCD105106107, BCCD108109110)**	Bait construct was co-transfected with the reporter plasmid pGAL/lacZ in the absence of prey construct	To check if bait protein can function as a transcriptional activator in the absence of prey protein

APPENDIX 7: REAGENTS USED IN LENTIVIRUS-MEDIATED KNOCK-DOWN AND OVER-EXPRESSION OF hSec3p

A. Primers used in the knock-down of hSec3p

Short hairpin oilgos used in hSec3p gene silencing	
Top strand oligo	5'-CACCGGAGGTAGATCAGATTGAATTCGAAAATTCAATCTGATCTACCTCC-3' 5'-CACCGCTAAAGAGTACAGATTATGGCGAACCATAATCTGTACTCTTTAGC-3'
Bottom strand oligo	5'-AAAAGGAGGTAGATCAGATTGAATTTTCGAATTCAATCTGATCTACCTCC-3' 5'-AAAAGCTAAAGAGTACAGATTATGGTTCGCCATAATCTGTACTCTTTAGC-3'
Short hairpin oilgos used for scrambled control	
Top strand oligo	5'-CACCTTGTGATGGAATAGGAAGCATCGAAATGCTTCCTATTCCATCACAA-3'
Bottom strand oligo	5'-AAAATTGTGATGGAATAGGAAGCATTTCGATGCTTCCTATTCCATCACAA-3'

B. Primers used in the over-expression of hSec3p

hSec3p over-expression	
Forward primer	5'-CACCATGGCAGCAATCAAGCAT-3'
Reverse primer	5'-GTGGGACTGTGCAATGCT-3'
Control vector	
Forward primer	5'-CACCATGCTACCCAAAGACCTC-3'
Reverse primer	5'-GAGGTCTTTGGGTAGCAT-3'

C. Growth medium, DMEM for hSec3p293OE and hSec3p293KD cells (~pH 7.3)

Items	Amount	Source
DMEM	1 bottle	Sigma, USA
Foetal bovine serum	100 ml	PAA Laboratories, Austria
$NaHCO_3$	3.7 g	Merck, Germany
Geneticin	50 mg/ml	Invitrogen, USA
L-glutamine	2 mM	Invitrogen, USA
Non-essential amino acids	0.1 mM	Invitrogen, USA
Pyruvic acid	1 mM	Invitrogen, USA
Deionised water	890 ml	Millipore, USA

The pH of the media was then adjusted to approximately 7.3 with a handheld pH meter (Beckman Coulter Inc., USA). The solution was then sterilised by filtration in a sterile environment through a 0.2 µm PES membrane bottle top filter unit (Nalge Nunc International, Denmark). A 20 ml aliquot of filtered media was used for screening of microbial contamination by incubation at 37°C for 3 days before the addition of FBS, geneticin, glutamine, non-essential amino acids and pyruvic acid. The serum supplemented media were kept at 4°C until further use. The cell culture media were warmed up in water bath to 37°C before use.

APPENDIX 8: REAGENTS USED IN PROTEIN-RNA INTERACTION ASSAYS

A. Wash buffer used in streptavidin-conjugated magnetic pull down assay

Items	Stock	Final	50 ml	Freshly add to 1 ml of wash buffer
HEPES	0.5 M	10 mM	1	-
$MgCl_2$	1 M	2 mM	0.1	-
KCl	1 M	10 mM	0.5	-
NP-40	100%	0.1%	0.05	-
EDTA	0.4 M	0.5 mM	0.0625	-
NaCl	5 M	150 mM	1.5	-
H_2O	-	-	46.7875	-
DTT	1 M	1 mM	-	1 µl
PMSF	100%	0.1%	-	1 µl
Protease cocktail	25 units/ml	1 unit/ml	-	40 µl

B. Binding buffer with BSA

Items	Final
HEPES (pH 7.4)	20 mM
$MgCl_2$	2.5 mM
KCl	75 mM
NP-40	0.05%
EDTA	0.1 mM
BSA	1%
DTT	1 mM
Protease cocktail	1 unit/ml

C. Binding buffer without BSA

Items	Final
HEPES (pH 7.4)	20 mM
$MgCl_2$	2.5 mM
KCl	75 mM
NP-40	0.05%
EDTA	0.1 mM
DTT	1 mM
Protease cocktail	1 unit/ml

APPENDIX 9: BIOINFORMATICS SOFTWARE USED IN THIS STUDY

Function	Name	URL or Manufacturer
Translation	Translate Tool	http://tw.expasy.org/tools/dna.html
Sequence comparison	BLAST	http://www.ncbi.nlm.nih.gov/BLAST (blastn; blastp; blastx algorithms)
Multiple Sequence Alignment	CLUSTALW	http://www.ebi.ac.uk/clustalw/index.html
Restriction enzyme site analysis	Webcutter 2.0	http://www.firstmarket.com/cutter/cut2.html
Analysis of protein sequences	ScanProsite Eukaryotic Linear Motif resources	http://tw.expasy.org/tools/scanprosite/
Prediction of protein MW	Compute pI/MW ProtParam	http://tw.expasy.org/tools/pi_tool.html http://tw.expasy.org/tools/protparam.html
Primer design	Bioportal Vector NTI version 7.1	http://bioportal.bic.nus.edu.sg/ Informax, Inc.
RNAi design	BLOCK-iT RNAi Designer	www.invitrogen.com/rnai
Nucleotide scrambling	siRNA Wizard	http://www.sirnawizard.com/scrambled.php